



UNIVERSITÀ
DI PAVIA

**DEPARTMENT OF BRAIN AND BEHAVIORAL SCIENCES
UNIT OF NEUROPHYSIOLOGY**

PhD IN BIOMEDICAL SCIENCES

PhD Director: **Prof. Egidio D'Angelo**

**Characterization of antioxidant and anti-inflammatory
profiles of new electrophilic/non-electrophilic
compounds: relevance for Nrf2/NF- κ B transcription
factors involvement**

PhD Tutors: **Prof. Marco Racchi**
Prof. Cristina Lanni

PhD Dissertation of
Catanzaro Michele

XXXIII cycle
academic years 2017-2020

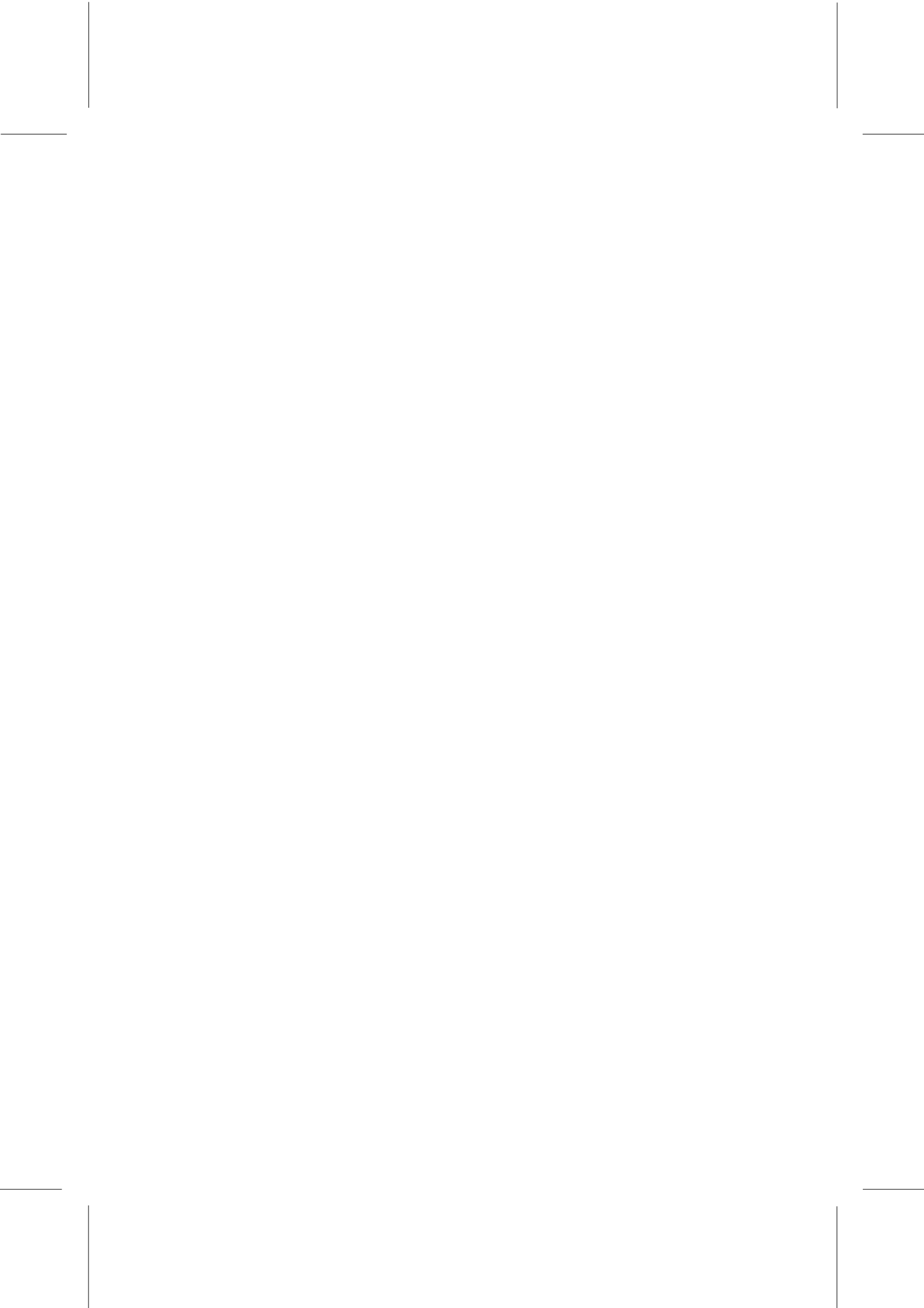


TABLE OF CONTENTS

PREFACE	p. 1
CHAPTER 1 - Curcumin- and diallyl sulfide- derived compounds: from the scientific rationale to the characterization of their antioxidant and antiinflammatory profiles	p. 9
PART I - Curcumin in Alzheimer's disease: can we think to new strategies and perspectives for this molecule?.....	p. 11
PART II - Immunomodulators inspired by nature: a review on Curcumin and Echinacea	p. 41
PART III - Modulation of oxidative stress response through activation of Keap1/Nrf2/ARE pathway by curcuma- and garlic-derived hybrids	p. 71
PART IV - Targeting cytokine release through the differential modulation of Nrf2 and NF- κ B pathways by electrophilic/non-electrophilic compounds	p. 97
PART V - <i>Eye-Light on Age-Related Macular Degeneration: Targeting Nrf2-Pathway as a Novel Therapeutic Strategy for Retinal Pigment Epithelium</i>	p. 131
CHAPTER 2 - Collaborative activities: characterization of the antioxidant profile of natural and nature-derived compounds through the investigation of the Nrf2 pathway	p. 163

PART I - Characterization of the antioxidant effects of gamma-Oryzanol: involvement of the Nrf2 pathway	p. 165
PART II - Prenylated Curcumin analogues as multipotent tools to tackle Alzheimer's disease.....	p. 187
PART III - Merging memantine and ferulic acid to probe connections between NMDA receptors, oxidative stress and amyloid- β peptide in Alzheimer's disease	p. 223
CHAPTER 3 - Immune response in COVID-19: a critical dissertation of potential pharmacological treatments.....	p. 253
PART I - Immune response in COVID-19: addressing a pharmacological challenge by targeting pathways triggered by SARS-CoV-2	p. 255
PART II - Molecular features of IGHV3-53-encoded antibodies elicited by SARS-CoV-2	p. 287
CHAPTER 4 - Other research activities.....	p. 293
PART I - The role of chitosan as coating of Nanostructured Lipid Carrier in skin delivery of fucoxanthin.....	p. 295
PART II - Targeting Infectious Agents as a Therapeutic Strategy in Alzheimer's Disease: Rationale and Current Status	p. 297
LIST OF PUBLICATIONS	p. 299





PREFACE

During my PhD research internship, I carried out the experimental activities at the Department of Drug Sciences of the University of Pavia, in the Pharmacology Section. My research activity mainly focused on the investigation of the antioxidant and antiinflammatory effects of some natural molecules and newly synthesized chemical compounds, through the fine dissection of the Nrf2 (NF-E2-related factor 2) and NF- κ B (Nuclear Factor kappa B) pathways, key regulators of oxidative stress and inflammation, respectively. Indeed, these conditions have been demonstrated to be involved in pathophysiological processes and one of which can be easily induced by another, as demonstrated by several studies (*Reuter et al., 2010; Biswas et al., 2016*). In particular, they are characterized by increased release of harmful reactive oxygen and nitrogen species (ROS and RNS), which further promote cellular damage and inflammation, thereby resulting in a feed-forward loop at the basis of many chronic diseases (*Khansari et al., 2009; Fischer et al., 2015*). Both conditions have been related to several disorders, such as neurodegenerative diseases, and the pharmacological research of new active molecules counteracting them is highly active.

In this context, thanks to a collaboration with the pharmaceutical chemist group held by Prof. Michela Rosini of the University of Bologna, we designed and tested a new set of electrophilic and non-electrophilic compounds, starting from the pharmacophoric moieties of two natural compounds, curcumin and diallyl sulphide.

As reported in the chapter 1 of this thesis, part I and part II, we analysed data from the literature concerning curcumin and other natural or hybrid molecules to rationally design our electrophilic/non-electrophilic compounds (*Serafini et al., 2017 and Catanzaro et al., 2018*). The idea raised

by the knowledge that hydroxycinnamoyl recurring motif, present in many natural polyphenols, has been shown to modulate several pathways related to aging and chronic diseases (*Upadhyay and Dixit, 2015*). Moreover, diallyl sulfides, garlic-derived organosulfur compounds carrying allyl mercaptan moieties, are able to counteract oxidative stress through the modulation of many antioxidant and defensive enzymes (*Koh et al., 2005; Rao et al, 2015*). After the chemical design and synthesis of compounds, we first investigated the antioxidant profile of these molecules by analysing their ability to modulate the Nrf2 pathway, a master regulator of intracellular redox homeostasis promoting the transcription of numerous cytoprotective genes (part III, *Serafini et al., 2020*).

Although it is widely known that the redox control acted by Nrf2 activation can suppress the inflammatory response, recent evidences directly linked the Nrf2 mediated anti-inflammatory activity to the crosstalk with the transcription factor NF- κ B, a key mediator of inflammatory response, cytokine production and cell survival (*Perkins et al., 2007*). However, the underlying molecular basis of this putative crosstalk has not been completely identified. In part IV, we investigated whether the activation of the Nrf2 pathway by our electrophilic compounds may interfere with the secretion of pro-inflammatory cytokines, dissecting the mechanistic connection between Nrf2 and NF- κ B transcription factors (*Fagiani et al., 2020*). However, our studies demonstrated that these compounds are able to induce a differential modulation of several cytokine and chemokines, by differently regulating the transcriptional activities of Nrf2 and NF- κ B pathways and that this regulation is not influenced by the crosstalk among them (*Fagiani et al., 2020*).

Furthermore, oxidative stress and inflammation, together with autophagy, are common features of a particular neurodegenerative disease called AMD (Age-related Macular Degeneration). This disease is a very common degenerative eye disease that affect the macula region and cause vision loss in elderly people worldwide still lacking effective therapies (*Lim et al., 2012*). AMD phenotypes are not homogeneous and the pathological mechanisms responsible for this illness are not completely understood. In the context of pharmacological interventions for AMD, it has been shown that a positive modulation of Nrf2 transcriptional activity may represent an efficient defensive strategy to prevent the oxidative and inflammatory-induced

damages responsible, at least in part, of macular degeneration (*Sachdeva et al., 2014*). Accordingly, in the last part of the chapter 1 (part V), we demonstrated that Nrf2 impairment predisposes ARPE-19 cells to a higher vulnerability, a typical early event triggering AMD (*Catanzaro et al. 2020*). Moreover, by using our compounds as a valuable pharmacological tool, we demonstrated that Nrf2 activation, leading to a downstream to up-regulation of HO-1 (Heme Oxygenase-1) and p62 (sequestosome 1) proteins, is a physiological protective response able to counteract cell damage and death (*Catanzaro et al. 2020*).

As reported in chapter 2, I was involved in other collaborative activities with different research groups, where I contributed with my skills to define the antioxidant profile of some natural or synthetic compounds. In particular, as reported in part I, thanks to a collaboration with Prof. Daniela Uberti of the University of Brescia, we investigated and demonstrated the Nrf2-mediated mechanism of action of γ -Oryzanol (ORY), a mixture of steryl ferulate compounds plentifully contained in rice (*Oryza sativa* L.) (*Rungratanawanich et al., 2018*). In this project we demonstrated the scavenger activity of ORY against hydrogen peroxide-induced ROS/RNS production and the ability of ORY to enhance the activity superoxide dismutase (SOD) and glutathione peroxidase (GPx) (*Rungratanawanich et al., 2018*). Deeping insight the molecular mechanism of ORY, we further demonstrated its capability to induce the nuclear translocation of Nrf2 and, consequentially, the upregulation of its target genes HO-1, NAD(P)H quinone reductase (NQO1), and glutathione synthetase (GSS) (*Rungratanawanich et al., 2018*).

In part II, thanks to a collaboration with Prof. Ersilia De Lorenzi of the University of Pavia, we investigated the antioxidant characteristic of a small library of synthetic compounds derived from curcumin (*Bisceglia et al., 2019*). In particular, we investigated the scavenger ability of these compounds when co-incubated with H₂O₂ comparing their activity with pure curcumin (*Bisceglia et al., 2019*). Moreover, we further demonstrated the ability of one of them to significantly induce the nuclear translocation of Nrf2 (*Bisceglia et al., 2019*). Finally, in part III, in a collaborative project with Prof. Michela Rosini and Prof. Anna Minarini of University of Bologna, we dissect the mechanism of action of a new set of compounds conjugating the anti-Alzheimer drug memantine

to the neuroprotective natural compound ferulic acid (*Rosini et al. 2019*). In particular, in this work, we contribute by investigating the cell-safety, the scavenging activity against ROS/RNS and the capability to modulate the intracellular Nrf2 pathway of these compounds in a model of human neuroblastoma cells (*Rosini et al. 2019*).

In the time of pandemic COVID-19 (COronaVirus Disease 2019), as described in chapter 3, part I, we critically reviewed in a paper the putative intracellular signaling pathways involved in viral infections, with particular emphasis on the relevance of coronaviruses. In particular, in the first phase of the pandemic, we tried to shed light to the immunopathological pathways triggered by SARS-CoV-2 (Severe Acute Respiratory Syndrome CoronaVirus 2) in order to identify the most relevant molecular cascades implicated in viral infections to suggest potential useful drug repurposing (*Catanzaro et al, 2020*). Then, in part II, we were asked by *Signal Transduction and Targeted Therapy* journal to critically resume the results presented in Science by Yuan *et al.* providing novel insights into the molecular features of neutralizing antibody responses to the SARS-CoV-2 (*Fagiani et al, 2020*).

In chapter 4, are reported the abstracts of two other collaborative papers not directly linked to my PhD project (for the full text of these articles please refer to the online sources). In particular, in part I, the abstract of a research paper about the design and develop of some nanostructured lipidic carriers loaded with fucoxanthin, a marine carotenoid characterized by antiproliferative properties against hyperproliferative cells, is reported (*Malgarim Cordenonsi et al., 2019*). The aim of this project was to create a lipidic formulation for skin application to prevent skin hyperproliferative diseases with particular emphasis on psoriasis. For this project we developed and characterized a psoriatic-like cellular model then used to evaluate the safety and the antiproliferative activities of these nano-formulations.

Finally, as described in part II, during the 6-months internship at the University of Sherbrooke (Quebec, Canada), under the supervision of Prof. Tamas Fülöp and Prof. Eric Frost, I worked in the lab of “Immuno-inflammation of Aging” in an immune-related research project investigating the involvement of bacterial and viral infections in Alzheimer’s Disease. In particular, in this thesis

is reported a review article that explain the rational background of the project (Fülöp et al, 2020). The review is based on the theory that systemic infections directly lead to neuroinflammation via microbial virulence factors responsible for β -amyloid production in the CNS (Central Nervous System) (Fülöp et al., 2018). In particular, with the progression of the disease, the overproduction of β -amyloid, displaying antimicrobial properties, becomes detrimental and, concomitantly with alterations of the immune system, lead to systemic inflammation, neurodegeneration, and the senescence of the immune cells (Fülöp et al, 2020).

REFERENCES

Bisceglia F., Seghetti F., Serra M., Zusso M., Gervasoni S., Verga L., Vistoli G., Lanni C., Catanzaro M., De Lorenzi E., Belluti F.; *Prenylated Curcumin analogues as multipotent tools to tackle Alzheimer's disease*, ACS Chem Neurosci. 2019 Mar 20; 10 (3): 1420-1433. doi: 10.1021/acscemneuro.8b00463.

Biswas S.K.; *Does the Interdependence between Oxidative Stress and Inflammation Explain the Antioxidant Paradox?*, Oxid Med Cell Longev. 2016; 2016: 5698931. doi: 10.1155/2016/5698931.

Catanzaro M., Corsini E., Rosini M., Racchi M., Lanni C.; *Immunomodulators inspired by nature: a review on Curcumin and Echinacea*, Molecules. 2018, 23 (11), 2778. doi: 10.3390/molecules23112778.

Catanzaro M., Fagiani F., Racchi M., Corsini E., Govoni S., Lanni C.; *Immune response in COVID-19: addressing a pharmacological challenge by targeting pathways triggered by SARS-CoV-2*, Signal Transduct Target Ther. 2020 May 29; 5 (1): 84. doi: 10.1038/s41392-020-0191-1.

Catanzaro M., Lanni C., Basagni F., Rosini M., Govoni S., Amadio M.; *Eye-Light on Age-Related Macular Degeneration: Targeting Nrf2-Pathway as a Novel Therapeutic Strategy for Retinal Pigment Epithelium*, Front Pharmacol. 2020; 11: 844. doi: 10.3389/fphar.2020.00844.

Fagiani F., Catanzaro M., Buoso E., Basagni F., Di Marino D., Raniolo S., Amadio M., Frost E.H., Corsini E., Racchi M., Fülöp T., Govoni S., Rosini M., Lanni C.; *Targeting cytokine release through the differential modulation of Nrf2 and NF- κ B pathways by electrophilic/non-electrophilic compounds*, Front Pharmacol. 2020; 11: 1256. doi: 10.3389/fphar.2020.01256.

Fagiani F., Catanzaro M., Lanni C.; *Molecular features of IGHV3-53-encoded antibodies elicited by SARS-CoV-2*, Signal Transduct Target Ther. 2020 Aug 25; 5 (1): 170. doi: 10.1038/s41392-020-00287-4.

- Fischer R., Maier O.; *Interrelation of oxidative stress and inflammation in neurodegenerative disease: role of TNF*, *Oxid Med Cell Longev*. 2015; 2015: 610813. doi: 10.1155/2015/610813.
- Fülöp T., Witkowski J.M., Bourgade K., Khalil A., Zerif E., Larbi A., Hirokawa K., Pawelec G., Bocti C., Lacombe G., Dupuis G., Frost E.H.; *Can an Infection Hypothesis Explain the Beta Amyloid Hypothesis of Alzheimer's Disease?*, *Front Aging Neurosci*. 2018 Jul 24; 10: 224. doi: 10.3389/fnagi.2018.00224.
- Fülöp T., Munawara U., Larbi A., Desroches M., Rodrigues S., Catanzaro M., Khalil A., Bernier F., Barron A., Beaugregard P.B., Dumoulin D., Bellenger J.P., Witkowski J.M., Frost E.H.; *Targeting Infectious Agents as a Therapeutic Strategy in Alzheimer's Disease: Rationale and Current Status*, *CNS Drugs*. 2020 May 26; doi: 10.1007/s40263-020-00737-1.
- Koh S.H., Kwon H., Park K.H., Ko J.K., Kim J.H., Hwang M.S., Yum Y.N., Kim O.H., Kim J., Kim H.T., Do B.R., Kim K.S., Kim H., Roh H., Yu H.J., Jung H.K., Kim S.H.; *Protective effect of diallyl disulfide on oxidative stress-injured neuronally differentiated PC12 cells*, *Brain Res Mol Brain Res*. 2005 Feb 18; 133 (2): 176-86. doi: 10.1016/j.molbrainres.2004.10.006.
- Lim L.S., Mitchell P., Seddon J.M., Holz F.G., Wong T.Y.; *Age-related macular degeneration*, *Lancet*. 2012 May 5; 379 (9827): 1728-38. doi: 10.1016/S0140-6736(12)60282-7.
- Malgarim Cordenonsi L., Faccendini A., Catanzaro M., Bonferoni M.C., Rossi S., Malavasi L., Platcheck Raffin R., Scherman Schapoval E.E., Lanni C., Sandri G., Ferrari F.; *The role of chitosan as coating of Nanostructured Lipid Carrier in skin delivery of fucoxanthin*, *Int J Pharm*. 2019 Aug 15; 567: 118487. doi: 10.1016/j.ijpharm.2019.118487.
- Perkins N.D.; *Integrating cell-signalling pathways with NF-kappaB and IKK function*, *Nat Rev Mol Cell Biol*. 2007 Jan; 8 (1): 49-62. doi: 10.1038/nrm2083.
- Rao P.S., Midde N.M., Miller D.D., Chauhan S., Kumar A., Kumar S.; *Diallyl Sulfide: Potential Use in Novel Therapeutic Interventions in Alcohol, Drugs, and Disease Mediated Cellular Toxicity by Targeting Cytochrome P450 2E1*, *Curr Drug Metab*. 2015; 16 (6): 486-503. doi: 10.2174/1389200216666150812123554.
- Reuter S., Gupta S.C., Chaturvedi M.M., Aggarwal B.B.; *Oxidative stress, inflammation, and cancer: how are they linked?*, *Free Radic Biol Med*. 2010 Dec 1; 49 (11): 1603-16. doi: 10.1016/j.freeradbiomed.2010.09.006.
- Rosini M., Simoni E., Caporaso R., Basagni F., Catanzaro M., Abu I.F., Fagiani F., Fusco F., Masuzzo S., Albani D., Lanni C., Mellor I.R., Minarini A.; *Merging memantine and ferulic acid to probe connections between NMDA receptors, oxidative stress and amyloid- β peptide in Alzheimer's disease*, *Eur J Med Chem*. 2019 Oct 15; 180: 111-120. doi: 10.1016/j.ejmech.2019.07.011.
- Rungratanawanich W., Abate G., Serafini M.M., Guarienti M., Catanzaro M., Marziano M., Memo M., Lanni C., Uberti D.; *Characterization of the antioxidant effects of gamma-Oryzanol: involvement of the Nrf2 pathway*, *Oxid Med Cell Longev*. 2018 Mar 14; 2018: 2987249. doi: 10.1155/2018/2987249.
- Sachdeva M.M., Cano M., Handa J.T.; *Nrf2 signaling is impaired in the aging RPE given an oxidative insult*, *Exp Eye Res*. 2014 Feb; 119: 111-4. doi: 10.1016/j.exer.2013.10.024.

Serafini M.M., Catanzaro M., Racchi M., Rosini M., Lanni C.; *Curcumin in Alzheimer's disease: can we think to new strategies and perspectives for this molecule?*, Pharm Res. 2017 Oct; 124: 146-155. doi: 10.1016/j.phrs.2017.08.004.

Serafini M.M., Catanzaro M., Fagiani F., Simoni E., Caporaso R., Dacrema M., Govoni S., Racchi M., Rosini M., Daglia M., Lanni C.; *Modulation of oxidative stress response through activation of Keap1/Nrf2/ARE pathway by curcuma- and garlic-derived hybrids*, Front Pharmacol. 2019; 10: 1597. doi: 10.3389/fphar.2019.01597.

Upadhyay S., Dixit M.; *Role of Polyphenols and Other Phytochemicals on Molecular Signaling*, Oxid Med Cell Longev. 2015; 2015: 504253. doi: 10.1155/2015/504253.

CHAPTER 1

Curcumin- and diallyl sulfide- derived compounds: from the scientific rationale to the characterization of their antioxidant and antiinflammatory profiles

PART I

The following manuscript was published in *Pharmacological Research* in 2017 as:

Curcumin in Alzheimer's disease: Can we think to new strategies and perspectives for this molecule?

Melania Maria Serafini, **Michele Catanzaro**, Michela Rosini, Marco Racchi and Cristina Lanni

Abstract

Population aging is an irreversible global trend with economic and socio-political consequences. One of the most invalidating outcomes of aging in the elderly is cognitive decline, leading to dementia and often related to neurodegenerative disorders. Among these latter, Alzheimer's disease (AD) is the major cause of dementia, affecting more than 30 million of individuals worldwide. To date, the treatment of AD remains a challenge because of an incomplete understanding of the events that lead to the selective neurodegeneration typical of Alzheimer's brains. There is an enormous global demand for new effective therapies and researchers are investigating new fields. One promising strategy is the use of nutraceuticals as integrative, complementary and preventive therapy. Curcumin is one example of natural product with anti-AD properties, with promising potential for prevention, treatment and diagnostic. The limitations in the use of curcumin as therapeutic are represented by its pharmacokinetics profile and the low bioavailability after oral administration. However, curcumin has been the focus of intense research for new drug development. Here we analyzed some new approaches that have been applied in the attempt to improve its use, particularly new formulations, changes in the way of administration, nanotechnology-based delivery systems and the hybridization strategy.

Keywords: Curcumin; Alzheimer's disease; Alternative formulations; Curcuminoids; Hybrids.

Contents lists available at [ScienceDirect](#)**Pharmacological Research**journal homepage: www.elsevier.com/locate/yphrs

Review

Curcumin in Alzheimer's disease: Can we think to new strategies and perspectives for this molecule?Melania Maria Serafini^{a,b}, Michele Catanzaro^b, Michela Rosini^c, Marco Racchi^b,
Cristina Lanni^{b,*}^a Scuola Universitaria Superiore IUSS Pavia, Italy^b Department of Drug Sciences, University of Pavia, Italy^c Department of Pharmacy and Biotechnology, University of Bologna, Italy**1. Introduction**

One of the most important demographic trends facing the world is the aging of the population. As the life expectancy has increased, the high prevalence of chronic disabilities represents one of the major causes of upward burden on the economy of Health Services, requiring a long-term clinical management of the affected subjects. Moreover, the morbidity often observed in aged people increases the healthcare costs since requires multiple intervention approaches. Among different comorbidities, cognitive decline leading to dementia remains the most invalidating one, because of the lack of efficacious treatments and its hard impact on both healthcare workers and families. The major cause of dementia among the elderly is Alzheimer's disease (AD) and current estimations predict that the number of people with dementia will increase and triple by 2050 [1]. For this reason, AD is a growing socio-economic problem worldwide and many researchers are focusing their efforts to come up with a cure. AD is a neurodegenerative disease clinically characterized by progressive loss of memory and cognitive functions. The main microscopic pathological features of AD include accumulation of intracellular fibrillary tangles (NFT) and extracellular senile plaques of β -amyloid peptide ($A\beta$), chronic neuro-inflammation, synaptic and neuronal loss. From the macroscopic point of view, brain atrophy is consistent with a brain volume and weight decrease [2]. The treatment of AD remains a major challenge because of an incomplete understanding of the events that

lead to the selective neurodegeneration typical of Alzheimer's brains. To date, there are not yet effective disease-modifying treatments available, but only therapeutics that slow down the disease progression and control symptoms in the short-term [3,4]. The failure of approved drugs to revert the disease is due to the lack of an early diagnosis for AD: synaptic loss, neuronal loss and brain shrinkage are already significant by the time of symptoms onset and AD diagnosis. There is an enormous global demand for new effective therapies and researchers are investigating different fields. One promising strategy is the cell-based therapy that aims at repopulation and regeneration of neuronal networks in AD brain. Some first clinical trials (NCT01297218 and NCT01696591) concluded that the neuroprotective effect of mesenchymal stem cells intracranial injections (MSCs), frequently reported in AD animal models, was not evident [5], but other trials are ongoing or recruiting patients. Another strategy deeply investigated in the last few years is the immunotherapy targeting A β peptide and/or tau protein, the two pathognomonic signs of the disease. Both, A β -directed immunization and tau immunotherapy have shown promising results in AD transgenic mouse models [6], but the translation to safe and efficient therapy for humans is still a challenge [7]. In this review we will focus our attention on another approach based on an integrative, complementary and preventive therapy for neurodegenerative disorders with alternative therapeutics, such as nutraceuticals. Natural products have already proven to be a rich source of therapeutics and, by offering a great chemical diversity, they can be of inspiration to create new bioactive compounds. Curcumin is one example of natural product with several properties useful in different clinical fields [8-10], whose antioxidant, A β -binding and anti-inflammatory properties make it a potential therapeutic for AD prevention, treatment and diagnostic.

2. Curcumin and its potential in Alzheimer's Disease

Curcumin is a natural product found in turmeric (*Curcuma longa*), a spice herb member of the ginger family (*Zingiberaceae*). Its chemical name is 1,7-bis[4-hydroxy-3-methoxyphenyl]-1,6heptadiene-3,5-dione, also named

diferuloylmethane, and it constitutes the 2-5% of the turmeric root. Dried turmeric root was a traditional remedy of Chinese medicine and Ayurvedic Indian medicine since ancient times; it was used in the treatment of different pathologies such as skin diseases, wounds, rheumatism, asthma, allergies, sinusitis, hepatic disorders, intestinal worms, generic inflammation and oxidative stress conditions [11]. Commercially available curcumin is a combination of three molecules, together called curcuminoids. Curcumin is the most representative (60-70%), followed by demethoxycurcumin (DMC, 20-27%) and bisdemethoxycurcumin (BDMC, 10-15%). Curcuminoids differ in potency and efficacy, with no clear supremacy of curcumin over the other two compounds or the whole mixture, thus suggesting that DMC and BDMC significantly contributed to the curcuminoid mixture effectiveness, that is not only due to curcumin. This concept is well reviewed by Ahmed and Gilani [12] in the context of Alzheimer's disease. The authors listed numerous papers that have demonstrated the neuroprotective potential of curcuminoids *in vitro* and *in vivo*, suggesting that curcuminoids act through multiple mechanisms as a mixture, but the contribution of the single components is distinct for activity and potency. For example, curcumin is more effective in inhibiting acetylcholinesterase activity [13], in protecting PC12 cells and HUVEC cells against A β [14,15], whereas DMC and BDMC have a stronger antioxidant activity measured with the DPPH (1,1-diphenyl-2-picrylhydrazyl) assay [15] and a higher IC₅₀ in the inhibition of A β 1-42 fibrillogenesis [16].

Concerning the potential effects of curcumin, in particular in AD, it can prevent AD development thanks to its anti-inflammatory [17-21] and antioxidant properties [22-24]. *In vitro* studies have shown that curcumin can bind A β , thus influencing the peptide aggregation and inhibiting fibril formation and elongation [25]. Moreover, curcumin can enhance A β cellular uptake [26] avoiding plaques deposition and preventing cellular insults induced by the peptide [16] and it can also downregulate A β production through BACE1 (beta-site APP-cleaving enzyme) expression [27]. *In vivo*, curcumin is able to rescue the distorted neuritic morphology near A β plaques [28], to decrease A serum level as well as A burden in the brain, especially in the neocortex and in the hippocampus, and to attenuate inflammation and microglia activation in AD mouse models [29]. Furthermore, curcumin can

modulate tau protein processing and phosphorylation avoiding NFTs formation (recently reviewed by [30,31]) (**Fig. 1**).

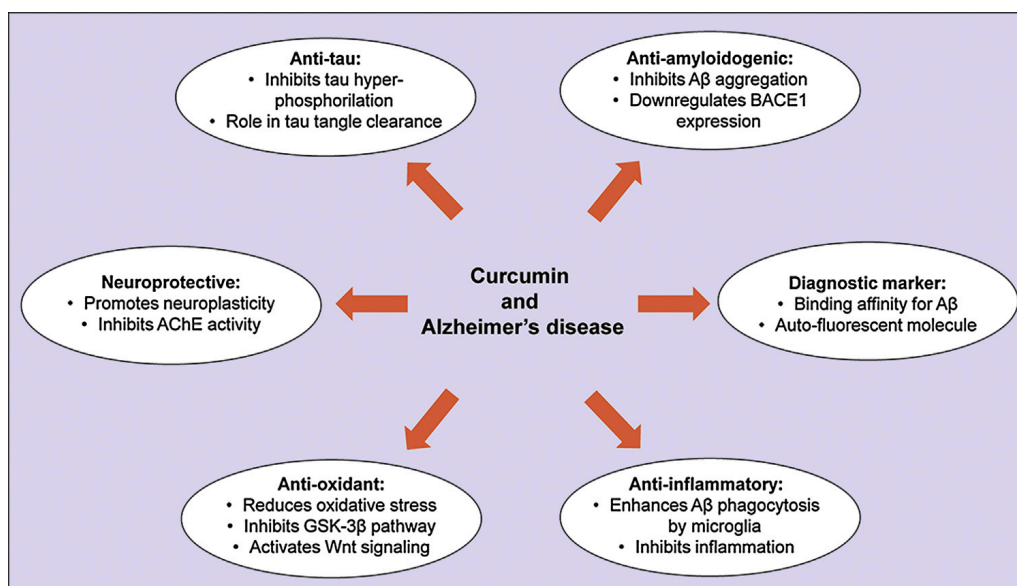


Fig. 1. Curcumin activities in Alzheimer's disease. Mechanisms of action of curcumin related to Alzheimer's disease pathological features. Figures have been done following the guidelines reported in [102].

Interestingly, curcumin has been shown to have a potential in the diagnostic field. Thanks to its fluorescent properties and A β -binding ability, curcumin has been also suggested as a detection agent for the early diagnosis of plaques deposition in the brain [32].

These findings were very promising; however, despite curcumin has a very safe nutraceutical profile with low side-effects and it has been reported to be well tolerated at doses up to 8 g per day in humans, the attempts to use curcumin in a therapeutic field were discouraging because the translation of these studies in clinical trials was not very successful [33]. Moreover, doubts about curcumin potential therapeutic use have recently raised because its classification as a PAINS (pan-assay interference compounds) candidate. PAINS are compounds that show activity in multiple assay, not through a specific interaction with the target, but by interfering with the assay readout.

Curcumin has numerous PAINS-type characteristics such as redox activity, metal chelation properties, auto-fluorescence and covalent protein labeling [34]. For this reason, results obtained with methods that can involve PAINS-like behaviors, need to be verified with other techniques to be confirmed. The classification of curcumin as a PAINS candidate is a very recent issue, and published data regarding the bioactivity of curcumin have to be read with a critical view. The limitations in the use of curcumin as therapeutic are represented by its pharmacokinetics profile. Curcumin is nearly insoluble in water, has a short half-life and a low bioavailability [35]. After oral administration it is rapidly metabolized by conjugation, sulfation and glucuronidation in the intestinal wall and in the liver and then excreted in feces. Moreover, it is chemically instable at neutral physiological pH and photodegradable, making its handling complicated and restricting its applications.

In addition to curcumin limitations, also the patient recruitment for clinical trial is challenging. AD is a multiple-stages pathology with different pathological markers, clinical features, and a final diagnosis only *post-mortem*. The patient recruitment is often based on the score in MMSE (Mini-Mental State Examination) that correlates with the severity of dementia, allowing the classification in no cognitive impairment, mild cognitive impairment and severe cognitive impairment. This classification correlates only partially with the pathological hallmarks observed in the brain, thus indicating that the sample of the patient are heterogeneous and not homogeneous as expected. To overcome these pharmaceutical issues related to curcumin pharmacokinetics and to improve therapeutic efficacy, new strategies have been applied and have been deepened in this review: new formulations, a change in the way of administration, alternative drug delivery taking advantage from the development of nanotechnology-based delivery systems, such as nanoparticles, liposomes and hydrogels and, finally, the hybridization approach.

3. Alternative formulation for curcumin

Considering the not significant results of the numerous clinical trials on humans [33,34], the oral administration of curcumin is not recommended. For these reasons alternative formulations have been tested *in vitro* and *in vivo*, with the final goal of optimizing curcumin absorption and efficacy.

The first approach for an alternative formulation was based on the combination of curcumin with other natural products as adjuvants. Piperine (1-piperoylpiperidine), an alkaloid extracted from black pepper fruits (*Piper nigrum*) and present also in long pepper (*Piper longum*) and other piper species (*Piperaceae*), was known for its ability to enhance the bioavailability of numerous drugs and phytochemicals thanks to its inhibition of uridine 5'-diphospho-glucuronosyltransferase (UDP-glucuronosyltransferase) [36]. In the context of AD, it was demonstrated, *in vivo*, that piperine significantly improved spatial memory because of its cytoprotective effect and the inhibition of AChE in hippocampus [37]. Moreover, piperine was combined with other nutraceuticals such as curcumin, epigallocatechin gallate, α -lipoic acid, N-acetylcysteine, B vitamins, vitamin C, and folate in a medical food cocktail that was administered for 6 months to the Tg2576 mouse model of AD. At the end of the treatment, the transgenic mice showed improved cortical- and hippocampal-dependent learning and their performance was indistinguishable from the non-transgenic control mice [38].

Basing on these already known properties of piperine, Suresh and Srinivasan orally administered 500 mg curcumin, 170 mg piperine or a combination of the two in a single formulation to Wistar male albino rats. Interestingly, they found that curcumin stayed significantly longer in the body tissues when administered concomitant with piperine; moreover, curcumin has been detected in the brain up to 96 h after the treatment [39].

Curcumin is only one of a multitude of compounds extracted from turmeric rhizome and the debate about the bioactivity of every single molecule is still open. It has been suggested that among the numerous non-curcuminoid components of turmeric, there are some, which could increase curcumin

absorption and bioavailability. Taking advantage of the synergism between these sesquiterpenoids naturally present in turmeric and the curcuminoids, Jäger and colleagues compared a combination of curcuminoids and volatile oils of turmeric rhizome (CTR), a curcumin inclusion in a lipophilic matrix composed by curcumin, soylécithin and microcrystalline cellulose 1:2:2 (CP), standard curcumin (CS) and a water soluble formulation of turmeric extract, hydrophilic carrier, cellulosic derivatives and natural antioxidants (CHC). All these formulations, with exception of CHC, were previously found to increase curcumin absorption with different potency [40,41]. After a single oral administered dose of 376 mg CP, CTR or CHC, or 1800 mg CS in human healthy volunteers, a 45.9-fold increase in CHC relative absorption compared to CS was observed, with a non statistically significant change of CTR (vs CS) and a weak increase of CP (vs CS) [42]. Thus, the volatile oils naturally occurring in turmeric rhizome are not increasing curcumin absorption, while the antioxidants tocopherol and ascorbyl palmitate combined with the polyvinyl pyrrolidone water-soluble carrier in the CHC formulation significantly improved it. This study suggests that the presence of a carrier is essential for ameliorating curcumin absorption and distribution. To further investigate the importance of an adequate profile for curcumin pharmacokinetics, a clinical study on human healthy volunteers was carried out with a patented formulation named BCM-95 CG (Biocurcumax™) in comparison with a combination of curcumin-lecithin-piperine, which was previously demonstrated to enhance curcumin bioavailability, and normal curcumin. BCM-95 CG is a formulation generated by micronizing curcumin and adding turmeric rhizome essential oils. The absorption of BCM-95 CG was faster than curcumin and curcumin-lecithin-piperine; moreover, it remained longer in the blood because of a lower elimination rate constant [40]. A more recent double-blind study compared the previous described Biocurcumax™ with other two commercial formulations: Meriva, curcumin complex with phosphatidylcholine from soy lecithin [41], and Theracurmin, curcumin dispersed with colloidal submicron particles [43]. In this study, the change of curcumin concentration in plasma, the maximum concentration and the bioavailability have been evaluated, indicating that Theracurmin possesses higher absorption efficiency in comparison with Meriva and BCM-95 CG curcumin commercial formulations [44].

4. Alternative drug delivery

In recent years, researchers have focused their attention in nanotechnology-based delivery systems because of their promising potential and advantages over the conventional approaches (**Fig. 2**).

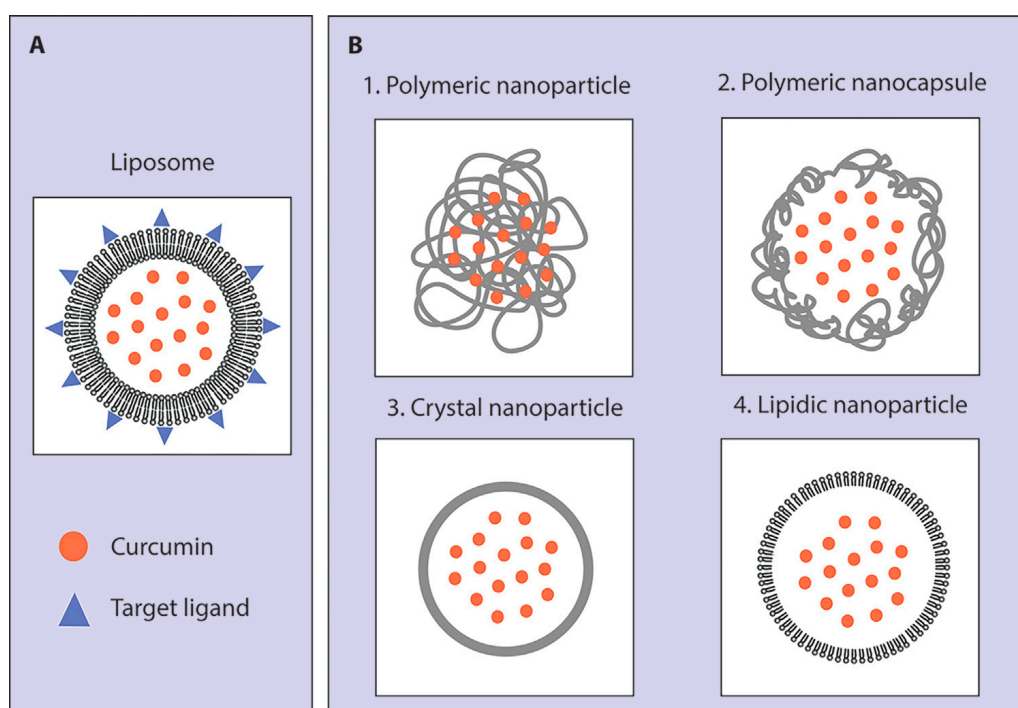


Fig. 2. Curcumin drug delivery. Examples of nanotechnology-based delivery systems. A) Liposomes entrapped with curcumin and decorated with molecules able to specifically target the brain; **B)** Different types of nanoparticles: 1. Polymeric nanoparticle; 2. Polymeric nanocapsule; 3. Crystal nanoparticle; 4. Lipidic nanoparticle. Figures have been done following the guidelines reported in [102].

The development of these systems could overcome the pharmaceutical issue related to curcumin delivery enhancing the dissolution rate, prolonging the residence in plasma, improving the pharmacokinetic profile and the cellular uptake. The ability of curcumin to penetrate organs and different brain regions has been shown to be affected by nanoparticulation. Curcumin-loaded PLGA nanoparticles (C-NPs) increased curcumin circulation time

when injected in the body of rats [45]. C-NPs were found mainly distributed in the spleen and the lung. Furthermore, C-NPs crossed the blood-brain barrier, thus prolonging retention time of curcumin in the cerebral cortex and hippocampus.

A system of PLGA (poly lactide-co-glycolide) nanoparticles encapsulated with curcumin (Nps-Cur) was studied by Doggui and colleagues *in vitro* using SK-N-SH human neuroblastoma cell line. Nps-Cur formulation has been shown to be stable up to six months, non-toxic to neurons and internalized by SK-N-SH cells due to their size of around 100 nm. Moreover, Nps-Cur can prevent ROS increase in dichlorofluorescein assay and protect cells against oxidative damage induced by a treatment with 500 μ M H₂O₂. Thus, PLGA-nanoparticles provide an efficient delivery system for encapsulated curcumin [46].

NanoCurc™ is a polymeric nanoparticle encapsulated curcumin formulation that has been developed to increase curcumin systemic bioavailability. It is soluble in aqueous media and readily administered parenterally by injection. This formulation showed to be protective *in vitro* in SK-N-SH differentiated cells against H₂O₂-induced oxidative stress. *In vivo* analysis demonstrated the presence of NanoCurc™ in the brain tissues of athymic mice and the ability of this formulation to downregulate the activity of caspase 3 and 7, critical mediators of the apoptotic pathway, in mice cortex. Moreover, after parenteral 25 mg/kg NanoCurc™ administration twice a day, in rodent brains a reduction in H₂O₂ content and an increase in the ratio of free *versus* oxidized glutathione [47] have been observed. These data suggest that this formulation could be promising also in AD, where oxidative stress and alterations in glutathione levels have been involved in the pathologic mechanism leading to the development of this type of dementia [48].

A novel lipopeptide composed by an aliphatic hydrophobic chain of palmitic acid, a microtubule stabilizing octapeptide and some hydrophilic residues, has been designed and synthesized by Ghosh's group [49]. This peptide spontaneously self-assembled in a β -sheet structure entrapping water molecule and forming a hydrogel with multiple functions. Furthermore, it slowly degrades releasing the neuroprotective octapeptide, and can be used

to encapsulate curcumin, being a delivery vehicle for hydrophobic and poor soluble drugs. Investigating the activity of the lipopeptide *in vitro* with Neuro-2a cells, Adak and colleagues found that it promotes neurite outgrowth in absence of external growth factors. Moreover, in PC-12 cells differentiated with nerve growth factor (NGF) and then treated with anti-NGF, a known inducer of A β overproduction and cell death, the hydrogel was able to ameliorate neural cell morphology and health, being neuroprotective [50]. These data are interesting since they suggest how a specific formulation may ameliorate the intrinsic properties of curcumin itself. Several and recent data of literature highlighted as curcumin may also have positive and very encouraging effects on neurogenesis and neuronal differentiation pathways, a very promising ability for incurable neurodegenerative and neuropsychiatric disorders that take a huge toll on society [51]. Curcumin has been related to hippocampal neurogenesis, since it can enhance neural plasticity and repair through the positive modulation of Wnt/beta-catenin pathway [52]. In addition, to overcome the problems related to pharmacokinetic limitations and improve the bioavailability of curcumin, the latter was encapsulated in polylactic-co-glycolic NPs (Cur PLGA NPs) to stimulate neural stem cells proliferation and neuronal differentiation *in vitro* and in adult rats [52]. The nanomaterials used in this paper have been demonstrated to ameliorate the availability of curcumin, since Cur PLGA NPs was effective at much lower doses *in vivo* in comparison of free curcumin that did not induce neurogenesis below a minimum threshold level. Moreover, curcumin can promote brain-derived neurotrophic factor (BDNF) release [53], and showed, only after a chronic administration, to ameliorate AD-related cognitive deficits (working and spatial reference memory) through an upregulation of BDNF-ERK signaling in the hippocampus of rats subjected to a ventricular injection of A β 1-42 [54]. In addition, curcumin has been recognized the potential as a DNA methyltransferase (DNMT) inhibitor, thus modulating DNA methylation patterns interfering with signaling pathways and transcriptional factors related to cell differentiation [55]. In this context, the effects of curcumin on neuronal differentiation and neurite outgrowth were investigated in the PC-12 Adh cell line alone and after NGF treatment [56]. The combination of curcumin and NGF has a more prominent effect on cell differentiation and neurite elongation than curcumin alone, with the

synergic effect related to the upregulation of GAP-43 and β -tubulin mRNA expression levels. These approaches suggest being corrective not only on curcumin, but also on other factors crucial for maintaining the integrity of neurons throughout an individual lifetime, such as NGF. There is growing evidence that an imbalance of neurotrophic support is significant in the pathogenesis of neurodegenerative diseases, but the implementation of neurotrophic factors is restricted by their poor penetration of the blood-brain barrier (BBB) and undesirable apoptotic effect.

As for NGF, the challenge of curcumin administration for brain disorders treatment is also represented by BBB penetration to reach the target organ. To achieve this goal, liposomes with cardiolipin (CL) and wheat germ agglutinin (WGA) carrying curcumin and NGF were developed and tested *in vitro* for their ability to permeate a monolayer of human brain-microvascular endothelial cells. Results were promising: WGA contributed to enhance the permeability of liposomes across the BBB and, at the same time, CL carried curcumin and NGF to A β fibrils inducing neuronal protection and apoptosis counteraction [57]. Mathew *et al.* adopted a different strategy to specifically target neurons and to reach the brain: they coupled curcumin-encapsulated PLGA-nanoparticles with Tet-1 peptide [58], which has affinity for neurons and retrograde transportation properties. Tet-1 is a 12 aminoacids peptide previously described by the groups of Boulis [58] and Pun [59]. This peptide possesses binding properties similar to the tetanus toxin, in fact it can specifically interact with motor neurons, being capable of retrograde delivery in neuronal cells. These peculiar characteristics of Tet-1 peptide were found interesting for an application in the drug delivery to the brain in the context of neurodegenerative diseases treatment. The study by Mathew *et al.* investigated the anti-amyloid and anti-oxidative properties mediated by the coupling of curcumin with PLGA-nanoparticles and Tet-1 peptide. This formulation slightly affected the free-radical scavenging activity of curcumin measured by DPPH assay becoming around 60% *versus* 80% of raw curcumin. On the contrary, anti-amyloid activity remained unchanged: Tet-1 conjugated PLGA-curcumin nanoparticles decreased the size of A β aggregates when co-incubated for 12, 24 or 48 h with a considerably reduction in plaques size [60].

Again, with the goal to specifically target the brain, Mulik and co-workers tested the possibility to use ApoE3 as a ligand for brain targeted delivery of curcumin [61]. Apolipoprotein E3 can form complexes with A β preventing its transport through the BBB, thus being neuroprotective. Furthermore, it can be taken up by the choroid plexus reaching the cerebrospinal fluid (CSF) by crossing the choroidal epithelium and enter brain parenchymal cells by low density lipoprotein receptor (LDL-R) mediated endocytosis, competing with A β [62]. Apolipoprotein E3-mediated poly(butyl)cyanoacrylate nanoparticles containing curcumin (ApoE3-C-PBCA NPs) have been formulated and have been shown to exhibit a protective role *in vitro* in SH-SY5Y cells against A β -induced cytotoxicity. This effect can be mainly ascribed to curcumin, whereasto ApoE3 to a lesser extent, because the control nanoparticles carrying ApoE, but without curcumin (ApoE-B-PBCA NPs), showed a slight protective effect. A similar result was obtained measuring the antioxidant and anti-apoptotic properties after A β treatment: ApoE3-C-PBCA NPs act counteracting oxidative stress and apoptosis with higher extent than ApoE-B-PBCA NPs [61].

Liposomes functionalized with a curcumin-alkyne derivative named TREG (described in [63]) can sequester A β 1-42 in human biological fluids from sporadic AD patients and Down syndrome subjects [64]. This interesting finding supports the idea that areduction in brain and plasma levels of A β 1-42 through the peripheral "sink effect" could be a useful therapeutic strategy. The same curcumin derivative was previously studied [65,66] for its ability to bind A β with high affinity, but only when the structure planarity was maintained. Moreover, different liposome formulations were tested and the more effective in A β inhibition of aggregation was the one with TREG molecules protruding from the liposome surface, rather than the one with TREG internalized in the bilayer. More recently, TREG liposomes were further functionalized with BBB-targeting ligands [67] to evaluate the co-presence of more ligands on their functionality. Interestingly, these multi-functional liposomes maintained their ability to bind A β and to inhibit its aggregation. In addition, they showed an increase in transport across monolayers suggesting the involvement of transporters for their translocation across the BBB [68]. The same liposomes were also injected intravenously in APP/PS1

mice for *in vivo* live animal imaging and *ex vivo* studies, and the results confirmed their high potential as theranostic (therapeutic and diagnostic) system for AD [69].

A functionalization strategy to specifically target A β , and inhibit its aggregation is the use of carriers conjugated with a combination of curcumin and specific antibodies. One example are the PEGylated biodegradable poly(alkyl cyanoacrylate) (PACA) nanoparticles (NPs) described by Le Droumaguet and co-workers. An anti-A β 1-42 antibody positioned at the PACA NPs surface showed a strong affinity towards A β 1-42 monomers and fibrils and curcumin functionalization offered a significant inhibition of A β aggregation [70].

In a context not specifically related to neurodegeneration and Alzheimer's disease, Storka *et al.* investigated safety and tolerability of Lipocurc™ in healthy humans. Lipocurc™ is a liposomal formulation of curcumin specifically developed for intravenous administration to overcome the bioavailability and pharmacokinetic limitations of the oral administration. A concentration of 6.9 mg/mL of curcumin was embedded into DMPC and DMPG liposomal membranes in a molar ratio of 9:1. The results of this study showed that a single intravenous infusion was well tolerated without symptoms or local reactions at doses up to 120 mg/m² and can be considered safe [71].

A change in the way of administration was further investigated by McClure and co-workers. In a very recent study they tested, in an animal model of Alzheimer's disease, the efficacy of aerosol delivered curcumin. The advantages of aerosolized drug administration are multiple: the absence of first-pass effect, the direct absorption via the olfactory epithelium, the absence of systemic delivery with the consequent limitation of systemic side effects and, important for targeting the brain, the ability to enter the central nervous system also for drugs incapable to permeate the BBB. 5XFAD mice treated with 5 mg/kg curcumin via aerosol showed improved cognitive functions, prevention of inflammation, reduction of plaque burden and dystrophic neurites [72].

5. Hybridation strategy for new efficient compounds

As for major chronic diseases, the pluralism of AD causes affords complex networks, suggesting that acting against a single pathogenic mechanism with high potency and selectivity might be insufficient to face the multifactorial nature of the disease [73]. The use of different drugs, as both drug cocktails or single pill drug combinations, represents the most simple and immediate way to modify AD phenotype by modulating simultaneously multiple nodes of the disease networks. Besides, a new polypharmacological approach has recently emerged, which proposes single chemical entities endowed with multiple biological activities as a promising strategy to obtaining potentially innovative medicines for multifactorial diseases. Interestingly, multitarget drugs offer the prospect of maintaining the positive outcomes of drug combinations, but with the benefits of a single-molecule therapy, as the issue of drug-drug interactions would be avoided, and the therapeutic regimen radically simplified [74].

Multitarget drugs can be rationally designed by linking, by means of suitable spacers, or fusing the key pharmacophoric functions, or through amalgamation of the pharmacophoric groups essential for activity into one hybrid molecule [75]. These strategies have led to the development of many multitarget neuroprotective agents, which are now tested as potential drug for Alzheimer's disease [76,77].

Because of its large spectrum of biological activities related to AD, curcumin represents a suitable starting point for multitarget drug design. Starting from this, many different curcumin analogues and hybrids have been synthesized and are now under testing phase.

5.1 Hybridation of curcumin and melatonin

Melatonin (N-acetyl-5-methoxytryptamine) is an indoleamine produced mainly in the pineal gland and plays a fundamental role in the regulation of circadian rhythms [78]. The decline in melatonin levels and the alteration of circadian rhythms during the aging contributes to the development of many

neurodegenerative disorders [79,80]. Searching for a new efficient compound as a potential AD-modifying agent, Chojnacki *et al.* developed various hybrids fusing curcumin and melatonin according to the hybrid molecule design strategy [81]. As the phenolic substitution pattern and the β -diketone moiety of curcumin have been demonstrated to be important for its antioxidant, anti-inflammatory, and metal-chelating properties [82] and, as the 5-methoxy group and the acetamide moiety of melatonin have been shown to be important for its antioxidant and free radical scavenging properties [83], the hybrid compounds were designed considering these structural features.

The neuroprotective activities of these compounds were evaluated in MC65 cells, a cellular AD model associated with A β - and oxidative stress-induced cellular toxicities, under tetracycline removal (-TC) conditions [84]. In this study, some compounds dose-dependently suppressed the production of A β -oligomers, but not the A β aggregation, counteracted the intracellular oxidative stress and significantly protected cells from induced toxicity. Neuroprotective activities of curcumin derivatives were strictly related to the hydroxy substituent on the phenyl ring, while the double bond and the conjugation system have been demonstrated to be not necessary. In addition, the ability of compounds to cross the BBB both *in vitro* and *in vivo* has also been evaluated, and one compound (**Table 1**, hybrid number 1) quickly and efficiently reached brain tissue after oral ingestion of a single daily dose. It has further been tested in a transgenic AD mice model showing an excellent bioavailability, thus encouraging further studies and optimizations for novel disease-modifying agents in AD [85].

5.2 Hybridation of curcumin and acetylcholinesterase inhibitors

One of the most accredited theories on the pathogenesis of AD is the cholinergic hypothesis that has been successfully applied in clinic with the development of acetylcholinesterase (AChE) inhibitors. Tacrine has been the first drug with this profile to be used. In this context, hybrids have been synthesized combining the pharmacophore of curcumin in monoanionic form with that of tacrine with the aim of obtaining a single more efficient molecule [86]. The choice to use monoanionic curcumin is due to the fact that in this

form curcumin may chelate metal ions [87], and it is well known that the imbalance of metal ions, such as copper (Cu^{2+}) and iron (Fe^{2+}) in turn increases the production of ROS [88]. Curcumin-tacrine hybrids have been tested in PC12 cell lines, showing a potent inhibition of AChE typical of tacrine. Particularly, one compound (**Table 1**, hybrid number 2) has been shown to have a higher potency when compared with tacrine. The higher potency has been related to the β -diketone moiety of curcumin that made this hybrid more neuroprotective against H_2O_2 - or $\text{A}\beta_{1-42}$ -induced toxicity than curcumin alone, and showed a remarkable ions-chelating ability, suggesting a potential of the hybrid compound to halt ion-induced $\text{A}\beta$ aggregation.

Among the acetylcholinesterase inhibitors, donepezil is the most used to date in the clinical treatment of AD. Yan *et al.* fused the pharmacophores of curcumin and donepezil to obtain a series of derivatives expected to be inhibitors of AChE activity and $\text{A}\beta$ aggregation, metal chelators and antioxidants [89]. In this library of hybrids, one of the compounds (**Table 1**, hybrid number 3) turned out to be a potent AChE and $\text{A}\beta$ aggregation inhibitor fusing the qualities of the original single molecules. Furthermore, this molecule has also been able to cross the BBB, indicating a great permeability and encouraging further studies.

5.3 Hybridation of curcumin and steroids

The addition of heterocyclic rings to steroids has often led to a change of their physiological activity and the appearance of new interesting pharmacological and biological properties [90]. On this basis, Elmegeed and co-workers synthesized novel curcumin hybrids fusing a promising steroidal heterocyclic nucleus to the essential phenolic feature of curcumin, one of which is shown in **Table 1** (hybrid number 4) [91]. When tested in an AD rat model, the hybrids showed to enhance acetylcholine synthesis and increase the levels of glutathione and paraoxenase, a protein with anti-inflammatory and anti-oxidative properties. Notably, conjugation of curcumin with cholesterol was previously exploited to direct the antioxidant and antiaggregating efficacy of the polyphenolic feature to cell membrane/lipid rafts, using cholesterol as the anchor motif [92,93]. As for other curcumin congeners [94,95], targeting of

antioxidant features to the main sites of ROS production through derivatization strategies was herein envisioned as a promising therapeutic approach.

5.4 Hybridation of curcumin and diallyl sulfide from garlic

The idea to synthesize new other hybrids raised by the knowledge that hydroxycinnamoyl recurring motif, present in curcumin, has been shown to modulate several pathways related to aging and dementia [96,97]. Simoni *et al.* [98,99] synthesized a set of new hybrids, by combining a hydroxycinnamoyl function from curcumin and diallyl sulfides from garlic. In addition, diallyl sulfides, garlic-derived organosulfur compounds carrying allyl mercaptan moieties, are able to counteract oxidative stress through antioxidant enzyme expression [100]. A catechol derivative with remarkable anti-aggregating ability and antioxidant properties (**Table 1**, hybrid number 5) has been initially identified. The characterization of the anti-aggregating and antioxidant profile of this new nature-inspired compound demonstrated that the activation of the Keap1-Nrf2 system is essential for counteracting oxidative stress and A β -induced toxicity [99]. This evidence suggests that this novel design strategy is an efficient and promising approach that, in the near future, could lead to the development of new efficient molecules to counteract multifactorial diseases like AD.

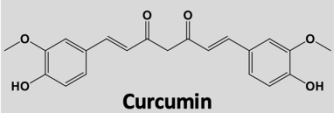
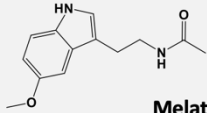
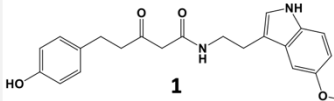
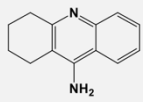
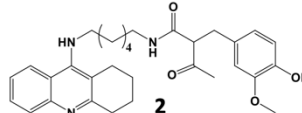
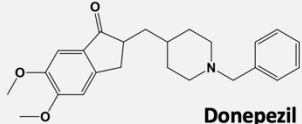
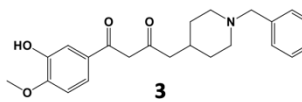
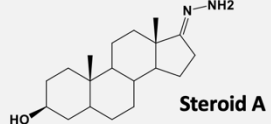
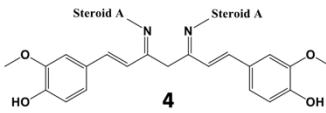
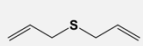
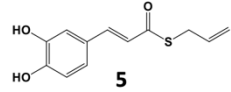
DRUG A	DRUG B	HYBRID COMPOUND
 <p>Curcumin</p>	 <p>Melatonin</p>	 <p>1</p>
	 <p>Tacrine</p>	 <p>2</p>
	 <p>Donepezil</p>	 <p>3</p>
	 <p>Steroid A</p>	 <p>4</p>
	 <p>Diallylsulfide</p>	 <p>5</p>

Table 1. Hybrids synthesis. Examples of different hybrid compounds from the combination of curcumin (drug A column) and other molecules (drug B column).

6. Conclusions

Curcumin is a minor constituent of the traditional medicine known as spice turmeric. Many scientific papers have been published on curcumin in different clinical fields ranging from cancer, neurodegenerative diseases, such as Alzheimer's disease, erectile dysfunction, hirsutism, to make some examples. These reported activities led to consider curcumin as a panacea. However, many limitations have been recognized for a therapeutic use of

curcumin: its poor pharmacokinetic/pharmacodynamic properties, its chemical instability, its low efficacy in different *in vitro* and *in vivo* disease models, its toxic profile under certain experimental settings [101], and very recently its PAINS character [34]. New formulations, changes in the way of administration, the direct delivery to the brain taking advantage from the development of nanotechnology-based delivery systems and the hybridization approach can overcome the critical pharmaceutical issues linked to curcumin pharmacokinetics improving therapeutic efficacy and giving new hopes for a clinical application of this natural compound. These approaches, besides possibly leading to new promising chemical entities, however, need further validation through expensive preclinical work to be approved for clinical trials.

REFERENCES

- [1] Alzheimer's Association. Alzheimer's disease facts and figures *Alzheimers Dement* 12 (Apr (4)) (2016) 459-509.
- [2] D.M. Walsh, D.J. Selkoe, Deciphering the molecular basis of memory failure in Alzheimer's disease, *Neuron* 44 (Sep (1)) (2004) 181-193, <http://dx.doi.org/10.1016/j.neuron.2004.09.010>.
- [3] J.L. Cummings, Treatment of Alzheimer's disease: current and future therapeutic approaches, *Rev. Neurol. Dis.* 1 (2) (2004 Spring) 60-69.
- [4] L.S. Schneider, F. Mangialasche, N. Andreasen, H. Feldman, E. Giacobini, R. Jones, V. Mantua, P. Mecocci, L. Pani, B. Winblad, M. Kivipelto, Clinical trials and late-stage drug development for Alzheimer's disease: an appraisal from 1984 to 2014, *J. Intern. Med.* 275 (Mar (3)) (2014) 251-283, <http://dx.doi.org/10.1111/joim.12191>.
- [5] K.S. Kim, H.S. Kim, J.M. Park, H.W. Kim, M.K. Park, H.S. Lee, D.S. Lim, T.H. Lee, M. Chopp, J. Moon, Long-term immunomodulatory effect of amniotic stem cells in an Alzheimer's disease model, *Neurobiol. Aging* 34 (Oct (10)) (2013) 2408-2420, <http://dx.doi.org/10.1016/j.neurobiolaging.2013.03.029>.
- [6] T. Wisniewski, A. Boutajangout, Immunotherapeutic approaches for Alzheimer's disease in transgenic mouse models, *Brain Struct. Funct.* 214(Mar 2-3) (2010) 201-218, <http://dx.doi.org/10.1007/s00429-009-0236-2>.
- [7] T. Wisniewski, F. Goñi, Immunotherapeutic approaches for Alzheimer's disease, *Neuron* 85 (Mar (6)) (2015) 1162-1176, <http://dx.doi.org/10.1016/j.neuron.2014.12.064>.

-
- [8] S. Jiang, J. Han, T. Li, Z. Xin, Z. Ma, W. Di, W. Hu, B. Gong, S. Di, D. Wang, Y. Yang, Curcumin as a potential protective compound against cardiac diseases, *Pharmacol. Res.* 119 (May) (2017) 373–383, <http://dx.doi.org/10.1016/j.phrs.2017.03.001>.
- [9] D. Lelli, A. Sahebkar, T.P. Johnston, C. Pedone, Curcumin use in pulmonary diseases: state of the art and future perspectives, *Pharmacol. Res.* 115 (Jan)(2017) 133–148, <http://dx.doi.org/10.1016/j.phrs.2016.11.017>.
- [10] M.C. Fadus, C. Lau, J. Bikhchandani, H.T. Lynch, Curcumin An age-old anti-inflammatory and anti-neoplastic agent, *J. Tradit. Complement. Med.* 7 (Sep (3)) (2016) 339–346, <http://dx.doi.org/10.1016/j.jtcme.2016.08.002>.
- [11] H.P. Ammon, M.A. Wahl, Pharmacology of curcuma longa, *Planta Med.* 57 (Feb (1))(1991) 1–7, <http://dx.doi.org/10.1055/s-2006-960004>.
- [12] T. Ahmed, A.H. Gilani, Therapeutic potential of turmeric in Alzheimer's disease: curcumin or curcuminoids? *Phytother. Res.* 28 (Apr (4)) (2014) 517–525, <http://dx.doi.org/10.1002/ptr.5030>.
- [13] T. Ahmed, A.H. Gilani, Inhibitory effect of curcuminoids on acetylcholinesterase activity and attenuation of scopolamine-induced amnesia may explain medicinal use of turmeric in Alzheimer's disease, *Pharmacol. Biochem. Behav.* 91 (Feb (4)) (2009) 554–559, <http://dx.doi.org/10.1016/j.pbb.2008.09.010>.
- [14] S.Y. Park, D.S. Kim, Discovery of natural products from *Curcuma longa* that protect cells from beta-amyloid insult: a drug discovery effort against Alzheimer's disease, *J. Nat. Prod.* 65 (Sep (9)) (2002) 1227–1231, <http://dx.doi.org/10.1021/np010039x>.
- [15] D.S. Kim, S.Y. Park, J.K. Kim, Curcuminoids from *Curcuma longa* L. (Zingiberaceae) that protect PC12 rat pheochromocytoma and normal human umbilical vein endothelial cells from beta-A (1–42) insult, *Neurosci. Lett.* 303 (Apr (1)) (2001) 57–61, [http://dx.doi.org/10.1016/S0304-3940\(01\)01677-9](http://dx.doi.org/10.1016/S0304-3940(01)01677-9).
- [16] H. Kim, B.S. Park, K.G. Lee, C.Y. Choi, S.S. Jang, Y.H. Kim, S.E. Lee, Effects of naturally occurring compounds on fibril formation and oxidative stress of beta-amyloid, *J. Agric. Food Chem.* 53 (Nov (2)) (2005) 8537–8541, <http://dx.doi.org/10.1021/jf051985c>.
- [17] X. Shi, Z. Zheng, J. Li, Z. Xiao, W. Qi, A. Zhang, Q. Wu, Y. Fang, Curcumin inhibits A β -induced microglial inflammatory responses *in vitro*: involvement of ERK1/2 and p38 signaling pathways, *Neurosci. Lett.* 6 (May (594)) (2015) 105–110, <http://dx.doi.org/10.1016/j.neulet.2015.03.045>.
- [18] A. Cianciulli, R. Calvello, C. Porro, T. Trotta, R. Salvatore, M.A. Panaro, PI3k/Akt signalling pathway plays a crucial role in the anti-inflammatory effects of curcumin in LPS-activated microglia, *Int. Immunopharmacol.* 36 (Jul) (2016) 282–290, <http://dx.doi.org/10.1016/j.intimp.2016.05.007>.
- [19] Z.J. Liu, Z.H. Li, L. Liu, W.X. Tang, Y. Wang, M.R. Dong, C. Xiao, Curcumin attenuates beta-Amyloid-Induced neuroinflammation via activation of peroxisome proliferator-Activated Receptor-Gamma function in a rat model of Alzheimer's disease, *Front. Pharmacol.* 19 (Aug (7)) (2016) 261, <http://dx.doi.org/10.3389/fphar.2016.00261>.
- [20] A. Sahebkar, A.F. Cicero, L.E. Simental-Mendía, B.B. Aggarwal, S.C. Gupta, Curcumin downregulates human tumor necrosis factor-alpha levels: a systematic review and meta-

- analysis of randomized controlled trials, *Pharmacol. Res.* 107 (May) (2016) 234-242, <http://dx.doi.org/10.1016/j.phrs.2016.03.026>.
- [21] G. Derosa, P. Maffioli, L.E. Simental-Mendía, S. Bo, A. Sahebkar, Effect of curcumin on circulating interleukin-6 concentrations: a systematic review and meta-analysis of randomized controlled trials, *Pharmacol. Res.* 111(Sep) (2016) 394-404, <http://dx.doi.org/10.1016/j.phrs.2016.07.004>.
- [22] L. Gibellini, E. Bianchini, S. De Biasi, M. Nasi, A. Cossarizza, Pinti M. natural compounds modulating mitochondrial functions, *Evid. Based Complement. Alternat. Med.* (2015), <http://dx.doi.org/10.1155/2015/527209>.
- [23] A.C. Uğuz, A. Öz, M. Nazıroğlu, Curcumin inhibits apoptosis by regulating intracellular calcium release, reactive oxygen species and mitochondrial depolarization levels in SH-SY5Y neuronal cells, *J. Recept. Signal Transduct. Res.* 36 (Aug (4)) (2016) 395-401, <http://dx.doi.org/10.3109/10799893.2015.1108337>.
- [24] C.D. Fan, Y. Li, X.T. Fu, Q.J. Wu, Y.J. Hou, M.F. Yang, J.Y. Sun, X.Y. Fu, Z.C. Zheng, B.L. Sun, Reversal of beta-Amyloid-Induced neurotoxicity in PC12Cells by curcumin, the important role of ROS-Mediated signaling and ERK pathway, *Cell. Mol. Neurobiol.* 37 (Mar 2) (2017) 211-222, <http://dx.doi.org/10.1007/s10571-016-0362-3>.
- [25] K. Ono, K. Hasegawa, H. Naiki, M. Yamada, Curcumin has potent anti-amyloidogenic effects for Alzheimer's beta-amyloid fibrils *in vitro*, *J. Neurosci. Res.* 75 (Mar (6)) (2004) 742-750, <http://dx.doi.org/10.1002/jnr.20025>.
- [26] L. Zhang, M. Fiala, J. Cashman, J. Sayre, A. Espinosa, M. Mahanian, J. Zaghi, V. Badmaev, M.C. Graves, G. Bernard, M. Rosenthal, Curcuminoids enhance amyloid-beta uptake by macrophages of Alzheimer's disease patients, *J. Alzheimers Dis.* 10 (1) (2006) 1-7, <http://dx.doi.org/10.3233/JAD-2006-10101>.
- [27] Y. Shimmyo, T. Kihara, A. Akaike, T. Niidome, H. Sugimoto, Epigallocatechin-3-gallate and curcumin suppress amyloid beta-induced beta-site APP cleaving enzyme-1 upregulation, *Neuroreport* 19 (Aug (13)) (2008) 1329-1333, <http://dx.doi.org/10.1097/wnr.0b013e32830b8ae1>.
- [28] M. Garcia-Alloza, L.A. Borrelli, A. Rozkalne, B.T. Hyman, B.J. Bacskai, Curcumin labels amyloid pathology *in vivo*, disrupts existing plaques, and partially restores distorted neurites in an Alzheimer mouse model, *J. Neurochem.* 102 (Aug (4)) (2007) 1095-1104, <http://dx.doi.org/10.1111/j.1471-4159.2007.04613>.
- [29] Y.J. Wang, P. Thomas, J.H. Zhong, F.F. Bi, S. Kosaraju, A. Pollard, M. Fenech, X.F. Zhou, Consumption of grape seed extract prevents amyloid-beta deposition and attenuates inflammation in brain of an Alzheimer's disease mouse, *Neurotox. Res.* 15 (Jan (1)) (2009) 3-14, <http://dx.doi.org/10.1007/s12640-009-9000-x>.
- [30] K.G. Goozee, T.M. Shah, H.R. Sahrabi, S.R. Rainey-Smith, B. Brown, G. Verdile, R.N. Martins, Examining the potential clinical value of curcumin in the prevention and diagnosis of Alzheimer's disease, *Br. J. Nutr.* 115 (Feb (3)) (2016) 449-465, <http://dx.doi.org/10.1017/S0007114515004687>.
- [31] M. Tang, C. Taghibiglou, The mechanisms of action of curcumin in alzheimer's disease, *J. Alzheimers Dis.* (May) (2017), <http://dx.doi.org/10.3233/JAD-170188>.

-
- [32] R. Patil, P.R. Gangalum, S. Wagner, J. Portilla-Arias, H. Ding, A. Rekechenetskiy, B. Konda, S. Inoue, K.L. Black, J.Y. Ljubimova, Holler E. Curcumin Targeted, Polymalic acid-Based MRI contrast agent for the detection of Abeta plaques in alzheimer's disease, *Macromol. Biosci.* 15 (Sep (9)) (2015) 1212-1217, <http://dx.doi.org/10.1002/mabi.201500062>.
- [33] N. Brondino, S. Re, A. Boldrini, A. Cuccomarino, N. Lanati, F. Barale, P. Politi, Curcumin as a therapeutic agent in dementia: a mini systematic review of human studies, *Sci. World J.* (Jan (22)) (2014) 174282, <http://dx.doi.org/10.1155/2014/174282>.
- [34] K.M. Nelson, J.L. Dahlin, J. Bisson, J. Graham, G.F. Pauli, M.A. Walters, The essential medicinal chemistry of curcumin, *J. Med. Chem.* 60 (Mar (5)) (2017) 1620-1637, <http://dx.doi.org/10.1021/acs.jmedchem.6b00975>.
- [35] P. Anand, A.B. Kunnumakkara, R.A. Newman, B.B. Aggarwal, Bioavailability of curcumin: problems and promises, *Mol. Pharm.* 4 (Nov-Dec (6)) (2007) 807-818, <http://dx.doi.org/10.1021/mp700113r>.
- [36] K. Srinivasan, Black pepper and its pungent principle-piperine: a review of diverse physiological effects, *Crit. Rev. Food Sci. Nutr.* 47 (8) (2007) 735-748, <http://dx.doi.org/10.1080/10408390601062054>.
- [37] P. Chonpathompikunlert, J. Wattanathorn, S. Muchimapura, Piperine, the main alkaloid of Thai black pepper, protects against neurodegeneration and cognitive impairment in animal model of cognitive deficit like condition of Alzheimer's disease, *Food Chem. Toxicol.* 48 (Mar (3)) (2010) 798-802, <http://dx.doi.org/10.1016/j.fct.2009.12.009>.
- [38] A. Parachikova, K.N. Green, C. Hendrix, F.M. La Ferla, Formulation of a medical food cocktail for Alzheimer's disease: beneficial effects on cognition and neuropathology in a mouse model of the disease, *PLoS One* 5 (Nov 11) (2010) e14015, <http://dx.doi.org/10.1371/journal.pone.0014015>.
- [39] D. Suresh, K. Srinivasan, Tissue distribution & elimination of capsaicin, piperine & curcumin following oral intake in rats, *Indian J. Med. Res.* 131(May) (2010) 682-691.
- [40] B. Antony, B. Merina, V.S. Iyer, N. Judy, K. Lennertz, S. Joyal, A pilot cross-Over study to evaluate human oral bioavailability of BCM-95CG (Biocurcumax), a novel bioenhanced preparation of curcumin, *Indian J. Pharm. Sci.* 70 (Jul-Aug (4)) (2008) 445-449, <http://dx.doi.org/10.4103/0250-474X.44591>.
- [41] J. Cuomo, G. Appendino, A.S. Dern, E. Schneider, T.P. McKinnon, M.J. Brown, S. Togni, B.M. Dixon, Comparative absorption of a standardized curcuminoid mixture and its lecithin formulation, *J. Nat. Prod.* 74 (Apr (4)) (2011) 664-669, <http://dx.doi.org/10.1021/np1007262>.
- [42] R. Jäger, R.P. Lowery, A.V. Calvanese, J.M. Joy, M. Purpura, J.M. Wilson, Comparative absorption of curcumin formulations, *Nutr. J.* 13 (Jan (11)) (2014), <http://dx.doi.org/10.1186/1475-2891-13-11>.
- [43] H. Sasaki, Y. Sunagawa, K. Takahashi, A. Imaizumi, H. Fukuda, T. Hashimoto, H. Wada, Y. Katanasaka, H. Takeya, M. Fujita, K. Hasegawa, T. Morimoto, Innovative preparation of curcumin for improved oral bioavailability, *Biol. Pharm. Bull.* 34 (5) (2011) 660-665, <http://dx.doi.org/10.1248/bpb.34.660>.

- [44] Y. Sunagawa, S. Hirano, Y. Katanasaka, Y. Miyazaki, M. Funamoto, N. Okamura, Y. Hojo, H. Suzuki, O. Doi, T. Yokoji, E. Morimoto, T. Takashi, H. Ozawa, A. Imaizumi, M. Ueno, H. Kakeya, A. Shimatsu, H. Wada, K. Hasegawa, T. Morimoto, Colloidal submicron-particle curcumin exhibits high absorption efficiency—a double-blind, 3-way crossover study, *J. Nutr. Sci. Vitaminol.* (Tokyo) 61 (1) (2015) 37–44, <http://dx.doi.org/10.3177/jnsv.61.37>.
- [45] Y.M. Tsai, C.F. Chien, L.C. Lin, T.H. Tsai, Curcumin and its nano-formulation: the kinetics of tissue distribution and blood-brain barrier penetration, *Int. J. Pharm.* 416 (Sep (1)) (2011) 331–338, <http://dx.doi.org/10.1016/j.ijpharm.2011.06.030>.
- [46] S. Doggui, J.K. Sahni, M. Arseneault, L. Dao, C. Ramassamy, Neuronal uptake and neuroprotective effect of curcumin-loaded PLGA nanoparticles on the human SK-N-SH cell line, *J. Alzheimers Dis.* 30 (2) (2012) 377–392, <http://dx.doi.org/10.3233/JAD-2012-112141>.
- [47] B. Ray, S. Bisht, A. Maitra, A. Maitra, D.K. Lahiri, Neuroprotective and neurorescue effects of a novel polymeric nanoparticle formulation of curcumin (NanoCurc™) in the neuronal cell culture and animal model: implications for Alzheimer's disease, *J. Alzheimers Dis.* 23 (1) (2011) 61–77, <http://dx.doi.org/10.3233/JAD-2010-101374>.
- [48] G.C. Chiang, X. Mao, G. Kang, E. Chang, S. Pandya, S. Vallabhajosula, R. Isaacson, L.D. Ravdin, Alzheimer's Disease Neuroimaging Initiative, D.C. Shungu, Relationships among cortical glutathione levels, brain amyloidosis, and memory in healthy older adults investigated *In vivo* with 1H-MRS and Pittsburgh compound-B PET, *AJNR Am. J. Neuroradiol.* 38 (Jun (6)) (2017) 1130–1137, <http://dx.doi.org/10.3174/ajnr.A5143>.
- [49] A. Biswas, P. Kurkute, B. Jana, A. Laskar, S. Ghosh, an amyloid inhibitor octapeptide forms amyloid type fibrous aggregates and affects microtubule motility, *Chem. Commun. (Camb)* 50 (Mar (20)) (2014) 2604–2607, <http://dx.doi.org/10.1039/c3cc49396b>.
- [50] A. Adak, G. Das, S. Barman, S. Mohapatra, D. Bhunia, B. Jana, S. Ghosh, Biodegradable neuro-Compatible peptide hydrogel promotes neurite outgrowth, shows significant neuroprotection, and delivers anti-Alzheimer drug, *ACS Appl. Mater. Interfaces* 9 (Feb (6)) (2017) 5067–5076, <http://dx.doi.org/10.1021/acsami.6b12114>.
- [51] E. Uliassi, A. Gandini, R.C. Perone, M.L. Bolognesi, Neuroregeneration versus neurodegeneration: toward a paradigm shift in Alzheimer's disease drug discovery, *Future Med. Chem.* 9 (Jun (10)) (2017) 995–1013, <http://dx.doi.org/10.4155/fmc-2017-0038>.
- [52] S.S.K. Tiwari, S. Agarwal, B. Seth, A. Yadav, S. Nair, P. Bhatnagar, *et al.*, Curcumin-loaded nanoparticles potently induce adult neurogenesis and reverse cognitive deficits in Alzheimer's disease model via canonical Wnt/b-catenin pathway, *ACS Nano* 8 (1) (2014) 76–103, <http://dx.doi.org/10.1021/nn405077y>.
- [53] D. Liu, Z. Wang, Z. Gao, K. Xie, Q. Zhang, H. Jiang, Q. Pang, Effects of curcumin on learning and memory deficits, BDNF, and ERK protein expression in rats exposed to chronic unpredictable stress, *Behav. Brain Res.* (2014) 116–121, <http://dx.doi.org/10.1016/j.bbr.2014.05.068> (271C).
- [54] L. Zhang, Y. Fang, Y. Xu, Y. Lian, N. Xie, T. Wu, H. Zhang, L. Sun, R. Zhang, Z. Wang, Curcumin improves amyloid (-Peptide (1–42) induced spatial memory deficits through

- BDNF-ERK signaling pathway, *PLoS One* 10 (Jun(6)) (2015) e0131525, <http://dx.doi.org/10.1371/journal.pone.0131525>.
- [55] G. Bora-Tatar, H. Erdem-Yurter, Investigations of curcumin and resveratrol on neurite outgrowth: perspectives on spinal muscular atrophy, *Biomed. Res. Int.* (2014), <http://dx.doi.org/10.1155/2014/709108>.
- [56] M. Dikmen, Comparison of the effects of curcumin and RG108 on NGF-Induced PC-12 adh cell differentiation and neurite outgrowth, *J. Med.Food* 20 (Apr (4)) (2017) 376-384, <http://dx.doi.org/10.1089/jmf.2016.3889>.
- [57] Y.C. Kuo, C.C. Lin, Rescuing apoptotic neurons in Alzheimer's disease using wheat germ agglutinin-conjugated and cardiolipin-conjugated liposomes with encapsulated nerve growth factor and curcumin, *Int. J. Nanomed.* 1(Apr (10)) (2015) 2653-2672, <http://dx.doi.org/10.2147/IJN.S79528>.
- [58] J.K. Liu, Q. Teng, M. Garrity-Moses, T. Federici, D. Tanase, M.J. Imperiale, N.M. Boulis, A novel peptide defined through phage display for therapeutic protein and vector neuronal targeting, *Neurobiol. Dis.* 19 (Aug (3)) (2005) 407-418, <http://dx.doi.org/10.1016/j.nbd.2005.01.022>.
- [59] I.K. Park, J. Lasiene, S.H. Chou, P.J. Horner, S.H. Pun, Neuron-specific delivery of nucleic acids mediated by Tet1-modified poly(ethylenimine), *J. GeneMed.* 9 (Aug (8)) (2007) 691-702, <http://dx.doi.org/10.1002/jgm.1062>.
- [60] A. Mathew, T. Fukuda, Y. Nagaoka, T. Hasumura, H. Morimoto, Y. Yoshida, T. Maekawa, K. Venugopal, D.S. Kumar, Curcumin loaded-PLGA nanoparticles conjugated with Tet-1 peptide for potential use in Alzheimer's disease, *PLoSOne* 7 (3) (2012), <http://dx.doi.org/10.1371/journal.pone.0032616>.
- [61] R.S. Mulik, J. Mönkkönen, R.O. Juvonen, K.R. Mahadik, A.R. Paradkar, ApoE3 mediated poly(butyl) cyanoacrylate nanoparticles containing curcumin: study of enhanced activity of curcumin against beta amyloid induced cytotoxicity using *in vitro* cell culture model, *Mol. Pharm.* 7 (Jun (3)) (2010) 815-825, <http://dx.doi.org/10.1021/mp900306x>.
- [62] C.L. Martel, J.B. Mackic, E. Matsubara, S. Governale, C. Miguel, W. Miao, J.G. McComb, B. Frangione, J. Ghiso, B.V. Zlokovic, Isoform-specific effects of apolipoproteins E2, E3, and E4 on cerebral capillary sequestration and blood-brain barrier transport of circulating Alzheimer's amyloid beta, *J. Neurochem.* 69 (Nov (5)) (1997) 1995-2004, <http://dx.doi.org/10.1046/j.1471-4159.1997.69051995.x>.
- [63] C. Airoidi, C. Zona, E. Sironi, L. Colombo, M. Messa, D. Aurilia, M. Gregori, M. Masserini, M. Salmona, F. Nicotra, B. La Ferla, Curcumin derivatives as new ligands of Aβ peptides, *J. Biotechnol.* 156 (Dec (4)) (2011) 317-324, <http://dx.doi.org/10.1016/j.jbiotec>.
- [64] E. Conti, M. Gregori, I. Radice, F. Da Re, D. Grana, F. Re, E. Salvati, M. Masserini, C. Ferrarese, C.P. Zoia, L. Tremolizzo, Multifunctional liposomes interact with Aβ in human biological fluids: therapeutic implications for Alzheimer's disease, *Neurochem. Int.* (Feb (24)) (2017), <http://dx.doi.org/10.1016/j.neuint.2017.02.012>.
- [65] M. Taylor, S. Moore, S. Mourtas, A. Niarakis, F. Re, C. Zona, B. La Ferla, F. Nicotra, M. Masserini, S.G. Antimisiaris, M. Gregori, D. Allsop, Effect of curcumin-associated and lipid

- ligand-functionalized nanoliposomes on aggregation of the Alzheimer's Abeta peptide, *Nanomedicine* 7 (Oct (5)) (2011) 541-550, <http://dx.doi.org/10.1016/j.nano.2011.06.015>.
- [66] S. Mourtas, M. Canovi, C. Zona, D. Aurilia, A. Niarakis, B. La Ferla, M. Salmona, F. Nicotra, M. Gobbi, S.G. Antimisiaris, Curcumin-decorated nanoliposomes with very high affinity for amyloid-beta 1-42 peptide, *Biomaterials* 32 (Feb (6)) (2011) 1635-1645, <http://dx.doi.org/10.1016/j.biomaterials.2010.10.027>.
- [67] E. Markoutsas, G. Pampalakis, A. Niarakis, I.A. Romero, B. Weksler, P.O. Couraud, S.G. Antimisiaris, Uptake and permeability studies of BBB-targeting immunoliposomes using the hCMEC/D3 cell line, *Eur. J. Pharm. Biopharm.* 77 (Feb (2)) (2011) 265-274, <http://dx.doi.org/10.1016/j.ejpb.2010.11.015>.
- [68] K. Papadia, E. Markoutsas, S. Mourtas, A.D. Giannou, B. La Ferla, F. Nicotra, M. Salmona, P. Klepetsanis, G.T. Stathopoulos, S.G. Antimisiaris, Multifunctional LUV liposomes decorated for BBB and amyloid targeting. A. *In vitro* proof-of-concept, *Eur. J. Pharm. Sci.* 101 (Apr) (2017) 140-148, <http://dx.doi.org/10.1016/j.ejps.2017.02.019>.
- [69] K. Papadia, A.D. Giannou, E. Markoutsas, C. Bigot, G. Vanhoute, S. Mourtas, A. Van der Linded, G.T. Stathopoulos, S.G. Antimisiaris, Multifunctional LUV liposomes decorated for BBB and amyloid targeting – B. *In vivo* brain targeting potential in wild-type and APP/PS1 mice, *Eur. J. Pharm. Sci.* 102 (May) (2017) 180-187, <http://dx.doi.org/10.1016/j.ejps.2017>.
- [70] B. Le Droumaguet, J. Nicolas, D. Brambilla, S. Mura, A. Maksimenko, L. De Kimpe, E. Salvati, C. Zona, C. Airoidi, M. Canovi, M. Gobbi, N. Magali, B. La Ferla, F. Nicotra, W. Schepers, O. Flores, M. Masserini, K. Andrieux, P. Couvreur, Versatile and efficient targeting using a single nanoparticulate platform: application to cancer and Alzheimer's disease, *ACS Nano* 6 (Jul (7)) (2012) 5866-5879, <http://dx.doi.org/10.1021/nn3004372>.
- [71] A. Storka, B. Vcelar, U. Klickovic, G. Gouya, S. Weisshaar, S. Aschauer, G. Bolger, L. Helson, M. Wolzt, Safety, tolerability and pharmacokinetics of liposomal curcumin in healthy humans, *Int. J. Clin. Pharmacol. Ther.* 53 (Jan (1)) (2015) 54-65, <http://dx.doi.org/10.5414/CP202076>.
- [72] R. McClure, H. Ong, V. Janve, S. Barton, M. Zhu, B. Li, M. Dawes, W.G. Jerome, A. Anderson, P. Massion, J.C. Gore, W. Pham, Aerosol delivery of curcumin reduced amyloid-beta deposition and improved cognitive performance in a transgenic model of Alzheimer's disease, *J. Alzheimers Dis.* 55 (2) (2017) 797-811, <http://dx.doi.org/10.3233/JAD-160289>.
- [73] M. Rosini, E. Simoni, R. Caporaso, A. Minarini, Multitarget strategies in Alzheimer's disease: benefits and challenges on the road to therapeutics, *Future Med. Chem.* 8 (Apr (6)) (2016) 697-711, <http://dx.doi.org/10.4155/fmc-2016-0003>.
- [74] M. Rosini, Polypharmacology: the rise of multitarget drugs over combination therapies, *Future Med. Chem.* 6 (Apr (5)) (2014) 485-487, <http://dx.doi.org/10.4155/fmc.14.25>.
- [75] G. Bottegioni, A.D. Favia, M. Recanatini, A. Cavalli, The role of fragment-based and computational methods in polypharmacology, *Drug Discov. Today* 17 (Jan (1-2)) (2012) 23-34, <http://dx.doi.org/10.1016/j.drudis.2011.08.002>.
- [76] O. Weinreb, T. Amit, O. Bar-Am, M.B. Youdim, Neuroprotective effects of multifaceted hybrid agents targeting MAO, cholinesterase, iron and (beta-amyloid in ageing and

- Alzheimer's disease, *Br. J. Pharmacol.* 173 (Jul (13)) (2016) 2080-2094, <http://dx.doi.org/10.1111/bph.13318>.
- [77] M. Rosini, E. Simoni, A. Minarini, C. Melchiorre, Multi-target design strategies in the context of Alzheimer's disease: acetylcholinesterase inhibition and NMDA receptor antagonism as the driving forces, *Neurochem. Res.* 39 (Oct (10)) (2014) 1914-1923, <http://dx.doi.org/10.1007/s11064-014-1250-1>.
- [78] P. Pévet, Melatonin and biological rhythms, *Biol. Signals Recept.* 9 (May-Aug (3-4)) (2000) 203-212 (14640).
- [79] J.N. Zhou, R.Y. Liu, W. Kamphorst, M.A. Hofman, D.F. Swaab, Early neuropathological Alzheimer's changes in aged individuals are accompanied by decreased cerebrospinal fluid melatonin levels, *J. Pineal Res.* 35 (Sep (2)) (2003) 125-130, <http://dx.doi.org/10.1034/j.1600-079X.2003.00065.x>.
- [80] C.F. Hatfield, J. Herbert, E.J. van Someren, J.R. Hodges, M.H. Hastings, Disrupted daily activity/rest cycles in relation to daily cortisol rhythms of home-dwelling patients with early Alzheimer's dementia, *Brain* 127 (May (Pt 5)) (2004) 1061-1074, <http://dx.doi.org/10.1093/brain/awh129>.
- [81] J.E. Chojnacki, K. Liu, X. Yan, S. Toldo, T. Selden, M. Estrada, M.I. Rodríguez-Franco, M.S. Halquist, D. Ye, S. Zhang, Discovery of 5-(4-hydroxyphenyl)-3-oxo-pentanoic acid [2-(5-methoxy-1H-indol-3-yl)-ethyl]-amide as a neuroprotectant for Alzheimer's disease by hybridization of curcumin and melatonin, *ACS Chem. Neurosci.* 20 (Aug (8)) (2014) 690-699, <http://dx.doi.org/10.1021/cn500081s>.
- [82] T. Esatbeyoglu, P. Huebbe, I.M. Ernst, D. Chin, A.E. Wagner, G. Rimbach, Curcumin? from molecule to biological function, *Angew. Chem. Int. Ed. Engl.* 22 (May (22)) (2012) 5308-5332, <http://dx.doi.org/10.1002/anie.201107724>.
- [83] S.A. Rosales-Corral, D. Acuña-Castroviejo, A. Coto-Montes, J.A. Boga, L.C. Manchester, L. Fuentes-Broto, A. Korkmaz, S. Ma, D.X. Tan, R.J. Reiter, Alzheimer's disease: pathological mechanisms and the beneficial role of melatonin, *J. Pineal Res.* 52 (Mar (2)) (2012) 167-202, <http://dx.doi.org/10.1111/j.1600-079X.2011.00937.x>.
- [84] B.L. Sopher, K. Fukuchi, T.J. Kavanagh, C.E. Furlong, G.M. Martin, Neurodegenerative mechanisms in Alzheimer disease. A role for oxidative damage in amyloid beta protein precursor-mediated cell death, *Mol. Chem. Neuropathol.* 29 (Oct-Dec (2-3)) (1996) 153-168.
- [85] G. Gerenu, K. Liu, J.E. Chojnacki, J.M. Saathoff, P. Martínez-Martín, G. Perry, X. Zhu, H.G. Lee, S. Zhang, Curcumin/melatonin hybrid 5-(4-hydroxy-phenyl)-3-oxo-pentanoic acid [2-(5-methoxy-1H-indol-3-yl)-ethyl]-amide ameliorates AD-like pathology in the APP/PS1 mouse model, *ACS Chem. Neurosci.* 6 (Aug (8)) (2015) 1393-1399, <http://dx.doi.org/10.1021/acschemneuro.5b00082>.
- [86] Z. Liu, L. Fang, H. Zhang, S. Gou, L. Chen, Design, synthesis and biological evaluation of multifunctional tacrine-curcumin hybrids as new cholinesterase inhibitors with metal ions-chelating and neuroprotective property, *Bioorg. Med. Chem.* 25 (Apr (8)) (2017) 2387-2398, <http://dx.doi.org/10.1016/j.bmc.2017.02.049>.

- [87] S. Banerjee, A.R. Chakravarty, Metal complexes of curcumin for cellular imaging, targeting, and photoinduced anticancer activity, *Acc. Chem. Res.* 48 (Jul (7)) (2015) 2075-2083, <http://dx.doi.org/10.1021/acs.accounts.5b00127>.
- [88] P. Zatta, D. Drago, S. Bolognin, S.L. Sensi, Alzheimer's disease, metal ions and metal homeostatic therapy, *Trends Pharmacol. Sci.* 30 (Jul (7)) (2009) 346-355, <http://dx.doi.org/10.1016/j.tips.2009.05.002>.
- [89] J. Yan, J. Hu, A. Liu, L. He, X. Li, H. Wei, Design, synthesis, and evaluation of multitarget-directed ligands against Alzheimer's disease based on the fusion of donepezil and curcumin, *Bioorg. Med. Chem.* 25 (Jun (12)) (2017) 2946-2955, <http://dx.doi.org/10.1016/j.bmc.2017.02.048>.
- [90] N.R. Mohamed, M.M. Abdelhalim, Y.A. Khadrawy, G.A. Elmegeed, O.M. Abdel-Salam, One-pot three-component synthesis of novel heterocyclic steroids as a central antioxidant and anti-inflammatory agents, *Steroids* 77 (Nov (13)) (2012) 1469-1476, <http://dx.doi.org/10.1016/j.steroids.2012.09.001>.
- [91] G.A. Elmegeed, H.H. Ahmed, M.A. Hashash, M.M. Abd-Elhalim, D.S. El-kady, Synthesis of novel steroidal curcumin derivatives as anti-Alzheimer's disease candidates: evidences-based on *in vivo* study, *Steroids* 101 (Sep) (2015) 78-89, <http://dx.doi.org/10.1016/j.steroids.2015.06.003>.
- [92] J.A. Lenhart, X. Ling, R. Gandhi, T.L. Guo, P.M. Gerk, D.H. Brunzell, S. Zhang, Clicked bivalent ligands containing curcumin and cholesterol as multifunctional abeta oligomerization inhibitors: design, synthesis, and biological characterization, *J. Med. Chem.* 53 (Aug (16)) (2010) 6198-6209, <http://dx.doi.org/10.1021/jm100601q>.
- [93] K. Liu, R. Gandhi, J. Chen, S. Zhang, Bivalent ligands targeting multiple pathological factors involved in Alzheimer's disease, *ACS Med. Chem. Lett.* 3 (Nov (11)) (2012) 942-946, <http://dx.doi.org/10.1021/ml300229y>.
- [94] E. Simoni, C. Bergamini, R. Fato, A. Tarozzi, S. Bains, R. Motterlini, A. Cavalli, M.L. Bolognesi, A. Minarini, P. Hrelia, G. Lenaz, M. Rosini, C. Melchiorre, Polyamine conjugation of curcumin analogues toward the discovery of mitochondria-directed neuroprotective agents, *J. Med. Chem.* 53 (Oct (19)) (2010) 7264-7268, <http://dx.doi.org/10.1021/jm100637k>.
- [95] E. Simoni, R. Caporaso, C. Bergamini, J. Fiori, R. Fato, P. Miszta, S. Filipek, F. Caraci, M.L. Giuffrida, V. Andrisano, A. Minarini, M. Bartolini, M. Rosini, Polyamine conjugation as a promising strategy to target amyloid aggregation in the framework of Alzheimer's disease, *ACS Med. Chem. Lett.* 7 (Sep (12)) (2016) 1145-1150, <http://dx.doi.org/10.1021/acsmchemlett.6b00339>.
- [96] C.B. Pocerlich, M.L. Lange, R. Sultana, D.A. Butterfield, Nutritional approaches to modulate oxidative stress in Alzheimer's disease, *Curr. Alzheimer Res.* 8 (Aug (5)) (2011) 452-469, <http://dx.doi.org/10.2174/156720511796391908>.
- [97] M. Stefani, S. Rigacci, Protein folding and aggregation into amyloid: the interference by natural phenolic compounds, *Int. J. Mol. Sci.* 14 (Jun (6)) (2013) 12411-12457, <http://dx.doi.org/10.3390/ijms140612411>.
- [98] E. Simoni, M.M. Serafini, M. Bartolini, R. Caporaso, A. Pinto, D. Necchi, J. Fiori, V. Andrisano, A. Minarini, C. Lanni, M. Rosini, Nature-Inspired multifunctional ligands:

-
- focusing on amyloid-Based molecular mechanisms of alzheimer's disease, *ChemMedChem* 11 (Jun (12)) (2016) 1309-1317, <http://dx.doi.org/10.1002/cmdc.201500422>.
- [99] E. Simoni, M.M. Serafini, R. Caporaso, C. Marchetti, M. Racchi, A. Minarini, M. Bartolini, C. Lanni, M. Rosini, Targeting the nrf2/Amyloid-Beta liaison in alzheimer's disease: a rational approach, *ACS Chem. Neurosci.* (Apr) (2017), <http://dx.doi.org/10.1021/acscemneuro.7b00100>.
- [100] S. Kim, H.G. Lee, S.A. Park, J.K. Kundu, Y.S. Keum, Y.N. Cha, H.K. Na, Y.J. Surh, Keap1 cysteine 288 as a potential target for diallyl trisulfide-induced Nrf2 activation, *PLoS One* 9 (Jan (1)) (2014) e85984, <http://dx.doi.org/10.1371/journal.pone.0085984>.
- [101] E. Burgos-Morón, J.M. Calderón-Montaño, J. Salvador, A. Robles, M. López-Lázaro, The dark side of curcumin, *Int. J. Cancer* 126 (Apr (7)) (2010) 1771-1775, <http://dx.doi.org/10.1002/ijc.24967>.
- [102] R. Roskoski Jr, Guidelines for preparing color figures for everyone including the colorblind, *Pharmacol. Res.* 119 (May) (2017) 240-241, <http://dx.doi.org/10.1016/j.phrs.2017.02.005>.

PART II

The following manuscript was published in *Molecules* in 2018 as:

Immunomodulators Inspired by Nature: A Review on Curcumin and Echinacea

Michele Catanzaro, Emanuela Corsini, Michela Rosini, Marco Racchi and Cristina Lanni



Abstract

The immune system is an efficient integrated network of cellular elements and chemicals developed to preserve the integrity of the organism against external insults and its correct functioning and balance are essential to avoid the occurrence of a great variety of disorders. To date, evidence from literature highlights an increase in immunological diseases and a great attention has been focused on the development of molecules able to modulate the immune response. There is an enormous global demand for new effective therapies and researchers are investigating new fields. One promising strategy is the use of herbal medicines as integrative, complementary and preventive therapy. The active components in medical plants have always been an important source of clinical therapeutics and the study of their molecular pharmacology is an enormous challenge since they offer a great chemical diversity with often multi-pharmacological activity. In this review, we mainly analysed the immunomodulatory/anti-inflammatory activity of *Echinacea* spp. and *Curcuma longa*, focusing on some issues of the phytochemical research and on new possible strategies to obtain novel agents to supplement the present therapies.

Keywords: immune system; immunomodulators; curcumin; curcumin analogues; Echinacea; signal transduction pathways.

Review

Immunomodulators Inspired by Nature: A Review on Curcumin and Echinacea

Michele Catanzaro ¹, Emanuela Corsini ^{2,*} , Michela Rosini ³, Marco Racchi ¹  and Cristina Lanni ¹

¹ Department of Drug Sciences—Pharmacology Section, University of Pavia, 27100 Pavia, Italy; michele.catanzaro01@universitadipavia.it (M.C.); racchi@unipv.it (M.R.); cristina.lanni@unipv.it (C.L.)

² Department of Environmental Science and Policy, University of Milano, 20133 Milano, Italy

³ Department of Pharmacy and Biotechnology, University of Bologna, 40126 Bologna, Italy; michela.rosini@unibo.it

* Correspondence: emanuela.corsini@unimi.it; Tel.: +39-02-50318241; Fax: +39-02-50318284

1. Immune System and Immunomodulators

In everyday life, humans are exposed to harmful pathogens and environmental pollutants that can affect the health status and homeostasis of the organism. The immune system (IS) is a complex integrated network of cells, tissues, organs and soluble mediators, evolved to defend the organism against any foreign insult that threatens the integrity of the organism. One of the key features of the IS is its capability to distinguish between the *self* (own cells and tissues) and the *non-self* (foreign molecules and microbes of the environment).

The IS involves many types of cells, tissues, and organs. In primary lymphoid organs, bone marrow and thymus, the immune cells are produced and mature; while in the secondary lymphoid organs, lymph nodes, spleen, tonsils and Peyer's patches in the small intestine, the immune cells circulate and reside during their lifetime. Phagocytic cells, which include monocytes, macrophages and neutrophils, are the most abundant cells of the IS. These cells are capable to engulf and digest pathogens and foreign molecules. Lymphocytes, the second most abundant cells of the IS, are important in the normal immune response to infection and tumors but also in mediating transplant rejection and auto-immunity [1]. They can be distinguished in two

different types, called T- and B-cells. All immune cells arise from common hematopoietic stem cells (HSCs) in the bone marrow following hematopoiesis. During the activation of an immune response, lymphocytes exponentially proliferate and differentiate: B-cells turn into plasma cells, a sort of antibody factories that release into the bloodstream thousands of antibodies, whereas T-cells differentiate into different subsets with different specialization [1].

The immune response is traditionally classified into *innate* and *adaptive* immunity covering different and specific roles in the immune defence responses. The innate immune system provides an imminent but incomplete defence against a foreign insult and it has not long-term memory [2]. This system includes phagocytic cells, the complement system and various classes of receptors utilized by innate cells, such as toll-like receptors (TLRs). These receptors are a member of pattern-recognition receptors family (PPPs) and able to detect conserved pathogens-associated molecular patterns (PAMPs), such as bacterial and fungal cell-wall components (i.e. lipopolysaccharides, bacterial lipopeptides and β -glucans) [3]. Although with some exceptions, TLRs and the other PPPs allow innate cells to discern self from non-self but lack of the capacity to discriminate among the non-self molecules. One exception is represented by TLR5 that seems to be able to respond differently to the flagellins of pathogenic and non-pathogenic bacteria [4]. The adaptive immune response is an antigen-specific system that includes long-lived lymphocytes (memory cells) and their highly specialized receptors [5].

The innate and adaptive systems are not strictly separated but work closely together in a fine-tuning machine. The innate system recognizes the infection and "alerts" the adaptive system through the antigen presentation, that occurs thanks the major histocompatibility complex (MHC) proteins. The innate cells release also other chemicals signals, such as cytokines and chemokines, to completely activate the adaptive system. Importantly, specialized B and T lymphocytes, known as regulatory cells, manage and stop the immune response once the insult has been counteracted, thus avoiding an excessive response of the IS [6,7].

Despite its high efficiency and specificity, the unbalance of immune responses can be responsible of a plethora of disorders, such as allergy, autoimmune diseases, immunosuppression and AIDS [8,9]. Nowadays, epidemiological data provide evidence of an increase in immunological diseases. This still-growing issue has led to the development of a particular class of molecules, overall called immunomodulators, able to enhance or suppress the immune response in IS-mediated diseases. Whereas immunostimulatory drugs have been developed for their potential applicability to infection, immunodeficiency, and cancer, immunosuppressive drugs are employed to inhibit the immune response in many immune-mediated diseases (i.e. in organ transplantation and autoimmune diseases). Within this context, new and innovative approaches are needed to develop more effective treatments, and nature may represent a source of inspiration.

2. Phytochemical Research

Scientific research of phytochemicals, the active components in medical plants, has always been an important source of clinical therapeutics by offering a great chemical diversity with often multi-pharmacological activity. Since ancient times, phytochemicals have been used in traditional medicine for their properties and health benefits [10]. Many of these natural products have pharmacological or biological activity that can be exploited in pharmaceutical drug discovery and drug design. As an example, polyphenols produced by plants as secondary metabolites are the most abundant antioxidants in the human diet. In the last years, a large number of studies demonstrated the beneficial health effects of their dietary contribution [11-13]. Some plant extracts have been proved to modulate the IS response and numerous phytochemicals, included not only polyphenols but also polysaccharides, flavonoids and alkaloids, have been studied for their immunomodulatory activities [14-18].

In this review, we focused on the immunomodulatory/antoinflammatory activity of Echinacea and turmeric, by analysing some issues of the

phytochemical research and, as consequence, new possible strategies to obtain novel agents to supplement the present therapies.

3. *Echinacea* sp.

Echinacea is a genus of nine herbaceous flowering plants in the daisy family (*Asteraceae*; *Compositae*), commonly called coneflowers, originating from eastern and central North America. *Echinacea* species, parts and preparations have different uses. In particular, three species of *Echinacea*, namely *E. purpurea*, *E. angustifolia* and *E. pallida*, have been used in Native Americans medicine for centuries as a treatment for respiratory tract infections and inflammatory conditions, including common cold, coughs, bronchitis, and inflammation of mouth and pharynx [19]. Fresh or dry herb, dried rhizome and roots, and alcoholic extracts are commercially available, often combined with ginseng, goldenseal, or garlic [20]. *Echinacea* preparations belong to the best-selling botanical drugs in the USA and Europe [21].

Inexpensive and effective natural immunomodulators could be of great value in medicine; however, lack of standardization to active ingredients, qualitative and quantitative changes in preparations, lack of rigorous test for efficacy, all contributes to inconsistencies in published results regarding immunomodulatory effects of herbal remedies. Several clinical trials have been carried out with *Echinacea* preparations and there is evidence of both therapeutic inefficacy and efficacy, depending on preparation and study design. *Echinacea* can be effective in reducing the duration and severity of cold symptoms, but this effect is noted only with certain preparations of *Echinacea*, mainly *E. purpurea* [19,22,23]. At this regards, interesting it is the study of Balan *et al.* [24], which comparing three different *E. purpurea*-based remedies commercially available, namely IMMUNAL drops (succus of *E. pupurea*), IMMUNAL FORTE tablets (*E. pupurea* herbae succus siccum) and ECHINACEA FORTE drops (juice squeezed from fresh flowers of *E. pupurea*), demonstrated important differences in the immunomodulatory effects

exerted by the remedies in female Balb/c mice, with stimulation (by IMMUNAL drops and ECHINACEA FORTE), inhibition (by IMMUNAL tablets and ECHINACEA FORTE) and no effects with ECHINACEA FORTE on antibody production or with IMMUNAL drops, depending on the product, highlighting how different preparations can have different modulatory effects.

Echinacea is best known as an immunostimulant, and there are a series of studies that support these immunomodulatory effects, with both increase in innate and specific immunity. However, anti-inflammatory activities are also reported [19,23,25], and anti-viral and anti-microbial effects have also been demonstrated, supporting its use in traditional medicine (see reviews [19,23,25]). This broad spectrum of action indicates that the plant contains in its parts, e.g. leaves, flowers, roots, different active ingredients and that depending on the preparation, e.g. water, alcoholic, oil extracts or dried forms, different compositions are obtained, which can explain its different effects. A thoroughly standardization and testing it is, therefore, critical prior to its use in various immune system malfunctions, as the phytochemical profiles of distinct Echinacea products are highly variable, depending on the harvested plant material, specie used, and extraction protocols.

The folk use of Echinacea is mainly meant to be therapeutic, not prophylactic, as in humans its benefits lies in its ability to shorten the duration and lessen the symptoms of illness, with a *post hoc* pooling of the available trial results suggesting a relative risk reduction of 10% to 20%, and not in its ability to prevent illness [19,21,26]. Rondanelli *et al.* [23] also suggested a prophylactic use of highly standardized Echinacea extracts, with a specific phytochemical profile (presence of the polysaccharide Polinacea™, the phenylethenoid echinacoside and substantial lack of alkamides), as a self-care for prevention of common cold and to improve the immune response to influence vaccination [23,27]. Authors suggest treatment over 4 months with 2400 mg/day for prophylactic use, and a dose of 4000 mg/day during acute stages of colds, as beneficial for preventing/treating cool [23].

Source	Model & Concentration	Effects	Ref.
In vitro studies			
Arabinogalactan	Isolated mice macrophages; 3.7–500 µg/mL	↑ Macrophages activation ↑ IL-1, TNF-α, IFN-β	[28]
<i>E. purpurea</i> extracts	Human Peripheral Blood Mononuclear Cells; ≥0.1 µg/mL	↑ NK function	[29]
<i>E. purpurea</i> extracts	Bone Marrow-derived Dendritic Cells; 400 mg/mL	↑ JNK ↑ p38 MAPK, NF-κB	[31]
<i>E. purpurea</i> extracts	Human Peripheral Blood Mononuclear Cells; ≥10 µg/mL	↑ DCs differentiation ↓ HLA-DR, CD32	[32]
<i>E. Purpurea</i> polysaccharide enriched extract	Bone Marrow-derived Dendritic Cells; 100 µg/mL	↑ Macrophages activation, CCR7 ↑ CD80, CD86, MHCII ↑ IL-1β, IL-6, IL-12p70, TNF-α, NO ↑ Phagocytosis and intracellular bactericidal activity	[33]
Alkylamides from <i>E. purpurea</i>	Human whole blood, 5 nM–5 µM	↑ Cannabinoid receptor type 2 ↓ TNF-α,	[38]
Alkylamides from <i>E. purpurea</i>	Human Peripheral Blood Mononuclear Cells; 10 µg/mL	↑ Cannabinoid receptor type 2 ↓ TNF-α, ↑ IL-10	[39]
Alkylamides from <i>E. purpurea</i>	Jurkat T cells, 330 ng/mL	↑ PPARγ	[40]
<i>E. Angustifolia</i> extract	Porcine leukocytes; 50 µM (for its major constituent)	↓ Cyclooxygenase, 5-lipoxygenase	[42]
<i>E. purpurea</i> extracts	Jurkat T cells, 10–250 µg/mL	↑ IL-2, IFNγ	[44]

Table 1. Main significant immunomodulatory and antiinflammatory effects of Echinacea in different *in vitro* studies.

Several modulatory effects on immune system have been demonstrated on both innate and acquired immunity (**Table 1**). Studies suggest that Echinacea stimulates immune functions in both healthy and immune suppressed animals [26]. In macrophages, phagocytosis and cytokine production (increased TNF-α, IL-1, IFN-β) have been enhanced following treatment with Echinacea extracts, increased leukocytes mobility as well as activation of natural killer cells has also been reasonably demonstrated in animals and humans [19,28–30]. *E. purpurea* polysaccharide enriched extracts can promote phenotypic and functional maturation of dendritic cells by modulation of JNK, p38 MAPK and NF-κB pathways [31,32] (**Figure 1**); and can favour M1 macrophage polarization by modulation of JNK pathway [33].

In the study of Wang *et al.* [32], dendritic cells treated for 24 h with whole plant, stem plus leaf, flower, and root extracts of *E. purpurea* displayed reduced levels of HLA-DR and CD32 expression in a dose-dependent manner compared to the control (untreated) cell samples, with whole plant and stem plus leaf extracts showing the greatest CD32 inhibition compared to the other preparations. These results suggest that whole plant and stem plus leaf extracts have the ability to inhibit dendritic cell maturation. In the study of Fu *et al.* [33], Echinacea extract (100 µg/mL) significantly activate murine bone-marrow derived macrophage by increasing the expression of CD80, CD86 and MHCII molecules, and by upregulating markers of classically activated macrophages (M1), including CCR7 and the production of IL-1 β , IL-6, IL-12p70, TNF- α and NO. In the same study, enhanced phagocytosis and intracellular bactericidal activity were observed [33]. Changes in the numbers and activities of T- and B-cell cells have also been described as well as enhanced host resistance, but data are less solid [24,28,30,34,35].

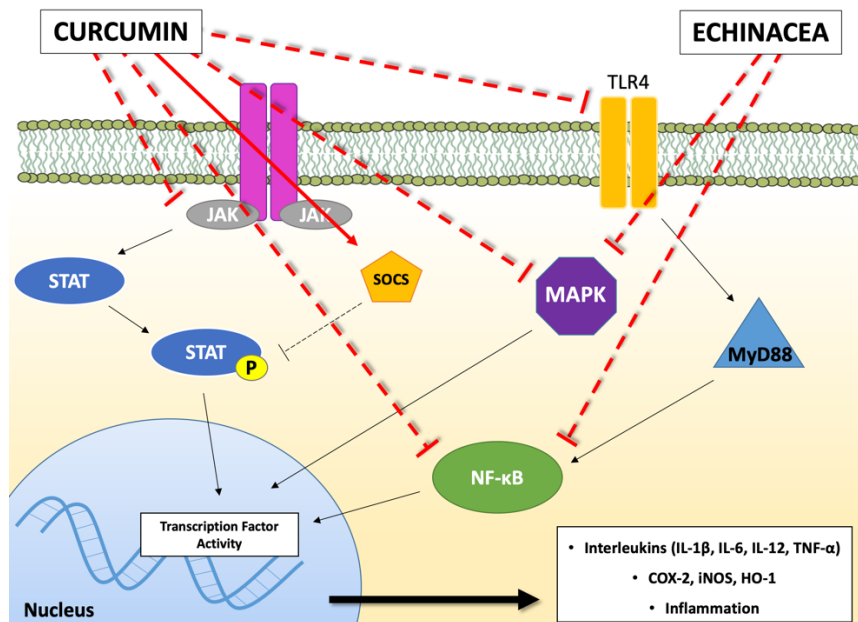


Figure 1. A schematic representation of the main molecular pathways linked to inflammatory and immunomodulatory activities modulated by Curcumin and Echinacea. The solid red line indicates the activation of the pathway, whereas the truncated red line

indicates inhibition of the pathway. JAK: Janus kinase; STAT: Signal Transducers and Activators of Transcription; SOCS: Suppressor of Cytokine Signalling proteins; TLR-4: Toll-like Receptor-4; MyD88: Myeloid Differentiation primary response 88; NF- κ B: Nuclear Factor kappa B; MAPK: Mitogen-Activated Protein Kinase; COX-2: cyclooxygenase-2; iNOS: inducible Nitric Oxide Synthase; HO-1: Heme Oxygenase-1; IL: Interleukin; TNF: Tumor Necrosis Factor.

Studying the molecular pharmacology of herbal medicines is an enormous challenge due to the fact that herbal extracts are multi-component drugs, working in concerted, with multileveled ways of actions [36]. Several bioactive phytochemicals have been identified [37]. Among its active ingredients, alkamides (e.g. dodeca-2E,4E,8Z,10Z-tetraenoic acid isobutylamide and dodeca- 2E,4E-dienoic acid isobutylamide), polyphenols (e.g. cihoric acid), and polysaccharides can be mentioned. The lipophilic fraction of *E. purpurea* tinctures consists of more than 15 different N-alkylamides. N-alkylamide lipids can activate the cannabinoid receptor type 2, with a K_i value of approximately 60 nM, and are supposed to have anti-inflammatory and immunomodulatory activities [38]. Ethanol extract of *E. purpurea* root and herbal extracts as well as N-alkylamide combinations have been shown to produce synergistic pharmacological effects on the endocannabinoid system *in vitro*, to affect calcium mobilization triggered by PMA, and peroxisome proliferator activated receptor-gamma [38-40], and alkylamides from *E. angustifolia* have been demonstrated to inhibit cyclooxygenase and 5-lipoxygenase *in vitro* [41,42]. In addition, while the expression of the anti-inflammatory cytokine IL-10 was significantly induced in human peripheral blood mononuclear cells, the expression of the pro-inflammatory cytokine TNF- α was inhibited [38,39]. Caffeic acid derivatives, including cihoric acid, cafteric acid, cynarin and chlorogenic acid are believed to be responsible for the wound-healing actions of *E. angustifolia* roots [43]. Besides alkamides, and phenolic compounds, the polysaccharide arabinogalactan (75 kDa) from *E. purpurea*, with a structure resembling bacteria lypopolisaccharide, has been identified as the main activators of macrophages [28]. While activating macrophages both *in vitro* and *in vivo*, this polysaccharide did not activate B, failed to induce T cells to produce IL-2, IFN- β or IFN- γ , and only caused a slight increase in T-cell proliferation [28]. In Jurkat T-cells, cultured at high density (5×10^6 /ml), treated with *E. purpurea* (10-250 μ g/ml), containing 80% polysaccharides,

predominantly a 10kDa entity; phenolic compounds, cynarin, cichoric and caftaric acids, but no detectable alkylamides, showed a strong dose-dependent enhancement of production of IL-2 and IFN- γ in response to PMA plus ionomycin was observed [44]. The extract alone had no effect. The high-molecular weight polysaccharides (30-100 kDa) purified by *E. angustifolia* have also been proposed as the anti-inflammatory principles of the plant in mice using the Croton oil ear test [41]. The root oil of *E. angustifolia*, containing 1,8-pentadecadiene, has been reported to inhibit tumor cell growth in mice and rats [45].

Different wide-spectrum bioactive components have been identified, which on the one hand indicate that Echinacea extracts have medical potential to be effective for the treatment and prevention of cold and other upper respiratory tract infections and possibly other diseases, on the other side, the inconsistent results published indicate that effective doses and preparations need to be clearly identified and standardized for a proper therapeutic or prophylactic use. Further studies are required to determine the immunological and pharmacologic potential of Echinacea preparations.

Regarding a possible long-term use Echinacea, this is still an open question, as its use in traditional medicine is therapeutic, not prophylactic, although some authors suggest a prophylactic use in wintertime [23], the consequences of long-term use (years) are unknown. Continuous ingestion of different Echinacea preparations up to 6 months did not showed toxicological concerns (see review by [46]), but possible consequences on longer time are unknown. Caution with immunostimulants is also warrant, as their use has been associated with development or exacerbation of autoimmunity in genetically predisposed individuals [47].

4. *Curcuma longa*

Turmeric (*Curcuma longa*), also known as "indian saffron" due to its brilliant yellow colour, is a spice herb, member of the ginger family (*Zingiberaceae*)

native to the Indian subcontinent and Southeast Asia, having more than a two centuries old scientific history [48]. The worldwide main producer of turmeric is India, which has been used as Ayurvedic remedy and flavouring agent since ancient times (more than 4000 years) [49].

Depending on its origin and the growth conditions, turmeric obtained from ground-dried root contains different percentages of volatile and non-volatile oils, proteins, fat, minerals, carbohydrates, curcuminoids and moisture. Commercially available curcumin is a combination of three molecules, together called curcuminoids. Curcumin is the most representative (60-70%), followed by demethoxycurcumin (20-27%) and bisdemethoxycurcumin (10-15%). Curcuminoids differ in potency, efficacy and stability, with no clear supremacy of curcumin over the other two compounds or the whole mixture [50]. Besides curcuminoids, the other active components of turmeric include sesquiterpenes, diterpenes, triterpenoids [51].

To date, many limitations have been recognized for a therapeutic use of curcumin: its poor pharmacokinetic/pharmacodynamic properties, its chemical instability, its low efficacy in different *in vitro* and *in vivo* disease models, its toxic profile under certain experimental settings [52], and the very recently suggestion that curcumin may be part of a series of molecules recognized for their interference with biological assays called PAINS (pan assay interference compounds) [53]. Different formulations, changes in the way of administration, the development of nanotechnology-based delivery systems have helped to overcome the critical pharmaceutical issues linked to curcumin pharmacokinetics improving therapeutic efficacy and giving new hopes for a clinical application of this natural compound [54]. Several preclinical and clinical data showing the effectiveness of curcumin in the prevention and treatment of various human diseases including cancer, cardiovascular, inflammatory, metabolic, neurological and skin diseases (reviewed in [55]). Among the different properties referred to curcumin, one of the most studied is the anti-inflammatory profile that may be useful in both acute and chronic inflammation. The immunomodulatory abilities of curcumin arise from its interaction with various immunomodulators, including not only cellular components, such as dendritic cells, macrophages, and both

B and T lymphocytes, but also molecular components involved in the inflammatory processes, such as cytokines and various transcription factors with their downstream signalling pathways [56] (**Table 2**).

Source	Model & Concentration	Effects	Ref.
In vitro studies			
Curcumin	Bone Marrow-derived Dendritic Cells; 25 μ M	↓ DC maturation ↓ CD80, CD86 ↓ IL-12, MAPK, NF- κ B	[57]
Curcumin	Bone Marrow-derived Dendritic Cells; 7.5 μ M	↑ STAT3	[63]
Curcumin	Murine macrophage; 10 μ M	↓ IL-6, TNF- α , PTGS-2 ↓ p38MAPK ↑ SOCS1, SOCS3	[67]
Curcumin	Myelogenous leukemia cells and human erythroleukemia cells; 20 μ M	↑ SOCS1, SOCS3 ↓ HDAC8	[68]
Curcumin	BV-2 microglia cells; ≥ 10 μ M	↓ NF- κ B, iNOS ↓ IL-6, TNF- α , IL-1 β	[72]
Curcumin	BV-2 microglia cells; ≥ 10 μ M	↓ iNOS, COX-2, HO-1 ↓ MAPK, NF- κ B ↓ TNF- α , NO, PGE-2	[73]
Curcumin	Microglial and cortical neurons co-cultures; 2 μ M	↓ TLR4, MyD88, NF- κ B	[76]
Curcumin	Human promonocytic cells; 30 μ M	↓ NF- κ B, caspase 3	[88]
α -Turmerone ar-Turmerone	Human Peripheral Blood Mononuclear Cells; 5–10 μ g/mL	↑ PBMC proliferation ↑ IL-2, TNF- α	[89]
Polar fraction of turmeric hot water extracts	Human Peripheral Blood Mononuclear Cells; 400 μ g/ μ L	↑ PBMC proliferation ↑ IL-6, TNF- α	[90]
In vivo studies			
Curcumin	Healthy rabbits; 2, 4 and 6 g/kg orally	↑ serum IgG, IgM	[58]
Curcumin	Mice with experimental colitis induced by dextran sulfate sodium (DSS); 50 mg/kg orally	↓ MPO, STAT3 ↓ IL-1 β , TNF- α	[62]
Curcumin	Mice with cyclophosphamide (CYP)-induced diabetes; 25 mg/kg intraperitoneally	↓ leucocyte infiltration ↓ NF- κ B, NO	[71]
Curcumin	Mice with traumatic brain injury; 100 mg/kg intraperitoneally	↑ activation of microglia/macrophages ↓ TLR4, MyD88, NF- κ B	[76]
Curcumin	Rats with traumatic spinal cord injury; 100 mg/kg intraperitoneally	↓ TNF- α , IL-1 β , IL-6 ↓ TLR4, NF- κ B	[77]
Curcumin	Rats with spinal cord injury; 6 mg/kg intraperitoneally	↓ MIP1 α , IL-2, RANTES ↓ NF- κ B	[78]
Curcumin	Mice with <i>K. pneumoniae</i> induced lung infection; 150 mg/kg orally	↓ leucocyte infiltration ↓ NO, MPO, TNF- α	[85,86]
Curcumin	Broilers with induced <i>Eimeria maxima</i> and <i>Eimeria tenella</i> infections; 35 mg/kg orally	↑ concanavalin A	[87]

Table 2. Main significant immunomodulatory and antiinflammatory effects of curcumin in different *in vitro* and *in vivo* studies.

Curcumin has been found to inhibit the immunostimulatory function of dendritic cells (DCs) and to interfere in the myeloid DC maturation. These effects have been related to the suppression of CD80 and CD86 expression, two co-working membrane proteins that provide stimulatory signal necessary for T cell activation, and the impairment in pro-inflammatory cytokine production (IL-12) due to inhibition of MAPK (Mitogen-Activated Protein Kinase) activation and NF- κ B (nuclear factor kappa B) translocation [57] (**Figure 1**). Furthermore, curcumin supplementation in rabbit diet (2, 4 and 6 g/kg) significantly increased serum levels of IgG and IgM, thus suggesting that curcumin can also improve immune functions [58].

The JAK/STAT (Janus kinase/signal transducers and activators of transcription) signalling is a signal transduction pathway directly involved in the cellular homeostasis and in the immune responses, modulating a wide array of cytokines and growth factors involved in cell proliferation, differentiation, cell migration and apoptosis [59]. *In vitro* concentrations of curcumin ranging from 20 to 50 μ M have been reported to inhibit STAT3 phosphorylation in multiple cell types [60,61]. This observation is consistent with data reported by Liu *et al.* on the capability of curcumin to modulate STAT3 pathway in a mice model with colitis induced by dextran sulfate sodium (DSS) [62]. A significant improvement in the disease activity index and histological injure score compared with control group has been observed following treatment with curcumin (50 mg/kg). Furthermore, also the myeloperoxidase activity (MPO), an index of leukocyte infiltration, and the phosphorylation of STAT3 resulted significantly reduced. Following the decreased DNA-binding activity of STAT3, also the expression of IL-1 β and TNF- α were significantly downregulated after treatment with curcumin [62]. More recently, low concentrations (7.5 μ M) of curcumin have been found to induce *in vitro* an anti-inflammatory profile in DCs enhancing the phosphorylation and the activity of STAT3, thus suggesting a biphasic effect of curcumin on STAT3 modulation depending on the range of curcumin concentrations [63]. This observation is quite intriguing and has been also observed when curcumin has been used together with opioids, the drugs of choice for the alleviation of acute and chronic pain and opioid tolerance. In particular, although curcumin seems to be relatively safe to use as a single

high dose orally [64], the effect of curcumin on morphine tolerance has been suggested to be biphasic and therefore should be used cautiously [65].

The JAK/STAT signalling pathway is antagonized by Suppressor of Cytokine Signaling proteins (SOCS) that is involved in the regulation of proinflammatory proteins and cytokines production [66]. Guimarães *et al.* demonstrated that curcumin potently inhibited lipopolysaccharide (LPS)-induced expression of IL-6, TNF- α and prostaglandin-endoperoxide synthase 2 mRNA in murine RAW 264.7 macrophages by preventing the inhibition of SOCS1 and 3 [67]. Curcumin further inhibited LPS-induced p38 MAPK activation by reducing both its phosphorylation and nuclear translocation pointing out the importance of this molecular pathway in inflammatory process [67] (**Figure 1**). These data are consistent with the ability of pure curcumin to increase the expression of SOCS1 and SOCS3 proteins in primary myeloproliferative neoplasms cells through suppressing class I histone deacetylases (especially HDAC8 activity) [68].

Beside JAK/STAT, another key molecular pathway involved in the inflammation is mediated by NF- κ B, a transcription factor regulating the inflammatory response and the immune system homeostasis. NF- κ B has been demonstrating to control the expression of inflammatory mediators such as COX-2, inducible nitric oxide synthase (iNOS) and interleukins and to regulate the expression of more 400 genes involved in inflammation and other chronic diseases [69]. In particular, the modulation of cytokine levels by curcumin has been related to the inhibition of NF- κ B signalling pathway [70]. In type 1 diabetes, a T cell-mediated autoimmune disease in which pancreatic β cells are destroyed by the IS, curcumin inhibited pancreatic leucocyte infiltration and preserve insulin-expressing cells [71]. These effects have been related to a reduced NF- κ B activation in T cell receptor (TCR)-stimulated NOD lymphocytes and to an impairment of the T cell stimulatory function of dendritic cells, thus leading to reduced secretion of proinflammatory cytokines and nitric oxide (NO) and antigen-presenting cell activity [71]. The involvement of NF- κ B and iNOS in anti-inflammatory curcumin effects has also been investigated by Cianciulli *et al.* [72] in BV-2 murine microglial cells, a specialised population of macrophages found in the central nervous system.

Curcumin significantly attenuated the LPS-induced release of NO and pro-inflammatory cytokines, as well as iNOS expression and NF- κ B activation [72]. These anti-inflammatory effects have been demonstrated to be mediated by iNOS, COX-2, HO-1, MAPK and NF- κ B [73], thus suggesting that curcumin plays an important role in the attenuation of inflammatory responses in the central nervous system by influencing microglial cells through modulation of NF- κ B activity. In particular, the induction of NF- κ B is dependent on the activation of TLR receptors. TLR4 is the most studied member of TLRs family and its crucial role in the regulation of immune system response has been well recognized, taking into account that TLR4 receptor agonists have been approved as vaccine adjuvants [74]. The activation of TLR4 recruits MyD88 (myeloid differentiation factor), thus resulting in the induction of NF- κ B [75]. The modulation of TLR4/MyD88/NF- κ B signalling pathway by curcumin has been demonstrated (**Figure 1**). Zhu *et al.* found that curcumin administration in mice following Traumatic Brain Injury (TBI) shown attenuated functional impairment, brain oedema and a reduced neuronal cell death with a general reduction in the activation of microglia/macrophages. In particular, curcumin normalized the LPS-induced upregulation of TLR4, MyD88 and NF- κ B both in C57BL/6 mice with an induced TBI *in vivo*, and in a co-culture system of microglia and neurons, *in vitro* [76]. Also in rats after spinal cord injury (SCI) curcumin decreased the release of proinflammatory cytokines TNF- α , IL-1 β , and IL-6 [77]. In particular, curcumin down-regulated TLR4 and NF- κ B inflammatory signalling pathway, thus ameliorating SCI-induced hind limb locomotion deficits, spinal cord oedema, and apoptosis [77]. Similar effects have been observed by Urdzikova *et al.* in a rat model of SCI, where curcumin, administrated both intraperitoneally and *in situ*, attenuated glial scar formation by decreasing the levels of MIP1 α , IL-2, and RANTES production and the NF- κ B activity [78]. MIP1 α (Macrophage Inflammatory Protein) and RANTES (Regulated on Activation, Normal T cell Expressed and Secreted) are two members of CC chemokine family also known as CCL3 and CCL5 respectively, involved in the inflammatory response and in the recruitment and activation of immune cells. The release of these (and other) chemokines it has been shown decreased by curcumin also in other different studies demonstrating the ability of these compound to modulate the chemotaxis process in the immune response [79,80].

The modulatory effects of curcumin on the TLR4/MyD88/NF- κ B signalling pathway have been reported not only in brain injury models but also in experimental colitis [81], in LPS-induced mastitis [82] and in *Helicobacter pylori*-induced gastritis [83], pointing out the importance of this pathway in the development of different diseases.

The anti-inflammatory effects of curcumin have been further used to enhance the efficacy of already approved antimicrobial agents through synergic effects [84]. Bansal *et al.* demonstrated that curcumin protected BALB/c mice from lung inflammation caused by *Klebsiella pneumoniae* [85]. In this study, mice that received orally curcumin alone or in combination with augmentin showed a significant decrease in neutrophil influx into the lungs and a significant decrease in the production of NO, MPO activity and TNF α levels [85]. Similar results have been obtained by combining curcumin and clarithromycin [86]. Kim *et al.* evaluated also the effects of a dietary supplementation with turmeric on systemic and local immune responses on experimental *Eimeria maxima* and *Eimeria tenella* infections in commercial broiler chickens [87]. Dietary supplementation with turmeric enhanced coccidiosis resistance in the chickens with enhanced systemic humoral immunity, as assessed by higher levels of serum antibodies to an *Eimeria* microneme protein, MIC2, and enhanced cellular immunity, as measured by concanavalin A-induced spleen cell proliferation [87]. The anti-inflammatory effects of curcumin have been tested also against *Mycobacterium tuberculosis* (MTB) infection in an *in vitro* human macrophage model and have been found to be partially mediated both by NF- κ B inhibition and caspase 3 activation [88].

Altogether these results underline that curcumin may modulate molecular pathways involved in the inflammation and in the immune response, thus suggesting its putative use as supplement therapy or nutritional approach.

Beyond curcumin, also other bioactive components of *Curcuma longa* have been investigated for their abilities to modulate the immune system. α -turmerone and ar-turmerone, two compounds isolated from the lipophilic fraction *Curcuma longa*, demonstrated to induce PBMC proliferation and

cytokine production [89]. The same effects were stimulated also by the polar fraction of turmeric hot water extracts [90]. Also other curcumin-free turmeric components, such as turmerin, elemene, furanodiene, curdione, bisacurone, cyclocurcumin, calebin A, and germacrone, have been found to exhibit different biological activities including anti-inflammatory and anticancer activity (for a review see [91]). These results suggest the potential use of whole *Curcuma longa* extract to enhance the IS activity in immunosuppressed patients.

5. Problematics and future perspectives

Nutraceuticals positively influence human health and include a variety of functional foods, fortified foods and dietary supplements (both herbal and not) [92] and their consumption amounts for approximately 20-25% of dietary supplements sales in the USA, pointing out their relevance on the market [93]. Herbal dietary supplements, mainly consisting of herbal extracts, are complex mixtures of phytochemicals that contain not only the principal active compound/s but also minor constituents that can enhance the pharmacological activity of the main active ingredient or lead to adverse effects. The chemical variability and the complexity of the herbal extracts makes the study of the pharmacological profile very difficult and this issue is exacerbated whether we consider that different preparations can have different pharmacological effects. One putative hypothesis for batch variability could be ascribed to additional factors that might interfere with the effects of the main active ingredient/s. The inadequate control of quality and standardization of productive processes represent a relevant problem related to the use of dietary supplements. In many studies conducted to determine the effect of natural extracts on immune system, no adequate microbial contamination control protocols have been applied even if it is recognized that microbial endotoxins can modify the parameters and the response of immune system [94]. As regarding the clinical use of curcumin, despite the multi-target activity and its safety at higher doses, one of the major limitations is due to its reduced bioavailability and its low solubility. Several

pharmacokinetics studies over the past decades related to absorption, distribution, metabolism and excretion of curcumin have confirmed its poor absorption and rapid metabolism that severely curtails its bioavailability [95].

To improve the pharmacokinetic profile of this molecule, alternative strategies have been adopted: new formulations, a change in the way of administration, alternative drug delivery taking advantage from the development of nanotechnology-based delivery systems, such as nanoparticles, liposomes and hydrogels and, finally, the hybridization approach [54, 95]. Kumari *et al.* derivatized curcumin and the lead compound derived, curcumin A, was able to decrease the cell cycle progression of T cells, indicating the anti-inflammatory activities of this new molecule [96]. Jantan *et al.* tested a series of 43 curcumin diarylpentanoid analogues evaluating their inhibitory effects on the chemotactic activity of phagocytes *in vitro*, and found that some of them inhibited the migration of human polymorphonuclear leukocytes, suggesting their potential for use as chemical leads for the development of new immunomodulatory agents [97].

Krishnakumar *et al.* investigated the bioavailability of a novel formulation of curcumin-impregnated soluble dietary fibre dispersions, which undergoes fermentation in the colon by the action of β -mannanase and may provide protection to curcumin from the degrading enzymes of the upper gastrointestinal tract [98]. This formulation, when orally administered, showed an improved bioavailability when compared to curcuminoids [98,99]. Recently, nanoformulations of curcumin are emerging as a novel substitute to increase aqueous solubility and bioavailability [100]. The entrapment in poly D,L-lactic-co-glycolic acid nanoparticles has been demonstrated to be suitable in the transportation of curcumin to target tissues through the epithelia and other biological barriers and in adjuvanting its activity increasing an early cell-mediated immune response [101]. Furthermore, curcumin-stabilized silver nanoparticles significantly inhibited the expression of IL-1 β , TNF- α , IL-6 and NF- κ B in a higher extent than curcumin alone [102]. In addition, lipid nanoparticles encapsulating curcumin were able to prevent metastasis formation and limited the progression of the disease by

modulating vascular inflammation in a highly metastatic breast cancer model [103].

Curcumin represents also a starting point for multitarget drug design. Multitarget drugs can be rationally designed by linking, by means of suitable spacers, or fusing the key pharmacophoric functions, or through amalgamation of the pharmacophoric groups essential for activity into one hybrid molecule [104]. Many different curcumin analogues and hybrids have been synthesized and are now under testing phase. The idea to synthesize new hybrids raised by the knowledge that hydroxycinnamoyl recurring motif, present in curcumin, has been shown to modulate several pathways related to aging-related disorders. As an example, Simoni *et al.* [105,106] synthesized a set of new hybrids, by combining a hydroxycinnamoyl function from curcumin and diallyl sulfides from garlic. This novel design strategy represented an efficient and promising approach, since a catechol derivative with remarkable biological modulating properties has been characterized. This approach could be useful in the near future the development of new efficient molecules to counteract multifactorial diseases.

6. Conclusions

The active components in medical plants have always represented an important source of clinical therapeutics since they offer a chemical diversity often associated with a multi-pharmacological activity. Their use in traditional medicine for their properties and health benefits is well recognized since ancient times. Many of these natural products, such as curcumin and Echinacea, have important biological activity that can be exploited in pharmaceutical drug discovery and drug design. However, inconsistencies in published results regarding immunomodulatory effects of herbal remedies have been highlighted, mainly due to limitations such as lack of standardization to active ingredients, qualitative and quantitative changes in preparations and lack of rigorous test for efficacy. There is evidence of both therapeutic inefficacy and efficacy of Echinacea on immune system,

depending on preparation and study design. In addition, curcumin show additional limitations related to its poor pharmacokinetic/pharmacodynamic properties, its chemical instability, and its PAINS character [53]. To overcome these critical pharmaceutical issues, new formulations, the direct delivery to the specific tissue taking advantage from the hybridization approach and the development of nanotechnology-based delivery systems have been characterized mainly for curcumin. The use of nanoparticles, in particular, can ensure controlled release of drugs and reduce their toxicity. Noteworthy, natural products might also contain prebiotic components, whose interaction with the host microbiome can significantly impact health and disease. This is a new area of research that would further help optimize the selection of natural products for the maintenance of health and treatment of autoimmune diseases, such as arthritis, systemic lupus and other diseases, and define their mechanisms of action [107]. These approaches may be promising, allowing developing new promising chemical entities, which, however, should be validated through expensive preclinical work to be approved for clinical trials. Within this context, an approach has been recently tried on subjects affected by rheumatoid arthritis, on which a novel, highly bioavailable form of curcumin in a natural turmeric matrix was evaluated for its ability to improve the clinical symptoms of this autoimmune, inflammatory disorder [108].

REFERENCES

1. Yatim, K. M.; Lakkis, F. G. A brief journey through the immune system. *Clin. J. Am. Soc. Nephrol. CJASN* **2015**, *10*, 1274–1281, doi:10.2215/CJN.10031014.
2. Netea, M. G.; Quintin, J.; van der Meer, J. W. M. Trained immunity: a memory for innate host defense. *Cell Host Microbe* **2011**, *9*, 355–361, doi:10.1016/j.chom.2011.04.006.
3. Kawai, T.; Akira, S. The role of pattern-recognition receptors in innate immunity: update on Toll-like receptors. *Nat. Immunol.* **2010**, *11*, 373–384, doi:10.1038/ni.1863.
4. Ueta, M.; Kinoshita, S. Innate immunity of the ocular surface. *Brain Res Bull.* **2010**, *81*, 219–228. doi: 10.1016/j.brainresbull.2009.10.001.
5. Pancer, Z.; Cooper, M. D. The evolution of adaptive immunity. *Annu. Rev. Immunol.* **2006**, *24*, 497–518, doi:10.1146/annurev.immunol.24.021605.090542.

6. Mauri, C.; Bosma, A. Immune regulatory function of B cells. *Annu. Rev. Immunol.* **2012**, *30*, 221-241, doi:10.1146/annurev-immunol-020711-074934.
7. Josefowicz, S. Z.; Lu, L.-F.; Rudensky, A. Y. Regulatory T cells: mechanisms of differentiation and function. *Annu. Rev. Immunol.* **2012**, *30*, 531-564, doi:10.1146/annurev.immunol.25.022106.141623.
8. Oberbarnscheidt, M. H.; Lakkis, F. G. Innate allorecognition. *Immunol. Rev.* **2014**, *258*, 145-149, doi:10.1111/imr.12153.
9. Lerner, A.; Jeremias, P.; Matthias, T. The World Incidence and Prevalence of Autoimmune Diseases is Increasing. *Int. J. Celiac Dis.* **2016**, *3*, 151-155, doi:10.12691/ijcd-3-4-8.
10. Nilius, B.; Appendino, G. Spices: the savory and beneficial science of pungency. *Rev. Physiol. Biochem. Pharmacol.* **2013**, *164*, 1-76, doi:10.1007/112_2013_11.
11. Estrela, J. M.; Mena, S.; Obrador, E.; Benlloch, M.; Castellano, G.; Salvador, R.; Dellinger, R. W. Polyphenolic Phytochemicals in Cancer Prevention and Therapy: Bioavailability versus Bioefficacy. *J. Med. Chem.* **2017**, *60*, 9413-9436, doi:10.1021/acs.jmedchem.6b01026.
12. Annucci, G.; Bozzetto, L.; Costabile, G.; Giacco, R.; Mangione, A.; Anniballi, G.; Vitale, M.; Vetrani, C.; Cipriano, P.; Della Corte, G.; Pasanisi, F.; Riccardi, G.; Rivellesse, A. A. Diets naturally rich in polyphenols improve fasting and postprandial dyslipidemia and reduce oxidative stress: a randomized controlled trial. *Am. J. Clin. Nutr.* **2014**, *99*, 463-471, doi:10.3945/ajcn.113.073445.
13. Afzal, M.; Safer, A. M.; Menon, M. Green tea polyphenols and their potential role in health and disease. *Inflammopharmacology* **2015**, *23*, 151-161, doi:10.1007/s10787-015-0236-1.
14. Farzaei, M.; Rahimi, R.; Abdollahi, M. The Role of Dietary Polyphenols in the Management of Inflammatory Bowel Disease. *Curr. Pharm. Biotechnol.* **2015**, *16*, 196-210, doi:10.2174/1389201016666150118131704.
15. Andreicut, A.-D.; Pârvu, A. E.; Mot, A. C.; Pârvu, M.; Fischer Fodor, E.; Cătoi, A. F.; Feldrihan, V.; Cecan, M.; Irimie, A. Phytochemical Analysis of Anti-Inflammatory and Antioxidant Effects of *Mahonia aquifolium* Flower and Fruit Extracts. *Oxid. Med. Cell. Longev.* **2018**, *2018*, 1-12, doi:10.1155/2018/2879793.
16. Ferreira, S. S.; Passos, C. P.; Madureira, P.; Vilanova, M.; Coimbra, M. A. Structure-function relationships of immunostimulatory polysaccharides: A review. *Carbohydr. Polym.* **2015**, *132*, 378-396, doi:10.1016/j.carbpol.2015.05.079.
17. Gandhi, G. R.; Neta, M. T. S. L.; Sathiyabama, R. G.; Quintans, J. de S. S.; de Oliveira e Silva, A. M.; Araújo, A. A. de S.; Narain, N.; Júnior, L. J. Q.; Gurgel, R. Q. Flavonoids as Th1/Th2 cytokines immunomodulators: A systematic review of studies on animal models. *Phytomedicine* **2018**, *44*, 74-84, doi:10.1016/j.phymed.2018.03.057.
18. Boland, J. W.; Foulds, G. A.; Ahmedzai, S. H.; Pockley, A. G. A preliminary evaluation of the effects of opioids on innate and adaptive human *in vitro* immune function. *BMJ Support. Palliat. Care* **2014**, *4*, 357-367, doi:10.1136/bmjspcare-2013-000573.
19. Percival, S. S. Use of echinacea in medicine. *Biochem. Pharmacol.* **2000**, *60*, 155-158, doi:10.1016/S0006-2952(99)00413-X.

20. Davis, J.; Cupp, M. J. Echinacea. In *Toxicology and Clinical Pharmacology of Herbal Products*; Cupp, M. J., Ed.; Humana Press: Totowa, NJ, 2000; pp. 85-93 ISBN 978-1-59259-020-9.
21. Barrett, B. Medicinal properties of Echinacea: A critical review. *Phytomedicine* **2003**, *10*, 66-86, doi:10.1078/094471103321648692.
22. Karsch-Völk, M.; Barrett, B.; Linde, K. *Echinacea* for Preventing and Treating the Common Cold. *JAMA* **2015**, *313*, 618, doi:10.1001/jama.2014.17145.
23. Rondanelli, M.; Miccono, A.; Lamburghini, S.; Avanzato, I.; Riva, A.; Allegrini, P.; Faliva, M. A.; Peroni, G.; Nichetti, M.; Perna, S. Self-Care for Common Colds: The Pivotal Role of Vitamin D, Vitamin C, Zinc, and *Echinacea* in Three Main Immune Interactive Clusters (Physical Barriers, Innate and Adaptive Immunity) Involved during an Episode of Common Colds—Practical Advice on Dosages and on the Time to Take These Nutrients/Botanicals in order to Prevent or Treat Common Colds. *Evid. Based Complement. Alternat. Med.* **2018**, *2018*, 1-36, doi:10.1155/2018/5813095.
24. Bařan, B. J.; Sokolnicka, I.; Skopińska-Róźewska, E.; Skopiński, P. The modulatory influence of some Echinacea -based remedies on antibody production and cellular immunity in mice. *Cent. Eur. J. Immunol.* **2016**, *1*, 12-18, doi:10.5114/ceji.2016.58813.
25. Sultan, M. T.; Buttxs, M. S.; Qayyum, M. M. N.; Suleria, H. A. R. Immunity: Plants as Effective Mediators. *Crit. Rev. Food Sci. Nutr.* **2014**, *54*, 1298-1308, doi:10.1080/10408398.2011.633249.
26. Melchart, D.; Walther, E.; Linde, K.; Brandmaier, R.; Lersch, C. Echinacea root extracts for the prevention of upper respiratory tract infections: a double-blind, placebo-controlled randomized trial. *Arch. Fam. Med.* **1998**, *7*, 541-545.
27. Di Pierro, F.; Rapacioli, G.; Ferrara, T.; Togni, S. Use of a standardized extract from *Echinacea angustifolia* (Polinacea) for the prevention of respiratory tract infections. *Altern. Med. Rev. J. Clin. Ther.* **2012**, *17*, 36-41.
28. Luettig, B.; Steinmüller, C.; Gifford, G. E.; Wagner, H.; Lohmann-Matthes, M. L. Macrophage activation by the polysaccharide arabinogalactan isolated from plant cell cultures of *Echinacea purpurea*. *J. Natl. Cancer Inst.* **1989**, *81*, 669-675.
29. See, D. M.; Broumand, N.; Sahl, L.; Tilles, J. G. *In vitro* effects of echinacea and ginseng on natural killer and antibody-dependent cell cytotoxicity in healthy subjects and chronic fatigue syndrome or acquired immunodeficiency syndrome patients. *Immunopharmacology* **1997**, *35*, 229-235, doi:10.1016/S0162-3109(96)00125-7.
30. Vetvicka, V.; Vetvickova, J. Natural immunomodulators and their stimulation of immune reaction: true or false? *Anticancer Res.* **2014**, *34*, 2275-2282.
31. Li, Y.; Wang, Y.; Wu, Y.; Wang, B.; Chen, X.; Xu, X.; Chen, H.; Li, W.; Xu, X. Echinacea pupurea extracts promote murine dendritic cell maturation by activation of JNK, p38 MAPK and NF-κB pathways. *Dev. Comp. Immunol.* **2017**, *73*, 21-26, doi:10.1016/j.dci.2017.03.002.
32. Wang, C.-Y.; Chiao, M.-T.; Yen, P.-J.; Huang, W.-C.; Hou, C.-C.; Chien, S.-C.; Yeh, K.-C.; Yang, W.-C.; Shyur, L.-F.; Yang, N.-S. Modulatory effects of *Echinacea purpurea* extracts

- on human dendritic cells: A cell- and gene-based study. *Genomics* **2006**, *88*, 801-808, doi:10.1016/j.ygeno.2006.08.011.
33. Fu, A.; Wang, Y.; Wu, Y.; Chen, H.; Zheng, S.; Li, Y.; Xu, X.; Li, W. *Echinacea purpurea* Extract Polarizes M1 Macrophages in Murine Bone Marrow-Derived Macrophages Through the Activation of JNK: *E CHINACEA P URPUREA E XTRACT P OLARIZES M1 M ACROPHAGES*. *J. Cell. Biochem.* **2017**, *118*, 2664-2671, doi:10.1002/jcb.25875.
 34. Steinmüller, C.; Roesler, J.; Gröttrup, E.; Franke, G.; Wagner, H.; Lohmann-Matthes, M. L. Polysaccharides isolated from plant cell cultures of *Echinacea purpurea* enhance the resistance of immunosuppressed mice against systemic infections with *Candida albicans* and *Listeria monocytogenes*. *Int. J. Immunopharmacol.* **1993**, *15*, 605-614.
 35. Vimalanathan, S.; Schoop, R.; Suter, A.; Hudson, J. Prevention of influenza virus induced bacterial superinfection by standardized *Echinacea purpurea*, via regulation of surface receptor expression in human bronchial epithelial cells. *Virus Res.* **2017**, *233*, 51-59, doi:10.1016/j.virusres.2017.03.006.
 36. Williamson, E. Synergy and other interactions in phytomedicines. *Phytomedicine* **2001**, *8*, 401-409, doi:10.1078/0944-7113-00060.
 37. Huntley, A. L.; Thompson Coon, J.; Ernst, E. The safety of herbal medicinal products derived from *Echinacea* species: a systematic review. *Drug Saf.* **2005**, *28*, 387-400.
 38. Raduner, S.; Majewska, A.; Chen, J.-Z.; Xie, X.-Q.; Hamon, J.; Faller, B.; Altmann, K.-H.; Gertsch, J. Alkylamides from *Echinacea* Are a New Class of Cannabinomimetics: *CANNABINOID TYPE 2 RECEPTOR-DEPENDENT AND -INDEPENDENT IMMUNOMODULATORY EFFECTS*. *J. Biol. Chem.* **2006**, *281*, 14192-14206, doi:10.1074/jbc.M601074200.
 39. Chicca, A.; Raduner, S.; Pellati, F.; Strompen, T.; Altmann, K.-H.; Schoop, R.; Gertsch, J. Synergistic immunopharmacological effects of N-alkylamides in *Echinacea purpurea* herbal extracts. *Int. Immunopharmacol.* **2009**, *9*, 850-858, doi:10.1016/j.intimp.2009.03.006.
 40. Spelman, K.; Iiams-Hauser, K.; Cech, N. B.; Taylor, E. W.; Smirnov, N.; Wenner, C. A. Role for PPAR γ in IL-2 inhibition in T cells by *Echinacea*-derived undeca-2E-ene-8,10-diyonic acid isobutylamide. *Int. Immunopharmacol.* **2009**, *9*, 1260-1264, doi:10.1016/j.intimp.2009.08.009.
 41. Tragni, E.; Galli, C. L.; Tubaro, A.; Del Negro, P.; Della Loggia, R. Anti-inflammatory activity of *Echinacea angustifolia* fractions separated on the basis of molecular weight. *Pharmacol. Res. Commun.* **1988**, *20 Suppl 5*, 87-90.
 42. Müller-Jakic, B.; Brey, W.; Pröbstle, A.; Redl, K.; Greger, H.; Bauer, R. *In vitro* inhibition of cyclooxygenase and 5-lipoxygenase by alkamides from *Echinacea* and *Achillea* species. *Planta Med.* **1994**, *60*, 37-40, doi:10.1055/s-2006-959404.
 43. Facino, R. M.; Carini, M.; Aldini, G.; Marinello, C.; Arlandini, E.; Franzoi, L.; Colombo, M.; Pietta, P.; Mauri, P. Direct characterization of caffeoyl esters with antihyaluronidase activity in crude extracts from *Echinacea angustifolia* roots by fast atom bombardment tandem mass spectrometry. *Farm. Soc. Chim. Ital.* **1989**, *1993*, *48*, 1447-1461.

44. Fonseca, F. N.; Papanicolaou, G.; Lin, H.; Lau, C. B. S.; Kennelly, E. J.; Cassileth, B. R.; Cunningham-Rundles, S. Echinacea purpurea (L.) Moench modulates human T-cell cytokine response. *Int. Immunopharmacol.* **2014**, *19*, 94-102, doi:10.1016/j.intimp.2013.12.019.
45. Voaden, D. J.; Jacobson, M. Tumor inhibitors. 3. Identification and synthesis of an oncolytic hydrocarbon from American coneflower roots. *J. Med. Chem.* **1972**, *15*, 619-623.
46. Ardjomand-Woelkart, K.; Bauer, R. Review and Assessment of Medicinal Safety Data of Orally Used Echinacea Preparations. *Planta Med.* **2016**, *82*, 17-31. doi:10.1055/s-0035-1558096.
47. Lee, A. N.; Werth, V. P. Activation of autoimmunity following use of immunostimulatory herbal supplements. *Arch Dermatol.* **2004**, *140*, 723-727.
48. Vogel, H. A.; Pelletier, J. Curcumin-biological and medicinal properties. *J. Pharma* **1815**, *2*, 50.
49. Priyadarsini, K. I. The chemistry of curcumin: from extraction to therapeutic agent. *Mol. Basel Switz.* **2014**, *19*, 20091-20112, doi:10.3390/molecules191220091.
50. Goel, A.; Kunnumakkara, A. B.; Aggarwal, B. B. Curcumin as "Curecumin": From kitchen to clinic. *Biochem. Pharmacol.* **2008**, *75*, 787-809, doi:10.1016/j.bcp.2007.08.016.
51. Abdel-Lateef, E.; Mahmoud, F.; Hammam, O.; El-Ahwany, E.; El-Wakil, E.; Kandil, S.; Abu Taleb, H.; El-Sayed, M.; Hassenein, H. Bioactive chemical constituents of *Curcuma longa* L. rhizomes extract inhibit the growth of human hepatoma cell line (HepG2). *Acta Pharm.* **2016**, *66*, 387-398, doi:10.1515/acph-2016-0028.
52. Burgos-Morón, E.; Calderón-Montaño, J. M.; Salvador, J.; Robles, A.; López-Lázaro, M. The dark side of curcumin. *Int. J. Cancer* **2010**, *126*, 1771-1775, doi:10.1002/ijc.24967.
53. Nelson, K. M.; Dahlin, J. L.; Bisson, J.; Graham, J.; Pauli, G. F.; Walters, M. A. The Essential Medicinal Chemistry of Curcumin. *J. Med. Chem.* **2017**, *60*, 1620-1637, doi:10.1021/acs.jmedchem.6b00975.
54. Serafini, M. M.; Catanzaro, M.; Rosini, M.; Racchi, M.; Lanni, C. Curcumin in Alzheimer's disease: Can we think to new strategies and perspectives for this molecule? *Pharmacol. Res.* **2017**, *124*, 146-155, doi:10.1016/j.phrs.2017.08.004.
55. Kunnumakkara, A. B.; Bordoloi, D.; Padmavathi, G.; Monisha, J.; Roy, N. K.; Prasad, S.; Aggarwal, B. B. Curcumin, the golden nutraceutical: multitargeting for multiple chronic diseases. *Br. J. Pharmacol.* **2017**, *174*, 1325-1348, doi:10.1111/bph.13621.
56. Momtazi-Borojeni, A. A.; Haftcheshmeh, S. M.; Esmaeili, S.-A.; Johnston, T. P.; Abdollahi, E.; Sahebkar, A. Curcumin: A natural modulator of immune cells in systemic lupus erythematosus. *Autoimmun. Rev.* **2018**, *17*, 125-135, doi:10.1016/j.autrev.2017.11.016.
57. Kim, G.-Y.; Kim, K.-H.; Lee, S.-H.; Yoon, M.-S.; Lee, H.-J.; Moon, D.-O.; Lee, C.-M.; Ahn, S.-C.; Park, Y. C.; Park, Y.-M. Curcumin inhibits immunostimulatory function of dendritic cells: MAPKs and translocation of NF-kappa B as potential targets. *J. Immunol. Baltim. Md* **1950** **2005**, *174*, 8116-8124.

-
58. Alagawany, M.; Ashour, E. A.; Reda, F. M. Effect of Dietary Supplementation of Garlic (*Allium Sativum*) and Turmeric (*Curcuma Longa*) on Growth Performance, Carcass Traits, Blood Profile and Oxidative Status in Growing Rabbits. *Ann. Anim. Sci.* **2016**, *16*, 489-505, doi:10.1515/aoas-2015-0079.
 59. Rawlings, J. S. The JAK/STAT signaling pathway. *J. Cell Sci.* **2004**, *117*, 1281-1283, doi:10.1242/jcs.00963.
 60. Bill, M. A.; Nicholas, C.; Mace, T. A.; Etter, J. P.; Li, C.; Schwartz, E. B.; Fuchs, J. R.; Young, G. S.; Lin, L.; Lin, J.; He, L.; Phelps, M.; Li, P.-K.; Lesinski, G. B. Structurally Modified Curcumin Analogs Inhibit STAT3 Phosphorylation and Promote Apoptosis of Human Renal Cell Carcinoma and Melanoma Cell Lines. *PLoS ONE* **2012**, *7*, e40724, doi:10.1371/journal.pone.0040724.
 61. Weissenberger, J.; Priester, M.; Bernreuther, C.; Rakel, S.; Glatzel, M.; Seifert, V.; Kögel, D. Dietary curcumin attenuates glioma growth in a syngeneic mouse model by inhibition of the JAK1,2/STAT3 signaling pathway. *Clin. Cancer Res. Off. J. Am. Assoc. Cancer Res.* **2010**, *16*, 5781-5795, doi:10.1158/1078-0432.CCR-10-0446.
 62. Liu, L.; Liu, Y. L.; Liu, G. X.; Chen, X.; Yang, K.; Yang, Y. X.; Xie, Q.; Gan, H. K.; Huang, X. L.; Gan, H. T. Curcumin ameliorates dextran sulfate sodium-induced experimental colitis by blocking STAT3 signaling pathway. *Int. Immunopharmacol.* **2013**, *17*, 314-320, doi:10.1016/j.intimp.2013.06.020.
 63. Brück, J.; Holstein, J.; Glocova, I.; Seidel, U.; Geisel, J.; Kanno, T.; Kumagai, J.; Mato, N.; Sudowe, S.; Widmaier, K.; Sinnberg, T.; Yazdi, A. S.; Eberle, F. C.; Hirahara, K.; Nakayama, T.; Röcken, M.; Ghoreschi, K. Nutritional control of IL-23/Th17-mediated autoimmune disease through HO-1/STAT3 activation. *Sci. Rep.* **2017**, *7*, doi:10.1038/srep44482.
 64. Lao, C. D.; Ruffin, M. T. 4th; Normolle, D.; Heath, D. D.; Murray, S. I.; Bailey, J. M.; Boggs, M. E.; Crowell, J.; Rock, C. L.; Brenner, D. E. Dose escalation of a curcuminoid formulation. *BMC Complement Altern Med.* **2006**, *17*, 6-10.
 65. Lin, J. A.; Chen, J. H.; Lee, Y. W.; Lin, C. S.; Hsieh, M. H.; Chang, C. C.; Wong, C. S.; Chen, J. J.; Yeh, G. C.; Lin, F. Y.; Chen, T. L. Biphasic effect of curcumin on morphine tolerance: a preliminary evidence from cytokine/chemokine protein array analysis. *Evid Based Complement Alternat Med.* **2011**, doi: 10.1093/ecam/neaq018.
 66. Duncan, S. A.; Baganizi, D. R.; Sahu, R.; Singh, S. R.; Dennis, V. A. SOCS Proteins as Regulators of Inflammatory Responses Induced by Bacterial Infections: A Review. *Front. Microbiol.* **2017**, *8*, doi:10.3389/fmicb.2017.02431.
 67. Guimarães, M. R.; Leite, F. R. M.; Spolidorio, L. C.; Kirkwood, K. L.; Rossa, C. Curcumin abrogates LPS-induced pro-inflammatory cytokines in RAW 264.7 macrophages. Evidence for novel mechanisms involving SOCS-1, -3 and p38 MAPK. *Arch. Oral Biol.* **2013**, *58*, 1309-1317, doi:10.1016/j.archoralbio.2013.07.005.
 68. Chen, C.; Yu, K.; Yan, Q.; Xing, C.; Chen, Y.; Yan, Z.; Shi, Y.; Zhao, K.-W.; Gao, S. Pure curcumin increases the expression of SOCS1 and SOCS3 in myeloproliferative neoplasms through suppressing class I histone deacetylases. *Carcinogenesis* **2013**, *34*, 1442-1449, doi:10.1093/carcin/bgt070.

69. Kunnumakkara, A. B.; Sailo, B. L.; Banik, K.; Harsha, C.; Prasad, S.; Gupta, S. C.; Bharti, A. C.; Aggarwal, B. B. Chronic diseases, inflammation, and spices: how are they linked? *J. Transl. Med.* **2018**, *16*, doi:10.1186/s12967-018-1381-2.
70. Liu, Y.; Chen, L.; Shen, Y.; Tan, T.; Xie, N.; Luo, M.; Li, Z.; Xie, X. Curcumin Ameliorates Ischemia-Induced Limb Injury Through Immunomodulation. *Med. Sci. Monit.* **2016**, *22*, 2035-2042, doi:10.12659/MSM.896217.
71. Castro, C. N.; Barcala Tabarozzi, A. E.; Winnewisser, J.; Gimeno, M. L.; Antunica Noguero, M.; Liberman, A. C.; Paz, D. A.; Dewey, R. A.; Perone, M. J. Curcumin ameliorates autoimmune diabetes. Evidence in accelerated murine models of type 1 diabetes: Curcumin ameliorates autoimmunity in NOD. *Clin. Exp. Immunol.* **2014**, *177*, 149-160, doi:10.1111/cei.12322.
72. Cianciulli, A.; Calvello, R.; Porro, C.; Trotta, T.; Salvatore, R.; Panaro, M. A. PI3k/Akt signalling pathway plays a crucial role in the anti-inflammatory effects of curcumin in LPS-activated microglia. *Int. Immunopharmacol.* **2016**, *36*, 282-290, doi:10.1016/j.intimp.2016.05.007.
73. Yu, Y.; Shen, Q.; Lai, Y.; Park, S. Y.; Ou, X.; Lin, D.; Jin, M.; Zhang, W. Anti-inflammatory Effects of Curcumin in Microglial Cells. *Front. Pharmacol.* **2018**, *9*, doi:10.3389/fphar.2018.00386.
74. Ireton, G. C.; Reed, S. G. Adjuvants containing natural and synthetic Toll-like receptor 4 ligands. *Expert Rev. Vaccines* **2013**, *12*, 793-807, doi:10.1586/14760584.2013.811204.
75. Vaure, C.; Liu, Y. A comparative review of toll-like receptor 4 expression and functionality in different animal species. *Front. Immunol.* **2014**, *5*, 316, doi:10.3389/fimmu.2014.00316.
76. Zhu, H.; Bian, C.; Yuan, J.; Chu, W.; Xiang, X.; Chen, F.; Wang, C.; Feng, H.; Lin, J. Curcumin attenuates acute inflammatory injury by inhibiting the TLR4/MyD88/NF- κ B signaling pathway in experimental traumatic brain injury. *J. Neuroinflammation* **2014**, *11*, 59, doi:10.1186/1742-2094-11-59.
77. Ni, H.; Jin, W.; Zhu, T.; Wang, J.; Yuan, B.; Jiang, J.; Liang, W.; Ma, Z. Curcumin modulates TLR4/NF- κ B inflammatory signaling pathway following traumatic spinal cord injury in rats. *J. Spinal Cord Med.* **2015**, *38*, 199-206, doi:10.1179/2045772313Y.0000000179.
78. Urdzikova, L.M.; Karova, K.; Ruzicka, J.; Kloudova, A.; Shannon, C.; Dubisova, J.; Murali, R.; Kubinova, S.; Sykova, E.; Jhanwar-Uniyal, M.; Jendelova, P. The Anti-Inflammatory Compound Curcumin Enhances Locomotor and Sensory Recovery after Spinal Cord Injury in Rats by Immunomodulation. *Int. J. Mol. Sci.* **2015**, *17*, doi:10.3390/ijms17010049.
79. Abe, Y.; Hashimoto, S.; Horie, T. Curcumin inhibition of inflammatory cytokine production by human peripheral blood monocytes and alveolar macrophages. *Pharmacol. Res.* **1999**, *39*, 41-47, doi:10.1006/phrs.1998.0404.
80. Lin, M.-S.; Sun, Y.-Y.; Chiu, W.-T.; Hung, C.-C.; Chang, C.-Y.; Shie, F.-S.; Tsai, S.-H.; Lin, J.-W.; Hung, K.-S.; Lee, Y.-H. Curcumin attenuates the expression and secretion of RANTES after spinal cord injury *in vivo* and lipopolysaccharide-induced astrocyte reactivation *in vitro*. *J. Neurotrauma* **2011**, *28*, 1259-1269, doi:10.1089/neu.2011.1768.

-
81. Lubbad, A.; Oriowo, M. A.; Khan, I. Curcumin attenuates inflammation through inhibition of TLR-4 receptor in experimental colitis. *Mol. Cell. Biochem.* **2009**, *322*, 127-135, doi:10.1007/s11010-008-9949-4.
 82. Fu, Y.; Gao, R.; Cao, Y.; Guo, M.; Wei, Z.; Zhou, E.; Li, Y.; Yao, M.; Yang, Z.; Zhang, N. Curcumin attenuates inflammatory responses by suppressing TLR4-mediated NF- κ B signaling pathway in lipopolysaccharide-induced mastitis in mice. *Int. Immunopharmacol.* **2014**, *20*, 54-58, doi:10.1016/j.intimp.2014.01.024.
 83. Santos, A. M.; Lopes, T.; Oleastro, M.; Gato, I. V.; Floch, P.; Benejat, L.; Chaves, P.; Pereira, T.; Seixas, E.; Machado, J.; Guerreiro, A. S. Curcumin inhibits gastric inflammation induced by *Helicobacter pylori* infection in a mouse model. *Nutrients* **2015**, *7*, 306-320, doi:10.3390/nu7010306.
 84. Moghadamtousi, S. Z.; Kadir, H. A.; Hassandarvish, P.; Tajik, H.; Abubakar, S.; Zandi, K. A review on antibacterial, antiviral, and antifungal activity of curcumin. *BioMed Res. Int.* **2014**, *2014*, 186864, doi:10.1155/2014/186864.
 85. Bansal, S.; Chhibber, S. Curcumin alone and in combination with augmentin protects against pulmonary inflammation and acute lung injury generated during *Klebsiella pneumoniae* B5055-induced lung infection in BALB/c mice. *J. Med. Microbiol.* **2010**, *59*, 429-437, doi:10.1099/jmm.0.016873-0.
 86. Bansal, S.; Chhibber, S. Phytochemical-induced reduction of pulmonary inflammation during *Klebsiella pneumoniae* lung infection in mice. *J. Infect. Dev. Ctries.* **2014**, *8*, doi:10.3855/jidc.3277.
 87. Kim, D. K.; Lillehoj, H. S.; Lee, S. H.; Jang, S. I.; Lillehoj, E. P.; Bravo, D. Dietary Curcuma longa enhances resistance against *Eimeria maxima* and *Eimeria tenella* infections in chickens. *Poult. Sci.* **2013**, *92*, 2635-2643, doi:10.3382/ps.2013-03095.
 88. Bai, X.; Oberley-Deegan, R. E.; Bai, A.; Ovrutsky, A. R.; Kinney, W. H.; Weaver, M.; Zhang, G.; Honda, J. R.; Chan, E. D. Curcumin enhances human macrophage control of *Mycobacterium tuberculosis* infection: Curcumin and tuberculosis in macrophages. *Respirology* **2016**, *21*, 951-957, doi:10.1111/resp.12762.
 89. Yue, G. G. L.; Chan, B. C. L.; Hon, P.-M.; Lee, M. Y. H.; Fung, K.-P.; Leung, P.-C.; Lau, C. B. S. Evaluation of *in vitro* anti-proliferative and immunomodulatory activities of compounds isolated from *Curcuma longa*. *Food Chem. Toxicol.* **2010**, *48*, 2011-2020, doi:10.1016/j.fct.2010.04.039.
 90. Yue, G. G. L.; Chan, B. C. L.; Hon, P.-M.; Kennelly, E. J.; Yeung, S. K.; Cassileth, B. R.; Fung, K.-P.; Leung, P.-C.; Lau, C. B. S. Immunostimulatory activities of polysaccharide extract isolated from *Curcuma longa*. *Int. J. Biol. Macromol.* **2010**, *47*, 342-347, doi:10.1016/j.ijbiomac.2010.05.019.
 91. Aggarwal, B. B.; Yuan, W.; Li, S.; Gupta, S. C. Curcumin-free turmeric exhibits anti-inflammatory and anticancer activities: Identification of novel components of turmeric. *Mol. Nutr. Food Res.* **2013**, *57*, 1529-1542, doi:10.1002/mnfr.201200838.
 92. Drake, P. M. W.; Szeto, T. H.; Paul, M. J.; Teh, A. Y.-H.; Ma, J. K.-C. Recombinant biologic products versus nutraceuticals from plants - a regulatory choice? *Br. J. Clin. Pharmacol.* **2017**, *83*, 82-87, doi:10.1111/bcp.13041.

93. Brown, A. C. An overview of herb and dietary supplement efficacy, safety and government regulations in the United States with suggested improvements. Part 1 of 5 series. *Food Chem. Toxicol.* **2017**, *107*, 449–471, doi:10.1016/j.fct.2016.11.001.
94. Jantan, I.; Ahmad, W.; Bukhari, S. N. A. Plant-derived immunomodulators: an insight on their preclinical evaluation and clinical trials. *Front. Plant Sci.* **2015**, *6*, doi:10.3389/fpls.2015.00655.
95. Anand, P.; Kunnumakkara, A. B.; Newman, R. A.; Aggarwal, B. B. Bioavailability of curcumin: problems and promises. *Mol. Pharm.* **2007**, *4*, 807–818, doi:10.1021/mp700113r.
96. Kumari, N.; Nekhai, S.; Kulkarni, A.; Lin, X.; McLean, C.; Ammosova, T.; Ivanov, A.; Hipolito, M.; Nwulia, E. Inhibition of HIV-1 by curcumin A, a novel curcumin analog. *Drug Des. Devel. Ther.* **2015**, 5051, doi:10.2147/DDDT.S86558.
97. Jantan, I.; Bukhari, S. N. A.; Lajis, N. H.; Abas, F.; Wai, L. K.; Jasamai, M. Effects of diarylpentanoid analogues of curcumin on chemiluminescence and chemotactic activities of phagocytes: Immunomodulatory effects of diarylpentanoids. *J. Pharm. Pharmacol.* **2012**, *64*, 404–412, doi:10.1111/j.2042-7158.2011.01423.x.
98. Krishnakumar, I.; Ravi, A.; Kumar, D.; Kuttan, R.; Maliakel, B. An enhanced bioavailable formulation of curcumin using fenugreek-derived soluble dietary fibre. *J. Funct. Foods* **2012**, *4*, 348–357, doi:10.1016/j.jff.2012.01.004.
99. Krishnakumar, I.; Maliakel, A.; G, G.; Kumar, D.; Maliakel, B.; Kuttan, R. Improved blood-brain-barrier permeability and tissue distribution following the oral administration of a food-grade formulation of curcumin with fenugreek fibre. *J. Funct. Foods* **2015**, *14*, 215–225, doi:10.1016/j.jff.2015.01.049.
100. Gera, M.; Sharma, N.; Ghosh, M.; Huynh, D. L.; Lee, S. J.; Min, T.; Kwon, T.; Jeong, D. K. Nanoformulations of curcumin: an emerging paradigm for improved remedial application. *Oncotarget* **2017**, *8*, 66680–66698, doi:10.18632/oncotarget.19164.
101. Afolayan, F. I. D.; Erinwusi, B.; Oyeyemi, O. T. Immunomodulatory activity of curcumin-entrapped poly d,l-lactic-co-glycolic acid nanoparticles in mice. *Integr. Med. Res.* **2018**, *7*, 168–175, doi:10.1016/j.imr.2018.02.004.
102. Sharma, R. K.; Cwiklinski, K.; Aalinkeel, R.; Reynolds, J. L.; Sykes, D. E.; Quaye, E.; Oh, J.; Mahajan, S. D.; Schwartz, S. A. Immunomodulatory activities of curcumin-stabilized silver nanoparticles: Efficacy as an antiretroviral therapeutic. *Immunol. Invest.* **2017**, *46*, 833–846, doi:10.1080/08820139.2017.1371908.
103. Palange, A. L.; Di Mascolo, D.; Carallo, C.; Gnasso, A.; Decuzzi, P. Lipid-polymer nanoparticles encapsulating curcumin for modulating the vascular deposition of breast cancer cells. *Nanomedicine.* **2014**, *10*, 991–1002. doi: 10.1016/j.nano.2014.02.004.
104. Bottegoni, G.; Favia, A. D.; Recanatini, M.; Cavalli, A. The role of fragment-based and computational methods in polypharmacology. *Drug Discov. Today* **2012**, *17*, 23–34, doi:10.1016/j.drudis.2011.08.002.
105. Simoni, E.; Serafini, M. M.; Bartolini, M.; Caporaso, R.; Pinto, A.; Necchi, D.; Fiori, J.; Andrisano, V.; Minarini, A.; Lanni, C.; Rosini, M. Nature-Inspired Multifunctional Ligands:

-
- Focusing on Amyloid-Based Molecular Mechanisms of Alzheimer's Disease. *ChemMedChem* **2016**, *11*, 1309-1317, doi:10.1002/cmdc.201500422.
106. Simoni, E.; Serafini, M. M.; Caporaso, R.; Marchetti, C.; Racchi, M.; Minarini, A.; Bartolini, M.; Lanni, C.; Rosini, M. Targeting the Nrf2/Amyloid-Beta Liaison in Alzheimer's Disease: A Rational Approach. *ACS Chem. Neurosci.* **2017**, *8*, 1618-1627, doi:10.1021/acscchemneuro.7b00100.
107. Dudics, S.; Langan, D.; Meka, R. R.; Venkatesha, S. H.; Berman, B. M.; Che, C. T.; Moudgil, K. D. Natural Products for the Treatment of Autoimmune Arthritis: Their Mechanisms of Action, Targeted Delivery, and Interplay with the Host Microbiome. *Int J Mol Sci.* **2018**, *19*, doi: 10.3390/ijms19092508.
108. Amalraj, A.; Varma, K.; Jacob, J.; Divya, C.; Kunnumakkara, A. B.; Stohs, S. J.; Gopi, S. A Novel Highly Bioavailable Curcumin Formulation Improves Symptoms and Diagnostic Indicators in Rheumatoid Arthritis Patients: A Randomized, Double-Blind, Placebo-Controlled, Two-Dose, Three-Arm, and Parallel-Group Study. *J Med Food.* **2017**, *20*, 1022-1030. doi:10.1089/jmf.2017.3930.

PART III

The following manuscript was published in *Frontiers in Pharmacology* in 2020 as:

Modulation of Keap1/Nrf2/ARE signaling pathway by curcuma- and garlic-derived hybrids

Melania Serafini, **Michele Catanzaro (co-first author)**, Francesca Fagiani, Elena Simoni, Roberta Caporaso, Marco Dacrema, Irene Romanoni, Stefano Govoni, Marco Racchi, Maria Daglia, Michela Rosini and Cristina Lanni

Abstract

Nrf2 is a basic leucine zipper transcription factor that binds to the promoter region of the antioxidant response element (ARE), inducing the coordinated up-regulation of antioxidant and detoxification genes. We recently synthesized a set of new molecules by combining the functional moieties of curcumin and diallyl sulfide, both known to induce the expression of antioxidant phase II enzymes by activating Nrf2 pathway. The aim of the study is to investigate the ability of such compounds to activate Keap1/Nrf2/ARE cytoprotective pathway, in comparison with two reference Nrf2-activators: curcumin and dimethyl fumarate, a drug approved for the treatment of relapsing-remitting multiple sclerosis. Furthermore, since Nrf2 pathway is known to be regulated also by epigenetic modifications, including key modifications in microRNA (miRNA) expression, the effects of the hybrids on the expression levels of selected miRNAs, associated with Nrf2 signaling pathway have also been investigated. The results show that compounds exert antioxidant effect by activating Nrf2 signaling pathway and inducing the ARE-regulated expression of its downstream target genes, such as HO-1 and NQO1, with two hybrids to a higher extent than curcumin. In addition, some molecules induce changes in the expression levels of miR-125b-5p, even if to a lesser extent than curcumin. However, no changes have been observed in the expression levels of mRNA coding for glutathione synthetase, suggesting that the modulation of this mRNA is not strictly under the control of miR-125b-5p, which could be influenced by other miRNAs.

Keywords: curcumin; Nrf2; Keap1; NQO1; HO-1; dimethyl fumarate; miRNA.



Modulation of Keap1/Nrf2/ARE Signaling Pathway by Curcuma- and Garlic-Derived Hybrids

Melania Maria Serafini^{1,2†}, Michele Catanzaro^{1†}, Francesca Fagiani^{1,2}, Elena Simoni³, Roberta Caporaso³, Marco Dacrema⁴, Irene Romanoni¹, Stefano Govoni¹, Marco Racchi¹, Maria Daglia⁴, Michela Rosini³ and Cristina Lanni^{1*}

OPEN ACCESS

Edited by:
Filippo Caraci,
University of Catania, Italy

¹ Department of Drug Sciences, University of Pavia, Pavia, Italy, ² Scuola Universitaria Superiore IUSS, Pavia, Italy, ³ Department of Pharmacy and Biotechnology, University of Bologna, Bologna, Italy, ⁴ Department of Pharmacy, University of Napoli Federico II, Naples, Italy

INTRODUCTION

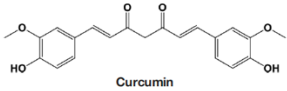
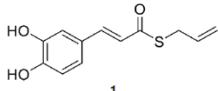
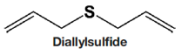
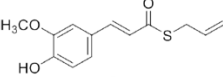
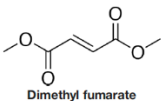
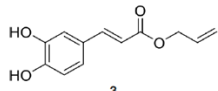
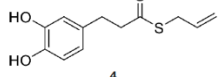
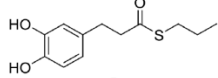
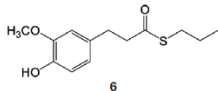
Nrf2 (NF-E2-related factor 2), a member of the Cap'n'collar (CNC) transcription factor family, is a redox-sensitive transcription factor that plays a key role in adaptation to cellular stress. Under normal homeostatic conditions, Keap1 anchors the Nrf2 transcription factor within the cytoplasm targeting it for ubiquitination and degradation by 26S proteasomes (Niture *et al.*, 2014). Under stress conditions, phosphorylation and/or redox modification of critical cysteines residues in Keap1 inhibits the enzymatic activity of the Keap1-Cul3-Rbx1 E3 ubiquitin ligase complex (Tebay *et al.*, 2015). Consequently, free Nrf2 translocates to the nucleus, where it dimerizes with Maf proteins (musculoaponeurotic fibrosarcoma) and binds to the antioxidant response element (ARE), also called electrophile response element (EpRE), a cis-acting enhancer sequence located in the promoter region of a battery of downstream genes encoding cyto-protective, antioxidant, and phase II detoxifying enzymes or proteins, such as NAD(P)H: quinone reductase-1 (NQO1), heme oxygenase-1 (HO-1), and glutathione synthetase (GSS) (Tebay *et al.*, 2015). The Nrf2/Keap1/ARE signaling pathway

can be activated by various exogenous and endogenous small molecules (Baird and Dinkova-Kostova, 2011; Paunkov *et al.*, 2019) and controls also the expression of genes involved in the regulation of cell proliferation and survival (Malhotra *et al.*, 2010).

Natural products have emerged as a great source of bioactive compounds with health beneficial impact. One example are polyphenols, phenolic compounds that act on biological systems exerting protective effects not only by direct antioxidant capacity, but also by interacting with signal-transduction pathways that regulate transcription factors and, consequently, the expression of genes and proteins (Auclair *et al.*, 2009; Spencer, 2010; Camargo *et al.*, 2010). Among the variety of pathways, it has been demonstrated that polyphenols such as curcumin, hydroxytyrosol contained in olive oil, resveratrol, and epigallocatechin-3-gallate extracted from green tea could modulate the transcription factor Nrf2, via translocation into the cell nucleus and induction of the expression of its target genes (Scapagnini *et al.*, 2011; Xicota *et al.*, 2017; Martínez-Huélamo *et al.*, 2017).

In our previous papers, we described and characterized the ability of a set of new curcuma- and garlic-derived compounds to inhibit A β oligomerization and fibrilization (Simoni *et al.*, 2016; Simoni *et al.*, 2017). The main structure of these hybrids combines the diallyl sulfide (DAS), which represents the mercaptan moiety of garlic-derived organosulfur compounds, and the hydroxycinnamoyl group, a recurring chemical function of polyphenols, such as curcumin, rosmarinic acid, and coumarin (Ho *et al.*, 2012; Witaicenis *et al.*, 2014; Nabavi *et al.*, 2015a). Our data demonstrated the ability of these molecules to act as scavenger agents in presence of oxidant stressors (Simoni *et al.*, 2016; Simoni *et al.*, 2017). In particular, we identified a catechol derivative (compound 1, see **Table 1**), with remarkable anti-aggregating ability and antioxidant properties (Simoni *et al.*, 2016). Starting from the results obtained with compound 1, which is considered the lead compound, its structure was systematically modified by focusing on the aryl substitution pattern, the thioester function, and the aliphatic skeleton with the aim of strategically tuning the pharmacological profile (Simoni *et al.*, 2017). Herein, to investigate the structure-dependent activation of intracellular defensive

pathways, we focused on a selection of these hybrids (compounds 1–6, **Table 1**). Two reference molecules, known to activate Nrf2 pathway, were used for comparison: curcumin (CURC) and dimethyl fumarate (DMF), whose structure are also reported in **Table 1**. CURC has been extensively studied in different pathological contexts and, while to date there are no confirmed applications in humans due to the failure of clinical trials, its antioxidant properties are well-known and confirmed by a plethora of publications (Darvesh *et al.*, 2012; Shen *et al.*, 2013; Vera-Ramirez *et al.*, 2013; Nabavi *et al.*, 2015b; Serafini *et al.*, 2017; Catanzaro *et al.*, 2018). DMF has been approved by the Food and Drug Administration (FDA) for the treatment of relapsing-remitting multiple sclerosis and its anti-inflammatory and antioxidant properties are widely reported in literature (for an extensive review see Suneetha and Raja Rajeswari, 2016; Saidu *et al.*, 2019).

Combined compounds	Derived hybrid compounds	
	Structure	Functional groups
 <p>Curcumin</p>	 <p>1</p>	<ul style="list-style-type: none"> • Michael acceptor • Catechol moiety • Thioester • Terminal double bond
 <p>Diallylsulfide</p>	 <p>2</p>	<ul style="list-style-type: none"> • Michael acceptor • Thioester • Terminal double bond
 <p>Dimethyl fumarate</p>	 <p>3</p>	<ul style="list-style-type: none"> • Michael acceptor • Catechol moiety • Terminal double bond
	 <p>4</p>	<ul style="list-style-type: none"> • Catechol moiety • Thioester • Terminal double bond
	 <p>5</p>	<ul style="list-style-type: none"> • Catechol moiety • Thioester
	 <p>6</p>	<ul style="list-style-type: none"> • Thioester

Compound 1: S-allyl (E)-3-(3,4-dihydroxyphenyl)prop-2-enethioate;
 Compound 2: S-allyl (E)-3-(4-hydroxy-3-methoxyphenyl)prop-2-enethioate;
 Compound 3: allyl (E)-3-(3,4-dihydroxyphenyl)acrylate;
 Compound 4: S-allyl 3-(3,4-dihydroxyphenyl)propanethioate;
 Compound 5: S-propyl 3-(3,4-dihydroxyphenyl)propanethioate;
 Compound 6: S-propyl 3-(4-hydroxy-3-methoxyphenyl)propanethioate

Table 1. Design strategy of curcuma- and garlic-derived compounds.

To investigate the potential interplay of compounds 1-6 with the Nrf2 cellular pathway, we first evaluated their ability to modulate the expression of the Nrf2 transcription factor and its negative regulator Kelch-like ECH-associated protein 1 (Keap1), as well as its nuclear translocation and the activation of Nrf2 downstream target genes in human neuroblastoma SH-SY5Y cells, a cell line commonly used to perform preliminary molecules screening and to dissect the underlying molecular mechanism (Narasimhan *et al.*, 2012; Park *et al.*, 2014; de Oliveira *et al.*, 2019). In addition, a growing body of evidence demonstrated that several natural products, such as polyphenols, exert their protective effect through the induction of different epigenetic changes, including key modifications in microRNAs (miRNAs) expression (Howell *et al.*, 2013; Curti *et al.*, 2014; Boyanapalli and Kong, 2015; Liang and Xi, 2016; Curti *et al.*, 2017; Pandima Devi *et al.*, 2017). MiRNAs are small non-coding RNA molecules of ~22 nucleotides in length, which are endogenously expressed and play a key role in RNA-silencing and post-transcriptional regulation of gene expression. Indeed, those noncoding RNAs modulate gene expression by suppressing translation and/or reducing the stability of their target mRNAs and consequently their target proteins. In fact, their binding to the target mRNAs, usually at the 3'-UTR, induces the recruitment of the RNA-induced silencing complex (RISC) that represses the translation of target mRNAs or enhances their cleavage (Bartel, 2004). MiRNAs can target in a combinatorial fashion a great variety of genes, which, in turn, indirectly modulate the expression of thousands of genes.

Recent studies revealed important roles of miRNAs in the control of Nrf2 activity. In addition, Nrf2 itself has been identified as a regulator of miRNAs, suggesting a loop system of mechanisms (Kurinna and Werner, 2015). In particular, miRNAs could directly target the Nrf2 mRNA and the mRNAs encoding for proteins that control the level and activity of Nrf2. As a transcription factor, Nrf2 can regulate not only the expression of protein coding parts of the genome, but also protein non-coding parts of the genome which, in turn, contains the majority of functional Nrf2-binding sites (Hirotsu *et al.*, 2012). In silico analysis by Papp and colleagues predicted 85 Nrf2-miRNA interactions, with 63 miRNAs able to directly or indirectly regulate Nrf2 (Papp *et al.*, 2012).

In line with these premises, the investigation of miRNA modulation could potentially be important in providing novel insights for a better understanding of the antioxidant activities of natural products and hybrids. Hence, we further investigated whether compounds are capable to exert epigenetic effects by modulating specific miRNAs associated with Nrf2 signaling pathway.

MATERIAL AND METHODS

Reagents

Compounds were synthesized according to previous procedures (Simoni *et al.*, 2016; Simoni *et al.*, 2017). Final compounds were >98% pure as determined by High Performance Liquid Chromatography (HPLC) analyses. The analyses were performed under reversed-phase conditions on a Phenomenex Jupiter C18 (150 × 4.6 mm I.D.) column, using a binary mixture of H₂O/acetonitrile (60/40, v/v for 1, 2; 65/35, v/v for 3; 50/50, v/v for 4, 5, 6) as the mobile phase, UV detection at $\lambda = 302$ nm (for 1, 2, 3) or 254 nm (for 4, 5, 6), and a flow rate of 0.7 ml/min. Analyses were performed on a liquid chromatograph model PU-1585 UV equipped with a 20 ml loop valve (Jasco Europe, Italy). CURC (CAS number 08511) and DMF (CAS number 242926) were $\geq 98\%$ and $\geq 97\%$ pure respectively, and were purchased by Sigma-Aldrich (Merck KGaA, Darmstadt, Germany). All compounds were solubilized in DMSO at stock concentrations of 10 mM, frozen (-20°C) in aliquots and diluted in culture medium immediately prior to use. For each experimental setting, a stock aliquot was thawed and diluted to minimize repeated freeze and thaw damage. The final concentration of DMSO in culture medium was less than 0.1%. Cell culture media and all supplements were purchased from Sigma-Aldrich (Merck KGaA, Darmstadt, Germany). Rabbit polyclonal anti-human Nrf2 (NBP1-32822), mouse monoclonal anti-human NQO1 (NB200-209), and rabbit polyclonal anti-human HO-1 (NBP1-31341) antibodies were purchased from Novus (Biotechnique, Minneapolis, USA). Mouse monoclonal anti-human Keap1 antibody (MAB3024) was purchased from R&D Systems

(Biotechne, Minneapolis, USA). Mouse monoclonal anti-human β -actin (612656) and mouse anti-human lamin A/C (612162) antibodies were purchased from BD Biosciences (Franklin Lakes, NJ, USA). Finally, mouse anti-human α -tubulin (sc-5286) and mouse anti-human GSS (sc-166882) antibodies were purchased from Santa Cruz Biotechnology (Dallas, Texas, USA).

SH-SY5Y Cell Cultures

Human neuroblastoma SH-SY5Y cells from the European Collection of Cell Cultures (ECACC No. 94030304) were cultured in a medium with equal amounts of Eagle's minimum essential medium and Nutrient Mixture Ham's F-12, supplemented with 10% heat-inactivated fetal bovine serum (FBS), 2 mM glutamine, 0.1 mg/ml streptomycin, 100 IU/ml penicillin and non-essential amino acids at 37°C in 5% CO₂-containing, and 95% air atmosphere. All culture media, supplements and FBS were purchased from Sigma-Aldrich (Merck KGaA, Darmstadt, Germany).

Cell Viability

The mitochondrial dehydrogenase activity that reduces 3-(4,5-dimethylthiazol-2-yl)-2,5-diphenyl-tetrazolium bromide (MTT, Sigma-Aldrich, Merck KGaA, Darmstadt, Germany) was used to determine cell viability using a quantitative colorimetric assay (van Meerloo *et al.*, 2011; Kumar *et al.*, 2018). At day 0, SH-SY5Y cells were plated in 96-well plates at a density of 2.5×10⁴ viable cells per well, respectively. After treatment, according to the experimental setting, cells were exposed to an MTT solution (1 mg/ml) in complete medium. After 4 hours of incubation with MTT, we lysed cells with sodium dodecyl sulfate (SDS) for 24 hours and cell viability was quantified by reading absorbance at 570 nm wavelength, using a Synergy HT multi-detection micro-plate reader (Bio-Tek).

Subcellular Fractionation for Nrf2 Nuclear Translocation

The expression of Nrf2 in nuclear SH-SY5Y cell lysates was assessed by Western blot analysis. Cell monolayers were washed twice with ice-cold PBS,

harvested, and subsequently homogenized 20 times using a glass-glass homogenizer in ice-cold fractionation buffer (20 mM Tris/HCl pH 7.4, 2 mM EDTA, 0.5 mM EGTA, 0.32 M sucrose, 50 mM β -mercaptoethanol). The homogenate was centrifuged at 300g for 5 minutes to obtain the nuclear fraction. An aliquot of the nuclear extract was used for protein quantification by Bradford method, whereas the remaining was boiled at 95°C for 10 minutes after dilution with 2 \times sample buffer (125 mM Tris-HCl pH 6.8, 4% SDS, 20% glycerol, 6% β -mercaptoethanol, 0.1% bromophenol blue). Equivalent amount of nuclear extracted proteins (30 μ g) were subjected to polyacrylamide gel electrophoresis and immunoblotting as described below.

Immunodetection of Nrf2, Keap1, NQO1, and HO-1

The expression of Nrf2, Keap1, NQO1, and HO-1 in whole cell lysates or nuclear extracts was assessed by Western blot analysis. After treatment, cell monolayers were washed twice with ice-cold PBS, lysed on the culture dish by the addition of ice-cold homogenization buffer (50 mM Tris-HCl pH 7.5, 150 mM NaCl, 5 mM EDTA, 0.5% Triton X-100, and protease inhibitor mix). Samples were sonicated and centrifuged at 13,000g for 10 seconds at 4°C. The resulting supernatants were transferred into new tubes, and protein content was determined by Bradford method. For Western blot analysis, equivalent amounts of both total and nuclear extracts (30 μ g) were electrophoresed in 10% acrylamide gel, under reducing conditions, then, electroblotted into PVDF membranes (Merck KGaA, Darmstadt, Germany), blocked for 1 hour with 5% w/v bovine serum albumin (BSA) in TBS-T (0.1 M Tris-HCl, pH 7.4, 0.15 M NaCl, and 0.1% Tween 20), and incubated overnight at 4°C with primary antibodies diluted in 5% w/v BSA in TBS-T. The proteins were visualized using primary antibodies for Nrf2 (1:2,000), Keap1 (1:1,000), NQO1 (1:2,000), or HO-1 (1:2,000). Detection was carried out by incubation with secondary horseradish peroxidase-conjugated antibodies (1:5,000) diluted in 5% w/v BSA in TBS-T for 1 hour at room temperature. Membranes were subsequently washed three times with TBS-T and proteins of interest were visualized using an enhanced chemiluminescent reagent (Pierce, Rockford, IL, USA). β -Actin, α -tubulin, and lamin A/C were performed as control for gel loading.

Real-Time PCR (RT-qPCR)

Total RNA was extracted from SH-SY5Y cells by using a RNeasy Plus Mini Kit (Qiagen, Valencia, CA, USA) following the manufacturer's instructions. QuantiTect reversion transcription kit and QuantiTect SYBR Green PCR kit (Qiagen, Valencia, CA, USA) were used for cDNA synthesis and gene expression analysis, following the manufacturer's specifications. Nrf2, Keap1, NQO1, HO-1, GSS, and GAPDH primers (genome wide bioinformatically validated primers sets) were provided by Qiagen (QuantiTect Primer Assays; Qiagen, Valencia, CA, USA). GAPDH was used as an endogenous reference.

MicroRNA Analysis

After the extraction procedure, the RNA quantification was assessed using a spectrophotometric method with FLUOstar® Omega (BMG LABTECH, Ortenberg, Germany) and the LVIS plate, following the operating manual instructions. RNA purity was assessed by calculating the 260/280 absorbance ratio. After quantification, a RTII Retrotranscription Kit (Qiagen) was used to promote the retrotranscription of exclusively mature miRNA following the manufacturer's instructions. The cDNA was diluted with RNase-free water prior to start the RT-qPCR procedure. To verify the expression of miRNA targets, a miScript® miRNA PCR Array (Qiagen) was used, following the manufacturer's instructions. We performed the RT-qPCR using StepOnePlus RT-qPCR (Applied Biosystem, Foster City, California, USA). The primers were purchased from Qiagen, with specific forward primers contained in the miScript® miRNA PCR Array and with reverse primers contained in the in miScript SYBR® Green PCR Array. For each plate the amplification conditions were set as follows: 95°C for 15 minutes, 94°C for 15 seconds, 55°C for 30 seconds, and 70°C for 30 seconds. The last three steps were repeated for 45 cycles. SNORD61 and RNU6-6P were used as endogenous controls.

Densitometry and Statistics

All experiments were performed at least three times. Data are expressed as mean \pm SEM. The acquisition of the Western blotting images was done

through a scanner and the relative densities of the bands were analyzed with ImageJ software. Statistical analyses were performed using GraphPad Software version 7.0 (La Jolla, CA, USA). Statistical differences were determined by analysis of variance (ANOVA) followed, when significant, by an appropriate *post hoc* test as indicated in figure legends. For miRNA expression, we used linear mixed models, including treatments as fixed terms and plates as random effects, which allowed for different intercepts for each run. In miRNA figures, the points indicate the mean value while the bars represent the SEM. In all reported statistical analyses, effects were designated as significant with a p-value < 0.05. Statistical analyses were performed using R software version 3.4.1 (R Core Team, 2018).

RESULTS

Cellular Toxicity of Curcuma- and Garlic- Derived Compounds

The cytotoxicity of compounds 1–6 has been assessed by MTT assay in SH-SY5Y human neuroblastoma cells, in comparison with CURC and DMF. Cells were exposed to the compounds and CURC at concentrations ranging from 1 to 12.5 μM for 24 hours. The concentrations for DMF were chosen basing on literature data (Brennan *et al.*, 2015; Campolo *et al.*, 2018) and a range of concentrations starting from 1 μM to 50 μM has been analyzed.

As shown in **Figure 1**, all the compounds were well tolerated (reduction of cell viability of about 10%) at a concentration up to 5 μM , with the exception of the prototype 1, that at 5 μM induced a slight decrease (about 20%) in cell viability, consistent with our previous data (Simoni *et al.*, 2017).

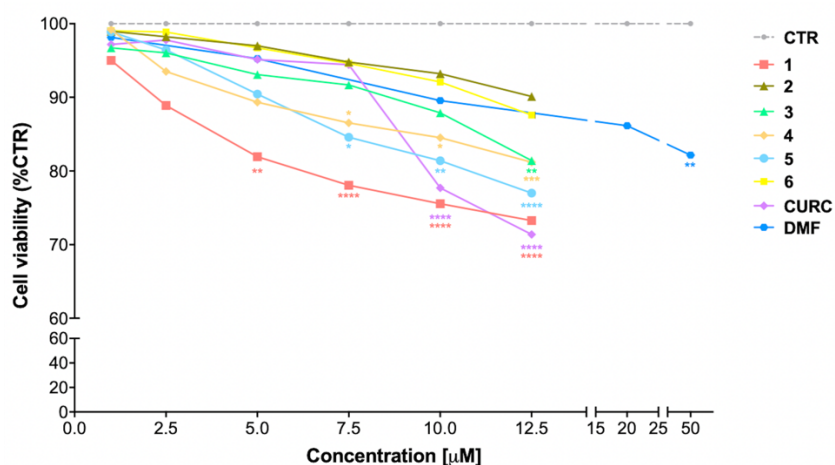


Figure 1. Cellular toxicity of hybrid compounds (1-6), curcumin (CURC), and dimethyl fumarate (DMF) on human neuroblastoma SH-SY5Y. Cells were treated with compounds 1-6 and CURC for 24 hours at different concentrations ranging from 1 to 12.5 µM. DMF was used in a range of concentrations starting from 0.5 µM till to 50 µM. Cell viability was assessed by MTT assay. Data are expressed as percentage of cell viability versus CTR; * $p < 0.05$, ** $p < 0.01$ and **** $p < 0.0001$ versus CTR; Dunnett's multiple comparison test ($n \geq 5$).

Modulation of Nrf2 and Its Negative Regulator Keap1

To understand the molecular mechanisms underlying the antioxidant activity of compounds 1-6, we decided to investigate the Nrf2 pathway, which plays a key role in orchestrating cellular antioxidant defenses and in maintaining cellular redox homeostasis. To analyze the modulation of the Nrf2-mediated detoxification pathway, we performed RT-qPCR and Western immunoblotting in SH-SY5Y human neuroblastoma cells exposed to compounds 1-6 and CURC at the concentration of 5 µM or to DMF at the concentration of 20 µM for 24 hours (**Figure 2**). All compounds tested did not affect the mRNA levels of Nrf2 (**Figure 2A**) and Keap1 (**Figure 2B**), neither Keap1 protein amount (**Figure 2D**). In contrast, a strong increase in Nrf2 protein expression (**Figure 2C**) is induced by all compounds, with the exception of compound 6. DMF treatment did not produce statistically significant results in our experimental setting, although an increase trend could be assumed. Altogether, these results show that all compounds tested,

with the exception of compound 6, modulate Nrf2 protein levels, but do not act at the transcriptional level.

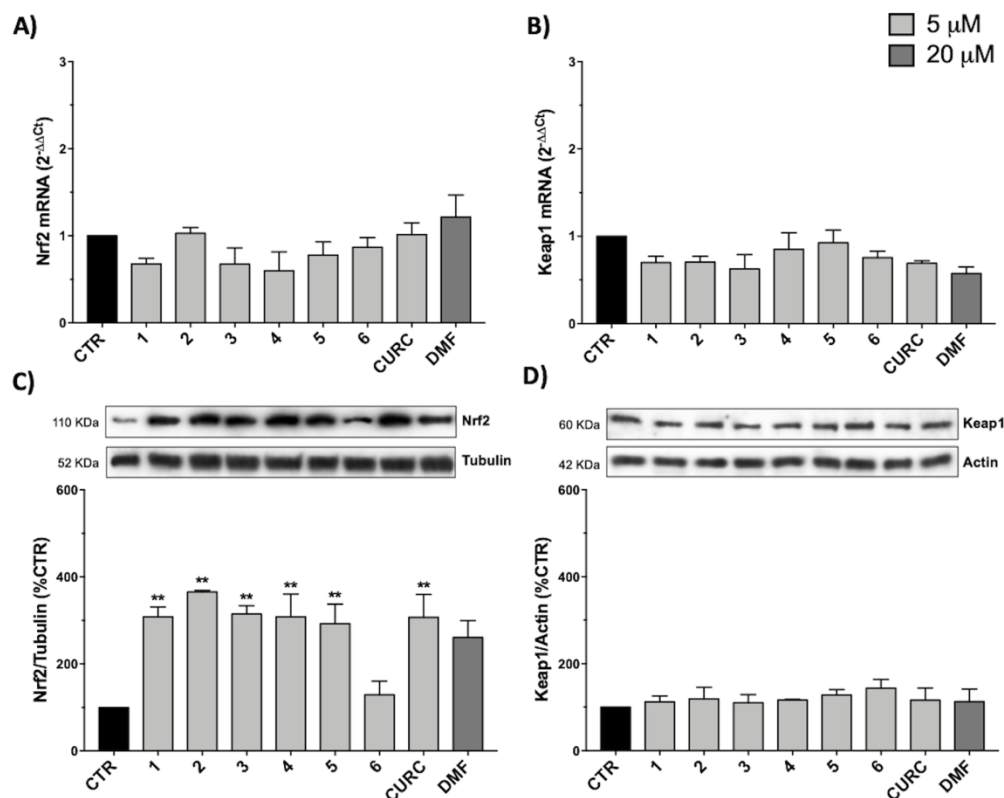


Figure 2. Modulation of Nrf2 and Keap1 mRNA and protein levels by compounds 1-6, curcumin (CURC), and dimethyl fumarate (DMF). (A-B) RNA from total cellular extracts of SH-SY5Y cells treated for 24 hours with 5 μ M compounds or 20 μ M DMF were analyzed for Nrf2 (A) and Keap1 (B) mRNA expression by RTqPCR. GAPDH was used as housekeeping gene. Results are shown as mean \pm SEM; no statistically significant data with Dunnett's multiple comparison test (A, $n = 3$, F ratio = 1.249; B, $n = 3$, F ratio = 1.671). (C-D) Cellular extracts of SH-SY5Y cells treated for 24 hours with compounds at 5 μ M or 20 μ M DMF were analyzed for Nrf2 (C) and Keap1 (D) protein levels by Western blot. Anti-tubulin was used as protein loading control. Results are shown as ratio (% of CTR) \pm SEM; ** $p < 0.01$, versus CTR; Dunnett's multiple comparison test (C, $n \geq 5$, F ratio = 3.981; D, $n = 3$, F ratio = 0.4049).

Nuclear Translocation of the Nrf2 Transcription Factor

Since Nrf2 nuclear translocation is an essential step for the complete activation of its pathway, we further examined the ability of the hybrids to induce the nuclear localization of Nrf2 in SH-SY5Y, by comparing their effects with CURC and DMF.

Data from literature suggest that a pro-electrophilic moiety (catechol) and/or an electrophilic moiety (the Michael acceptor α,β -unsaturated carbonyl group) are important structural functions for Nrf2 induction (Tanigawa *et al.*, 2007; Satoh *et al.*, 2013). The tested compounds were selected to delineate the structural requirements responsible for the activation of the transcription factor and its downstream signaling pathway. The six hybrids investigated in this study differ from each other by the presence or absence of the mentioned key functional groups (**Table 1**). Indeed, the compounds 1 and 3 provide the catechol moiety as well as the Michael acceptor group. The compounds 4 and 5 lack the Michael acceptor function but have the catechol moiety, whereas 2 shows only the Michael acceptor. The compound 6 was chosen as negative control, lacking for both Michael acceptor and catechol function. Moreover, the effects of CURC and DMF as positive controls have also been investigated.

SH-SY5Y cells were treated with the compounds at different concentrations: 5 μ M, 500 nM, and 50 nM of 1–6 and CURC or 20 μ M, 10 μ M, and 5 μ M of DMF. As indicated in **Figure 3A**, all tested hybrids, except 6, lacking for both electrophilic features, are capable to significantly induce Nrf2 nuclear translocation at their highest concentration. This result indicates that Nrf2 nuclear translocation may rely on the presence of both the α,β -unsaturated carbonyl function and the catechol group, either alone or in combination, thus suggesting that nucleophilic addition of Keap1 cysteine residues to (pro)- electrophilic portions of the molecule might activate the Nrf2 pathway. Moreover, 1 and 5 significantly induce Nrf2 nuclear localization at the intermediate concentration of 500 nM, whereas 1 also at a concentration of 50 nM. None of the molecules, with the exception of 1, were found to act on the Nrf2 pathway at the lowest concentrations investigated (i.e., 50 nM).

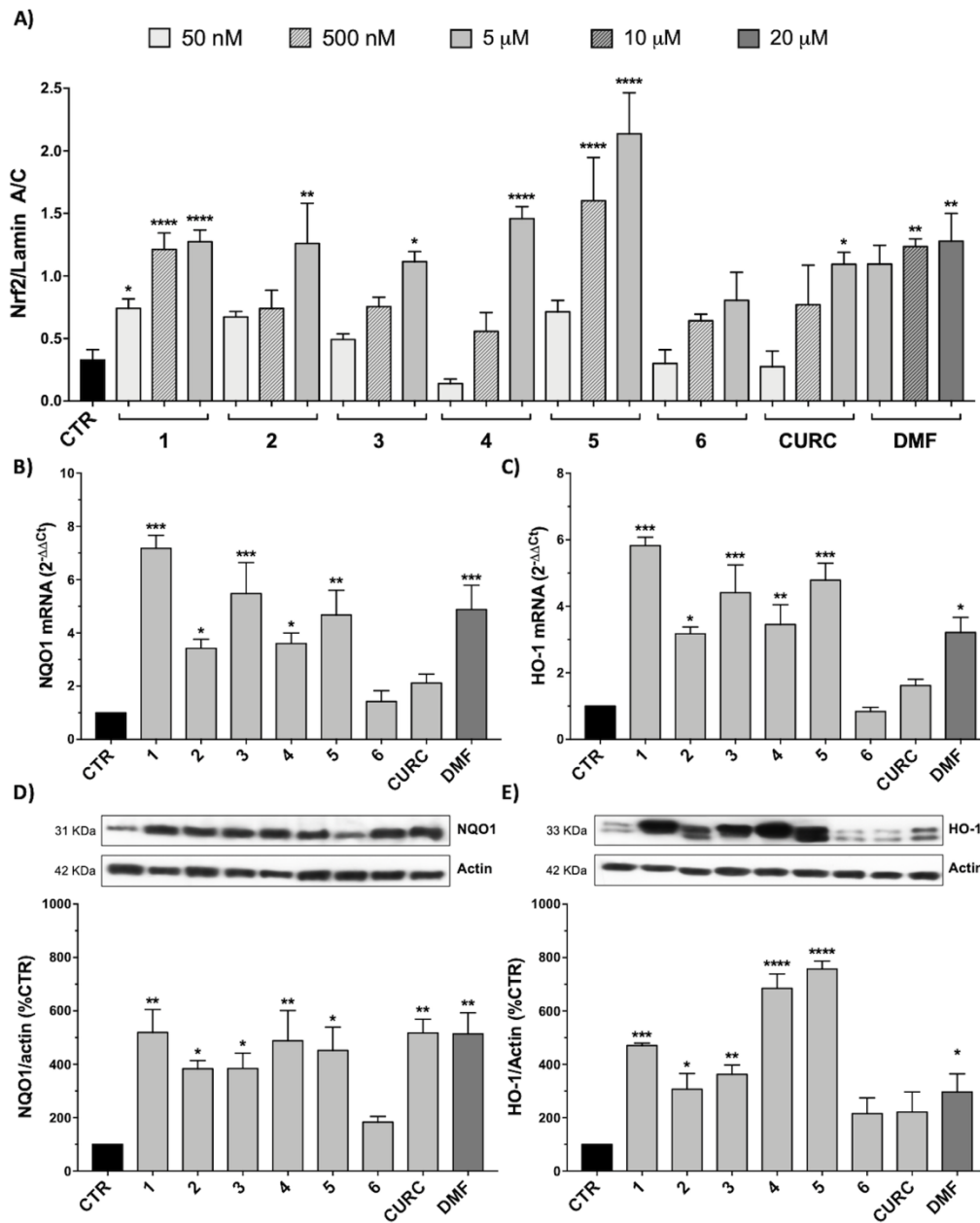


Figure 3. Nrf2-pathway activation by hybrids: nuclear translocation and targets induction. (A) Nuclear cellular extracts of SH-SY5Y cells were treated for 3 hours with compounds at 5 μM, 500 nM, and 50 nM or with 20, 10, and 5 μM dimethyl fumarate (DMF). Nrf2 protein content in the nucleus was determined by Western blot. Anti-lamin A/C was used

as a protein loading control. Results are shown as ratio Nrf2/lamin A/C \pm SEM; * p < 0.05, ** p < 0.01 and **** p < 0.0001 *versus* CTR; Dunnett's multiple comparison test (F ratio = 6.797, $n \geq 3$). **(B-C)** RNA from total cellular extracts of SH-SY5Y cells, treated for 24 hours with 5 μ M compounds or 20 μ M DMF, were analyzed for NQO1 **(B)** and HO-1 **(C)** mRNA expression by RT-qPCR. GAPDH was used as housekeeping gene. Results are shown as mean \pm SEM; * p < 0.05, ** p < 0.01, and **** p < 0.001 *versus* CTR; Dunnett's multiple comparison test (B, $n \geq 3$, F ratio = 10.44; C, $n \geq 3$, F ratio = 13.95). **(D-E)** Cellular extracts of SH-SY5Y cells treated for 24 hours with compounds at 5 μ M or 20 μ M DMF were analyzed for NQO1 **(D)** and HO-1 **(E)** protein levels by Western blot. Anti-actin was used as protein loading control. Results are shown as ratio (% of CTR) \pm SEM; * p < 0.05, ** p < 0.01, *** p < 0.001, and **** p < 0.0001 *versus* CTR; Dunnett's multiple comparison test (D, $n \geq 3$, F ratio = 5.144; E, $n \geq 3$, F ratio = 17.26).

Activation of the Nrf2 Target Genes

To demonstrate the complete activation of Nrf2 pathway by the synthesized hybrids, the expression of two Nrf2 target genes has also been evaluated. Indeed, once in the nucleus, Nrf2 binds to the ARE sequences in the promoter region of its target genes, inducing the expression of phase II cyto-protective genes related to cellular stress response, such as those codifying for NQO1 and HO-1. The mRNA expression and protein levels of these two genes were evaluated by RT-qPCR and Western blot in SH-SY5Y, treated with compounds 1-6 and CURC at the concentration of 5 μ M and with 20 μ M DMF for 24 hours. As shown in **Figure 3**, all compounds, with the exception of 6 and CURC, induced an increase in NQO1 mRNA levels (**Figure 3B**), followed by an increase in NQO1 protein with the exception of 6 (**Figure 3D**). In a similar way, the mRNA (**Figure 3C**) and protein (**Figure 3E**) levels of HO-1 are positively modulated by all hybrids except 6, and CURC. The increase in transcription and translation of two Nrf2 target genes demonstrates the complete activation of the Nrf2 pathway.

To explain the discrepancy between the obtained data showing the loss of efficacy of CURC on Nrf2 target gene activation, we further evaluated whether such result may rely on the timing of the treatment. Thus, we performed a time course using CURC and compound 1, as an example of the most active hybrid compound. SH-SY5Y cells were treated with compound 1 or CURC at the concentration of 5 μ M for 3, 6, 9, 16, and 24 hours. NQO1 (**Figures 4A,**

B) and HO-1 (**Figures 4C, D**) mRNAs levels were differently regulated in time, with NQO1 slowly increasing and HO-1 being boosted for 3 hours and, then, decreasing with time. Treatment with compound 1 induced a significant increase in relative NQO1 mRNA levels from 6 hours to 16 hours (**Figure 4A**), whereas CURC treatment induced an increase at 6 hours, which reached a peak at 9 hours and then lost statistical significance by 16 hours (**Figure 4B**). Treatment with compound 1 induced a strong increase in HO-1 mRNA levels, already statistically significant at 3 hours, then decreasing with time (**Figure 4C**). Here, the effect of curcumin was similar to that induced by hybrid 1, though the increase in the HO-1 mRNA levels was smaller (**Figure 4C**). Taken together, these data demonstrate that CURC induces a significant increase in NQO1 and HO-1 mRNA and protein levels at different times of treatment compared to compound 1. These results suggest that compounds may affect the Nrf2 pathway through different temporal kinetics.

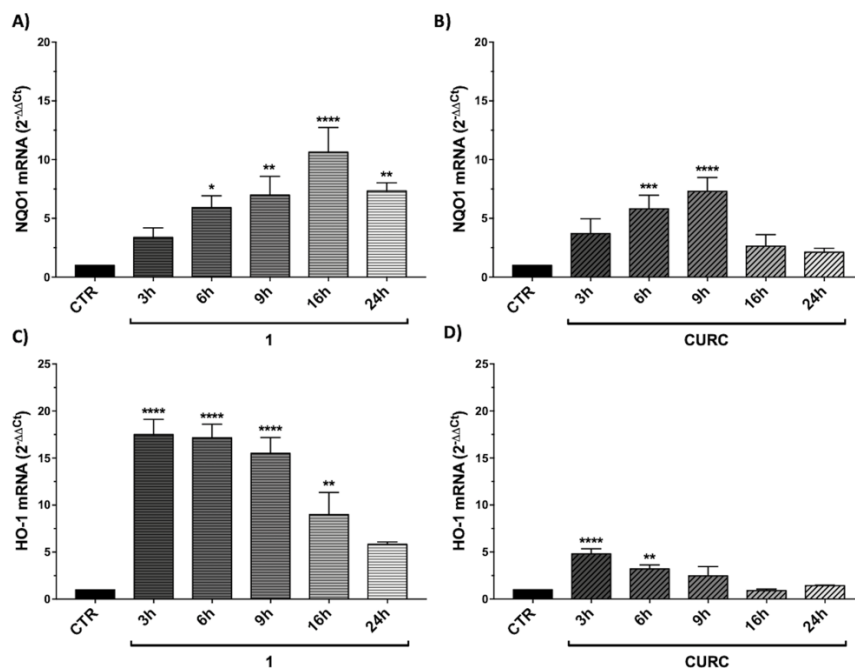


Figure 4. Time-dependent modulation of Nrf2 targets by compound 1 and curcumin. RNA from total cellular extracts of SH-SY5Y cells, treated for 3, 6, 9, 16, and 24 hours with 5 μ M compounds 1 and curcumin (CURC), were analyzed for NQO1 (**A-B**) or HO-1 (**C-D**) relative

mRNA expression by RT-qPCR. GAPDH was used as housekeeping gene. Results are shown as mean \pm SEM; * p < 0.05, ** p < 0.01, *** p < 0.001, and **** p < 0.0001 versus CTR; Dunnett's multiple comparison test (A, $n \geq 3$, F ratio = 9.346; B, $n \geq 3$, F ratio = 10.44; C, $n \geq 3$, F ratio = 18.02; D, $n \geq 3$, F ratio = 13.87).

Modulation of miRNAs Related to the Nrf2 Signaling Pathway

To deepen the understanding of the mechanism through which the selected hybrids exert their antioxidant activities, in comparison to CURC, we determined the expression levels of different miRNAs in SH-SY5Y cell cultures. MiRNAs were chosen on the basis of their predicted targets with the aid of miRTarBase (<http://miRTarBase.mbc.nctu.edu.tw/>) an open access database which provides information about experimentally validated miRNA-target interactions (Chou *et al.*, 2018). One single miRNA could have multiple targets, thus we focused our attention on miRNAs, which could modulate the mRNA, and consequently the protein amount, of genes involved in the Nrf2 signaling pathway, such as those codifying for HO-1 (hsa-miR-196a-5p), GSS (hsa-miR-125b-5p), and SOD2 (hsa-miR-222-3p, hsa-miR-17-3p).

SH-SY5Y human neuroblastoma cells were treated with compounds 1-6 and CURC at different concentrations (5 μ M, 500 nM, and 50 nM) for 24 hours. Total RNA was extracted from treated and control cell cultures, as according to the Material and Methods section, and RT-qPCR assays were performed.

Among all the miRNAs analyzed, only hsa-miR-125b-5p results to be modulated with a statistically significant p-value. Data from literature indicate that hsa-miR-125b-5p is involved in oxidative stress, since it has mRNA coding for GSS as target (Chou *et al.*, 2016). As far as hsa-miR-125b-5p is concerned, the results obtained following statistical analysis suggest that the expression level of this miRNA is downregulated after treatment with CURC at all concentrations (**Figure 5**). In addition, significant differences in miRNA expression levels were registered between the control and the following treatments: 5 μ M and 500 nM of 2, 5 μ M of 3, 50 nM of 4, 50 nM and 500 nM of 5, and 50 nM and 500 nM of 6. The decrease in miR-125b-5p after

treatment with compounds 2-6 and CURC at different concentrations confirms that they have the capacity to modulate miRNAs involved in protection against oxidative stress. Nevertheless, the compounds tested did not significantly modulate the expression of mRNA coding for GSS, even if CURC at all concentrations shows an increased trend in line with the reduction of miR-125b-5p (**Table 2**). These data suggest that the process of GSS synthesis is regulated by other molecular mechanisms and the modulation of this mRNA is not strictly under the control of miR-125b-5p.

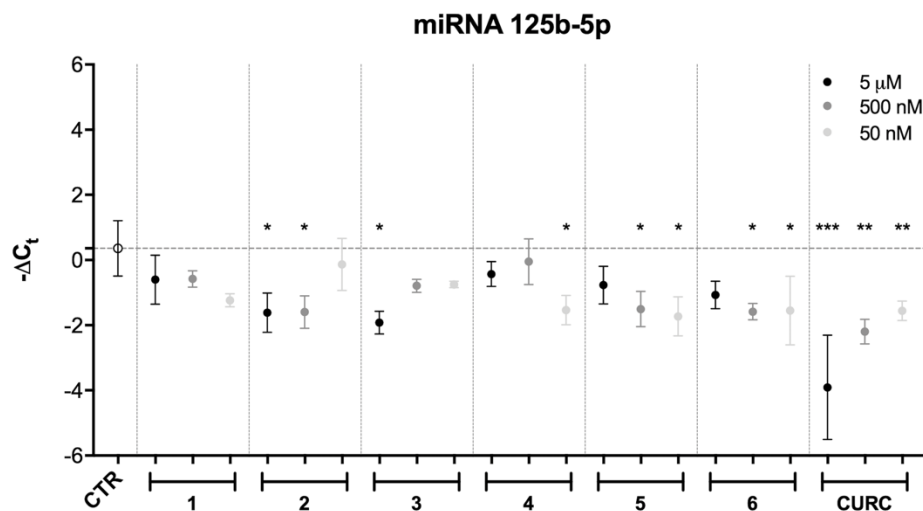


Figure 5. miRNA modulation by hybrids and curcumin. Expression levels (-Delta CT) of hsa-miR-125b-5p in SH-SY5Y cells treated with different newly synthesized compounds at different concentrations (50 and 500 nM). Results are shown as mean \pm SEM; * p < 0.05, ** p < 0.01, and *** p < 0.001 versus CTR; Dunnett's multiple comparison test (n = 3, F ratio = 4.584).

GSS mRNA ($2^{-\Delta\Delta C_t}$)			
Compound	Concentration		
	5 μ M	500 nM	50 nM
1	0.83 \pm 0.25	1.16 \pm 0.12	0.61 \pm 0.10
2	1.07 \pm 0.14	1.04 \pm 0.35	1.14 \pm 0.05
3	1.17 \pm 0.03	0.96 \pm 0.02	1.08 \pm 0.24
4	1.25 \pm 0.22	1.31 \pm 0.25	1.10 \pm 0.10
5	1.42 \pm 0.29	0.97 \pm 0.25	1.90 \pm 0.44
6	1.18 \pm 0.21	1.22 \pm 0.42	1.19 \pm 0.23
CURC	1.81 \pm 0.25	1.93 \pm 0.45	2.24 \pm 0.61

Table 2. GSS mRNA levels modulation. RNA from total cellular extracts of SHSY5Y cells treated for 24 hours at different concentrations (50, 500 nM, and 5 μ M) of compounds were analyzed for GSS mRNA expression by RT-qPCR. GAPDH was used as housekeeping gene. Results are shown as mean \pm SEM.

DISCUSSION

Nrf2 is a redox-sensitive transcription factor that has been described to play a critical role in adaptation to cellular stress and affords cellular defense by initiating transcription of antioxidant phase II and detoxification genes (Tebay *et al.*, 2015). The hybrids here tested have been demonstrated to modulate in an *in vitro* model the activation of Nrf2-pathway and the ARE-controlled expression of its target genes codifying cyto-protective enzymes (i.e., NQO1 and HO-1).

The mechanism at the basis of the effects exerted by the compounds has been shown not to be related to the modulation in the transcription levels of Nrf2 and Keap1 (**Figures 2A, B**), as well as in the protein levels of Keap1 (**Figure 2D**), thus suggesting that in our experimental setting the increase in Nrf2 (**Figure 2C**) protein expression is not due to a decreased transcription or translation of the negative regulator Keap1. We hypothesize that compounds may directly interact with Keap1, preventing its binding to Nrf2 and, consequently, the ubiquitination process, by possibly modifying the

sulfhydryl groups of cysteine residues on Keap1 and inhibiting Keap1-Nrf2 protein-protein interaction.

Subsequently, free Nrf2 in the cytoplasm could escape proteasome-targeted degradation and migrate into the nucleus to carry out its activities as a transcription factor. A proof of the hypothesis of an electrophile-based modulation of the Nrf2- pathway [consistently with what reviewed by (Basagni *et al.*, 2019)] is the lack of efficacy in activating Nrf2 observed for compound 6, which, lacking a (pro)electrophile feature is not able to engage covalent bond with cysteine residues of Keap-1 (**Figure 3**). Combining virtual screening/molecular docking with focused exploration of structure-activity relationships (SAR) of our compounds could significantly contribute to investigate the mode of action of the hybrid compounds at a molecular level, opening prospects for further investigation. Beyond the activation of the Nrf2 pathway in a Keap1-dependent manner, data from literature further indicate that polyphenols, such as CURC, and DMF are capable to activate Nrf2 by other pathways or alternative mechanisms, including glutathione (GSH) depletion (Schmidt *et al.*, 2007; Satoh *et al.*, 2013; Brennan *et al.*, 2015). GSH is known to play an important role in cellular defense against various stressors and its depletion has been also suggested to be protective against inflammation and neurodegeneration (Ewing and Maines, 1993; Aschner, 2000). Electrophiles such as curcumin and DMF have been found to induce severe side effects, due to their non-specific interaction with cysteine thiols of GSH, consequently reducing GSH levels (Satoh *et al.*, 2013; Brennan *et al.*, 2015). In our hand, we found that, unlike CURC, the curcuma- and garlic-inspired compounds seem not to affect the expression of GSS (**Table 2**), thus suggesting a lack of modulation in glutathione levels. This hypothesis is also supported by the results that only CURC at all the concentrations tested induces epigenetic changes through modifications in miR-125b-5p expression (**Figure 5**), in turn modulating the expression levels of mRNA coding for glutathione synthetase. Taking into account that electrophiles have complex time- and dose-dependent relationships with cellular GSH (Jobbagy *et al.*, 2019), whether this different effect on the regulation of glutathione levels is specific only for CURC and not for our hybrids requires further investigation.

In conclusion, we have characterized, by using *in vitro* techniques, a pathway by our hybrids, which emerge as promising pharmacological tools. However, we are conscious that to translate these positive outcomes in a potential therapeutic benefit, the obtained results require to be validated in *in vivo* models. Indeed, also curcumin, whose antioxidant properties are well recognized by a plethora of publications (Darvesh *et al.*, 2012; Shen *et al.*, 2013; Vera-Ramirez *et al.*, 2013; Nabavi *et al.*, 2015b; Serafini *et al.*, 2017; Catanzaro *et al.*, 2018), to date does not show confirmed applications in humans due to the failure of clinical trials. Some considerations can be made on this point. A direct antioxidant effect *in vivo* may be limited by several factors, such as bioavailability, metabolic reactions, and modification of intracellular concentrations (Crespo *et al.*, 2015). Furthermore, recent data highlight attention when referring to the use of antioxidants for supplement practice. Not only positive effects, but also negative outcomes have been observed when analyzing large numbers of studies (Visioli, 2015). As an example, the use of antioxidant mixtures (a combination of vitamins A, C, E, beta-carotene, selenium, and zinc) in the cardiovascular disease prevention has been found in several studies not to show benefits, but to result in an increase in all-cause mortality (Jenkins *et al.*, 2018). Hence, a careful evaluation also concerning the lifestyle or other dietary factors adopted by supplement users requires multiple assessments over time.

Based on these considerations, we believe that the results here exposed evaluating the activity of hybrids 1-6 in *in vitro* studies, are promising. However, whether these profiles might result in better translational outcomes require further *in vivo* investigations to verify bioavailability issues and to test their potential in pathological models characterized by deficit in the redox system.

REFERENCES

Aschner, M. (2000). Neuron-astrocyte interactions: implications for cellular energetics and antioxidant levels. *Neurotoxicology* 21, 1101-1107.

- Auclair, S., Milenkovic, D., Besson, C., Chauvet, S., Gueux, E., Morand, C., *et al.* (2009). Catechin reduces atherosclerotic lesion development in apo E-deficient mice: a transcriptomic study. *Atherosclerosis* 204 (2), e21–e27. doi: 10.1016/j.atherosclerosis.2008.12.007.
- Baird, L., and Dinkova-Kostova, A. T. (2011). The cytoprotective role of the Keap1-Nrf2 pathway. *Arch. Toxicol.* 85, 241–272. doi: 10.1007/s00204-011-0674-5.
- Bartel, D. P. (2004). MicroRNAs: genomics, biogenesis, mechanism, and function. *Cell* 116 (2), 281–297. doi: 10.1016/s0092-8674(04)00045-5.
- Basagni, F., Lanni, C., Minarini, A., and Rosini, M. (2019). Lights and shadows of electrophile signaling: focus on the Nrf2-Keap1 pathway. *Future Med. Chem.* 11, 707–721. doi: 10.4155/fmc-2018-0423.
- Boyanapalli, S. S. S., and Kong, A. N. T. (2015). “Curcumin, the King of Spices”: epigenetic regulatory mechanisms in the prevention of cancer, neurological, and inflammatory diseases. *Curr. Pharmacol. Rep.* 1, 129–139. doi: 10.1007/s40495-015-0018-x.
- Brennan, M. S., Matos, M. F., Li, B., Hronowski, X., Gao, B., Juhasz, P., *et al.* (2015). Dimethyl fumarate and monoethyl fumarate exhibit differential effects on KEAP1, NRF2 activation, and glutathione depletion *In Vitro*. *PLoS One* 10, e0120254. doi: 10.1371/journal.pone.0120254.
- Camargo, A., Ruano, J., Fernandez, J. M., Parnell, L. D., Jimenez, A., Santos- Gonzalez, M., *et al.* (2010). Gene expression changes in mononuclear cells in patients with metabolic syndrome after acute intake of phenol-rich virgin olive oil. *BMC Genomics* 11, 253. doi: 10.1186/1471-2164-11-253.
- Campolo, M., Casili, G., Lanza, M., Filippone, A., Paterniti, I., Cuzzocrea, S., *et al.* (2018). Multiple mechanisms of dimethyl fumarate in amyloid b-induced neurotoxicity in human neuronal cells. *J. Cell Mol. Med.* 22 (2), 1081–1094. doi: 10.1111/jcmm.13358.
- Catanzaro, M., Corsini, E., Rosini, M., Racchi, M., and Lanni, C. (2018). Immunomodulators inspired by nature: a review on curcumin and echinacea. *Mol. Basel Switz.* 23 (11), 2778. doi: 10.3390/molecules23112778.
- Chou, C.-H., Chang, N.-W., Shrestha, S., Hsu, S.-D., Lin, Y.-L., Lee, W.-H., *et al.* (2016). miRTarBase 2016: updates to the experimentally validated miRNA-target interactions database. *Nucleic Acids Res.* 44, D239–D247. doi: 10.1093/nar/gkv1258.
- Chou, C. H., Shrestha, S., Yang, C. D., Chang, N. W., Lin, Y. L., Liao, K. W., *et al.* (2018). miRTarBase update 2018: a resource for experimentally validated microRNA-target interactions. *Nucleic Acids Res.* 46 (D1), D296–D302. doi: 10.1093/nar/gkx1067.
- Crespo, M. C., Tomé-Carneiro, J., Burgos-Ramos, E., Loria Kohen, V., Espinosa, M. I., Herranz, J., *et al.* (2015). One-week administration of hydroxytyrosol to humans does not activate Phase II enzymes. *Pharmacol. Res.* 95–96, 132–137. doi: 10.1016/j.phrs.2015.03.018.
- Curti, V., Capelli, E., Boschi, F., Nabavi, S. F., Bongiorno, A. I., Habtemariam, S., *et al.* (2014). Modulation of human miR-17-3p expression by methyl 3-O-methyl gallate as explanation of its *in vivo* protective activities. *Mol. Nutr. Food Res.* 58, 1776–1784. doi: 10.1002/mnfr.201400007.
- Curti, V., Di Lorenzo, A., Rossi, D., Martino, E., Capelli, E., Collina, S., *et al.* (2017). Enantioselective modulatory effects of naringenin enantiomers on the expression levels of miR-

17-3p involved in endogenous antioxidant defenses. *Nutrients* 9, 215. doi: 10.3390/nu9030215.

Darvesh, A. S., Carroll, R. T., Bishayee, A., Novotny, N. A., Geldenhuys, W. J., and Van der Schyf, C. J. (2012). Curcumin and neurodegenerative diseases: a perspective. *Expert Opin. Investig. Drugs* 21, 1123–1140. doi: 10.1517/13543784.2012.693479.

de Oliveira, M. R., Custódio de Souza, I. C., and Fürstenau, C. R. (2019). Promotion of mitochondrial protection by naringenin in methylglyoxal-treated SH-SY5Y cells: involvement of the Nrf2/GSH axis. *Chem. Biol. Interact.* 310, 108728. doi: 10.1016/j.cbi.2019.108728.

Ewing, J. F., and Maines, M. D. (1993). Glutathione depletion induces heme oxygenase-1 (HSP32) mRNA and protein in rat brain. *J. Neurochem.* 60, 1512–1519. doi: 10.1111/j.1471-4159.1993.tb03315.x.

Hirotsu, Y., Katsuoka, F., Funayama, R., Nagashima, T., Nishida, Y., Nakayama, K., *et al.* (2012). Nrf2-MafG heterodimers contribute globally to antioxidant and metabolic networks. *Nucleic Acids Res.* 40 (20), 10228–10239. doi: 10.1093/nar/gks827.

Ho, C.-Y., Cheng, Y.-T., Chau, C.-F., and Yen, G.-C. (2012). Effect of diallyl sulfide on *in vitro* and *in vivo* Nrf2-mediated pulmonary antioxidant enzyme expression via Activation ERK/p38 Signaling Pathway. *J. Agric. Food Chem.* 60, 100–107. doi: 10.1021/jf203800d.

Howell, J. C., Chun, E., Farrell, A. N., Hur, E. Y., Caroti, C. M., Iuvone, P. M., *et al.* (2013). Global microRNA expression profiling: curcumin (diferuloylmethane) alters oxidative stress-responsive microRNAs in human ARPE-19 cells. *Mol. Vis.* 19, 544–560.

Jenkins, D. J. A., Spence, J. D., Giovannucci, E. L., Kim, Y.-I., Josse, R., Vieth, R., *et al.* (2018). Supplemental vitamins and minerals for CVD prevention and treatment. *J. Am. Coll. Cardiol.* 71, 2570–2584. doi: 10.1016/j.jacc.2018.04.020.

Jobby, S., Vitturi, D. A., Salvatore, S. R., Turell, L., Pires, M. F., Kansanen, E., *et al.* (2019). Electrophiles modulate glutathione reductase activity via alkylation and upregulation of glutathione biosynthesis. *Redox Biol.* 21, 101050. doi: 10.1016/j.redox.2018.11.008.

Kumar, P., Nagarajan, A., and Uchil, P. D. (2018). Analysis of cell viability by the MTT assay. *Cold Spring Harb. Protoc.* 2018 (6). doi: 10.1101/pdb.prot095505.

Kurinna, S., and Werner, S. (2015). NRF2 and microRNAs: new but awaited relations. *Biochem. Soc. Trans.* 43 (4), 595–601. doi: 10.1042/BST20140317.

Liang, Z., and Xi, Y. (2016). MicroRNAs mediate therapeutic and preventive effects of natural agents in breast cancer. *Chin. J. Nat. Med.* 14, 881–887. doi: 10.1016/S1875-5364(17)30012-2.

Malhotra, D., Portales-Casamar, E., Singh, A., Srivastava, S., Arenillas, D., Happel, C., *et al.* (2010). Global mapping of binding sites for Nrf2 identifies novel targets in cell survival response through ChIP-Seq profiling and network analysis. *Nucleic Acids Res.* 38 (17), 5718–5734. doi: 10.1093/nar/gkq212.

Martínez-Huélamo, M., Rodríguez-Morató, J., Boronat, A., and De La Torre, R. (2017). Modulation of Nrf2 by olive oil and wine polyphenols and neuroprotection. *Antioxidants (Basel)* 6 (4), E73. doi: 10.3390/antiox6040073.

- Nabavi, S. F., Tenore, G. C., Daglia, M., Tundis, R., Loizzo, M. R., and Nabavi, S. M. (2015a). The cellular protective effects of rosmarinic acid: from bench to bedside. *Curr. Neurovasc. Res.* 12, 98-105. doi: 10.2174/1567202612666150109113638.
- Nabavi, S. F., Thiagarajan, R., Rastrelli, L., Daglia, M., Sobarzo-Sánchez, E., Alinezhad, H., *et al.* (2015b). Curcumin: a natural product for diabetes and its complications. *Curr. Top. Med. Chem.* 15, 2445-2455. doi: 10.2174/1568026615666150619142519.
- Narasimhan, M., Patel, D., Vedpathak, D., Rathinam, M., Henderson, G., and Mahimainathan, L. (2012). Identification of novel microRNAs in post-transcriptional control of Nrf2 expression and redox homeostasis in neuronal, SH-SY5Y cells. *PLoS One* 7, e51111. doi: 10.1371/journal.pone.0051111.
- Niture, S. K., Khatri, R., and Jaiswal, A. K. (2014). Regulation of Nrf2-an update. *Free Radic. Biol. Med.* 66, 36-44. doi: 10.1016/j.freeradbiomed.2013.02.008.
- Pandima Devi, K., Rajavel, T., Daglia, M., Nabavi, S. F., Bishayee, A., and Nabavi, S. M. (2017). Targeting miRNAs by polyphenols: novel therapeutic strategy for cancer. *Semin. Cancer Biol.* 46, 146-157. doi: 10.1016/j.semcancer.2017.02.001.
- Papp, D., Lenti, K., Módos, D., Fazekas, D., Dúl, Z., Túrei, D., *et al.* (2012). The NRF2-related interactome and regulome contain multifunctional proteins and fine-tuned autoregulatory loops. *FEBS Lett.* 586 (13), 1795-1802. doi: 10.1016/j.febslet.2012.05.016.
- Park, S. Y., Kim, D. Y., Kang, J.-K., Park, G., and Choi, Y.-W. (2014). Involvement of activation of the Nrf2/ARE pathway in protection against 6-OHDA-induced SH-SY5Y cell death by a-iscubebenol. *Neurotoxicology* 44, 160-168. doi: 10.1016/j.neuro.2014.06.011.
- Paunkov, A., Chartoumpakis, D. V., Ziros, P. G., and Sykiotis, G. P. (2019). A Bibliometric Review of the Keap1/Nrf2 Pathway and its Related Antioxidant Compounds. *Antioxidants* 8 (9), E353. doi: 10.3390/antiox8090353.
- R Core Team (2018). R: A Language and Environment for Statistical Computing. R Foundation for Statistical Computing (Vienna).
- Saidu, N. E. B., Kavian, N., Leroy, K., Jacob, C., Nicco, C., Batteux, F., *et al.* (2019). Dimethyl fumarate, a two-edged drug: current status and future directions. *Med. Res. Rev.* 39 (5), 1923-1952. doi: 10.1002/med.21567.
- Satoh, T., McKercher, S. R., and Lipton, S. A. (2013). Nrf2/ARE-mediated antioxidant actions of pro-electrophilic drugs. *Free Radic. Biol. Med.* 65, 645-657. doi: 10.1016/j.freeradbiomed.2013.07.022.
- Scapagnini, G., Sonya, V., Abraham, N. G., Calogero, C., Zella, D., and Fabio, G. (2011). Modulation of Nrf2/ARE pathway by food polyphenols: a nutritional neuroprotective strategy for cognitive and neurodegenerative disorders. *Mol. Neurobiol.* 44, 192-201. doi: 10.1007/s12035-011-8181-5.
- Schmidt, T. J., Ak, M., and Mrowietz, U. (2007). Reactivity of dimethyl fumarate and methylhydrogen fumarate towards glutathione and N-acetyl-L-cysteine- preparation of S-substituted thiosuccinic acid esters. *Bioorg. Med. Chem.* 15, 333-342. doi: 10.1016/j.bmc.2006.09.053.

Serafini, M. M., Catanzaro, M., Rosini, M., Racchi, M., and Lanni, C. (2017). Curcumin in Alzheimer's disease: Can we think to new strategies and perspectives for this molecule? *Pharmacol. Res.* 124, 146-155. doi: 10.1016/j.phrs.2017.08.004.

Shen, L.-R., Parnell, L. D., Ordovas, J. M., and Lai, C.-Q. (2013). Curcumin and aging. *BioFactors* 39, 133-140. doi: 10.1002/biof.1086.

Simoni, E., Serafini, M. M., Bartolini, M., Caporaso, R., Pinto, A., Necchi, D., *et al.* (2016). Nature-inspired multifunctional ligands: focusing on amyloid-based molecular mechanisms of Alzheimer's disease. *ChemMedChem* 11, 1309-1317. doi: 10.1002/cmdc.201500422.

Simoni, E., Serafini, M. M., Caporaso, R., Marchetti, C., Racchi, M., Minarini, A., *et al.* (2017). Targeting the Nrf2/Amyloid-Beta Liaison in Alzheimer's Disease: a rational approach. *ACS Chem. Neurosci.* 8, 1618-1627. doi: 10.1021/acschemneuro.7b00100.

Spencer, J. P. (2010). Beyond antioxidants: the cellular and molecular interactions of flavonoids and how these underpin their actions on the brain. *Proc. Nutr. Soc.* 69 (2), 244-260. doi: 10.1017/S0029665110000054.

Suneetha, A., and Raja Rajeswari, K. (2016). Role of dimethyl fumarate in oxidative stress of multiple sclerosis: a review. *J. Chromatogr. B.* 1019, 15-20. doi: 10.1016/j.jchromb.2016.02.010.

Tanigawa, S., Fujii, M., and Hou, D.-X. (2007). Action of Nrf2 and Keap1 in ARE-mediated NQO1 expression by quercetin. *Free Radic. Biol. Med.* 42, 1690-1703. doi: 10.1016/j.freeradbiomed.2007.02.017.

Tebay, L. E., Robertson, H., Durant, S. T., Vitale, S. R., Penning, T. M., Dinkova-Kostova, A. T., *et al.* (2015). Mechanisms of activation of the transcription factor Nrf2 by redox stressors, nutrient cues, and energy status and the pathways through which it attenuates degenerative disease. *Free Radic. Biol. Med.* 88 (Pt B), 108-146. doi: 10.1016/j.freeradbiomed.2015.06.021.

van Meerloo, J., Kaspers, G. J., and Cloos, J. (2011). Cell sensitivity assays: the MTT assay. *Methods Mol. Biol.* 731, 237-245. doi: 10.1007/978-1-61779-080-5_20.

Vera-Ramirez, L., Pérez-Lopez, P., Varela-Lopez, A., Ramirez-Tortosa, M., Battino, M., and Quiles, J. L. (2013). Curcumin and liver disease. *BioFactors* 39, 88-100. doi: 10.1002/biof.1057.

Visioli, F. (2015). Xenobiotics and human health: a new view of their pharmanutritional role. *PharmaNutrition* 3 (2), 60-64. doi: 10.1016/j.phanu.2015.04.001.

Witaicenis, A., Seito, L. N., da Silveira Chagas, A., de Almeida, L. D., Luchini, A. C., Rodrigues-Orsi, P., *et al.* (2014). Antioxidant and intestinal anti-inflammatory effects of plant-derived coumarin derivatives. *Phytomedicine* 21, 240-246. doi: 10.1016/j.phymed.2013.09.001.

Xicota, L., Rodriguez-Morato, J., Dierssen, M., and De La Torre, R. (2017). Potential Role of (-)-epigallocatechin-3-gallate (EGCG) in the secondary prevention of Alzheimer disease. *Curr. Drug Targets* 18, 174-195. doi: 10.2174/1389450116666150825113655.

PART IV

The following manuscript was published in *Frontiers in Pharmacology* in 2020 as:

Targeting cytokine release through the differential modulation of Nrf2 and NF- κ B pathways by electrophilic/non-electrophilic compounds

Francesca Fagiani, **Michele Catanzaro (co-first author)**, Erica Buoso, Filippo Basagni, Daniele Di Marino, Stefano Raniolo, Marialaura Amadio, Eric Frost, Emanuela Corsini, Marco Racchi, Tamas Fulop, Stefano Govoni, Michela Rosini and Cristina Lanni

Abstract

The transcription factor Nrf2 coordinates a multifaceted response to various forms of stress and to inflammatory processes, maintaining a homeostatic intracellular environment. Nrf2 anti-inflammatory activity has been related to the crosstalk with the transcription factor NF- κ B, a pivotal mediator of inflammatory responses and of multiple aspects of innate and adaptive immune functions. However, the underlying molecular basis has not been completely clarified. By combining into new chemical entities, the hydroxycinnamoyl motif from curcumin and the allyl mercaptan moiety of garlic organosulfur compounds, we tested a set of molecules, carrying (pro)electrophilic features responsible for the activation of the Nrf2 pathway, as valuable pharmacologic tools to dissect the mechanistic connection between Nrf2 and NF- κ B. We investigated whether the activation of the Nrf2 pathway by (pro)electrophilic compounds may interfere with the secretion of pro-inflammatory cytokines, during immune stimulation, in a human immortalized monocyte-like cell line (THP-1). The capability of compounds to affect the NF- κ B pathway was also evaluated. We assessed the compounds-mediated regulation of cytokine and chemokine release by using Luminex X-MAP[®] technology in human primary peripheral blood mononuclear cells (PBMCs) upon LPS stimulation. We found that all compounds, also in the

absence of electrophilic moieties, significantly suppressed the LPS-evoked secretion of pro-inflammatory cytokines such as TNF α and IL-1 β , but not of IL-8, in THP-1 cells. A reduction in the release of pro-inflammatory mediators similar to that induced by the compounds was also observed after siRNA mediated-Nrf2 knockdown, thus indicating that the attenuation of cytokine secretion cannot be directly ascribed to the activation of Nrf2 signaling pathway. Moreover, all compounds, with the exception of compound 1, attenuated the LPS-induced activation of the NF- κ B pathway, by reducing the upstream phosphorylation of I κ B, the NF- κ B nuclear translocation, as well as the activation of NF- κ B promoter. In human PBMCs, compound 4 and CURC attenuated TNF α release as observed in THP-1 cells, and all compounds acting as Nrf2 inducers significantly decreased the levels of MCP-1/CCL2, as well as the release of the proinflammatory cytokine IL-12. Altogether, the compounds induced a differential modulation of innate immune cytokine release, by differently regulating Nrf2 and NF- κ B intracellular signaling pathways.

Keywords: Nrf2; NF- κ B; curcumin; antioxidant; inflammation; cytokine release; TNF α ; MCP-1.



Targeting Cytokine Release Through the Differential Modulation of Nrf2 and NF- κ B Pathways by Electrophilic/Non-Electrophilic Compounds

Francesca Fagiani^{1,2†}, Michele Catanzaro^{1†}, Erica Buoso¹, Filippo Basagni³, Daniele Di Marino⁴, Stefano Raniolo⁵, Marialaura Amadio¹, Eric H. Frost⁶, Emanuela Corsini⁷, Marco Racchi¹, Tamas Fulop⁸, Stefano Govoni¹, Michela Rosini^{3*} and Cristina Lanni^{1*}

OPEN ACCESS

Edited by:
Filippo Caraci,
University of Catania, Italy

Reviewed by:
Rosalia Crupi,
University of Messina, Italy
Raffaella Gozzelino,
New University of Lisbon, Portugal

¹ Department of Drug Sciences, Pharmacology Section, University of Pavia, Pavia, Italy, ² Scuola Universitaria Superiore IUSS Pavia, Pavia, Italy, ³ Department of Pharmacy and Biotechnology, University of Bologna, Bologna, Italy, ⁴ Department of Life and Environmental Sciences, New York-Marche Structural Biology Center (NY-MaSBIC), Polytechnic University of Marche, Ancona, Italy, ⁵ Università della Svizzera Italiana (USI), Faculty of Biomedical Sciences, Institute of Computational Science—Center for Computational Medicine in Cardiology, CH-Lugano, Switzerland, ⁶ Department of Microbiology and Infectiology, Centre de Recherches Cliniques, Faculty of Medicine and Health Sciences, University of Sherbrooke, Sherbrooke, QC, Canada, ⁷ Department of Environmental Science and Policy, Università degli Studi di Milano, Milan, Italy, ⁸ Geriatric Division, Department of Medicine, Faculty of Medicine and Health Sciences, Research Center on Aging, University of Sherbrooke, Sherbrooke, QC, Canada

INTRODUCTION

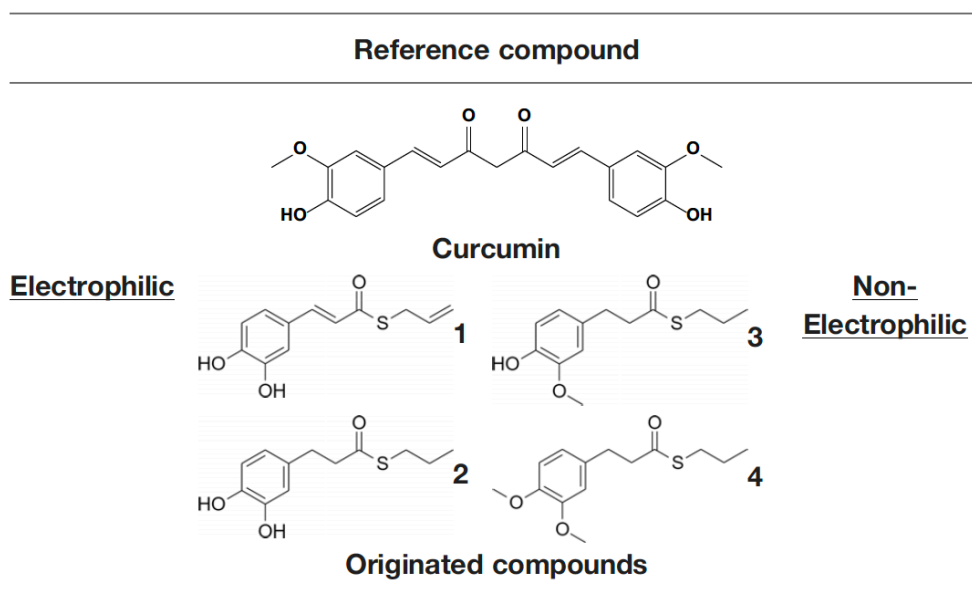
Nuclear factor (erythroid-derived 2)-like 2 (Nrf2) is a transcription factor regulating the expression of about 250 genes encoding a network of cooperating enzymes involved in endobiotic and xenobiotic biotransformation reactions, antioxidant metabolism, protein degradation and regulation of inflammation (Hayes and Dinkova-Kostova, 2014). By governing such complex transcriptional networks, Nrf2 coordinates a multifaceted response to various forms of stress, maintaining a homeostatic intracellular environment. Several studies demonstrate that Nrf2 plays also a key role in the resolution of inflammatory processes. Consistently, Nrf2 is abundant in monocytes and granulocytes, proving its crucial involvement in immune response driven by these cell types. Data from the literature demonstrate that genetic or pharmacological activation of Nrf2 strongly

suppresses the production of proinflammatory cytokines (Innamorato *et al.*, 2008; Knatko *et al.*, 2015; Kobayashi *et al.*, 2016; Quinti *et al.*, 2017) and Nrf2-deficiency induces an exacerbation of inflammation in a variety of murine models such as sepsis, pleurisy, and emphysema (Iizuka *et al.*, 2005; Ishii *et al.*, 2005; Thimmulappa *et al.*, 2006). However, while the contribution of Nrf2 in inflammatory processes has been widely recognized, the underlying molecular basis has not been completely clarified. Its anti-inflammatory activity has been related to several mechanisms, including crosstalk with the transcription factor nuclear factor- κ B (NF- κ B), the modulation of redox balance, and the direct downregulation of some antioxidant response element (ARE)-dependent expression of pro-inflammatory cytokines, such as IL-6 and IL-1 β (Kobayashi *et al.*, 2016). Among them, the crosstalk between Nrf2 and NF- κ B relies on both transcriptional and post-transcriptional mechanisms, allowing fine-tuning of dynamic responses to ever-changing environmental cues. NF- κ B is a key transcription factor governing the expression of a plethora of genes involved in diverse biological processes, including immune and inflammatory responses, cell proliferation, death, angiogenesis, cell survival, and oncogenesis (Häcker and Karin, 2006; Perkins, 2007). In particular, NF- κ B controls the transcription of genes encoding pro-inflammatory cytokines, such as TNF α and IL-1 β . In the absence of a stimulant, NF- κ B remains inactive and sequestered in the cytoplasm by binding to an inhibitory protein, I κ B. The exposure of cells to pro-inflammatory stimuli, such as cytokines and infectious agents, triggers the activation of the I κ B kinase (IKK) complex that phosphorylates I κ B protein on two serine residues. Phosphorylated I κ B is ubiquitinated and, subsequently, degraded via proteasome (Hayden *et al.*, 2006; Perkins, 2007). The degradation of I κ B allows NF- κ B translocation into the nucleus to drive the expression of target genes; within the nucleus it interacts with other transcription factors and transcriptional co-factors to regulate expression of an array of genes, many of which are involved in inflammatory signaling (e.g. cytokines, chemokines, adhesion molecules, and acute phase proteins) (Baeuerle and Baltimore, 1996). Notably, several pharmacological and genetic studies suggest a functional crosstalk between Nrf2 and NF- κ B transcription factors, with a range of complex molecular interactions depending on the cell type and tissue context (Wardyn *et al.*, 2015). A strong

activity in both NF- κ B and Nrf2 has been found fundamental for well-coordinated responses to counteract a cellular inflammatory status (Fusco *et al.*, 2017; D'amico *et al.*, 2019). Indeed, an imbalance between Nrf2 and NF- κ B pathways has been associated with a variety of diseases ranging from neurodegeneration, cardiovascular and autoimmune disorders.

The transcriptional factor Nrf2, with its redox sensitive repressor Keap1 (Kelch-like ECH-associated protein 1), orchestrates adaptive responses to diverse forms of stress through regulatory cysteine switches. Thus, precise electrophilic addition is emerging as a valuable opportunity to shed light on previously untapped roles of this redox sensing system (Basagni *et al.*, 2019). By combining into new chemical entities the hydroxycinnamoyl motif derived from curcumin and the allyl mercaptan moiety of garlic organosulfur compounds, we previously synthesized a set of molecules (compounds 1-3), carrying, with the exception of compound 3, a catechol moiety and/or an α,β -unsaturated carbonyl group (**Table 1**). These (pro)electrophilic features were shown to be responsible for the activation of the Nrf2 pathway and the subsequent induction of ARE-dependent target genes, possibly by covalent conjugation with Keap1 cysteine sensors (Simoni *et al.*, 2017; Serafini *et al.*, 2019). Notably, alkylation of functionally significant cysteines of NF- κ B was also shown to play a prominent role in the inhibition of pro-inflammatory transcriptional pathways (Kastrati *et al.*, 2016), albeit alternative mechanisms have been proposed, such as the inhibition of IKK β , or promotion of RelA polyubiquitination and proteasomal degradation (Woodcock *et al.*, 2018).

Herein, we considered the abovementioned compounds as valuable pharmacologic tools to explore the mechanistic connection between Nrf2 and NF- κ B. To exclude possible oxidative activation of the methoxyphenol ring of compound 3 into reactive metabolites such as quinone methide, which could provide an additional electrophilic site (Luis *et al.*, 2018), an additional new compound 4 was synthesized (**Table 1**).



Compound 1: *S*-allyl (*E*)-3-(3,4-dihydroxyphenyl)prop-2-enethioate;

Compound 2: *S*-propyl 3-(3,4-dihydroxyphenyl)propanethioate;

Compound 3: *S*-propyl 3-(4-hydroxy-3-methoxyphenyl)propanethioate;

Compound 4: *S*-propyl 3-(3,4-dimethoxyphenyl)propanethioate.

Table 1. Design strategy of electrophilic and non-electrophilic compounds.

In the present work, we investigated whether the modulation in Nrf2 pathway activation by our molecules was able to interfere with the LPS-induced secretion of pro-inflammatory cytokines, during immune stimulation, in a human immortalized monocyte-like cell line (THP-1), a well-established cell model for the immune modulation approach (Chanput *et al.*, 2014), using curcumin (CURC) as a reference compound. Moreover, the capability of compounds to affect the NF- κ B intracellular pathway, a pivotal mediator of inflammatory responses and critical regulator of multiple aspects of both innate and adaptive immune functions, was also investigated. To validate the results obtained in THP-1 cells in a human primary cellular model, we assessed the regulation of cytokine and chemokine (e.g. IFN γ , IL-1 β , IL-4, IL-6, IL-8, IL-12 (p40), IL-12 (p70), IL-13, IL-27, MCP-1, MCP-3, TNF α) release by the described compounds, upon immune LPS stimulation, in human

peripheral blood mononuclear cells (PBMCs), obtained from venous whole blood of healthy patients, by using Luminex X-MAP® technology.

Altogether, we demonstrated that compounds modulated the innate immune cytokine release, by differently regulating Nrf2 and NF- κ B intracellular signaling pathways.

MATERIALS AND METHODS

Compounds Synthesis

Compounds 1-3 were synthesized according to procedures reported in (Simoni *et al.*, 2016; Simoni *et al.*, 2017); details on the newly synthesized compound 4 are reported here below.

Synthesis of S-Propyl 3-(3,4-Dimethoxyphenyl)propanethioate (Compound 4)

To a solution of compound 2 (110 mg, 0.46 mmol) in 1.80 mL of DMF potassium carbonate (222.5 mg, 1.61 mmol) and methyl iodide dropwise (0.10 mL, 1.61 mmol) were added. The reaction mixture was left stirring at room temperature overnight. The reaction was quenched by adding 3 mL of water and the mixture obtained was further extracted with diethyl ether (2 x 5 mL). Organic phases were collected, reunited, dried with anhydrous sodium sulphate and solvent was evaporated under vacuum. The crude oil was purified by column chromatography on silica gel using petroleum ether/ethyl acetate (8/2) as mobile phase. 4 was obtained as colorless oil (110 mg, 89%). ¹H NMR (400 MHz, CDCl₃) δ 6.74 (d, J = 8 Hz, 1H), 6.69-6.67 (m, 2H), 3.82 (s, 3H), 3.80 (s, 3H), 2.89 (t, J = 8 Hz, 2H), 2.83-2.77 (m, 4H), 1.59-1.50 (m, 2H), 0.91 (t, J = 8 Hz, 3H). ¹³C NMR (100 MHz, CDCl₃) δ 198.79, 148.98, 147.61, 132.83, 120.27, 111.77, 111.41, 55.98, 55.89, 45.88, 31.23, 30.87, 23.06, 13.39. MS [ESI+] m/z 291.10 + [M+Na]⁺.

Chromatographic separations were performed on silica gel columns (Kieselgel 40, 0.040–0.063 mm, Merck). Reactions were followed by TLC on Merck (0.25 mm) glass-packed precoated silica gel plates (60 F254), then visualized with a UV lamp. NMR spectra were recorded at 400 MHz for ¹H and 100 MHz for ¹³C on a Varian VXR 400 spectrometer (**Supplementary Figure 1**). Chemical shifts (δ) are reported in parts per million (ppm) relative to tetramethylsilane (TMS), and spin multiplicities are given as s (singlet), br s (broad singlet), d (doublet), t (triplet), q (quartet), or m (multiplet). Direct infusion ESI-MS mass spectra were recorded on a Waters ZQ 4000 and Xevo G2-XS QToF apparatus. Final compounds were >95% pure as determined by High Performance Liquid Chromatography (HPLC) analyses. The analyses were performed under reversed-phase conditions on a Phenomenex Jupiter C18 (150 × 4.6 mm I.D.) column, using a binary mixture of H₂O/acetonitrile (60/40, v/v for 1; 50/50, v/v for 2 and 3; 40/60, v/v for 4) as the mobile phase, UV detection at λ=302 nm (for 1) or 254 nm (for 2–4), and a flow rate of 0.7 mL/min. Analyses were performed on a liquid chromatograph model PU-1587 UV equipped with a 20 μL loop valve (Jasco Europe, Italy).

All compounds were solubilized in DMSO (dimethyl sulfoxide) at stock concentrations of 10 mM, frozen (–20°C) in aliquots and diluted in culture medium immediately prior to use. For each experimental setting, a stock aliquot was thawed and diluted to minimize repeated freeze and thaw damage. The final concentration of DMSO in culture medium was less than 0.1%.

Reagents

CURC (#08511) was ≥98% pure (HPLC) and purchased by Sigma-Aldrich (Merck KGaA, Darmstadt, Germany). Cell culture media and all supplements were purchased from Sigma Aldrich (Merck KGaA, Darmstadt, Germany). Rabbit polyclonal anti-human Nrf2 (NBP1-32822) and anti-human HO-1 (NBP1-31341) antibodies were purchased from Novus (Biotechnie, Minneapolis USA). Mouse monoclonal anti-human IκBα (#4814T), mouse monoclonal anti-human phospho-IκBα (Ser32/36) (#9246T), and rabbit monoclonal anti-human NF-κB p65 (D14E12) XP® (#8242) were purchased

from Cell Signaling (Cell Signaling Technology, Danvers, MA, USA). Mouse monoclonal anti-human lamin A/C (612162) antibody was purchased from BD Biosciences (Franklin Lakes, NJ, USA). Mouse anti-human α -tubulin (sc-5286) was purchased from Sigma-Aldrich (Merck KGaA, Darmstadt, Germany). Peroxidase conjugate-goat anti-mouse (A4416) was purchased from Sigma-Aldrich (Merck KGaA, Darmstadt, Germany). Anti-rabbit peroxidase-linked antibody (#7074) was purchased from Cell Signaling (Cell Signaling Technology, Danvers, MA, USA). Lipopolysaccharide (LPS) from *Escherichia coli* O111:B4 (L2630) was purchased from Sigma-Aldrich (Merck KGaA, Darmstadt, Germany). The proteasome inhibitor MG132 (474790) was purchased from Calbiochem (San Diego, CA).

Cell Culture and Treatments

Human THP-1 cells were purchased from the European Collection of Authenticated Cell Cultures (ECACC, Salisbury, UK) and diluted to 106 cells/mL in RPMI 1640 medium supplemented with 10% heat-inactivated Fetal Bovine Serum (FBS), 2 mM glutamine, 0.1 mg/mL streptomycin, 100 IU·mL penicillin, and 0.05 mM 2-mercaptoethanol (complete medium) and maintained at 37°C in 5% CO₂-containing and 95% air atmosphere. The experiments were carried out on passages 5-15. Cells were treated as reported in figure legends. Control cells were exposed only to solvent (DMSO).

Cell Viability

The mitochondrial dehydrogenase activity that reduces 3-(4,5-dimethylthiazol-2-yl)-2,5-diphenyl-tetrazolium bromide (MTT, Sigma Aldrich, Merck KGaA, Darmstadt, Germany) was used to determine cell viability using a quantitative colorimetric assay (Kumar *et al.*, 2018). At day 0, THP-1 cells were plated in 96-well plates at a density of 50×10^3 viable cells per well. After treatment, according to the experimental setting, cells were exposed to an MTT solution (1 mg/mL) in complete medium. After 4 h of incubation with MTT, cells were lysed with sodium dodecyl sulfate (SDS) for 24 h and cell

viability was quantified by reading absorbance at 570 nm wavelength, using Synergy HT multi-detection microplate reader (Bio-Tek, Winooski, VT, USA).

Subcellular Fractionation for Nrf2 and NF- κ B Nuclear Translocation

The expression of Nrf2 and NF- κ B in nuclear THP-1 lysates was assessed by Western blot analysis. Suspended cells were collected, centrifugated, and washed twice with ice-cold PBS (phosphate buffered saline), and, subsequently, homogenized 20 times using a glass-glass homogenizer in ice-cold fractionation buffer (20 mM Tris/HCl pH 7.4, 2 mM EDTA, 0.5 mM EGTA, 0.32 M sucrose, 50 mM β -mercaptoethanol). The homogenate was centrifuged at $300 \times g$ for 5 min to obtain the nuclear fraction. An aliquot of the nuclear extract was used for protein quantification by the Bradford method, whereas the remaining sample was boiled at 95°C for 5 min after dilution with 2X sample buffer (125 mM Tris-HCl pH 6.8, 4% SDS, 20% glycerol, 6% β -mercaptoethanol, 0.1% bromophenol blue). Equivalent amounts of nuclear extracted proteins (30 mg) were subjected to polyacrylamide gel electrophoresis and immunoblotting, as described below.

Immunodetection of Nrf2, HO-1, p-I κ B α , I κ B α , and NF- κ B

The expression of Nrf2, HO-1, p-I κ B α , I κ B α , and NF- κ B in whole cell lysates or nuclear extracts was assessed by Western blot analysis. After treatments, suspended cells were collected, centrifugated, and washed twice with ice-cold PBS, lysed by the addition of ice-cold homogenization buffer (50 mM Tris-HCl pH 7.5, 150 mM NaCl, 5 mM EDTA, 0.5% Triton X-100 and protease-phosphatase inhibitors mix). Samples were sonicated and centrifuged at $13,000 \times g$ for 10 s at 4°C. The resulting supernatants were transferred into new tubes, and protein content was determined by Bradford method. After that, the samples were boiled at 95°C for 5 min after dilution with 5X sample buffer. For Western blot analysis, equivalent amounts of both total and nuclear extracts (30 mg) were electrophoresed in 10% acrylamide gel, under reducing conditions, then, electroblotted into PVDF membranes (Sigma Aldrich, Merck KGaA, Darmstadt, Germany), blocked for 1 h with 5% w/v

bovine serum albumin (BSA) in TBS-T (0.1 M Tris-HCl pH 7.4, 0.15 M NaCl, and 0.1% Tween 20), and incubated overnight at 4°C with primary antibodies diluted in 5% w/v BSA in TBS-T. The proteins were visualized using primary antibodies for Nrf2 (1:1000), HO-1 (1:1000), I κ B α (1:1000), p-I κ B α (1:1000), or NF- κ B (1:1000). Detection was carried out by incubation with secondary horseradish peroxidase-conjugated antibodies (1:5000) diluted in 5% w/v BSA in TBS-T for 1 h at room temperature. Membranes were subsequently washed three times with TBS-T and proteins of interest were visualized using an enhanced chemiluminescent reagent (Pierce, Rockford, IL, USA). α -tubulin and lamin A/C were performed as controls for gel loading.

Small Interference RNA (siRNA) for Nrf2

Nrf2 siRNA designed for the human gene Nrf2 was purchased from Sigma Aldrich, Merck KGaA (Darmstadt, Germany). A scrambled siRNA, without known homology with any gene, was used as negative control (Sigma Aldrich, Merck KGaA, Darmstadt, Germany). RNA interference experiments in THP-1 cells were performed by transient transfection for 24 h, using RNAiMAX Lipofectamine (Invitrogen, Thermo Fisher Scientific, Waltham, MA, USA), according to manufacturer's protocol. To confirm Nrf2 silencing, the proteasome inhibitor MG132 (Calbiochem) was added to the medium of selected plates at a final concentration of 5 μ M. After 24 h, cells were analyzed for Nrf2 expression by Western blot analysis.

Enzyme-Linked Immunosorbent Assay (ELISA) Determination of TNF α , IL-8, and IL-1 β

THP-1 cells were treated with compounds 1-4 and CURC at a concentration of 5 μ M for 24 h, and then stimulated with LPS for 3 h, as described in the legends to figures. TNF α , IL-8, and IL-1 β released from THP-1 cells were measured in cell-free supernatants obtained by centrifugation at 250 x g for 5 min and immediately processed for ELISA, according to the manufacturer's protocol. TNF α , IL-8 and IL-1 β production was assessed by specific sandwich ELISA (Invitrogen, Thermo Fisher Scientific, Waltham, MA, USA; Immunotools GmbH, Friesoythe, Germany). Results were expressed as stimulation index.

The limit of detection under optimal conditions was 4 pg/mL for TNF α , 2.6 pg/mL for IL-8, and 18 pg/mL for IL-1 β .

Plasmid DNA Preparation, Transient Transfections, and Luciferase Assay

Plasmids for transfections were purified with the HiSpeed[®] Plasmid Midi Kit (Qiagen, Valencia, CA). DNA was quantified and assayed for purity using QuantusTM Fluorometer (Promega, Madison, WI). Transient transfections were performed in 12- multiwell culture plates; for each well 5 x 10⁵ cells were seeded in RPMI 1640 complete medium. Transfections were carried out using Lipofectamin 2000 Transfection Reagent (Invitrogen, Thermo Fisher Scientific, Waltham, MA, USA), according to manufacturer's instructions. pGL4.32 vector (E8491, Promega, Madison, WI) luciferase-reporter construct plasmid DNA was co-transfected with pRL-TK Renilla (E2241, Promega, Madison, WI) luciferase expressing vector to measure transfection efficiency, as described in Buoso *et al.* (2019). During transfection THP-1 cells were incubated at 37°C in 5% CO₂ overnight and, then, treated with 5 μ M compounds and CURC for 24 h and, then, stimulated with 10 ng/mL LPS for 6 h. At the end of the treatments, cells were lysed with Passive Lysis Buffer provided by Dual-Luciferase[®] Reporter Assay System, following manufacturer's instructions (Promega, Madison, WI). The luminescent signals were measured using a 20/20 Luminometer with 10 s of integration (Turner BioSystems, Sunnyvale, CA).

PBMCs Purification and Culture

Human peripheral blood mononuclear cells (PBMCs) were obtained from the blood of five (5) healthy individuals (mean age \pm SD: 71 \pm 5.22 years; gender: 3 females and 2 males) satisfying the SENIEUR standard protocol for immunogerontological studies (Pawelec *et al.*, 2001). Subjects having a history or physical signs of atherosclerosis or inflammation were excluded. All subjects gave written informed consent in accordance with the Declaration of Helsinki (Ethical Committee Project approval: Fulop_2019-2877). Heparinized blood was subjected to density gradient centrifugation over Ficoll-Paque Plus medium (GE Healthcare Life Sciences, Marlborough, MA, USA) as described

in (Le Page *et al.*, 2017). Briefly, PBS-diluted blood was carefully layered onto the Ficoll- Paque density gradient and centrifuged for 20 min at 400 x g at slow acceleration and with the brake off at room temperature. After centrifugation, the PBMCs layer, consisting of monocytes, T and B lymphocytes, was collected and washed three times with fresh PBS. Cell viability, assessed by Trypan blue exclusion, was more than 95%. For experiments, PBMCs were resuspended at a density of 1x10⁶ cells/mL in complete culture medium consisting of RPMI 1640 supplemented with 10% heat-inactivated FBS, 2 mM glutamine, 0.1 mg/mL streptomycin and 100 IU mL penicillin and maintained at 37°C in 5% CO₂ and 95% air atmosphere.

Luminex X-MAP® Assay

Human cytokine MILLIPLEX® MAP Kit (customized for IFN γ , IL-1 β , IL-4, IL-6, IL-8, IL-12 (p40), IL-12 (p70), IL-13, IL-27, MCP-1, MCP-3, TNF α) was purchased from Millipore-Sigma (Merck KGaA). The assay was performed in a 96-well plate and all reagents were prepared according to the manufacturer's instructions. Each well was cleaned and pre-wet with 200 μ L of wash buffer on plate at 450 rpm during 10 min at RT. Wash buffer was removed by inverting the plate. Assay buffer, matrix solution or culture medium was used as a blank, each standard from a range of concentrations (different for each analyte), quality controls and samples were added to the appropriate wells. The mixed magnetic microbead solution was sonicated and vortexed prior to adding 25 μ L into each well. The plates were sealed and incubated with agitation on a plate shaker at 750 rpm overnight at 4°C in a darkroom. Plates were put on the magnetic support to retain microbeads, then fluid was removed by inverting the plate to avoid touching the beads. Each well was washed three times with 200 μ L of wash buffer with a plate shaker at 450 rpm for 30 s at RT. 25 μ L of biotinylated detection antibodies were added per well, and plates were incubated in dark room at RT on a plate shaker at 750 rpm for 1 h. Then, 25 μ L of streptavidin-phycoerythrin solution were added to each well, and plates were incubated on a plate shaker at 750 rpm for 30 min at RT and protected from light. Plates were washed three times with 200 μ L of wash buffer. Microbeads were resuspended in 150 μ L/well of sheath fluid on a plate shaker at 450 rpm for 5 min at RT. Data were acquired on a

Luminex® 200TM System using the Luminex xPonent® software. An acquisition gate of between 8,000 and 15,000 was set to discriminate against any doublet events and ensure that only single microbeads were measured. Fifty beads/assay were collected and median fluorescence intensities (MFIs) were measured. Sensitivity limits (in pg/mL) were 0.86 for IFN γ ; 0.52 for IL-1 β ; 0.2 for IL-4; 0.14 for IL-6; 0.52 for IL-8; 2.24 for IL-12 (p40); 0.88 for IL-12 (p70); 2.58 for IL-13; 50.78 for IL-27; 3.05 for MCP-1; 8.61 for MCP-3 and 5.39 for TNF α . MFIs were converted to concentrations using the equation of standard range of the appropriate cytokine using Milliplex® Analyst 5.1 Software.

Densitometry and Statistics

All the experiments were performed at least three times with representative results being shown. Data are expressed as mean \pm SEM. The relative densities of the acquired images of Western blotting bands were analyzed with ImageJ software. Statistical analyses were performed using Prism software (GraphPad software, San Diego, CA, USA; version 8.0). Statistical differences were determined by analysis of variance (ANOVA) followed, when significant, by an appropriate *post hoc* test, as indicated in the figure legends. In all reported statistical analyses, effects were designated as non-significant for $p > 0.05$, significant (*) for $p < 0.05$ or less as indicated.

Quantum Mechanics Calculations

The study for the conformational freedom of compounds 1-4 was conducted with the software Gaussian 09 (Gaussian Inc., Wallingford, CT, USA; Revision A.02). Each molecule underwent a protocol of geometrical optimization, involving an increasing level of precision of basis sets [i.e., from 3-21 (Binkley *et al.*, 1980) to 6-31G* (Petersson and Al-Laham, 1991)], with the Hartree-Fock (HF) method (Kohn and Sham, 1965). The "Scan" functionality was used to estimate the barrier hindering conformational variability in the compounds for two different dihedral angles (**Supplementary Figure 2**). During this step, a Møller-Plesset correlation energy correction truncated at the second order (MP2) (Møller and Plesset, 1934) was added to the HF method and the torsions were rotated by intervals of 5 degrees until they completed the 360-

degree turn. For each of these steps, the dihedral angle under study was fixed and the energy of the structure was computed after few steps of minimization.

RESULTS

Cellular Toxicity of Compounds

The cytotoxicity of compounds 1–4 was assessed by MTT assay in THP-1 cells, in comparison with CURC, as a reference compound. Cells were exposed to compounds 1–4 and CURC at concentrations of 1 μ M, 2.5 μ M, 5 μ M, and 10 μ M for 24 h. Consistently with our previous data on a different cellular model (Simoni *et al.*, 2016; Simoni *et al.*, 2017; Serafini *et al.*, 2019; Catanzaro *et al.*, 2020), all the compounds were well-tolerated, with a slight reduction of cell viability of about 10% observed for compounds 3 and 4 (**Figure 1**). Based on these results and according to our previous investigations (Simoni *et al.*, 2017; Serafini *et al.*, 2019; Catanzaro *et al.*, 2020), all further experiments were conducted using the concentration of 5 μ M.

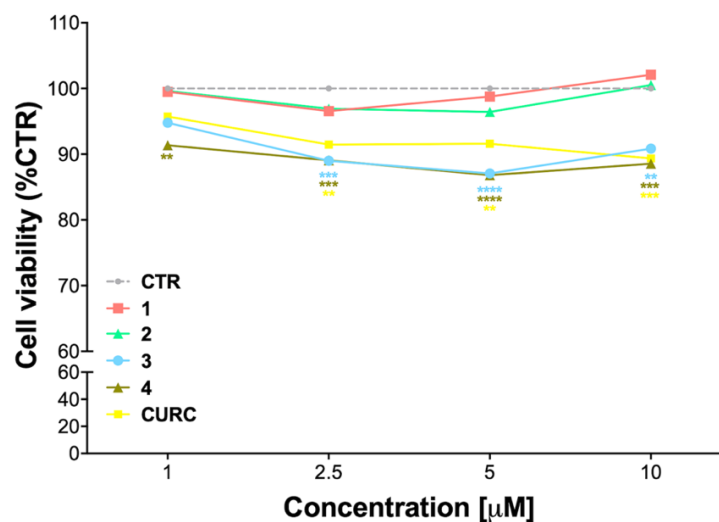


Figure 1. Cell viability in undifferentiated THP-1 exposed to compounds and CURC. THP-1 cells were treated with compounds 1–4 and CURC at the indicated concentrations for 24 h.

Cell viability was assessed by MTT assay. Data are expressed as means of percentage of cell viability \pm SEM. Dunnett's multiple comparison test; ** $p < 0.01$; *** $p < 0.001$ and **** $p < 0.0001$ versus CTR; $n = 4$.

Modulation of Nrf2 Nuclear Translocation and HO-1 Target by Compounds

Nrf2 is a redox-sensitive transcription factor orchestrating the expression and coordinated induction of a wide battery of genes encoding phase II and detoxifying enzymes. Under unstressed conditions, Nrf2 is retained in the cytoplasm by its negative repressor Keap1 and rapidly subjected to ubiquitination and proteasomal degradation, mediated by the binding of Keap1 to the Cul3/Rbx1 E1 ubiquitin ligase complex (Niture *et al.*, 2014). After exposure to oxidative and/or electrophilic stimuli, Nrf2 is released from structurally modified Keap1 and translocates into the nucleus, forms a heterodimer with one of the small musculoaponeurotic fibrosarcoma (Maf) proteins, and activates the ARE-mediated expression of cytoprotective genes. Since Nrf2 nuclear translocation is a fundamental step for the complete activation of its pathway, we tested the ability of compounds to induce the nuclear translocation of Nrf2 in THP-1 cells, by comparing their effects to CURC, used as a positive control.

Notably, evidence from the literature demonstrates that pro-electrophilic (catechol) and/or electrophilic moieties (the Michael acceptor α,β -unsaturated carbonyl group) are important structural functions necessary for the induction of the Nrf2 pathway (Tanigawa *et al.*, 2007; Satoh *et al.*, 2013). Compounds were synthesized and screened to identify the structural moieties responsible for the activation of Nrf2 and its downstream signaling pathway. The four compounds investigated in this study differ from each other by the presence or absence of the mentioned key functional groups (as shown in **Table 1**). Indeed, while compound 1 provides the catechol moiety, as well as the Michael acceptor group, 2 displays only the catechol moiety. Conversely, compounds 3 and 4 lack for both the Michael acceptor group and the catechol function.

Thus, THP-1 cells were treated with DMSO as vehicle control, compounds 1-4 and CURC at a concentration of 5 μ M for 3 h. After treatment, Nrf2 nuclear content was assessed by Western blot analysis. As shown in **Figure 2A**, compounds 1, 2, as well as CURC, significantly induced Nrf2 nuclear translocation, whereas compounds 3 and 4 did not increase Nrf2 nuclear content (**Figure 2A**). Such results are consistent with our previous work (Simoni *et al.*, 2017; Serafini *et al.*, 2019; Catanzaro *et al.*, 2020), where the ability of compounds 1 and 2, but not 3, to activate the Nrf2 pathway in SH-SY5Y and ARPE-19 cells suggested that the addition of Keap1 nucleophilic cysteines to (pro)electrophilic portions of the molecule could represent the initiating event. The finding that the newly synthesized molecule, compound 4, was also unable to induce Nrf2 nuclear translocation corroborates this hypothesis.

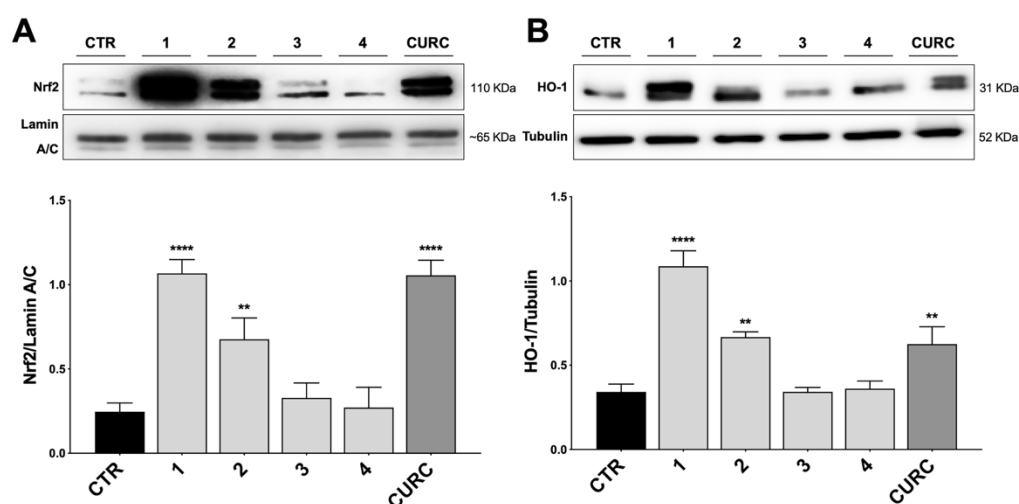


Figure 2. Nrf2 nuclear translocation and modulation of HO-1 protein content in THP-1 cells. (A) THP-1 cells were treated with compounds 1-4 and CURC at a concentration of 5 μ M for 3 h. After isolation, nuclear extracts were examined by Western blot analysis and Nrf2 expression was determined using an anti-Nrf2 antibody. Anti-lamin A/C was used as protein loading control. Results are shown as means of Nrf2/lamin A/C ratio \pm SEM. Dunnett's multiple comparison test; ** $p < 0.01$ and **** $p < 0.0001$ versus CTR; $n = 5-7$. **(B)** Total protein extracts of THP-1 cells, treated with compounds 1-4 and CURC at the concentration of 5 μ M for 24 h, were analyzed for HO-1 protein content by Western blot analysis. Anti-tubulin was used as

protein loading control. Results are shown as means of HO-1/Tubulin ratio \pm SEM. Dunnett's multiple comparison test; ** $p < 0.01$ and **** $p < 0.0001$ versus CTR; $n = 7$.

To demonstrate the downstream activation of the Nrf2 signaling pathway, the protein amount of HO-1, one of the main targets of Nrf2, was evaluated by Western blot analysis. THP-1 cells were treated with DMSO as vehicle control, compounds 1-4 and CURC at a concentration of 5 μ M for 24 h. As shown in **Figure 2B**, compounds 1, 2 and CURC positively modulated HO-1 protein levels, confirming the activation of the Nrf2 pathway. In contrast, compounds 3 and 4 did not affect the protein amount of HO-1 in THP-1 whole cell lysates, confirming their inability to promote Nrf2 pathway activation.

Compounds Attenuate TNF α and IL-1 β , but Not IL-8 Release, in LPS-Stimulated THP-1 Cells

To investigate the immunomodulatory potential of compounds acting as Nrf2 inducers, we exposed THP-1 cells to LPS from *E. coli*, resulting in enhanced production and secretion of pro-inflammatory mediators (**Supplementary Figure 3** and **Figure 4A**). Thus, THP-1 cells were treated with DMSO as vehicle control, compounds 1-4 and CURC at a concentration of 5 μ M for 24 h and, then, exposed to 10 ng/mL LPS for 3 h in order to evoke the inflammatory response (**Figure 3**). TNF α (**Figure 3A**) and IL-8 protein release (**Figure 3B**) were measured by ELISA in the supernatants of LPS-stimulated THP-1 cells. Notably, all compounds, independently from their ability to act as Nrf2 inducers, significantly reduced TNF α protein release into cell culture medium (**Figure 3A**). In contrast, in the same experimental setting, all compounds, as well as CURC, did not affect IL-8 protein release into cell culture medium (**Figure 3B**).

We further investigated the effects of compounds 1-4 and CURC on the release of the pro-inflammatory mediator IL-1 β upon stimulation. Unlike TNF α and IL-8, no increase in IL-1 β protein release was observed in THP-1 cells exposed to 10 ng/mL LPS, but only after stimulation with 1 mg/mL LPS for 3 h, as reported in **Figure 4A**. Then, THP-1 cells were treated with DMSO as vehicle control, compounds 1-4 and CURC at a concentration of 5 μ M for 24

h, exposed to 1 mg/mL LPS for 3 h to promote the inflammatory response, and tested for IL-1 β release by ELISA (**Figure 4B**). All the compounds, as well as CURC, significantly reduced IL-1 β protein release into cell culture medium. As observed for TNF α , both compounds acting as Nrf2 inducers (1 and 2) and those inactive on the Nrf2 pathway (3 and 4) counteracted the LPS-driven inflammatory response, thus suggesting the involvement of different intracellular pathways.

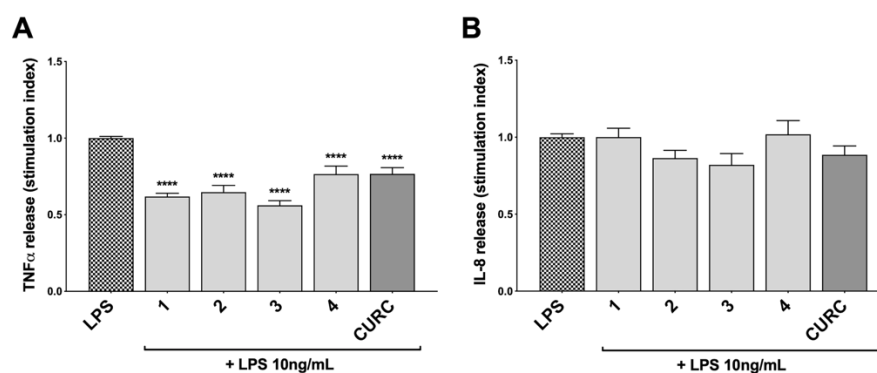


Figure 3. Modulation of TNF α and IL-8 release in LPS-stimulated THP-1 cells exposed to compounds. THP-1 cells were treated with compounds 1-4 and CURC at a concentration of 5 μ M for 24 h, and then stimulated with 10 ng/mL LPS for 3 h. TNF α (**A**) and IL-8 (**B**) protein release was measured in THP-1 supernatants by ELISA. Data are presented as means of stimulation index \pm SEM. Dunnett's multiple comparison test; **** p < 0.0001 versus CTR; n = 5.

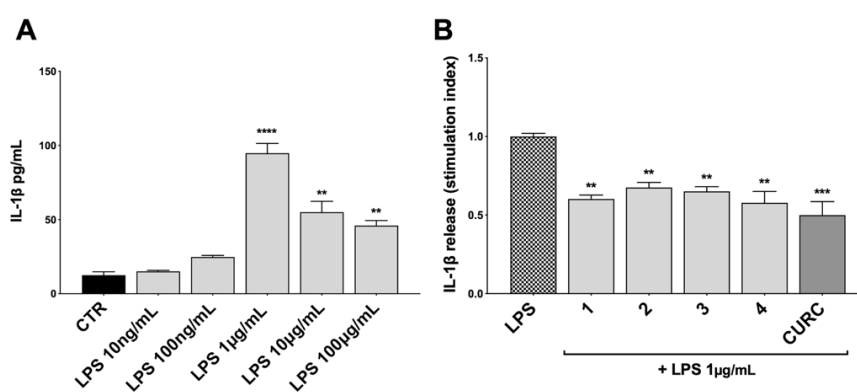


Figure 4. Modulation of IL-1 β release in LPS-stimulated THP-1 cells. (**A**) IL-1 β protein secretion was measured in THP-1 cell supernatants stimulated with LPS at the indicated

concentrations for 3 h. At the end of the treatment, IL-1 β protein release was assessed by ELISA. Data are presented as means of released picograms per mL (pg/mL) \pm SEM. Dunnett's multiple comparison test; ** p < 0.01 and **** p < 0.0001 *versus* CTR; n = 3. **(B)** IL-1 β protein release was measured in THP-1 cells supernatants, treated for 24 h with compounds 1–4 and CURC at a concentration of 5 μ M and then stimulated with 1 mg/mL LPS for 3 h. The level of IL-1 β was assessed by ELISA. Data are presented as means of stimulation index \pm SEM. Dunnett's multiple comparison test; ** p < 0.01 and *** p < 0.001 *versus* CTR; n = 3.

siRNA Mediated Nrf2 Knockdown Does Not Affect TNF α Release in LPS-Stimulated THP-1 Cells

Based on the effect elicited by compounds 3 and 4 on cytokine release, the Nrf2 gene was knocked down by siRNA in THP-1 cells with the aim to evaluate the weight of the Nrf2 pathway in pro-inflammatory cytokine modulation upon LPS stimulation. Accordingly, cells were transfected with scrambled (siRNA_{CTR}) and Nrf2 siRNA (siRNA_{Nrf2}) for 24 h and the proteasome inhibitor MG132 (5 μ M) was added 4 h before the end of the experiment to the medium of selected plates in order to assess Nrf2 silencing. Nrf2 shows a short half-life, with a rapid ubiquitin-proteasome-mediated degradation (Kobayashi and Yamamoto, 2006). Thus, to properly appreciate Nrf2 silencing, we blocked Nrf2 degradation using the proteasome inhibitor MG132. After treatments, the Nrf2 protein content was measured in whole cell lysates by Western blot analysis. As reported in **Figure 5A**, the proteasome inhibitor MG132 induced an increase in Nrf2 protein levels in comparison with control. No statistically significant difference in Nrf2 protein levels between wild type (WT) and scrambled treated cells, treated with MG132, was found, whereas a marked decrease in Nrf2 protein content between WT and siRNA_{Nrf2}-treated cells was observed (**Figure 5A**). Then, WT and siRNA_{Nrf2} cells were treated for 24 h with 5 μ M of selected compounds (the Nrf2 inducer 1, and the inactive 3 and 4), stimulated with 10 ng/mL LPS for 3 h to evoke the inflammatory response, and analysed for TNF α release by ELISA. Notably, all the selected compounds significantly suppressed LPS-induced release of TNF α both in WT and siRNA_{Nrf2} cells (**Figure 5B**), indicating that the observed reduction in pro-inflammatory cytokines release upon LPS

stimulation, cannot be explained on the basis of the activation of Nrf2 pathway.

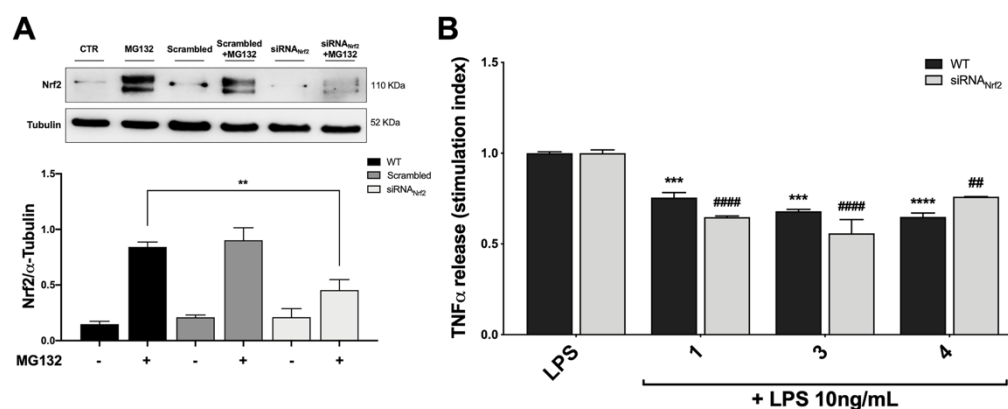


Figure 5. Optimization of Nrf2-silenced THP-1 model (A) and effect of Nrf2-knockdown on modulation of TNF α release by compounds 1, 3 and 4, upon LPS stimulation (B). (A) THP-1 cells were treated either with vehicle (WT), scrambled or siRNA_{Nrf2} for 24 h. Where indicated MG132 was added 4 h before the end of the experiment to block the proteasomal degradation of Nrf2. After treatments, Nrf2 expression was determined in total protein extracts by Western blot analysis using an anti-Nrf2 antibody. Anti- α -tubulin was used as protein loading control. Results are shown as means of Nrf2/ α -Tubulin ratio \pm SEM. Unpaired Student t-test; ** p < 0.01; n = 3. (B) TNF α amount was measured in the supernatants of THP-1 Nrf2-knockdown cells, treated with compounds 1, 3, and 4 at a concentration of 5 μ M for 24 h and then stimulated with 10 ng/mL LPS for 3 h. The protein secretion of TNF α was determined by ELISA. Data are shown as means of stimulation index \pm SEM. Dunnett's multiple comparison test; *** p < 0.001 and **** p < 0.0001 versus WT LPS; # p < 0.01 and #### p < 0.0001 versus siRNA_{Nrf2} LPS; n = 3.

Modulation of the NF- κ B Cellular Pathway by Compounds

To better understand the mechanism of action underlying the reduction of cytokines induced by compounds, we investigated their potential effect on the NF- κ B pathway. Exposure of THP-1 cells to LPS from *E. coli* resulted in activation of the NF- κ B transcription factor (Gomes *et al.*, 2015; Sakai *et al.*, 2017). To assess the effect of compounds on the NF- κ B signaling pathway, we investigated the modulation of the upstream signaling molecule I κ B α . In our

experimental setting, THP-1 cells were treated with DMSO as vehicle control, compounds 1-4 and CURC at a concentration of 5 μ M and, then, stimulated for 45 min with 10 ng/mL LPS. The phosphorylation of I κ B α was measured in whole cell lysates by Western blot analysis. As shown in **Figure 6A**, LPS stimulation markedly increased the level of p-I κ B α compared to controls, whereas treatments with compounds 2, 3, 4, and CURC significantly prevented I κ B α phosphorylation, thus indicating that they might hinder the activation of the NF- κ B pathway by preventing I κ B α phosphorylation. Compound 1 did not produce statistically significant results in our experimental setting, although a slight trend to decrease in I κ B α phosphorylation could be observed (**Figure 6A**).

To further evaluate the capability of compounds to influence NF- κ B nuclear translocation, THP-1 cells were treated with vehicle, 5 μ M compounds 1-4 and CURC and, then, stimulated for 1 h and 30 min with 10 ng/mL LPS, as inflammatory stimulus promoting NF- κ B nuclear translocation. Compounds 3 and 4, and CURC markedly suppressed NF- κ B nuclear translocation, whereas compound 2 acted to a lower extent (**Figure 6B**). Compound 1 did not produce statistically significant results in our experimental setting, although a slight trend to decrease could be observed (**Figure 6B**).

Finally, we investigated the activation of the NF- κ B promoter by luciferase assay. To evaluate whether compounds may exert a basal activity on NF- κ B promoter, THP-1 cells were transiently transfected with pGL4.32 luciferase reporter construct, containing NF- κ B-response elements (RE), and treated with vehicle, 5 μ M compounds 1-4 and CURC for 24 h and, then, analyzed for NF- κ B luciferase. No difference in NF- κ B luciferase activity between untreated and treated cells was observed, thus suggesting that compounds did not basally influence NF- κ B pathways (**Figure 6C**). THP-1 cells were then stimulated with 10 ng/mL LPS for 6 h after treatment with vehicle and 5 μ M compounds 1-4 and CURC for 24 h. As reported in **Figure 6D**, upon LPS stimulation, NF- κ B luciferase activity significantly increased, as expected, and treatments with compounds 2, 3, 4, and CURC significantly reduced it. In accordance with the slight effect on I κ B α phosphorylation and NF- κ B nuclear translocation, compound 1 did not hinder the activation of the NF- κ B

promoter, thus suggesting that the modulation of cytokine release by this molecule seems not to be driven by NF- κ B signaling pathway (**Figure 6D**).

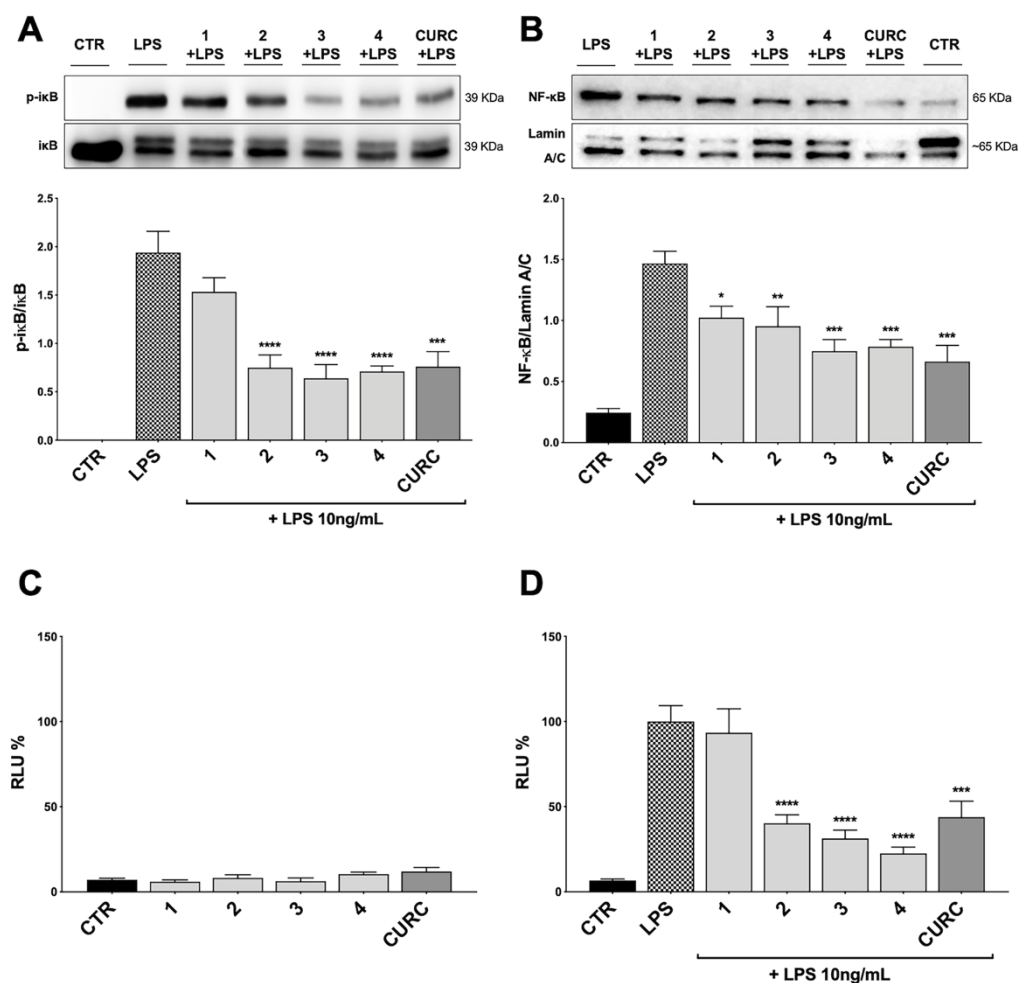


Figure 6. Modulation of NF- κ B pathway by compounds and CURC in LPS-stimulated THP-1 cells. (A) THP-1 cells were treated with 5 μ M compounds 1-4 and CURC for 24 h and then stimulated with 10 ng/mL LPS for 45 min. After stimulation, p-I κ B α expression was determined in total protein extracts by Western blot analysis, using an anti-p-I κ B α antibody. Anti-I κ B α (total) was used to normalize the data. Results are shown as means of p-I κ B α /I κ B α ratio \pm SEM. Dunnett's multiple comparison test; *** p < 0.001 and **** p < 0.0001 versus LPS; n = 5. **(B)** THP-1 cells were treated for 24 h with compounds 1-4 and CURC at a concentration of 5 μ M and then stimulated with 10 ng/mL LPS for 90 min. After isolation, nuclear extracts were examined

by Western blot analysis and NF- κ B expression was determined using an anti-NF- κ B antibody. Anti-lamin A/C was used as protein loading control. Results are shown as means of NF- κ B/Lamin A/C ratio \pm SEM. Dunnett's multiple comparison test; * p < 0.05, ** p < 0.01 and *** p < 0.001 versus LPS; n = 5. **(C, D)** THP-1 cells were transiently transfected with pGL4.32 [luc2P/NF- κ B-RE/Hygro] Vector reporter construct, and subsequently treated with compounds 1-4 and CURC at a concentration of 5 μ M for 24 h. After treatments, the cells were stimulated **(D)** or not **(C)** with 10 ng/mL LPS for 6 h. For each condition, luciferase activity was expressed as RLU% and compared to CTR values assumed at 100%. Results are shown as means \pm SEM. Dunnett's multiple comparison test; *** p < 0.001 and **** p < 0.0001 versus LPS; n = 3.

Differential Regulation of Innate Immune Cytokine Release in Human PBMCs From Healthy Donors

To further study the differential capability of compounds in modulating cytokine and chemokine release, we moved from THP-1 cells to human primary PBMCs from healthy donors. Human PBMCs were stimulated with 10 ng/mL LPS for 3 h after having been treated with vehicle and 5 μ M compounds 1-4 and CURC for 24 h. The release of a panel of the most common cytokines and chemokines [e.g. IFN γ , IL-1 β , IL-4, IL-6, IL-8, IL-12 (p40), IL-12 (p70), IL-13, IL-27, MCP-1, MCP-3, TNF α] was measured in culture medium by Luminex X-MAP[®] technology. Protein release of IFN γ , IL-4, IL-12 (p70), IL-13 and IL-27 was undetectable both in untreated and LPS-stimulated PBMCs from healthy donors, while, exposure of human PBMCs to LPS significantly increased protein release of IL-6, IL-8, IL-12 (p40), MCP-1, and TNF α compared to controls (**Table 2**). A differential regulation of cytokine and chemokine release by compounds was observed during immune stimulation. In particular, compounds 1 and CURC, significantly reduced the release of the pro-inflammatory cytokine IL-6 in LPS-stimulated human PBMCs. In accordance with preliminary results obtained in THP-1 cells, no effect on IL-8 release was observed for 1-4 and CURC, further indicating that all compounds, as well as CURC, did not influence the intracellular pathways regulating IL-8 release. In addition, compounds 1 and 2 significantly decreased IL-12 (p40) release in human PBMCs upon LPS stimulation (**Table 2**). No differences in IL-1 β and MCP-3 release were observed between PBMCs that were stimulated by LPS, untreated, or treated with compounds or CURC

PBMCs (**Table 2**). Interestingly, compounds 1, 2, and CURC were capable to significantly attenuate the release of the chemokine MCP-1 in LPS-stimulated PBMCs from healthy patients. In contrast, compounds 3 and 4 did not affect MCP-1 release, revealing the same activity trend observed for Nrf2 induction (**Table 2**). Notably, such results are consistent with evidence from literature reporting that, after innate immune stimulation, treatment of human PBMCs with Nrf2 activators, such as the Nrf2 agonist CDDO-Me (bardoxolone methyl), markedly reduced LPS-evoked MCP-1/ CCL2 production and that this effect was not specific to LPS- induced immune responses, as Nrf2 activation also reduced MCP-1/CCL2 production after stimulation with IL-6 (Eitas *et al.*, 2017). Furthermore, compound 4 and CURC confirmed their capability to significantly reduce TNF α release in LPS-stimulated PBMCs, as previously observed in the THP-1 cell line (**Table 2**).

	CTR	LPS10 ng/mL	Luminex xMAP [®] Technology				CURC+ LPS
			1+ LPS	2+ LPS	3+ LPS	4+ LPS	
IFN γ	Nd	Nd	Nd	Nd	Nd	nd	nd
IL-1 β	2.76 \pm 0.56	2.43 \pm 0.49	1.36 \pm 0.14	1.58 \pm 0.16	1.85 \pm 0.30	2.59 \pm 0.56	1.31 \pm 0.17
IL-4	Nd	Nd	nd	Nd	Nd	nd	nd
IL-6	33.20 \pm 6.38****	164.4 \pm 12.1	129.2 \pm 7.68*	139.9 \pm 8.32	147.1 \pm 10.5	156.0 \pm 11.4	99.65 \pm 6.71****
IL-8	1659 \pm 178****	3349 \pm 292	4012 \pm 141	3272 \pm 224	2794 \pm 124	3026 \pm 333	2665 \pm 221
IL-12 (p40)	2.44 \pm 0.14**	5.56 \pm 0.57	2.40 \pm 0.12**	3.28 \pm 0.27*	4.82 \pm 0.87	5.30 \pm 0.90	3.61 \pm 0.70
IL-12 (p70)	nd	Nd	nd	nd	Nd	nd	nd
IL-13	nd	Nd	nd	nd	Nd	nd	nd
IL-27	nd	Nd	nd	nd	nd	nd	nd
MCP-1	1149 \pm 89.2*	1627 \pm 139	899 \pm 163***	819 \pm 89.5****	1243 \pm 125	1198 \pm 105	625 \pm 76.9****
MCP-3	38.9 \pm 8.2	50.6 \pm 8.9	36.7 \pm 6.0	35.11 \pm 5.7	43.0 \pm 8.3	42.1 \pm 6.9	25.3 \pm 3.3
TNF α	13.75 \pm 2.76****	350.2 \pm 18.6	264.8 \pm 6.74	295.2 \pm 18.7	328.3 \pm 16.3	220.8 \pm 31.1**	252.8 \pm 38.6*

PBMCs were treated with compounds 1–4 and CURC at a concentration of 5 μ M for 24 h, and then stimulated with 10 ng/mL LPS for 3 h. IFN γ , IL-1 β , IL-4, IL-6, IL-8, IL-12 (p40), IL-12 (p70), IL-13, IL-27, MCP-1, MCP-3, TNF α protein release was measured in PBMC supernatants by Luminex xMAP[®] Technology. Data are presented as means of released picograms per mL (pg/mL) \pm SEM. Dunnett's multiple comparison test; * p < 0.05; ** p < 0.01; *** p < 0.001 and **** p < 0.0001 versus LPS; n = 5.

Table 2. Differential regulation of innate immune cytokine release in human PBMCs from healthy donors.

DISCUSSION

The transcription factor Nrf2 regulates a complex network of cellular responses to oxidative stress and inflammation. Cysteine residues of its repressor Keap1 act as sensor sites for Nrf2 electrophilic activators. Thus, we studied a set of previously synthesized compounds (1, 2, and 3), for which the ability to induce the Nrf2 pathway was strictly related to the (pro)-

electrophilic character of the molecule in THP-1 cells, a widely used cellular model for the immune modulation approach (Chanput *et al.*, 2014). In agreement with previous results (Simoni *et al.*, 2017; Serafini *et al.*, 2019; Catanzaro *et al.*, 2020), a significant effect was detected for the Nrf2 inducers 1 and 2, carrying a catechol moiety and/or an α,β -unsaturated carbonyl group, while no effect was observed for compound 3, lacking both (pro)-electrophilic features (**Table 1**). The same lack of effect was observed for compound 4, which was included in the study to exclude possible oxidative activation into electrophilic metabolites such as quinone methide, which could provide an additional site for adduct formation.

Based on these results, we investigated the potential effects of the compounds on the secretion of pro-inflammatory cytokines upon immune stimulation (e.g. LPS from *E. coli*) in the same cellular model. We found that both compounds which induced Nrf2 (1 and 2) as well as compounds inactive on the Nrf2 pathway (3 and 4) were capable to attenuate the release of the pro-inflammatory cytokines TNF α (**Figure 3A**) and IL-1 β (**Figure 4B**), but not IL-8 secretion (**Figure 3B**), thus suggesting that the reduction of cytokine release by compounds could not be directly ascribed to the activation of Nrf2 pathway. Accordingly, the ability of compounds to attenuate the secretion of TNF α , upon immune stimulation, was also observed after siRNA mediated Nrf2 knockdown (**Figure 5**). To further dissect the molecular mechanism underlying the reduction of cytokine release induced by compounds 1-4, we investigated their potential interplay with other signaling cascades, specifically focusing on the NF- κ B pathway, a pivotal mediator of inflammatory responses and critical regulator of multiple aspects of innate and adaptive immune functions (Häcker and Karin, 2006; Perkins, 2007). All compounds, with the exception of compound 1, significantly attenuated the LPS-induced activation of the NF- κ B canonical pathway, by impairing the upstream phosphorylation of I κ B α , NF- κ B nuclear translocation, as well as the activation of the NF- κ B promoter (**Figure 5**). As a consequence, the ability of compounds 2, 3, and 4 to reduce the activation of NF- κ B pathway may account, at least in part, for their observed effect on pro-inflammatory cytokine release. Notably, both Nrf2 and NF- κ B offer unique patterns of thiol modifications, indicating electrophilic signaling mediators as a valuable

instrument to control their redox-sensitive transcriptional regulatory function. However, while a (pro)-electrophilic feature is required for Nrf2 induction, suggesting covalent adduction as the triggering event, both (pro)-electrophile 2 and non-electrophilic compounds 3 and 4 were able to inhibit NF- κ B activation, revealing a different mode of interaction (**Figure 7**).

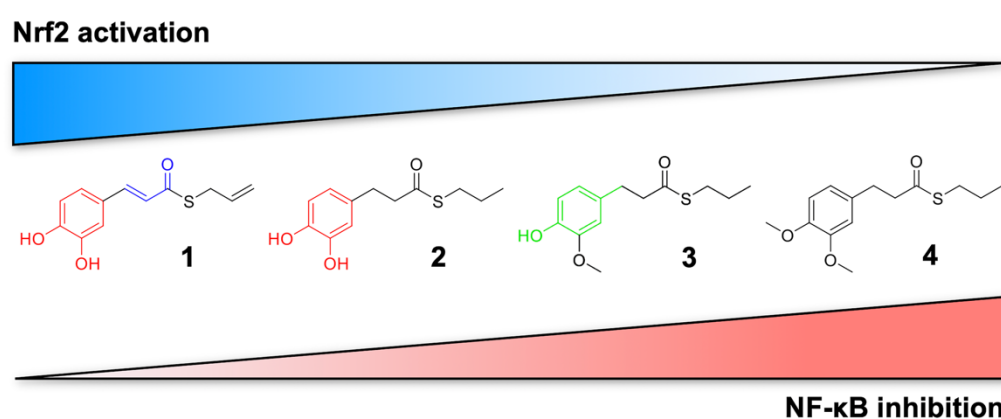


Figure 7. Differential modulation of Nrf2 and NF- κ B intracellular signaling pathways by compounds. Electrophile 1, carrying both the catechol moiety (red) and the α,β -unsaturated carbonyl group (blue), is the most active Nrf2 inducer, while being devoid of activity on NF- κ B pathway. Conversely, the non-electrophilic compound 4, synthesized to exclude eventual oxidative transformation of the methoxyphenol ring (green) of 3 into reactive metabolites, is the most potent NF- κ B inhibitor, with no impact on Nrf2 activation.

Noteworthy, compound 1, carrying both the catechol moiety and the α,β -unsaturated carbonyl group, was unable to significantly modulate the NF- κ B pathway. The modulation of cytokine release by this molecule might be, at least in part, related to anti-inflammatory effect mediated by the induction of Nrf2 targets, such as HO-1 (Roach *et al.*, 2009). Accordingly, HO-1 expression has been demonstrated to decrease the LPS-stimulated secretion of cytokines and chemokines such as MCP-1, IL-6, IL-10, and TNF α in murine and human macrophages (Roach *et al.*, 2009). Altogether, these results indicate that an electrophilic moiety is neither necessary nor per se sufficient to guarantee inhibition of the pro-inflammatory transcriptional activity of NF- κ B,

with shape complementarity emerging as a plausible feature of target recognition. The different biological behavior of electrophiles 1 and 2, which only varies in the presence or absence of two double bonds, might indeed reflect the more constrained conformation assumed by compound 1 with respect to flexible compound 2. The conjugation extended throughout most of the backbone stabilized compound 1 in a planar conformation, as opposed to the sp³ counterparts which manifested a maximum in energy for the same state (**Supplementary Figure 2**). Moreover, the possibility for compounds 2-4 to populate several conformations due to lower energy barriers might indicate that a conformational selection or induced fit effect in the ligand is necessary to execute the desired activity. The overall effects of compounds 1-4 on Nrf2 and NF- κ B intracellular pathways were summarized in **Figure 8**.

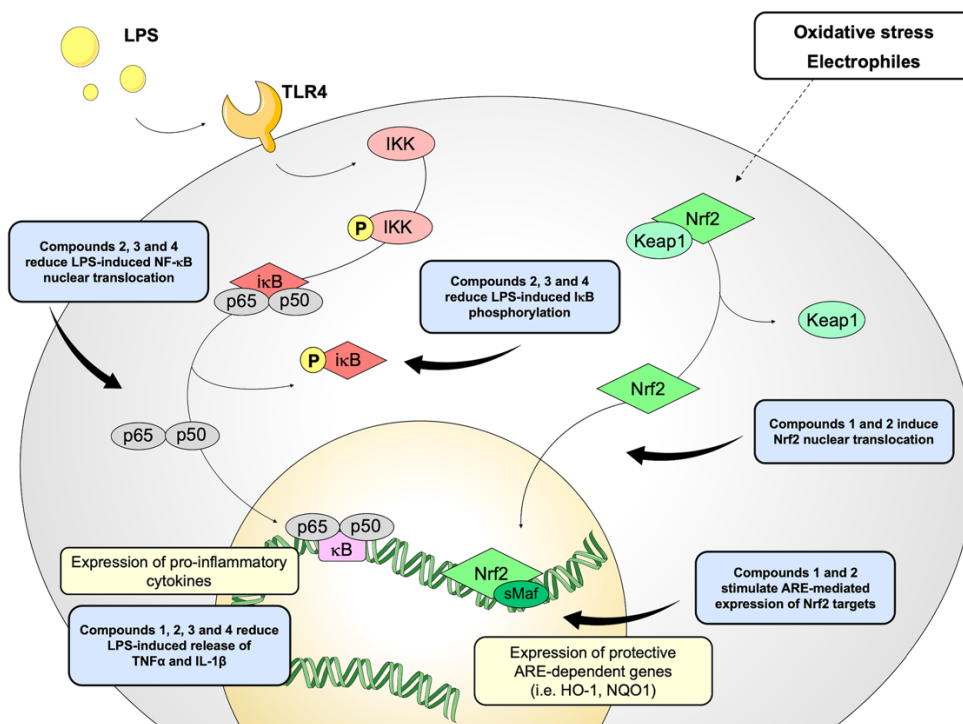


Figure 8. Schematic representation of the effects induced by compounds 1-4 on Nrf2 and NF- κ B pathways.

When moving in a human primary model, by Luminex X- MAP® technology, we screened the effects of compounds on a panel of cytokines and chemokines (e.g. IFN γ , IL-1 β , IL-4, IL-6, IL-8, IL-12 (p40), IL-12 (p70), IL-13, IL-27, MCP-1, MCP-3, TNF α) in order to unveil their potential modulatory effect on other inflammatory mediators (**Table 2**). Compared to data observed in THP-1 cells, we found a differential regulation of innate immune cytokine production by compounds, in line with previous data (Schildberger *et al.*, 2013). In particular, compounds 1 and CURC significantly reduced the secretion of the pro-inflammatory cytokine IL-6 in LPS-stimulated human PBMCs, while compound 4 and CURC attenuated TNF α release (**Table 2**). Furthermore, compounds acting as Nrf2 inducers (1 and 2) also suppressed the secretion of IL-12 (p40), corroborating the hypothesis that inhibition of IL-12 expression may be mediated by Nrf2 activation, as suggested by Macoch *et al.* (2015). Consistently, tert-butylhydroquinone, a well-known Nrf2 inducer, has been reported to activate Nrf2 and to inhibit the induction of IL-12 expression by LPS (Macoch *et al.*, 2015). However, further investigations are required to unravel the molecular mechanism by which Nrf2 represses IL-12 production and secretion.

In human PBMCs, we further found that only compounds acting as Nrf2 inducers (1 and 2) significantly suppressed the release of MCP-1, after LPS stimulation (**Table 2**). In accordance with data from the literature (Eitas *et al.*, 2017), this result indicates that MCP-1 production may rely on activation of the transcription factor Nrf2. Thus, the effect of Nrf2 inducers on MCP-1/CCL2 suggests a novel aspect of Nrf2 pharmacological activation as a regulator of key immunomodulatory functions. This finding represents a potentially generalizable aspect of pharmacological Nrf2 activation occurring with different stimuli (e.g. LPS, IL-6) and consistent across more than 60 individual human samples, as reported by Eitas *et al.* (2017). Thus, contrary to the prevalent view that Nrf2 represses inflammatory processes through redox control, we demonstrated that Nrf2 activation also directly counteracts the production of a key chemokine, by possibly regulating the expression of its encoding gene. Such hypothesis is consistent with data reporting Nrf2-mediated downregulation of proinflammatory mediator gene expression (Kobayashi *et al.*, 2016). However, the precise molecular mechanism

underlying Nrf2 and MCP-1 crosstalk is still elusive. Interestingly, by regulating the production of the chemokine MCP-1, Nrf2 can be considered an upstream regulator of MCP-1 production, thereby providing a molecular basis for a Nrf2-mediated anti-inflammatory approach. In this regard, elevated systemic MCP-1 system levels have been linked to worse outcomes in patients with cardiovascular disease (Martín-Ventura *et al.*, 2009), and pulmonary accumulation of MCP-1 has been reported in patients with acute respiratory distress syndrome (Rosseau *et al.*, 2000). Hence, targeting transcriptional accumulation of MCP-1 through pharmacological Nrf2 activation may represent a promising therapeutic approach.

Although the THP-1 and human PBMCs response can hint to potential responses that may occur *in vivo*, these results need to be validated in *in vivo* studies to draw more definite conclusions. Moreover, further mechanistic investigations are required to unravel the biological connection among Nrf2 activation, innate immune cytokine production, and the regulation of the NF- κ B pathway.

SUPPLEMENTARY MATERIAL

The Supplementary Material for this article can be found online at: <https://www.frontiersin.org/articles/10.3389/fphar.2020.01256/full#supplementary-material>.

REFERENCES

- Baeuerle, P. A., and Baltimore, D. (1996). NF-kappa B: ten years after. *Cell* 87, 13–20. doi: 10.1016/s0092-8674(00)81318-5
- Basagni, F., Lanni, C., Minarini, A., and Rosini, M. (2019). Lights and shadows of electrophile signaling: focus on the Nrf2-Keap1 pathway. *Future Med. Chem.* 11, 707–721. doi: 10.4155/fmc-2018-0423

- Binkley, J. S., Pople, J. A., and Hehre, W. J. (1980). Self-consistent molecular orbital methods. 21. Small split-valence basis sets for first-row elements. *J. Am. Chem. Soc.* 102, 939-947. doi: 10.1021/ja00523a008
- Buoso, E., Ronfani, M., Galasso, M., Ventura, D., Corsini, E., and Racchi, M. (2019). Cortisol-induced SRSF3 expression promotes GR splicing, RACK1 expression and breast cancer cells migration. *Pharmacol. Res.* 143, 17-26. doi: 10.1016/j.phrs.2019.03.008
- Catanzaro, M., Lanni, C., Basagni, F., Rosini, M., Govoni, S., and Amadio, M. (2020). Eye-Light on Age-Related Macular Degeneration: Targeting Nrf2-Pathway as a Novel Therapeutic Strategy for Retinal Pigment Epithelium. *Front. Pharmacol.* 11, 844. doi: 10.3389/fphar.2020.00844
- Chanput, W., Mes, J. J., and Wichers, H. J. (2014). THP-1 cell line: an *in vitro* cell model for immune modulation approach. *Int. Immunopharmacol.* 23, 37-45. doi: 10.1016/j.intimp.2014.08.002
- D'amico, R., Fusco, R., Gugliandolo, E., Cordaro, M., Siracusa, R., Impellizzeri, D., *et al.* (2019). Effects of a new compound containing Palmitoylethanolamide and Baicalein in myocardial ischaemia/reperfusion injury *in vivo*. *Phytomed. Int. J. Phytother. Phytopharm.* 54, 27-42. doi: 10.1016/j.phymed.2018.09.191
- Eitas, T. K., Stepp, W. H., Sjeklocha, L., Long, C. V., Riley, C., Callahan, J., *et al.* (2017). Differential regulation of innate immune cytokine production through pharmacological activation of Nuclear Factor-Erythroid-2-Related Factor 2 (NRF2) in burn patient immune cells and monocytes. *PLoS One* 12, e0184164. doi: 10.1371/journal.pone.0184164
- Fusco, R., Gugliandolo, E., Biundo, F., Campolo, M., Di Paola, R., and Cuzzocrea, S. (2017). Inhibition of inflammasome activation improves lung acute injury induced by carrageenan in a mouse model of pleurisy. *FASEB J.* 31, 3497- 3511. doi: 10.1096/fj.201601349R
- Gomes, A., Capela, J. P., Ribeiro, D., Freitas, M., Silva, A. M. S., Pinto, D. C. G. A., *et al.* (2015). Inhibition of NF- κ B activation and cytokines production in THP-1 monocytes by 2-styrylchromones. *Med. Chem. Shariqah United Arab Emir.* 11, 560-566. doi: 10.2174/1573406411666150209114702
- Häcker, H., and Karin, M. (2006). Regulation and function of IKK and IKK-related kinases. *Sci. STKE Signal Transduction Knowl. Environ.* 2006, re13. doi: 10.1126/stke.3572006re13
- Hayden, M. S., West, A. P., and Ghosh, S. (2006). NF- κ B and the immune response. *Oncogene* 25, 6758-6780. doi: 10.1038/sj.onc.1209943
- Hayes, J. D., and Dinkova-Kostova, A. T. (2014). The Nrf2 regulatory network provides an interface between redox and intermediary metabolism. *Trends Biochem. Sci.* 39, 199-218. doi: 10.1016/j.tibs.2014.02.002
- Iizuka, T., Ishii, Y., Itoh, K., Kiwamoto, T., Kimura, T., Matsuno, Y., *et al.* (2005). Nrf2-deficient mice are highly susceptible to cigarette smoke-induced emphysema. *Genes Cells Devoted Mol. Cell. Mech.* 10, 1113-1125. doi: 10.1111/j.1365-2443.2005.00905.x
- Innamorato, N. G., Rojo, A. II, Garcíá -Yaguë, A. J., Yamamoto, M., de Ceballos, M. L., and Cuadrado, A. (2008). The transcription factor Nrf2 is a therapeutic target against brain inflammation. *J. Immunol. Baltim. Md* 1950 181, 680-689. doi: 10.4049/jimmunol.181.1.680

- Ishii, Y., Itoh, K., Morishima, Y., Kimura, T., Kiwamoto, T., Iizuka, T., *et al.* (2005). Transcription factor Nrf2 plays a pivotal role in protection against elastase- induced pulmonary inflammation and emphysema. *J. Immunol. Baltim. Md* 1950 175, 6968-6975. doi: 10.4049/jimmunol.175.10.6968
- Kastrati, I., Siklos, M.II, Calderon-Gierszal, E. L., El-Shennawy, L., Georgieva, G., Thayer, E. N., *et al.* (2016). Dimethyl Fumarate Inhibits the Nuclear Factor κ B Pathway in Breast Cancer Cells by Covalent Modification of p65 Protein. *J. Biol. Chem.* 291, 3639-3647. doi: 10.1074/jbc.M115.679704
- Knatko, E. V., Ibbotson, S. H., Zhang, Y., Higgins, M., Fahey, J. W., Talalay, P., *et al.* (2015). Nrf2 Activation Protects against Solar-Simulated Ultraviolet Radiation in Mice and Humans. *Cancer Prev. Res. Phila. Pa* 8, 475-486. doi: 10.1158/1940-6207.CAPR-14-0362
- Kobayashi, M., and Yamamoto, M. (2006). Nrf2-Keap1 regulation of cellular defense mechanisms against electrophiles and reactive oxygen species. *Adv. Enzyme Regul.* 46, 113-140. doi: 10.1016/j.advenzreg.2006.01.007
- Kobayashi, E. H., Suzuki, T., Funayama, R., Nagashima, T., Hayashi, M., Sekine, H., *et al.* (2016). Nrf2 suppresses macrophage inflammatory response by blocking proinflammatory cytokine transcription. *Nat. Commun.* 7:11624. doi: 10.1038/ncomms11624
- Kohn, W., and Sham, L. J. (1965). Self-Consistent Equations Including Exchange and Correlation Effects. *Phys. Rev.* 140, A1133-A1138. doi: 10.1103/PhysRev.140.A1133
- Kumar, P., Nagarajan, A., and Uchil, P. D. (2018). Analysis of Cell Viability by the MTT Assay. *Cold Spring Harb. Protoc.* 2018. doi: 10.1101/pdb.prot095505
- Le Page, A., Garneau, H., Dupuis, G., Frost, E. H., Larbi, A., Witkowski, J. M., *et al.* (2017). Differential Phenotypes of Myeloid-Derived Suppressor and T Regulatory Cells and Cytokine Levels in Amnesic Mild Cognitive Impairment Subjects Compared to Mild Alzheimer Diseased Patients. *Front. Immunol.* 8:783. doi: 10.3389/fimmu.2017.00783
- Luis, P. B., Boeglin, W. E., and Schneider, C. (2018). Thiol Reactivity of Curcumin and Its Oxidation Products. *Chem. Res. Toxicol.* 31, 269-276. doi: 10.1021/acs.chemrestox.7b00326
- Macoch, M., Morzadec, C., Génard, R., Pallardy, M., Kerdine-Römer, S., Fardel, O., *et al.* (2015). Nrf2-dependent repression of interleukin-12 expression in human dendritic cells exposed to inorganic arsenic. *Free Radic. Biol. Med.* 88, 381-390. doi: 10.1016/j.freeradbiomed.2015.02.003
- Martín-Ventura, J.L., Blanco-Colio, L.M., Tuñón, J., Muñoz-García, B., Madrigal-Matute, J., Moreno, J. A., *et al.* (2009). Biomarkers in cardiovascular medicine. *Rev. Esp. Cardiol.* 62, 677-688. doi: 10.1016/s1885-5857(09)72232-7
- Møller, C., and Plesset, M. S. (1934). Note on an Approximation Treatment for Many-Electron Systems. *Phys. Rev.* 46, 618-622. doi: 10.1103/PhysRev.46.618
- Niture, S. K., Khatri, R., and Jaiswal, A. K. (2014). Regulation of Nrf2-an update. *Free Radic. Biol. Med.* 66, 36-44. doi: 10.1016/j.freeradbiomed.2013.02.008
- Pawelec, G., Ferguson, F. G., and Wikby, A. (2001). The SENIEUR protocol after 16 years. *Mech. Ageing Dev.* 122, 132-134. doi: 10.1016/s0047-6374(00)00240-2

- Perkins, N. D. (2007). Integrating cell-signalling pathways with NF-kappaB and IKK function. *Nat. Rev. Mol. Cell Biol.* 8, 49-62. doi: 10.1038/nrm2083
- Petersson, G. A., and Al-Laham, M. A. (1991). A complete basis set model chemistry. II. Open-shell systems and the total energies of the first-row atoms. *J. Chem. Phys.* 94, 6081-6090. doi: 10.1063/1.460447
- Quinti, L., Dayalan Naidu, S., Träger, U., Chen, X., Kegel-Gleason, K., Llères, D., *et al.* (2017). KEAP1-modifying small molecule reveals muted NRF2 signaling responses in neural stem cells from Huntington's disease patients. *Proc. Natl. Acad. Sci. U. S. A.* 114, E4676-E4685. doi: 10.1073/pnas.1614943114
- Roach, J. P., Moore, E. E., Partrick, D. A., Damle, S. S., Silliman, C. C., McIntyre, R. C., *et al.* (2009). Heme oxygenase-1 induction in macrophages by a hemoglobin-based oxygen carrier reduces endotoxin-stimulated cytokine secretion. *Shock Augusta Ga* 31, 251-257. doi: 10.1097/SHK.0b013e3181834115
- Rosseau, S., Hammerl, P., Maus, U., Walmrath, H. D., Schütte, H., Grimminger, F., *et al.* (2000). Phenotypic characterization of alveolar monocyte recruitment in acute respiratory distress syndrome. *Am. J. Physiol. Lung Cell. Mol. Physiol.* 279, L25-L35. doi: 10.1152/ajplung.2000.279.1.L25
- Sakai, J., Cammarota, E., Wright, J. A., Cicuta, P., Gottschalk, R. A., Li, N., *et al.* (2017). Lipopolysaccharide-induced NF- κ B nuclear translocation is primarily dependent on MyD88, but TNF α expression requires TRIF and MyD88. *Sci. Rep.* 7, 1428. doi: 10.1038/s41598-017-01600-y
- Satoh, T., McKercher, S. R., and Lipton, S. A. (2013). Nrf2/ARE-mediated antioxidant actions of pro-electrophilic drugs. *Free Radic. Biol. Med.* 65, 645-657. doi: 10.1016/j.freeradbiomed.2013.07.022
- Schildberger, A., Rossmannith, E., Eichhorn, T., Strassl, K., and Weber, V. (2013). Monocytes, peripheral blood mononuclear cells, and THP-1 cells exhibit different cytokine expression patterns following stimulation with lipopolysaccharide. *Mediators Inflamm.* 2013, 697972. doi: 10.1155/2013/697972
- Serafini, M. M., Catanzaro, M., Fagiani, F., Simoni, E., Caporaso, R., Dacrema, M., *et al.* (2019). Modulation of Keap1/Nrf2/ARE Signaling Pathway by Curcuma- and Garlic-Derived Hybrids. *Front. Pharmacol.* 10, 1597. doi: 10.3389/fphar.2019.01597
- Simoni, E., Serafini, M. M., Bartolini, M., Caporaso, R., Pinto, A., Necchi, D., *et al.* (2016). Nature-Inspired Multifunctional Ligands: Focusing on Amyloid-Based Molecular Mechanisms of Alzheimer's Disease. *ChemMedChem* 11, 1309-1317. doi: 10.1002/cmdc.201500422
- Simoni, E., Serafini, M.M., Caporaso, R., Marchetti, C., Racchi, M., Minarini, A., *et al.* (2017). Targeting the Nrf2/Amyloid-Beta Liaison in Alzheimer's Disease: A Rational Approach. *ACS Chem. Neurosci.* 8, 1618-1627. doi: 10.1021/acschemneuro.7b00100
- Tanigawa, S., Fujii, M., and Hou, D.-X. (2007). Action of Nrf2 and Keap1 in ARE-mediated NQO1 expression by quercetin. *Free Radic. Biol. Med.* 42, 1690-1703. doi: 10.1016/j.freeradbiomed.2007.02.017

Thimmulappa, R. K., Lee, H., Rangasamy, T., Reddy, S. P., Yamamoto, M., Kensler, T. W., *et al.* (2006). Nrf2 is a critical regulator of the innate immune response and survival during experimental sepsis. *J. Clin. Invest.* 116, 984–995. doi: 10.1172/JCI25790

Wardyn, J. D., Ponsford, A. H., and Sanderson, C. M. (2015). Dissecting molecular crosstalk between Nrf2 and NF- κ B response pathways. *Biochem. Soc Trans.* 43, 621–626. doi: 10.1042/BST20150014

Woodcock, C.-S. C., Huang, Y., Woodcock, S. R., Salvatore, S. R., Singh, B., Golin-Bisello, F., *et al.* (2018). Nitro-fatty acid inhibition of triple-negative breast cancer cell viability, migration, invasion, and tumor growth. *J. Biol. Chem.* 293, 1120–1137. doi: 10.1074/jbc.M117.814368

PART V

The following manuscript was published in *Frontiers in Pharmacology* in 2020 as:

Eye-light on Age-related Macular Degeneration: Targeting Nrf2-pathway as a Novel Therapeutic Strategy for Retinal Pigment Epithelium

Michele Catanzaro, Cristina Lanni, Filippo Basagni, Michela Rosini, Stefano Govoni and Marialaura Amadio

Abstract

Age-related macular degeneration (AMD) is a common disease with a multifactorial aetiology, still lacking effective and curative therapies. Among the early events triggering AMD is the deterioration of the retinal pigment epithelium (RPE), whose fundamental functions assure good health of the retina. RPE is physiologically exposed to high levels of oxidative stress during its lifespan; thus, the integrity and well-functioning of its antioxidant systems are crucial to maintain RPE homeostasis. Among these defensive systems, the Nrf2-pathway plays a primary role. Literature evidence suggests that, in aged and especially in AMD RPE, there is an imbalance between the increased pro-oxidant stress, and the impaired endogenous detoxifying systems, finally reverberating on RPE functions and survival. In this *in vitro* study on wild type (WT) and Nrf2-silenced (siNrf2) ARPE-19 cells exposed to various AMD-related *noxae* (H₂O₂, 4-HNE, MG132+Bafilomycin), we show that the Nrf2-pathway activation is a physiological protective stress response, leading downstream to an up-regulation of the Nrf2-targets HO1 and p62, and that a Nrf2 impairment predisposes the cells to a higher vulnerability to stress. In search of new pharmacologically active compounds potentially useful for AMD, four nature-inspired hybrids (NIH) were individually characterized as Nrf2 activators, and their pharmacological activity was investigated in ARPE-19 cells. The Nrf2 activator dimethyl-fumarate (DMF; 10 μM) was used as a positive control. Three out of the four tested NIH (5 μM) display both direct

and indirect antioxidant properties, in addition to cytoprotective effects in ARPE-19 cells under pro-oxidant stimuli. The observed pro-survival effects require the presence of Nrf2, with the exception of the lead compound NIH1, able to exert a still significant, albeit lower, protection even in siNrf2 cells, supporting the concept of the existence of both Nrf2-dependent and independent pathways mediating pro-survival effects. In conclusion, by using some pharmacological tools as well as a reference compound, we dissected the role of the Nrf2-pathway in ARPE-19 stress response, suggesting that the Nrf2 induction represents an efficient defensive strategy to prevent the stress-induced damage.

Keywords: Nrf2; age-related macular degeneration (AMD); retinal pigment epithelium (RPE); oxidative stress; pharmacological modulation; cytoprotection; HO1; p62.



Eye-Light on Age-Related Macular Degeneration: Targeting Nrf2-Pathway as a Novel Therapeutic Strategy for Retinal Pigment Epithelium

Michele Catanzaro¹, Cristina Lanni¹, Filippo Basagni², Michela Rosini², Stefano Govoni¹ and Marialaura Amadio^{1*}

¹ Section of Pharmacology, Department of Drug Sciences, University of Pavia, Pavia, Italy, ² Department of Pharmacy and Biotechnology, University of Bologna, Bologna, Italy

INTRODUCTION

Age-related macular degeneration (AMD) is one of the most common neurodegenerative diseases and leading causes of irreversible blindness in the elderly worldwide (Lim *et al.*, 2012). AMD is characterized by a progressive loss of central vision due to degenerative and vascular changes in the macula, the retinal region responsible for fine and colour vision (Jager *et al.*, 2008). AMD is classified in dry (~90%) and wet (~10%) AMD forms, in early and late stages (Lim *et al.*, 2012). Presently, no cure is available for dry AMD. In the wet form, monthly intravitreal injections of anti-VEGF drugs are used to contrast the neoangiogenesis, though they can only delay the symptoms and present several limits (Amadio *et al.*, 2016).

The degeneration of retinal pigment epithelium (RPE), fundamental for photoreceptor homeostasis and, in general, for retina health, is among the earliest factors triggering AMD pathology (Bhutto and Lutty, 2012). Compared with normal RPE, AMD RPE presents increased susceptibility to oxidative stress, autophagy impairment and higher levels of reactive oxygen species (ROS) under stress conditions (Golestaneh *et al.*, 2018). The most comprehensive transcription system used by RPE to neutralize oxidative

stress and maintain cellular homeostasis is the Keap1-Nrf2-ARE pathway (Sachdeva *et al.*, 2014; Lambros and Plafker, 2016). The nuclear factor E2-related factor 2 (Nrf2) is a transcription factor that is activated/upregulated under oxidative stress. In basal conditions, in the cytosol Nrf2 is anchored by Kelch-like ECH-associated protein 1 (Keap1), which mediates Nrf2 proteasomal degradation, maintaining Nrf2 at a low level (McMahon *et al.*, 2003). Upon oxidative stress, Keap1 undergoes a conformational change and dissociates from Nrf2, that is free to translocate to the nucleus, where it binds to the antioxidant response element (ARE) in the promoter of target genes, thus initiating their transcription (Motohashi and Yamamoto, 2004). Nrf2 activation has been shown to protect against oxidative stress, protein deposition, inflammation (Zhang *et al.*, 2015; Pajares *et al.*, 2016). Since oxidative stress is one of the main factors contributing to the AMD pathogenesis, and literature evidence suggests that Nrf2-signalling pathway is compromised in AMD-like animal models (Sachdeva *et al.*, 2014; Batliwala *et al.*, 2017), we evaluated the relevance of Nrf2 in RPE under adverse conditions.

In particular, in wild type and Nrf2-deficient ARPE-19 cells, we studied the effects of the following pro-oxidant AMD-related *noxae*: H₂O₂, 4-hydroxynonenal (4-HNE), MG132+Bafilomycin. H₂O₂ is a strong oxidant leading to an immediate ROS production, widely used in *in vitro* study on RPE cells (Zhu *et al.*, 2017; Hu *et al.*, 2019; Zhao *et al.*, 2019), that are physiologically subjected to elevated ROS levels due to their high metabolism and functions (Strauss, 2005). 4-HNE is a product of lipid peroxidation accumulating in AMD retina (Ethen *et al.*, 2007); it is pro-oxidant and toxic for RPE (Kaarniranta *et al.*, 2005; Kaemmerer *et al.*, 2007; Chen *et al.*, 2009), but its effects on Nrf2-pathway have been not fully elucidated. MG132+Bafilomycin co-stimulus inhibits autophagy in RPE (Viiri *et al.*, 2010, 2013), leading to accumulation of protein aggregates, a condition that predisposes to a more oxidant intracellular environment and dysfunction of RPE (Hytinen *et al.*, 2014; Ferrington *et al.*, 2016). In stressed ARPE-19 cells, among Nrf2-responsive genes, we studied the modulation of both *Heme Oxygenase 1 (HO1)* and *p62/sequestosome 1 (p62/SQSTM1)*, in virtue of their acknowledged functions in the maintenance and survival of RPE in the adult

retina (Loboda *et al.*, 2016; Wang *et al.*, 2016). In particular, HO1 is a detoxifying enzyme with a role in retina physiopathology and ocular diseases (Zhao *et al.*, 2012), while p62 is a key regulator of proteostasis in RPE (Kaarniranta *et al.*, 2017), and it mediates Keap1 degradation, contributing to Nrf2 activation in a positive feedback loop (Jain *et al.*, 2010; Jiang *et al.*, 2015).

With the aim to find new pharmacological tools potentially useful in AMD, we also tested a small set of nature-inspired hybrids (here called NIH) carrying the hydroxycinnamoyl function recurring in polyphenols, and the allyl mercaptan moiety of garlic-derived organosulfur compounds. These compounds, previously characterized in other cellular models (Simoni *et al.*, 2016, 2017; Serafini *et al.*, 2019), were herein studied for their antioxidant potential, their capability to activate Nrf2-pathway, and to promote protection in both wild type and Nrf2-deficient ARPE-19 cells under challenging stressful conditions.

MATERIALS AND METHODS

Cell culture, reagents and treatments

The human RPE cell line ARPE-19 was obtained from American Type Culture Collection. Cells were grown in a humidified 5% CO₂ atmosphere at 37°C in Dulbecco's Modified Eagle Medium: F12 (1:1; Gibco, Invitrogen, Carlsbad, CA, USA), including 10% inactivated foetal bovine serum, 100 units/ml penicillin, 100 µg/ml streptomycin, and 2 mM L-glutamine (Merck KGaA, Darmstadt, Germany). The experiments were carried out on passages 15-20. Cells were exposed to either the solvent (0.05% DMSO), or H₂O₂ (300-500 µM; Merck KGaA), the lipid peroxidation product 4-HNE; 50-100 µM; Cayman, Ann Arbor, MI, USA), the proteasome inhibitor MG132 (5 µM; Calbiochem, San Diego, CA, USA), the Vacuolar H⁺-ATPase Inhibitor bafilomycin (50 nM; Merck KGaA). Nature-inspired hybrids (NIH) were synthesized according to previous procedures (Simoni *et al.*, 2016, 2017) and were >98% pure. Each NIH and dimethyl-fumarate (DMF, Merck KGaA) were dissolved in DMSO to obtain 10- and 20-mM stock solutions, respectively.

NIH and DMF were diluted until 5 and 10 μM , respectively. Treatments were performed in triplicates, if not otherwise indicated.

Silencing of Nrf2 expression

A siRNA designed for the human *Nrf2* gene (Merck KGaA) was incubated for at least 24 hrs to obtain the siNrf2 ARPE-19 cell line. A commercial negative siRNA (siNEG, Merck KGaA) having no known homology with any gene was used as a negative control in preliminary experiments to confirm the specificity of the transient Nrf2 silencing. The siRNAs were transfected into ARPE-19 cells using the lipofectamin RNAiMAX transfection reagent (Invitrogen, Thermo Scientific, Waltham, MA, USA) following the manufacturer's instructions; siRNA treatment was maintained throughout the experiments (up to 72 hrs). To confirm that Nrf2 expression was silenced, 4 hrs before the end of the experiment, the proteasome inhibitor MG132 (5 μM) was added to the medium of selected plates to block the degradation of Nrf2 protein, that was evaluated by Western blotting.

Immunocytochemistry

ARPE-19 cells were seeded onto poly-L-lysine-coated coverslips for 24 hrs before exposure to either solvent, NIH or DMF, for 3 hrs. Immunocytochemistry was performed as previously described, with minor modifications (Marchesi *et al.*, 2018). Briefly, cells were fixed in ethanol 70% at -20°C , washed with phosphate-buffered saline (PBS), and permeabilized for 15 min with 0.01% Triton X-100 in PBS. Nonspecific binding sites were blocked at room temperature by incubation for 30 min with PBS containing 1% bovine serum albumin (BSA). Cells were then incubated for 1 hr with a polyclonal antibody recognizing Nrf2 (NBP1-32822; Novus Biologicals, Centennial, CO, USA) diluted 1:50 in PBS/1% BSA solution. After a brief rinse with PBS solution, cells were incubated for 1 hr with the Alexa Fluor 488-conjugated anti-rabbit secondary antibody (A27034; Invitrogen) diluted at 1:200 in PBS/1% BSA. Cells were rinsed in PBS, then incubated for 10 min with Hoechst solution to counterstain the nucleus. After rinse with PBS and distilled water, the cells were finally mounted up-side-down on a glass slide

in a drop of Mowiol mounting medium (Merck KGaA). Cells were photographed with AxioCam MRc5 mounted on Zeiss Axioskop 40 microscopy.

Cell fractioning, protein extraction, and Western blotting

ARPE-19 cells plated in either 35 or 100 mm dishes were subjected to treatments, then washed twice with cold PBS, scraped, and collected. For study on total homogenates, cells were lysed in an appropriate buffer (50 mM Tris-HCl pH 7.5, 150 mM NaCl, 5 mM EDTA, 0.5% Triton X-100, and protease inhibitors mix), and sonicated 2 times for 10 sec. For Nrf2 translocation study, nuclear extracts were obtained by using the Nuclear Extract kit (Active Motif, Carlsbad, CA, USA) according to our previous publication (Viiri *et al.*, 2013). Protein contents of total homogenates and nuclear fractions were determined by Bradford method (SERVA GmbH, Heidelberg, Germany) using BSA as a standard. Total lysate and nuclear fractions were diluted in 2x SDS protein gel loading solution and separated on 10% SDS-polyacrylamide gel electrophoresis, transferred into a nitrocellulose membrane, and processed following the standard procedures. The antibodies were diluted in 5% BSA in TBS-T Buffer (10 mM Tris-HCl, 100 mM NaCl, 0.1% Tween, pH 7.5) as follows: the anti-Nrf2 (NBP1-32822) and anti-HO1 (NBP1-31341) rabbit polyclonal antibodies (Novus Biologicals) at 1:1000; the anti-p62 (sc-28359), anti-lamin A (sc-71481) (both by Santa Cruz Biotechnology, Inc., Dallas, TX, USA), anti- β -actin (612656; BD Biosciences, San José, CA, USA) mouse monoclonal antibodies at 1:1000, 1:3000, and 1:1000, respectively. The horseradish peroxidase-conjugated secondary anti-mouse (A4416; Merck KGaA) and anti-rabbit (sc-2357; Santa Cruz Biotechnology, Inc.) antibodies were diluted in 5% BSA/TBS-T Buffer. The nitrocellulose membranes signals were detected by chemiluminescence. Experiments were performed in duplicate for each different cell preparation. As loading controls, β -actin was used for total homogenate, while lamin A for the rough nuclear fraction. Statistical analysis of the Western blotting data was performed on the densitometric values obtained by the Scion Image software (Scion Corporation).

RNA extraction, retro-transcription, and real-time quantitative PCR

Total RNA was extracted from ARPE-19 cells by the Direct-zol RNA MiniPrep Kit (Zymo Research, Irvine, CA, USA) and subjected to reverse transcription by the QuantiTect Reverse Transcription Kit (Qiagen, Hilden, Germany) following standard procedures. Real-time quantitative PCR (RT-qPCR) amplifications were carried out using the QuantiTect SYBR Green PCR Kit (Qiagen) and the Lightcycler instrument (Roche, Basel, Switzerland), with the following primers:

Nrf2: 5'- TTCTGTTGCTCAGGTAGCCCC-3' (upstream)

and 5'- TCAGTTTGGCTTCTGGACTTGG -3' (downstream);

HO1: 5'- AGCAACAAAGTGCAAGATTCTGC -3' (upstream)

and 5'- CAGCATGCCTGCATTCACATG -3' (downstream);

GAPDH: 5'- CAGCAAGAGCACAAAGAGGAAG-3' (upstream)

and 5'- CAACTGTGAGGAGGGGAGATT -3' (downstream).

GAPDH mRNA was the reference on which all the other values were normalized, due to its substantial stability in our experimental conditions as in most cases in literature. $2^{-\Delta\Delta C_t}$ method was used for quantification of mRNAs.

Cell viability assays

ARPE-19 cells were plated 20,000/well in a 96-well plate, and cell viability was determined by either MTT (Merck KGaA) or PrestoBlue® (Invitrogen) assays. MTT assay was performed according to a published method (Amadio *et al.*, 2008); absorbance was measured at 495 nm in a UV spectrophotometer and the results were expressed as a percentage of the absorbance of the samples in comparison to control. PrestoBlue® assay was used following manufacturer's instruction. After treatments, cells were loaded for 10 min with PrestoBlue® reagent prior to assay readout. Fluorescence was measured by the Synergy HT multidetection microplate reader (BioTek, Winooski, VT, USA) with excitation and emission wavelengths of 530 and 590 nm, respectively.

The results were expressed as a percentage of the fluorescence of the samples in comparison to control.

Measurement of reactive oxygen species

Measurement of intracellular reactive oxygen species (ROS) was performed by 2',7'-Dichlorofluorescein diacetate (DCFH-DA) assay (Merck KGaA) following manufacturer's instruction. Two different experimental settings were followed, as described in the relative figure legends. In each setting, at the end of the H₂O₂ treatments, cells were detached by trypsin, counted, incubated with 25 μM DCFH-DA for 45 min, and centrifuged (1,200 x g for 5 min at 37°C), to remove the DCFH-DA. The cells were re-suspended in medium without FBS, plated in black-bottom 96-well plate, and the 2',7'-dichlorofluorescein (DCF) was measured ($\lambda_{\text{ex}} = 485 \text{ nm}$, $\lambda_{\text{em}} = 530 \text{ nm}$) by Synergy HT multidetection microplate reader (BioTek).

Heme oxygenase activity

Cells cultured in 100 mm diameter petri dishes were collected after incubation with either solvent, NIH1, NIH4 (5 μM for 6 hrs), or hemin (10 μM for 4 hrs), a well-known HO1 inducer (Amadio *et al.*, 2014). Heme oxygenase activity was assessed according to a published method with minor modifications (Foresti *et al.*, 2015). Briefly, samples were incubated with the substrate hemin, biliverdin reductase, NADPH, glucose-6-phosphate (G6P), G6P dehydrogenase (Merck KGaA), and other reagents to sustain heme oxygenase activity. The assay is based on the spectrophotometric determination of bilirubin as the final product of a reaction where hemin is transformed by heme oxygenase to biliverdin, which is in turn converted by biliverdin reductase to bilirubin. The reaction was allowed to proceed for 1 h at 37°C in the dark and was stopped by addition of chloroform to extract the bilirubin formed. The extracted bilirubin was measured spectrophotometrically (wavelengths of 464 and 530 nm) and calculated in picomoles bilirubin/mg ARPE-19 cell protein/hr.

NIH stability assay

NIH1 was dissolved in DMSO to obtain a stock solution 10 mM. Samples of this stock solution were diluted until 1 mM in cell-free complete culture medium and left incubating at 37°C for up to three days. At selected time points (0, 24, 48, and 72 hrs) samples were collected, diluted at 0.1 mM with mobile phase ACN/H₂O 40:60, and analysed through HPLC reversed-phase conditions on a Phenomenex Jupiter C18 (150 × 4.6 mm I.D.) column, UV detection at $\lambda = 302$ nm and a flow rate of 1 ml/min. Analyses were performed on a liquid chromatograph model PU 2089 PLUS equipped with a 20 μ l loop valve and linked to MD 2010 Plus UV detector (Jasco Europe, Lecco, Italy). Areas of NIH1 peak, identified by co-injection, were analysed and their percentage reductions vs time were reported in the graph.

Statistical analysis

For the statistical analyses the GraphPad InStat program (GraphPad software, San Diego, CA, USA) was used. Data were subjected to the analysis of variance (either one-way or two-way ANOVA) followed, when significant, by an appropriate *post hoc* comparison test, as specifically indicated. Differences were considered statistically significant when $p < 0.05$.

RESULTS

The Nrf2-deficit reverberates on the cell viability in ARPE-19 cells under stress

To evaluate the efficiency rate of our Nrf2-silencing RNA, we first measured, by both RT-qPCR and Western blotting, the Nrf2 expression in wild type (WT), negative-siRNA (siNEG), and Nrf2-silenced (siNrf2) ARPE-19 cells, confirming in the latter ones a specific and marked decrease of both Nrf2 mRNA and protein content (**Supplementary Figure 1**). No difference in Nrf2 expression between WT and siNEG cells was found.

To determine whether the Nrf2 impairment affects the susceptibility of ARPE-19 to stress in term of cell viability, according to both our previous experience and new explorative experiments, we preliminary selected the best conditions (time/concentration) for each stress inducing a significant mortality in WT ARPE-19 cells.

WT ARPE-19 cells were either non-stressed, or exposed to 30, 50, or 100 μM 4-HNE, for 8 and 24 hrs, and analysed by a cell viability assay (**Supplementary Figure 2A**). Upon 8 hrs exposure to either 30 or 50 μM 4-HNE, no reduction in the cell viability was detected, while a significant mortality was observed following 100 μM 4-HNE. At 24 hrs, we found a dose-response proportional decrease in the viability of 4-HNE-stressed ARPE-19 cells. Therefore, WT, siNEG, and siNrf2 ARPE-19 cells were either non-stressed, or exposed to 100 μM 4-HNE, for 8 and 24 hrs, and analysed for cell viability (**Figure 1A**). In basal conditions, there is no difference in the viability among the three cell lines. At both 8 and 24 hrs under 4-HNE, siNrf2 cells show a lower survival than WT cells. Under stress, siNEG cells show a mortality fully comparable to WT cells; for this reason, we performed the following experiments only in WT and siNrf2 cells.

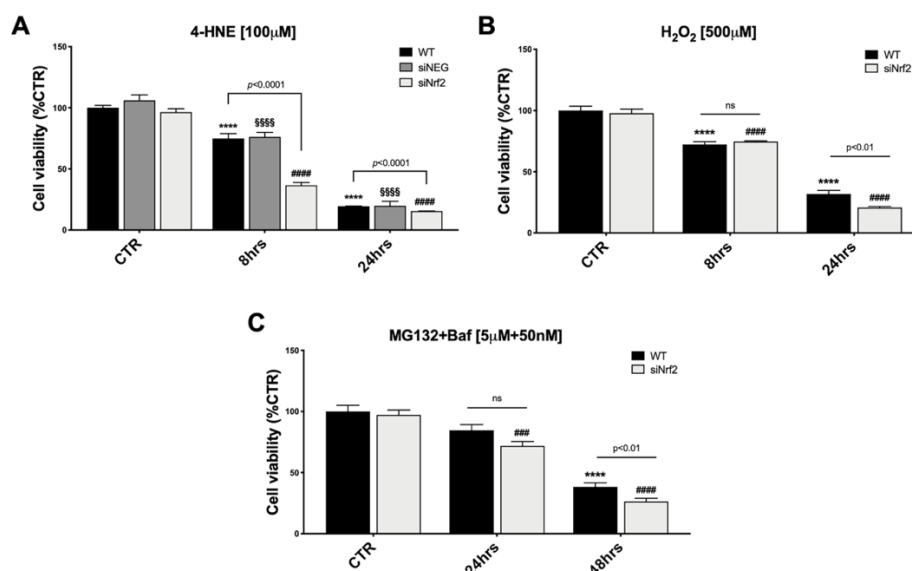


Figure 1. The Nrf2-impaired ARPE-19 cells are more susceptible to stress than their WT counterpart. Cell viability was assessed by a fluorometric assay (PrestoBlue[®]) and results are

expressed as mean of percentages \pm SEM. **(A)** WT, siNEG, and siNrf2 ARPE-19 cells were treated with either solvent (DMSO, CTR) or 4-HNE [100 μ M] for 8 and 24 hrs. Dunnett's multiple comparisons test; **** p <0.0001 versus WT CTR; §§§§ p <0.0001 versus siNEG CTR; and ##### p <0.0001 versus siNrf2 CTR; n=5-8. **(B)** WT and siNrf2 ARPE-19 cells were treated with either solvent (DMSO, CTR) or H₂O₂ [500 μ M] for 8 and 24 hrs. Sidak's multiple comparisons test; **** p =0.0001 versus WT CTR; ##### p <0.0001 versus siNrf2 CTR; n=6-8. **(C)** WT and siNrf2 ARPE-19 cells were treated with either solvent (DMSO, CTR) or MG132+Bafilomycin [5 μ M + 50 nM] for 24 and 48 hrs. Sidak's multiple comparisons test; **** p <0.0001 versus WT CTR; ### p <0.001 and ##### p <0.0001 versus siNrf2 CTR; n=5-9.

We also analysed the viability of WT ARPE-19 cells that were either non-stressed, or exposed to 100, 300, or 500 μ M H₂O₂, for 8 and 24 hrs (**Supplementary Figure 2B**), and then we selected 500 μ M H₂O₂ for 24 hrs as the best condition for our purpose. Both WT and siNrf2 ARPE-19 cells were either non-stressed, or exposed to 500 μ M H₂O₂, for 8 and 24 hrs, and analysed for viability; we found that siNrf2 cells show a lower survival than WT cells at 24 hrs (**Figure 1B**).

According to our previous experience with autophagy inhibitors in ARPE-19 cells (Viiri *et al.*, 2013), that require longer times to display cytotoxicity, we evaluated the impact of MG132+Bafilomycin (MG132+Baf; 5 μ M + 50 nM) co-treatment, for 24 and 48 hrs, in both WT and siNrf2 cells, and found a more consistent mortality in the latter ones at 48 hrs (**Figure 1C**).

Overall, these results indicate that the viability of WT and siNrf2 cells is fully comparable in normal conditions, while in prolonged adverse conditions the Nrf2 impairment predisposes the ARPE-19 cells to a higher stress-induced mortality.

Different stress stimuli activate Nrf2-pathway in wild type ARPE-19 cells

To study the Nrf2-pathway activation under pro-oxidant injury without causing cell mortality, both WT and siNrf2 ARPE-19 cells were either non-stressed, or exposed to 4-HNE (50 μ M), H₂O₂ (300 μ M), and MG132+Baf (5 μ M + 50 nM) co-treatment for 6 hrs. We first evaluated Nrf2 protein levels in total cellular homogenates by Western blotting, finding that each of these stressful conditions up-regulates Nrf2 protein expression in WT but not in siNrf2 cells, as expected (**Figure 2, panels A-C**).

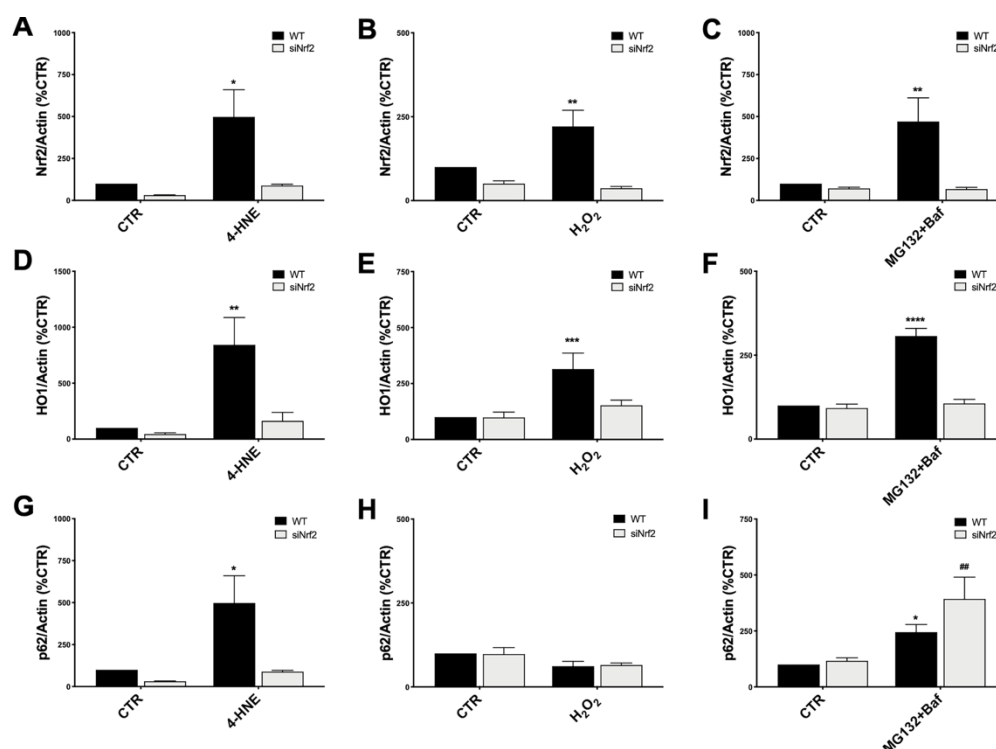


Figure 2. Nrf2-pathway activation in wild type ARPE-19 cells under different stress conditions. Both WT and siNrf2 ARPE-19 cell lines were treated for 6 hrs with either solvent (DMSO, CTR), 4-HNE [50 μ M] (panels A,D,G), H₂O₂ [300 μ M] (panels B,E,H), or MG132+Bafilomycin [5 μ M + 50 nM] (panels C,F,I). Total cellular homogenates were examined by Western blot using an antibody against Nrf2 (A-C), HO1 (D-F), and p62 (G-I); Actin content was used as a loading control to normalize the data. Results are expressed as percentage means \pm SEM. Sidak's multiple comparisons test; * p <0.05, ** p <0.01, *** p <0.001, and **** p <0.0001 versus WT CTR; ## p <0.01 versus siNrf2 CTR; n =4-6.

In order to highlight potential specificities in the stress-induced activation of Nrf2-targets, we then evaluated downstream the expression of HO1 and p62 protein levels in the same cellular total homogenates by Western blotting. We found that HO1 protein content is increased in WT cells in all the noxious conditions examined; no significant change in HO1 levels was detected in the stressed siNrf2 cells, suggesting the strong dependence of HO1 expression on Nrf2 (Figure 2, panels D-F). The p62 protein level varies in function of the stress condition: it is not changed in H₂O₂-treated WT cells, while it is

increased in WT cells exposed to either 4-HNE or MG132+Baf co-treatment (**Figure 2, panels G-I**). In siNrf2 cells exposed to either 4-HNE or H₂O₂, there are no alterations in p62 protein amount. Instead, a marked increase of p62 level occurs in siNrf2 cells under MG132+Baf, in accordance to the degradation of p62 via autophagy which is indeed blocked by this co-treatment. The increase of p62 protein level triggered by MG132+Baf seems even higher in siNrf2 than in WT cells, suggesting that siNrf2 cells are featured by a less efficient autophagy flux that may be further compromised in the presence of autophagy inhibitors.

NIH are well tolerated and activate Nrf2-pathway in ARPE-19 cells

In order to find new pharmacological tools potentially useful in AMD, we tested some nature-inspired hybrids (NIH1-4; **Supplementary Figure 3A**) for their capability to activate Nrf2-pathway in ARPE-19 cells. Previous *in vitro* studies showed that NIH allow Nrf2 activation when at least a (pro)electrophilic feature, such as the catechol moiety or the α,β -unsaturated carbonyl group, is present (Simoni *et al.*, 2017; Serafini *et al.*, 2019). First, preliminary experiments on the lead compound NIH1 were performed to evaluate its capability to induce Nrf2 nuclear translocation in ARPE-19 cells. According to our evidence in another cellular line (Serafini *et al.*, 2019), ARPE-19 cells were exposed for 3 hrs to either the solvent or lead compound NIH1 at two concentrations (0.5 and 5 μ M), and Nrf2 protein content within the nuclear fractions was evaluated by Western blotting experiments. We found that ARPE-19 cells exposed to 5 μ M NIH1 display significantly higher Nrf2 nuclear levels compared to control cells (control: 100.0% \pm 12.6; 0.5 μ M NIH1: 110.0% \pm 8.2; 5 μ M NIH1: 166.7%* \pm 11.4; values expressed as mean percentage \pm SEM; Dunnett's multiple comparisons test, *p<0.05 vs control; n=4). Consistently, 5 μ M concentration was selected and used for each NIH in the following experiments. As a positive control of Nrf2 activation we used dimethyl-fumarate (DMF, 10 μ M).

We determined the tolerability of NIH1, NIH2, NIH3, and NIH4 by MTT assay, finding that 48 hrs exposure does not affect the ARPE-19 cell viability (**Figure 3A**). A stability test on NIH1 performed in the complete culture medium at 24,

48, and 72 hrs, indicates that, compared to time 0, NIH1 concentration is reduced to $74.18\% \pm 2.80$, $46.26\% \pm 1.56$, and $18.17\% \pm 0.6$, respectively (**Supplementary Figure 3B**).

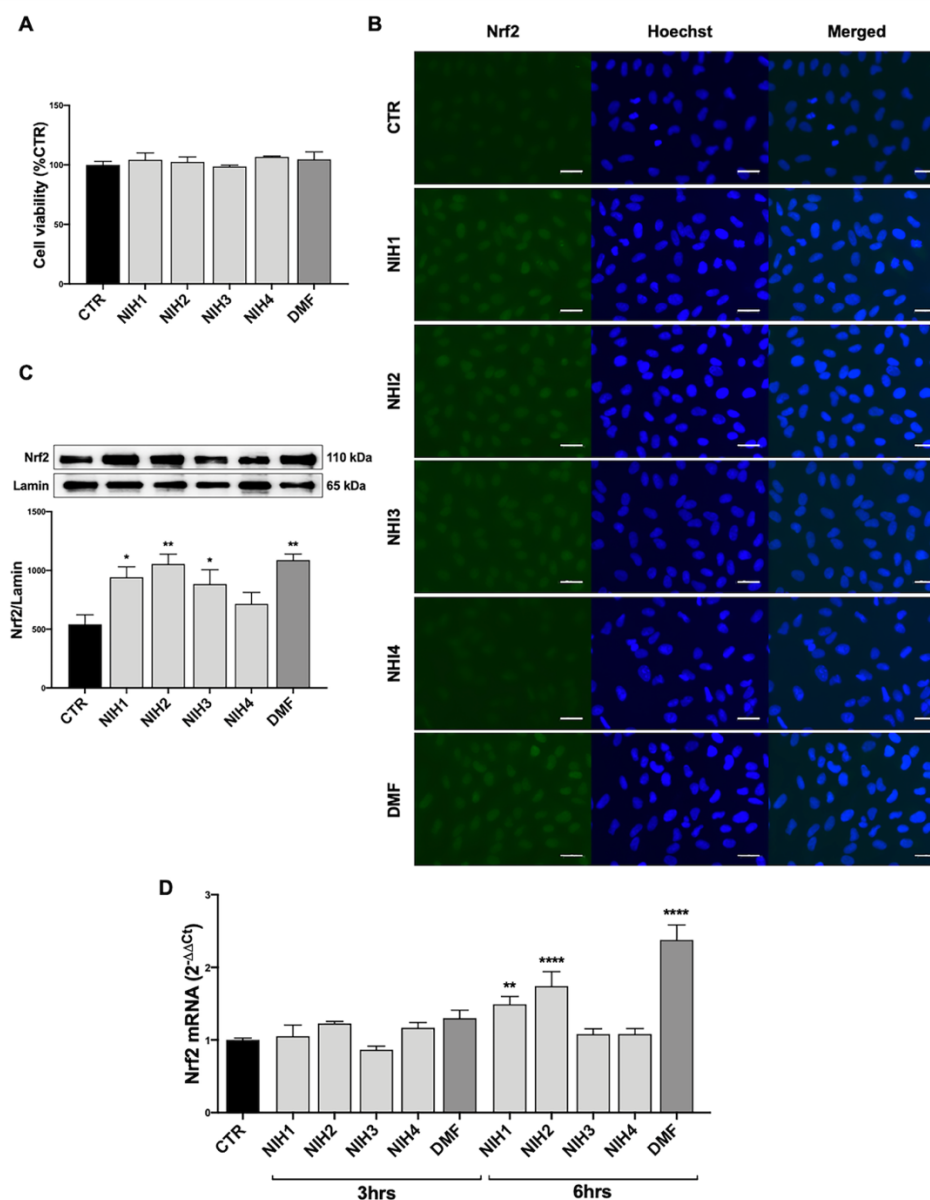


Figure 3. Pharmacological activation of Nrf2 protein by NIH in ARPE-19 cells. (A) Tolerability of NIH in ARPE-19 cells. ARPE-19 cells were treated for 48 hrs with solvent

(DMSO, CTR), NIH1, NIH2, NIH3 and NIH4 [5 μ M], or DMF [10 μ M], and their viability was assessed by MTT assay. Results are expressed as mean of percentages \pm SEM (CTR: 100%); Dunnett's multiple comparisons test; no statistical differences versus CTR; n=3-5. **(B-C) Evaluation of NIH-induced Nrf2 nuclear translocation.** ARPE-19 cells were treated for 3 hrs with either solvent (DMSO, CTR), NIH1, NIH2, NIH3, NIH4 [5 μ M], or DMF [10 μ M]. **(B)** Immunocytochemistry for Nrf2 protein localization was performed by using a green fluorescent-conjugated secondary antibody. Nuclei (blue) were stained by Hoechst. Scale bar: 20 μ m. **(C)** Nuclear fraction was isolated and examined by Western blot using an antibody against Nrf2. Lamin A content was used as a loading control to normalize the data. Results are expressed as means of Nrf2/Lamin A (ratio \times 1000) \pm SEM. Dunnett's multiple comparisons test; * p <0.05 and ** p <0.01 versus CTR; n=5. **(D) Study of Nrf2 mRNA expression following NIH treatment.** Total Nrf2 mRNA levels were measured by RT-qPCR in ARPE-19 cells exposed to either solvent (DMSO, CTR), NIH1, NIH2, NIH3, NIH4 [5 μ M], or DMF [10 μ M] for 3 hrs and 6 hrs. GAPDH mRNA content was used as a housekeeping to normalize the data. Results are expressed as means of $2^{-\Delta\Delta C_t} \pm$ SEM. Dunnett's multiple comparisons test; ** p <0.01 and *** p <0.0001 versus CTR; n=3.

We then evaluated the capability of hybrids to activate Nrf2 in ARPE-19 cells. Following 3 hrs exposure, the NIH1, NIH2, NIH3, having in their structure the chemical group(s) responsible for the Nrf2-pathway activation (Simoni *et al.*, 2016) (**Supplementary Figure 3A**), induce an increase of Nrf2 content within the nucleus, as shown by both immunocytochemistry (**Figure 3B**) and Western blotting experiments (**Figure 3C**). Immunocytochemistry revealed a general increment of Nrf2-immunostaining in the whole ARPE-19 cells exposed to either NIH1, NIH2, or NIH3. To confirm a possible up-regulation of Nrf2 expression upon these hybrids, by RT-qPCR we measured total Nrf2 mRNA levels at both 3 and 6 hrs, finding a statistically significant increase after 6 hrs treatment with NIH1 and NIH2 (**Figure 3D**), consistent with a self-sustaining positive feedback of Nrf2 itself. On the contrary, the fact that NIH3 does not increase Nrf2 mRNA levels after 3 and 6 hrs may be ascribed to our previous observation that some of the investigated compounds may affect the Nrf2-pathway following different temporal kinetics (Serafini *et al.*, 2019). DMF is well tolerated after 48 hrs exposure; it induces Nrf2 nuclear translocation at 3 hrs, and up-regulates Nrf2 mRNA expression at 6 hrs (**Figure 3**). NIH4, lacking the Nrf2-activating functional groups (**Supplementary Figure 3A**), instead displays effects not different from the solvent (**Figure 3**); therefore, NIH4 will be mentioned as "inactive" NIH since now.

The Nrf2-target HO1 gene can be differently induced by the active NIH in ARPE-19 cells

Because of the above results and tight dependence on Nrf2, we selected *HO1* gene to evaluate the effects of NIH downstream Nrf2 in WT ARPE-19 cells. In line with data on *Nrf2* mRNA levels, we found that total HO1 mRNA levels are significantly higher after 3 and 6 hrs exposure to NIH1 and NIH2 (**Figure 4A**). NIH1, NIH2, and NIH3, up-regulate total HO1 protein expression, although with extents and/or time-courses that vary among molecules (**Figure 4B**). In particular, after 3 hrs treatment, both NIH1 and NIH2 lead to a significant increase of HO1 protein content, that is maintained for the longer times here considered, and is still sustained at 24 hrs. The NIH1-mediated increase of HO1 protein is relevant even after 48 hrs treatment. For NIH3, we found an increase of total HO1 protein after 16 and 24 hrs (**Figure 4B**). DMF induces an up-regulation of *HO1* mRNA at both 3 and 6 hrs (**Figure 4A**); we also observed a trend to increase of HO1 protein levels upon 9, 16, 24 hrs DMF treatment, but without statistical significance in the overall group (**Figure 4B**). However, when comparing DMF and control alone (by an Unpaired t test), in DMF-treated cells HO1 protein levels are significantly higher than control after 9 hrs (+84.3% \pm 37.7; n=3-5, p<0.05), 16 hrs (+157.1% \pm 43.0; n=5, p<0.001), and 24 hrs (+58.9% \pm 19.8; n=5, p<0.01). No effects on *HO1* mRNA and protein expression are observed for the inactive NIH4 (**Figure 4**).

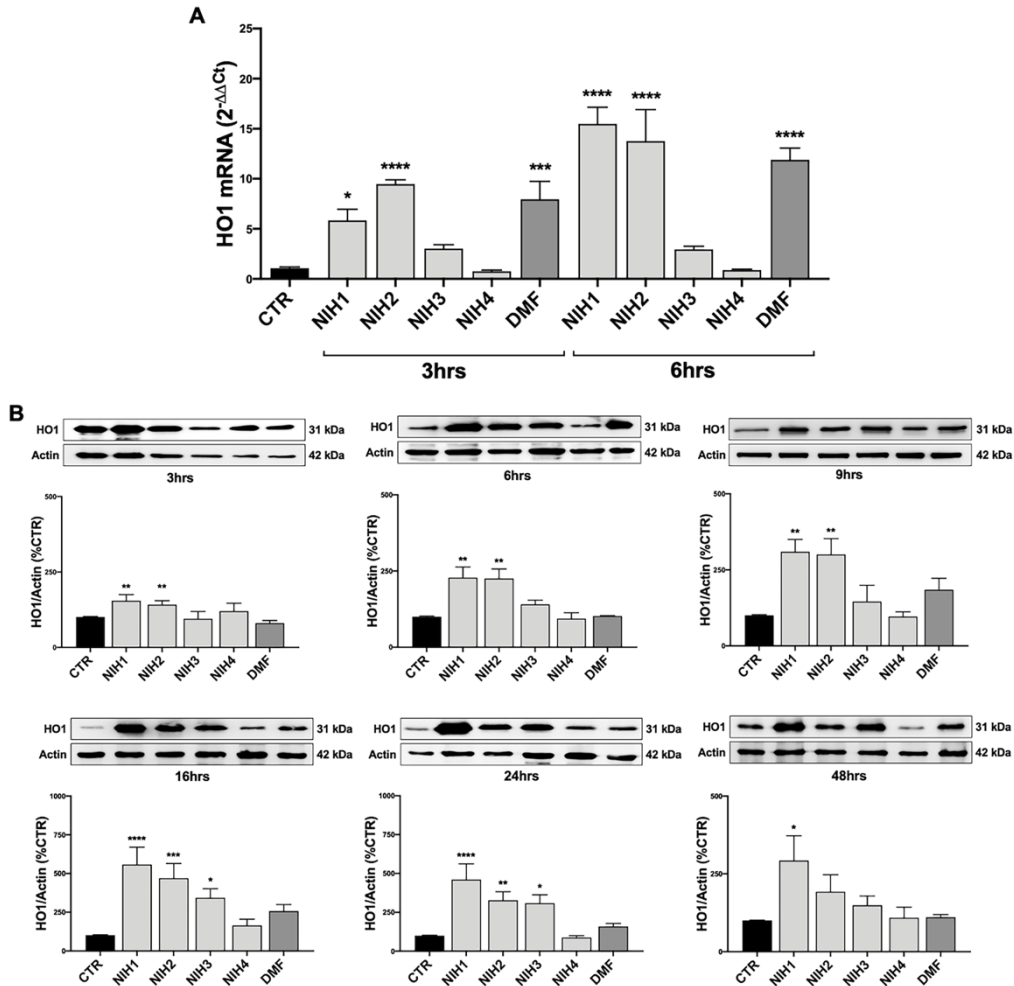


Figure 4. The NIH-mediated increase of HO1 expression vary among molecules. (A) Total HO1 mRNA levels were measured by RT-qPCR in ARPE-19 cells exposed to either solvent (DMSO, CTR), NIH1, NIH2, NIH3 and NIH4 [5 μ M], or DMF [10 μ M], for 3 and 6 hrs. GAPDH mRNA content was used as a housekeeping to normalize the data. Results are expressed as means of $2^{-\Delta\Delta C_t} \pm$ SEM. Dunnett's multiple comparisons test; * $p < 0.05$, *** $p < 0.001$ and **** $p < 0.0001$ versus CTR; $n = 3$. **(B)** ARPE-19 cells were exposed to either solvent (DMSO, CTR), NIH1, NIH2, NIH3, NIH4 [5 μ M], or DMF [10 μ M], for increasing times (up to 48 hrs), and total homogenates were examined by Western blot using an antibody against HO1. Actin was used as a loading control to normalize the data. Results are expressed as mean percentages \pm SEM. Dunnett's multiple comparisons test; * $p < 0.05$, ** $p < 0.01$, *** $p < 0.001$ and **** $p < 0.0001$ versus CTR; $n = 5$.

NIH1, NIH2, NIH3 have both direct and indirect antioxidant properties in ARPE-19 cells

We then evaluated the potential direct and indirect antioxidant properties of each NIH in H₂O₂-exposed ARPE-19 cells. To determine the direct antioxidant activity, ARPE-19 cells were either non-stressed, or exposed to 300 μM H₂O₂ with/without NIH, or DMF. By the DCF-DA assay, we measured ROS levels every 30 min during the following 4.5 hrs, finding that all the active NIH display ROS-scavenging capability, which is the highest for NIH1, followed by NIH2 and NIH3, respectively (**Figure 5A**). The ROS levels detected in ARPE-19 cells exposed to H₂O₂ plus NIH4 are slightly lower, while in DMF-treated cells they are comparable to those of H₂O₂-treated cells.

In order to evaluate whether the active NIH may provide protection from H₂O₂ not only by acting directly, as radical scavengers, but also because of the ability to induce an antioxidant cellular response, the ARPE-19 cells were pre-treated for 24 hrs with NIH, and then exposed to 300 μM H₂O₂. The ROS production was detected every 10 min for 1.5 hrs. We found that, compared to those in stressed cells, the ROS levels are progressively lower in cells pre-treated with NIH1, NIH2, followed by NIH3, NIH4 and, to a less extent, DMF (**Figure 5B**). The antioxidant effect observed here in NIH4-treated cells should be further studied.

According to these results, by selecting the most active among our hybrids, we evaluated the impact of NIH1 on the HO enzymatic activity at 6 hrs and found a significant increase of the HO metabolic product biliverdin in NIH1-treated ARPE-19 cells compared to control and NIH4-treated cells (**Supplementary Figure 4**).

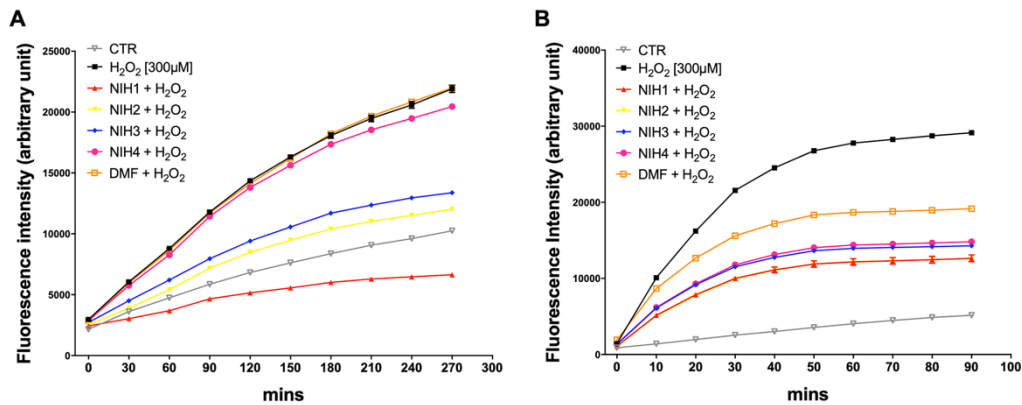


Figure 5. NIH are endowed of antioxidant properties. (A) ARPE-19 cells were exposed to H_2O_2 [300 μM] +/- NIH1, NIH2, NIH3 and NIH4 [5 μM], or DMF [10 μM] for 4.5 hrs. Control cells were exposed only to solvent (DMSO). ROS levels were measured every 30 min by the fluorometric 2',7'-Dichlorofluorescein diacetate (DCF-DA) assay. Results are expressed as mean \pm SEM. Fluorescence intensity for the NIH1, NIH2, NIH3, is significantly different from H_2O_2 at any time starting from 30 min with $p < 0.001$. Dunnett's multiple comparisons test versus H_2O_2 ; $n=4$. **(B)** ARPE-19 cells were pre-treated for 24 hrs with either solvent (DMSO, CTR), NIH1, NIH2, NIH3, NIH4 [5 μM], or DMF [10 μM], and then exposed to H_2O_2 [300 μM] for 1.5 hrs. ROS levels were measured every 10 min by the DCF-DA assay. Results are expressed as mean \pm SEM. Fluorescence intensity for all the NIH and DMF is significant at any time starting from 10 min with $p < 0.0001$. Dunnett's multiple comparisons test versus H_2O_2 ; $n=5$.

NIH1 provides protection from stress stimuli in both WT and Nrf2-silenced ARPE-19 cells

We then determined whether NIH provide cytoprotection to ARPE-19 from long-term injury. Both WT and siNrf2 ARPE-19 cells were pre-treated, or not, for 24 hrs with either NIH or DMF, and then exposed to the most challenging stress conditions selected in our previous experiments: 500 μM H_2O_2 , 100 μM 4-HNE, both for 24 hrs, or MG132+Baf (5 μM + 50 nM), for 48 hrs (**Figure 6**).

NIH1, NIH2, and NIH3, significantly protect WT cells from 24 hrs H_2O_2 exposure. In particular, NIH1 displays the best pro-survival effect in stressed cells, by restoring the cell viability to levels not statistically different from control (**Figure 6A**). ARPE-19 cells pre-treated with NIH4 show no change in the cell viability when compared to H_2O_2 -exposed cells; DMF moderately

counteracts the H₂O₂-induced mortality, although to a much less extent than any active NIH. In siNrf2 ARPE-19, only NIH1 counteracts the H₂O₂-induced mortality, doubling cell survival.

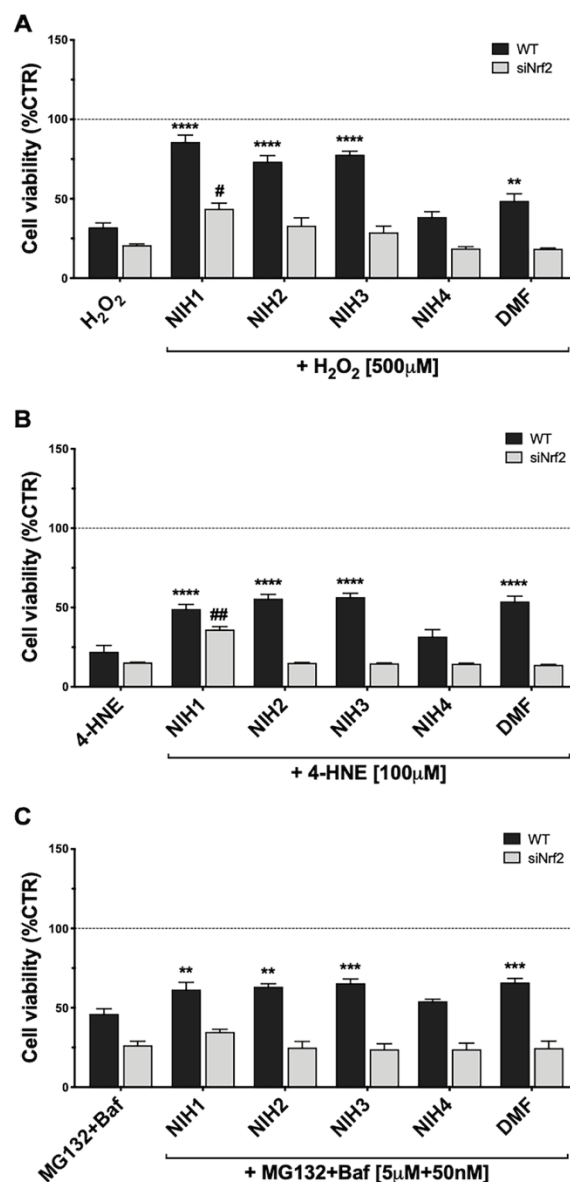


Figure 6. Study of NIH-mediated protection in WT and siNrf2 ARPE-19 cells under different stress. Cell viability was assessed by a fluorometric assay (PrestoBlue®) in WT and

siNrf2 ARPE-19 cells pre-treated for 24 hrs with either solvent (DMSO, CTR), NIH1, NIH2, NIH3, NIH4 [5 μ M], or DMF [10 μ M], and then exposed to either H₂O₂ [500 μ M, for 24 hrs] (**panel A**), 4-HNE [100 μ M, for 24 hrs] (**panel B**), or MG132+Bafilomycin [5 μ M+50 nM, for 48 hrs] (**panel C**). Results are expressed as mean of percentages \pm SEM in comparison with control (dot line, 100%). Dunnett's multiple comparisons test; * p <0.05, ** p <0.01, *** p <0.001, and **** p <0.0001 versus WT stress; # p <0.05 and ## p <0.01 versus siNrf2 stress; n =5-10.

In 24-hrs 4-HNE-exposed WT cells, NIH1, NIH2, NIH3, as well as DMF, display similar beneficial effects (**Figure 6B**). Analogously to that observed under H₂O₂, only the pre-treatment with NIH1 assures a protection from 4-HNE in siNrf2 cells, leading again to a 2.4-fold increase in the cell viability. In WT cells exposed to MG132+Baf for 48 hrs, the NIH1, NIH2 and NIH3, as well as DMF, show a significant protective effect, that is abolished in siNrf2 cells (**Figure 6C**).

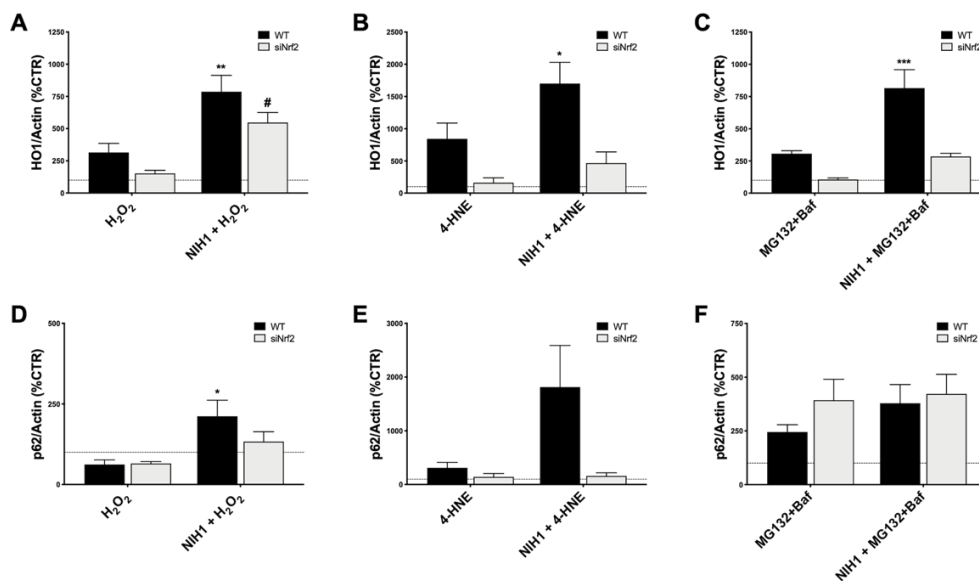


Figure 7. NIH1-mediated modulation of HO1 and p62 protein expression in stressed WT and siNrf2 ARPE-19 cells. Both WT and siNrf2 ARPE-19 cell lines were pre-treated for 24 hrs with either solvent (DMSO, CTR), or NIH1 [5 μ M], and then stressed, or not, for 6 hrs with H₂O₂ [300 μ M] (**panels A,D**), 4-HNE [50 μ M] (**panels B,E**), or MG132+Bafilomycin [5 μ M + 50 nM] (**panels C,F**). Total cellular homogenates were examined by Western blot using antibodies against HO1 (**A-C**) and p62 (**D-F**); Actin content was used as a loading control to normalize the data. Results are expressed as percentage means \pm SEM in comparison with control (dot line, 100%). Sidak's multiple comparisons test; * p <0.05, ** p <0.01; and *** p <0.001 versus WT stress; # p <0.05 versus siNrf2 stress; n =4-6.

Last, focusing on NIH1 and the same conditions used for our previous study of Nrf2/HO1 activation, we evaluated the HO1 and p62 protein levels in both WT and siNrf2 cells, that were pre-treated or not with NIH1 for 24 hrs, and then exposed for 6 hrs to either H₂O₂ (300 μM), 4-HNE (50 μM), or MG132+Baf (5 μM + 50 nM) (**Figure 7**). When pre-exposed to NIH1, stressed WT cells present higher levels of HO1 than their stressed counterparts, an effect that is index of preventive, NIH1-mediated activation of Nrf2, and that may contribute to the better cell viability profile observed in these cells. Similarly, we found an increment of p62 protein amount in NIH1-pre-treated WT cells. Surprisingly, we found a trend to increase of HO1 protein expression also in NIH1-pre-exposed siNrf2 cells, reaching statistical significance in the H₂O₂ group.

Overall these results demonstrate that a pre-treatment with the active NIH1 protects ARPE-19 cells by different pro-oxidant *noxae*, and suggest that NIH1 may confer resistance upon adverse conditions to both normal and Nrf2-silenced cells.

DISCUSSION

AMD is a complex disease whose aetiology is multifactorial: aging, genetic components, unhealthy environment and behavior, are all risk factors. Though AMD phenotype can dramatically change with progression, a common feature among the dry and wet forms, and the various stages of this pathology, is the degeneration of RPE, primarily responsible, among many other functions, for phagocytosis of photoreceptor outer segments and ROS scavenging (Strauss, 2005). RPE degeneration causes secondarily adverse effects on photoreceptors and choriocapillaris, finally leading to retinal alterations, visual loss and, in the worst cases, irreversible blindness (Ambati and Fowler, 2012). A consistent body of evidence elucidates the importance of dysregulated antioxidant mechanisms and oxidative stress in the development of AMD, and supports the possible association between Nrf2 deficiency and AMD (Datta *et al.*, 2017; Abokyi *et al.*, 2020). Nrf2-pathway is a master regulator of stress response in RPE; beside the well-documented role in the antioxidant cell defense, Nrf2 is also a key component of the

transduction machinery to maintain proteostasis, that is altered in AMD (Pajares *et al.*, 2016). Experimental evidence suggests that Nrf2 decreases in aged retina (Batliwala *et al.*, 2017), and its signaling is impaired in aged RPE exposed to an oxidative insult (Sachdeva *et al.*, 2014); KO animals for *Nrf2* or its downstream genes (i.e. *HO1*) develop age-related RPE degeneration and other AMD-like features (Zhao *et al.*, 2011; Felszeghy *et al.*, 2019). These findings strongly suggest that Nrf2-pathway impairment contributes to RPE degeneration in AMD, and that molecules enhancing Nrf2 activity may be of interest for this pathology (Lu *et al.*, 2016).

In the present study on ARPE-19 cells, we show that different types of pro-oxidant *noxae* activate Nrf2, whose importance in the stress defense has been corroborated by siRNA experiments. We found that, in term of viability, siNrf2 cells present a higher susceptibility than WT cells to H₂O₂, 4-HNE, MG132+Baf (**Figure 1**), all stresses able to up-regulate Nrf2 in WT, but not in siNrf2 cells (**Figure 2A-C**). Moreover, by focusing on two Nrf2-targets, we observed a different stress-related response in the gene expression of *HO1* and *p62*. In WT cells, HO1 protein is up-regulated upon any stress (**Figure 2D-F**), while p62 is increased following 4-HNE and MG132+Baf, but not H₂O₂ (**Figure 2G-I**). The stress-induced raising of HO1 and p62 protein amounts requires the presence of Nrf2, with the exception of p62 in MG132+Baf-treated siNrf2 cells, that show p62 levels even higher than the stressed WT counterpart (**Figure 2D-I**). This may be explained because p62 is degraded by autophagy, which is likely less efficient in siNrf2 cells, and it is further compromised and engulfed upon autophagy inhibition, thus leading to an accumulation of the autophagy marker p62 (Tang *et al.*, 2019).

Keap1/Nrf2/ARE pathway represents a promising pharmacological target to control common pathological features of many chronic diseases characterized by oxidative stress and inflammation (Robledinos-Antón *et al.*, 2019). Accordingly, many studies suggest the potential cytoprotective role of small molecules as Nrf2 activators in retinal tissues and relative pathologies, such as AMD (Batliwala *et al.*, 2017). With this purpose, we tested in ARPE-19 cells some compounds able to induce Nrf2 pathway (Simoni *et al.*, 2017) (**Supplementary Figure 3A**), by comparing their effects with DMF, a Nrf2-activator currently used in clinic for multiple sclerosis (Montes Diaz *et al.*,

2018). We show that, similarly to 10 μ M DMF, each active hybrid (NIH1, NIH2, and NIH3), at 5 μ M concentration, is able to induce an early activation of Nrf2, accompanied by an up-regulation of its own expression (**Figure 3B-D**). NIH1, NIH2, and NIH3, activate Nrf2, which translocates to the nucleus and escapes from proteasomal degradation, explaining the higher Nrf2 protein levels in comparison with cells exposed to either the solvent or the inactive NIH4. *Nrf2* mRNA levels significantly increase in ARPE-19 cells upon either NIH1 or NIH2, as well as DMF (**Figure 3D**), indicating that, once activated, nuclear Nrf2 also induces its own gene expression in a self-sustaining feedback, in accordance with previous evidence for other Nrf2 activators (Giudice *et al.*, 2010). Downstream, after exposure to either NIH1 or NIH2, we found an early up-regulation of *HO1* gene expression at both mRNA and protein level (**Figure 4A, B**). NIH3 favors HO1 protein expression, although at a longer time. The most consistent increase of HO1 protein [half-life: about 6 hrs (Lin *et al.*, 2008)] content is detected for these three NIH at 16 hrs (NIH1: 5.6-fold, NIH2: 4.7-fold, and NIH3: 3.4-fold the control level, respectively). For all, the increase of HO1 protein is persistent, up to 24 hrs for NIH2 and NIH3, and up to 48 hrs for NIH1. Moreover, beside increase of *HO1* gene expression, we demonstrate that NIH1 also favors heme oxygenase activity at 6 hrs in ARPE-19 cells similarly to hemin, a well-known HO1 inducer (**Supplementary Figure 4**).

Concerning DMF, to our knowledge, this is the first literature study of DMF effects on HO1 protein expression in RPE cells. Intriguingly, despite its capability to induce *HO1* mRNA transcription at 3 and 6 hrs, DMF is less powerful than NIH1 to up-regulate HO1 protein levels at the longer times considered (9, 16 and 24 hrs). We cannot exclude that this narrow effect may be due to the low concentration of DMF used in our study, and that higher DMF concentration may instead robustly induce HO1 protein expression.

The catechol motif, present in both NIH1 and NIH2 structures, becomes active electrophilic ortho-quinone on oxidation, which should provide protection in oxidative conditions (Simoni *et al.*, 2017; Serafini *et al.*, 2019). Furthermore, the electrophilic α,β -unsaturated carbonyl group in Michael-type acceptor compounds, such as NIH1, NIH3, as well as DMF, represents an additional source for Nrf2 activation (Basagni *et al.*, 2019). Coherently, in ARPE-19 cells

exposed to H₂O₂, NIH1, NIH2, and NIH3, display both direct and indirect antioxidant properties, by counteracting the increase of intracellular ROS levels (**Figure 5**). The direct antioxidant capacity of the active NIH is proportional to the number of functional groups within the chemical structure, with NIH1 showing the best profile (**Figure 5A**). The active NIH protect ARPE-19 cells from H₂O₂ not only in virtue of their pro-electrophilic chemical structure, but also of the induction of a Nrf2-mediated antioxidant cellular defense. Indeed, following 24 hrs NIH pre-treatment, H₂O₂-exposed WT cells show lower intracellular ROS levels (**Figure 5B**) and mortality (**Figure 6A**) than stressed cells; strikingly, NIH1 is able to fully preserve the cell viability. The active NIH display cytoprotective effects also in WT ARPE-19 upon 4-HNE and MG132+Baf, although to a less extent (**Figure 6B,C**). In our conditions, the DMF-mediated cytoprotective effects are lower than those observed with any active NIH (**Figure 6**). Moreover, contrary to NIH, DMF does not display direct antioxidant properties (**Figure 5A**), albeit it protects ARPE-19 cells from pro-oxidant stress via Nrf2-pathway activation; in agreement, DMF shows no protective effects in siNrf2 cells upon injury (**Figure 6**). In all the stress conditions, the pro-survival effects of each Nrf2 activator require the presence of Nrf2, being no more observable in siNrf2 cells, with the exception of NIH1 (**Figure 6**), that is able to prevent cell death by doubling the number of still viable cells following the exposure to either H₂O₂ or 4-HNE. One-day pre-treatment with NIH1 provides WT cells of preventive Nrf2 activation, and thus higher HO1 and p62 protein levels (**Figure 7**), effects that likely predispose the ARPE-19 cells to counteract more efficiently the following stressors and contribute to increase cell survival.

Last, we also discovered that a 24-hrs pre-treatment with NIH1 significantly up-regulates HO1 protein levels even in H₂O₂-stressed siNrf2 cells (**Figure 7A**), an effect that may contribute to their higher viability. The observation that Nrf2 silencing does not abolish the cytoprotective effects of NIH1 pre-treatment suggests that NIH1 may act on a Nrf2-independent pathway and/or on the remaining Nrf2 amount anyhow present in siNrf2 cells. However, further studies will be performed in future to test these hypotheses.

In the context of Keap1/Nrf2/ARE signaling pathway as a druggable target for AMD and other pathologies, various natural and synthetic Nrf2 activators

have been recently tested in both *in vitro* and *in vivo* studies to evaluate their protective effects against different pro-oxidant stimuli (Cui *et al.*, 2019; Shao *et al.*, 2019; Zhou *et al.*, 2019; Fresta *et al.*, 2020). In this panorama, our NIHs look as noteworthy pharmacological molecules, displaying a good profile of tolerability (**Figure 3**) and uncommon cytoprotective effects in RPE cells under three different types of AMD-related oxidative stress.

In conclusion, our study corroborates the relevance of Nrf2 in the RPE stress response, and shows that, beside WT, siNrf2 ARPE-19 cells exposed to different stress may be a useful *in vitro* model to test pharmacologically active molecules potentially interesting in AMD. Our findings also suggest that the active NIH are potentially valuable protective, preventive tools for cells physiologically facing challenging, high pro-oxidant stress, as RPE. In particular, NIH1 is worthy of further studies on RPE, AMD and other retinal degenerative diseases, and may be useful to reinforce the endogenous cellular protective mechanisms in both normal and Nrf2 impaired conditions.

SUPPLEMENTARY MATERIAL

The Supplementary Material for this article can be found online at: <https://www.frontiersin.org/articles/10.3389/fphar.2020.00844/full#supplementary-material>.

REFERENCES

- Abokyi, S., To, C.-H., Lam, T. T., and Tse, D. Y. (2020). Central Role of Oxidative Stress in Age-Related Macular Degeneration: Evidence from a Review of the Molecular Mechanisms and Animal Models. *Oxid. Med. Cell. Longev.* 2020, 1–19. doi:10.1155/2020/7901270.
- Amadio, M., Govoni, S., and Pascale, A. (2016). Targeting VEGF in eye neovascularization: What's new? *Pharmacol. Res.* 103, 253–269. doi:10.1016/j.phrs.2015.11.027.
- Amadio, M., Scapagnini, G., Davinelli, S., Calabrese, V., Govoni, S., and Pascale, A. (2014). Involvement of ELAV RNA-binding proteins in the post-transcriptional regulation of HO-1. *Front. Cell. Neurosci.* 8, 459. doi:10.3389/fncel.2014.00459.

- Amadio, M., Scapagnini, G., Laforenza, U., Intrieri, M., Romeo, L., Govoni, S., et al. (2008). Post-transcriptional regulation of HSP70 expression following oxidative stress in SH-SY5Y cells: the potential involvement of the RNA-binding protein HuR. *Curr. Pharm. Des.* 14, 2651-2658. doi:10.2174/138161208786264052.
- Ambati, J., and Fowler, B. J. (2012). Mechanisms of Age-Related Macular Degeneration. *Neuron* 75, 26-39. doi:10.1016/j.neuron.2012.06.018.
- Basagni, F., Lanni, C., Minarini, A., and Rosini, M. (2019). Lights and shadows of electrophile signaling: focus on the Nrf2-Keap1 pathway. *Future Med. Chem.* 11, 707-721. doi:10.4155/fmc-2018-0423.
- Batlwala, S., Xavier, C., Liu, Y., Wu, H., and Pang, I.-H. (2017). Involvement of Nrf2 in Ocular Diseases. *Oxid. Med. Cell. Longev.* 2017, 1703810. doi:10.1155/2017/1703810.
- Bhutto, I., and Luttj, G. (2012). Understanding age-related macular degeneration (AMD): relationships between the photoreceptor/retinal pigment epithelium/Bruch's membrane/choriocapillaris complex. *Mol. Aspects Med.* 33, 295-317. doi:10.1016/j.mam.2012.04.005.
- Chen, J., Wang, L., Chen, Y., Sternberg, P., and Cai, J. (2009). Phosphatidylinositol 3 Kinase Pathway and 4-Hydroxy-2-Nonenal-Induced Oxidative Injury in the RPE. *Investig. Ophthalmology Vis. Sci.* 50, 936. doi:10.1167/iovs.08-2439.
- Cui, R., Tian, L., Lu, D., Li, H., and Cui, J. (2019). Exendin-4 Protects Human Retinal Pigment Epithelial Cells from H₂O₂-Induced Oxidative Damage via Activation of NRF2 Signaling. *Ophthalmic Res.*, 1-9. doi:10.1159/000504891.
- Datta, S., Cano, M., Ebrahimi, K., Wang, L., and Handa, J. T. (2017). The impact of oxidative stress and inflammation on RPE degeneration in non-neovascular AMD. *Prog. Retin. Eye Res.* 60, 201-218. doi:10.1016/j.preteyeres.2017.03.002.
- Ethen, C. M., Reilly, C., Feng, X., Olsen, T. W., and Ferrington, D. A. (2007). Age-related macular degeneration and retinal protein modification by 4-hydroxy-2-nonenal. *Invest. Ophthalmol. Vis. Sci.* 48, 3469-3479. doi:10.1167/iovs.06-1058.
- Felszeghy, S., Viiri, J., Paterno, J. J., Hyttinen, J. M. T., Koskela, A., Chen, M., et al. (2019). Loss of NRF-2 and PGC-1 α genes leads to retinal pigment epithelium damage resembling dry age-related macular degeneration. *Redox Biol.* 20, 1-12. doi:10.1016/j.redox.2018.09.011.
- Ferrington, D. A., Sinha, D., and Kaarniranta, K. (2016). Defects in retinal pigment epithelial cell proteolysis and the pathology associated with age-related macular degeneration. *Prog. Retin. Eye Res.* 51, 69-89. doi:10.1016/j.preteyeres.2015.09.002.
- Foresti, R., Bucolo, C., Platania, C. M. B., Drago, F., Dubois-Randé, J.-L., and Motterlini, R. (2015). Nrf2 activators modulate oxidative stress responses and bioenergetic profiles of human retinal epithelial cells cultured in normal or high glucose conditions. *Pharmacol. Res.* 99, 296-307. doi:10.1016/j.phrs.2015.07.006.
- Fresta, C. G., Fidilio, A., Lazzarino, G., Musso, N., Grasso, M., Merlo, S., et al. (2020). Modulation of Pro-Oxidant and Pro-Inflammatory Activities of M1 Macrophages by the Natural Dipeptide Carnosine. *Int. J. Mol. Sci.* 21. doi:10.3390/ijms21030776.
- Giudice, A., Arra, C., and Turco, M. C. (2010). "Review of Molecular Mechanisms Involved in the Activation of the Nrf2-ARE Signaling Pathway by Chemopreventive Agents," in *Transcription*

Factors, ed. P. J. Higgins (Totowa, NJ: Humana Press), 37-74. doi:10.1007/978-1-60761-738-9_3.

Golestaneh, N., Chu, Y., Xiao, Y.-Y., Stoleru, G. L., and Theos, A. C. (2018). Dysfunctional autophagy in RPE, a contributing factor in age-related macular degeneration. *Cell Death Dis.* 8, e2537-e2537. doi:10.1038/cddis.2016.453.

Hu, X., Liang, Y., Zhao, B., and Wang, Y. (2019). Thymoquinone protects human retinal pigment epithelial cells against hydrogen peroxide induced oxidative stress and apoptosis. *J. Cell. Biochem.* 120, 4514-4522. doi:10.1002/jcb.27739.

Hyttinen, J. M. T., Amadio, M., Viiri, J., Pascale, A., Salminen, A., and Kaarniranta, K. (2014). Clearance of misfolded and aggregated proteins by autophagy and implications for aggregation diseases. *Ageing Res. Rev.* 18, 16-28. doi:10.1016/j.arr.2014.07.002.

Jager, R. D., Mieler, W. F., and Miller, J. W. (2008). Age-related macular degeneration. *N. Engl. J. Med.* 358, 2606-2617. doi:10.1056/NEJMra0801537.

Jain, A., Lamark, T., Sjøttem, E., Larsen, K. B., Awuh, J. A., Øvervatn, A., et al. (2010). p62/SQSTM1 is a target gene for transcription factor NRF2 and creates a positive feedback loop by inducing antioxidant response element-driven gene transcription. *J. Biol. Chem.* 285, 22576-22591. doi:10.1074/jbc.M110.118976.

Jiang, T., Harder, B., Rojo de la Vega, M., Wong, P. K., Chapman, E., and Zhang, D. D. (2015). p62 links autophagy and Nrf2 signaling. *Free Radic. Biol. Med.* 88, 199-204. doi:10.1016/j.freeradbiomed.2015.06.014.

Kaarniranta, K., Ryhänen, T., Karjalainen, H. M., Lammi, M. J., Suuronen, T., Huhtala, A., et al. (2005). Geldanamycin increases 4-hydroxynonenal (HNE)-induced cell death in human retinal pigment epithelial cells. *Neurosci. Lett.* 382, 185-190. doi:10.1016/j.neulet.2005.03.009.

Kaarniranta, K., Tokarz, P., Koskela, A., Paterno, J., and Blasiak, J. (2017). Autophagy regulates death of retinal pigment epithelium cells in age-related macular degeneration. *Cell Biol. Toxicol.* 33, 113-128. doi:10.1007/s10565-016-9371-8.

Kaemmerer, E., Schutt, F., Krohne, T. U., Holz, F. G., and Kopitz, J. (2007). Effects of Lipid Peroxidation-Related Protein Modifications on RPE Lysosomal Functions and POS Phagocytosis. *Investig. Ophthalmology Vis. Sci.* 48, 1342. doi:10.1167/iovs.06-0549.

Lambros, M. L., and Plafker, S. M. (2016). "Oxidative Stress and the Nrf2 Anti-Oxidant Transcription Factor in Age-Related Macular Degeneration," in *Retinal Degenerative Diseases*, eds. C. Bowes Rickman, M. M. LaVail, R. E. Anderson, C. Grimm, J. Hollyfield, and J. Ash (Cham: Springer International Publishing), 67-72. doi:10.1007/978-3-319-17121-0_10.

Lim, L. S., Mitchell, P., Seddon, J. M., Holz, F. G., and Wong, T. Y. (2012). Age-related macular degeneration. *The Lancet* 379, 1728-1738. doi:10.1016/S0140-6736(12)60282-7.

Lin, P.-H., Chiang, M.-T., and Chau, L.-Y. (2008). Ubiquitin-proteasome system mediates heme oxygenase-1 degradation through endoplasmic reticulum-associated degradation pathway. *Biochim. Biophys. Acta* 1783, 1826-1834. doi:10.1016/j.bbamcr.2008.05.008.

Loboda, A., Damulewicz, M., Pyza, E., Jozkowicz, A., and Dulak, J. (2016). Role of Nrf2/HO-1 system in development, oxidative stress response and diseases: an evolutionarily conserved mechanism. *Cell. Mol. Life Sci. CMLS* 73, 3221-3247. doi:10.1007/s00018-016-2223-0.

- Lu, M.-C., Ji, J.-A., Jiang, Z.-Y., and You, Q.-D. (2016). The Keap1-Nrf2-ARE Pathway As a Potential Preventive and Therapeutic Target: An Update: THE KEAP1-NRF2-ARE PATHWAY. *Med. Res. Rev.* 36, 924–963. doi:10.1002/med.21396.
- Marchesi, N., Thongon, N., Pascale, A., Provenzani, A., Koskela, A., Korhonen, E., et al. (2018). Autophagy Stimulus Promotes Early HuR Protein Activation and p62/SQSTM1 Protein Synthesis in ARPE-19 Cells by Triggering Erk1/2, p38^{MAPK}, and JNK Kinase Pathways. *Oxid. Med. Cell. Longev.* 2018, 1–15. doi:10.1155/2018/4956080.
- McMahon, M., Itoh, K., Yamamoto, M., and Hayes, J. D. (2003). Keap1-dependent proteasomal degradation of transcription factor Nrf2 contributes to the negative regulation of antioxidant response element-driven gene expression. *J. Biol. Chem.* 278, 21592–21600. doi:10.1074/jbc.M300931200.
- Montes Diaz, G., Hupperts, R., Fraussen, J., and Somers, V. (2018). Dimethyl fumarate treatment in multiple sclerosis: Recent advances in clinical and immunological studies. *Autoimmun. Rev.* 17, 1240–1250. doi:10.1016/j.autrev.2018.07.001.
- Motohashi, H., and Yamamoto, M. (2004). Nrf2-Keap1 defines a physiologically important stress response mechanism. *Trends Mol. Med.* 10, 549–557. doi:10.1016/j.molmed.2004.09.003.
- Pajares, M., Jiménez-Moreno, N., García-Yagüe, Á. J., Escoll, M., de Ceballos, M. L., Van Leuven, F., et al. (2016). Transcription factor NFE2L2/NRF2 is a regulator of macroautophagy genes. *Autophagy* 12, 1902–1916. doi:10.1080/15548627.2016.1208889.
- Robledinos-Antón, N., Fernández-Ginés, R., Manda, G., and Cuadrado, A. (2019). Activators and Inhibitors of NRF2: A Review of Their Potential for Clinical Development. *Oxid. Med. Cell. Longev.* 2019, 9372182. doi:10.1155/2019/9372182.
- Sachdeva, M. M., Cano, M., and Handa, J. T. (2014). Nrf2 signaling is impaired in the aging RPE given an oxidative insult. *Exp. Eye Res.* 119, 111–114. doi:10.1016/j.exer.2013.10.024.
- Serafini, M. M., Catanzaro, M., Fagiani, F., Simoni, E., Caporaso, R., Dacrema, M., et al. (2019). Modulation of Keap1/Nrf2/ARE Signaling Pathway by Curcuma- and Garlic-Derived Hybrids. *Front. Pharmacol.* 10, 1597. doi:10.3389/fphar.2019.01597.
- Shao, Y., Yu, H., Yang, Y., Li, M., Hang, L., and Xu, X. (2019). A Solid Dispersion of Quercetin Shows Enhanced Nrf2 Activation and Protective Effects against Oxidative Injury in a Mouse Model of Dry Age-Related Macular Degeneration. *Oxid. Med. Cell. Longev.* 2019, 1479571. doi:10.1155/2019/1479571.
- Simoni, E., Serafini, M. M., Bartolini, M., Caporaso, R., Pinto, A., Necchi, D., et al. (2016). Nature-Inspired Multifunctional Ligands: Focusing on Amyloid-Based Molecular Mechanisms of Alzheimer's Disease. *ChemMedChem* 11, 1309–1317. doi:10.1002/cmdc.201500422.
- Simoni, E., Serafini, M. M., Caporaso, R., Marchetti, C., Racchi, M., Minarini, A., et al. (2017). Targeting the Nrf2/Amyloid-Beta Liaison in Alzheimer's Disease: A Rational Approach. *ACS Chem. Neurosci.* 8, 1618–1627. doi:10.1021/acscchemneuro.7b00100.
- Strauss, O. (2005). The retinal pigment epithelium in visual function. *Physiol. Rev.* 85, 845–881. doi:10.1152/physrev.00021.2004.
- Tang, Z., Hu, B., Zang, F., Wang, J., Zhang, X., and Chen, H. (2019). Nrf2 drives oxidative stress-induced autophagy in nucleus pulposus cells via a Keap1/Nrf2/p62 feedback loop to protect

intervertebral disc from degeneration. *Cell Death Dis.* 10, 510. doi:10.1038/s41419-019-1701-3.

Viiri, J., Amadio, M., Marchesi, N., Hyttinen, J. M. T., Kivinen, N., Sironen, R., *et al.* (2013). Autophagy activation clears ELAVL1/HuR-mediated accumulation of SQSTM1/p62 during proteasomal inhibition in human retinal pigment epithelial cells. *PLoS One* 8, e69563. doi:10.1371/journal.pone.0069563.

Viiri, J., Hyttinen, J. M. T., Ryhänen, T., Rilla, K., Paimela, T., Kuusisto, E., *et al.* (2010). p62/sequestosome 1 as a regulator of proteasome inhibitor-induced autophagy in human retinal pigment epithelial cells. *Mol. Vis.* 16, 1399-1414.

Wang, L., Ebrahimi, K. B., Chyn, M., Cano, M., and Handa, J. T. (2016). "Biology of p62/sequestosome-1 in Age-Related Macular Degeneration (AMD)," in *Retinal Degenerative Diseases*, eds. C. Bowes Rickman, M. M. LaVail, R. E. Anderson, C. Grimm, J. Hollyfield, and J. Ash (Cham: Springer International Publishing), 17-22. doi:10.1007/978-3-319-17121-0_3.

Zhang, H., Davies, K. J. A., and Forman, H. J. (2015). Oxidative stress response and Nrf2 signaling in aging. *Free Radic. Biol. Med.* 88, 314-336. doi:10.1016/j.freeradbiomed.2015.05.036.

Zhao, H., Wang, R., Ye, M., and Zhang, L. (2019). Genipin protects against H₂O₂-induced oxidative damage in retinal pigment epithelial cells by promoting Nrf2 signaling. *Int. J. Mol. Med.* 43, 936-944. doi:10.3892/ijmm.2018.4027.

Zhao, J., Tan, S., Liu, F., Zhang, Y., Su, M., and Sun, D. (2012). Heme oxygenase and ocular disease: a review of the literature. *Curr. Eye Res.* 37, 955-960. doi:10.3109/02713683.2012.700753.

Zhao, Z., Chen, Y., Wang, J., Sternberg, P., Freeman, M. L., Grossniklaus, H. E., *et al.* (2011). Age-Related Retinopathy in NRF2-Deficient Mice. *PLoS ONE* 6, e19456. doi:10.1371/journal.pone.0019456.

Zhou, Y., Zhou, L., Zhou, K., Zhang, J., Shang, F., and Zhang, X. (2019). Celastrol Protects RPE Cells from Oxidative Stress-Induced Cell Death via Activation of Nrf2 Signaling Pathway. *Curr. Mol. Med.* 19, 172-182. doi:10.2174/1566524019666190424131704.

Zhu, C., Dong, Y., Liu, H., Ren, H., and Cui, Z. (2017). Hesperetin protects against H₂O₂-triggered oxidative damage via upregulation of the Keap1-Nrf2/HO-1 signal pathway in ARPE-19 cells. *Biomed. Pharmacother.* 88, 124-133. doi:10.1016/j.biopha.2016.11.089.

CHAPTER 2

Collaborative activities: characterization of the antioxidant profile of natural and nature-derived compounds through the investigation of the Nrf2 pathway

PART I

The following manuscript was published in *Oxidative Medicine and Cellular Longevity* in 2018 as:

Characterization of the Antioxidant Effects of γ -Oryzanol: Involvement of the Nrf2 Pathway

Wiramon Rungratanawanich, Giulia Abate, Melania Maria Serafini, Michela Guarienti, **Michele Catanzaro**, Mariagrazia Marziano, Maurizio Memo, Cristina Lanni and Daniela Uberti



Abstract

γ -Oryzanol (ORY) is well known for its antioxidant potential. However, the mechanism by which ORY exerts its antioxidant effect is still unclear. In this paper, the antioxidant properties of ORY were investigated for its potential effects as a reactive oxygen and nitrogen species (ROS/RNS) scavenger and in activating antioxidant-promoting intracellular pathways utilizing the human embryonic kidney cells (HEK-293). The 24 h ORY exposure significantly prevented hydrogen peroxide- (H_2O_2 -) induced ROS/RNS production at 3 h, and this effect was sustained for at least 24 h. ORY pretreatment also enhanced the activity of antioxidant enzymes: superoxide dismutase (SOD) and glutathione peroxidase (GPx). Interestingly, ORY induced the nuclear factor (erythroid-derived 2)-like 2 (Nrf2) nuclear translocation and upregulation of Nrf2-dependent defensive genes such as NAD(P)H quinone reductase (NQO1), heme oxygenase-1 (HO-1), and glutathione synthetase (GSS) at mRNA and protein levels in both basal condition and after H_2O_2 insult. Thus, this study suggested an intriguing effect of ORY in modulating the Nrf2 pathway, which is also involved in regulating longevity as well as age-related diseases.

Keywords: Orizanol; oxidative stress; Reactive Oxygen Species (ROS); Reactive Nitrogen Species (RNS); Nrf2; NQO1; HO-1.

Research Article

Characterization of the Antioxidant Effects of γ -Oryzanol: Involvement of the Nrf2 Pathway

W. Rungratanawanich,¹ G. Abate ¹, M. M. Serafini,^{2,3} M. Guarienti,¹ M. Catanzaro,³ M. Marziano,¹ M. Memo,¹ C. Lanni,³ and D. Uberti ¹

¹Department of Molecular and Translational Medicine, University of Brescia, Brescia, Italy

²Scuola Universitaria Superiore IUSS Pavia, Pavia, Italy

³Department of Drug Sciences, University of Pavia, Pavia, Italy

1. Introduction

According to the Harman theory of aging, oxidative stress is at the base of the mechanisms involved in aging processes [1] and contributes to the development of many age-related diseases including cancer, atherosclerosis, hypertension, diabetes, and neurodegenerative disorders [2–4]. Oxidative stress is defined as the imbalance of the production of free radicals, and the efficiency of antioxidant enzyme systems and the ability to activate antioxidant-promoting intracellular pathways. ROS/RNS are usually produced by living organisms as a result of normal cellular metabolism, but they can also be induced by different endogenous and exogenous insults [5]. Thus, during the life span, the organism is continuously at risk to be exposed to ROS/RNS beyond such a threshold level which the body tissues fail to counteract the damage. It is well known that ROS/RNS take part in physiological cell processes from low to moderate concentrations, but at high concentrations, they produce adverse modifications to the cellular macromolecules such as lipids, proteins, and DNA, affecting cell functions and survival [3, 6]. Antioxidant enzyme cascade such as superoxide dismutase (SOD), catalase (CAT), and glutathione peroxidase (GPx) acts as the first line of protection in counteracting ROS/RNS generation. These three enzymes work sequentially to neutralize free radicals. SOD catalyzes the dismutation of

superoxide anion to H_2O_2 , which is in turn neutralized to H_2O by CAT or GPx [7]. In addition, antioxidant-promoting intracellular pathways contribute in maintaining redox steady state and in preventing ROS/RNS detrimental effects induced by stressors. The nuclear factor (erythroid-derived 2)-like 2 (Nrf2) transcription factor has emerged as a master regulator of cellular detoxification response and redox status since it protects the organism from pathologies caused or exacerbated by oxidative stress. A key role of the Nrf2 pathway has also emerged in the aging processes and in age-related diseases [8-10].

The Nrf2 pathway is an intrinsic mechanism to defense oxidative stress by inducing the transcription of up to 10% of human genes, which take part in different cellular functions such as ROS/RNS elimination, detoxification, xenobiotic metabolism, drug excretion, and nicotinamide adenine dinucleotide phosphate (NADPH) synthesis. Among the antioxidant pathways, the Nrf2 pathway promotes the transcription of NQO1, HO-1, and GSS because of the presence of an antioxidant responsive element (ARE) sequence in their promoter region [11, 12]. In basal condition, the activation of Nrf2 is mediated by disrupting its interaction and binding to Kelch-like ECH-associated protein 1 (Keap1), a cytosolic Nrf2 repressor, resulting in recruitment the Cul3 ubiquitin ligase to induce Nrf2 degradation via proteasome, thus acting as a sensor of oxidative stress [13].

In recent years, natural compounds have gained more attention since their therapeutic effects have been found important in the improvement of a lifestyle as well as in the protection against age-related diseases such as hyperlipidemia, inflammatory disorders, cardiovascular diseases, and cancer [14-16]. These observations might change the concept of food consumption and nutrition, not only for diminishing starvation and malnutrition but also for preventing morbidity and mortality of chronic diseases particularly related to free radical damage. Thus, dietary antioxidants containing antioxidative phytochemicals become crucial to counteract oxidative stress, consequently maintaining body homeostasis and redox balance [17].

Rice (*Oryza sativa* L.), a natural source of antioxidant, is rich in plenty of antioxidative components such as essential vitamin E complex, anthocyanins, and phenolic compounds [18]. As compared to other cereal grains, rice contains the highest special phenolic compound that is ferulic acid, which is presented in the form of a steryl ferulate called "γ-oryzanol." ORY derived its name from rice because it was first discovered in rice bran oil and it is composed of a hydroxyl group [19-21]. ORY is a mixture of ferulic acid esters of phytosterols: triterpene alcohols and plant sterols [22]. The quantity of ORY and its compositions vary in the different types of rice. Some varieties of rice may exhibit an amount of ORY 8-10 times higher than vitamin E considered as one of the most potent natural antioxidants [23, 24].

The antioxidant properties of ORY have been investigated in *in vivo* and *in vitro* experiments, demonstrating its ability in preventing and reducing the ROS/RNS formation [16, 22]. Son *et al.* illustrated that mice subjected to a highfat diet supplemented with ORY showed significantly lower amount of oxidative stress and lipid peroxidation when compared to mice fed with highfat diet alone [25]. Similarly, in *Drosophila melanogaster*, ORY was found to ameliorate antioxidant activities, thereby preventing the oxidative damage [26]. However, how ORY exerts its antioxidant effects is still unclear. Here, the antioxidant mechanism of action of ORY was investigated by using HEK-293 cell line subjected to a subtoxic oxidative insult elicited by H₂O₂. This cellular model has been well recognized as a suitable tool to investigate the intracellular pathways involved in oxidative stress [27-29]. In particular, the mechanisms involved in ROS/RNS scavenging and the antioxidant-promoting intracellular pathway were characterized.

2. Material and Methods

2.1 Cell Culture and Treatments

Human embryonic kidney cells (HEK-293) were cultured in Dulbecco's modified Eagle's medium containing 10% fetal bovine serum, 2 mmol/L

glutamine, 100 U/mL penicillin, and 100 µg/mL streptomycin at 37°C in a 5% CO₂-containing atmosphere. Oxidative insult was induced by adding 100 µM of H₂O₂ to cells at 80% confluent monolayers for different times in accordance with the experimental paradigms.

2.2 Oryzanol and H₂O₂ Treatments

ORY was purchased from Sigma-Aldrich, Merck KGaA, Darmstadt, Germany. The powder was resuspended in ethanol at a concentration of 1 mg/mL. ORY was used at different concentration ranging from 1 to 20 µg/mL in different period of time according with the experiments. H₂O₂ 30% w/w (Sigma-Aldrich, Merck KGaA, Darmstadt, Germany) was used to prepare an initial concentration of 1mM that was then diluted in culture medium to obtain a final concentration of 100 µM for different period of time as per the experiments.

2.3 Cell Viability

Cell viability was evaluated 24 h after the oxidative insult by MTT assay. Cells were incubated with 500 mg/mL of MTT (3-(4,5-dimethylthiazol-2-yl)-2,5-diphenyltetrazolium bromide) for 3 h at 37°C. Then, it was removed, and cells were lysed with dimethyl sulfoxide. The absorbance at 595nm was measured using a Bio-Rad 3350 microplate reader (Bio Rad Laboratories, Richmond, CA, USA). Cells treated with 0.2% Triton-X100 solution (Sigma-Aldrich, Merck KGaA, Darmstadt, Germany) were used to calculate the maximum toxicity. Data were expressed as percentage of cell viability over the corresponding controls.

2.4 Measurement of ROS/RNS Generation

Intracellular ROS levels were measured using the fluorescent dye 2',7' - dichlorodihydrofluorescein diacetate (H₂DCF-DA) (Thermo Fisher Scientific, Waltham, Massachusetts USA), a nonpolar compound that is converted into a nonfluorescent polar derivative (H₂DCF) by cellular esterase after incorporation into cells. H₂DCF is membrane permeable and is rapidly oxidized to the high fluorescent 2',7' -DCF (DCF) in the presence of

intracellular ROS. For the experiments, HEK-293 cells were pretreated with ORY24h and then exposed to H₂O₂ oxidative insult at the different time points. At the end of the treatment, cells were washed in Hanks' balanced salt solution (HBSS) and then incubated in nitrogensaturated HBSS with 20mM H₂DCF-DA dissolved in dimethyl sulfoxide (DMSO) for 30 minutes at 37°C 5% CO₂. After washing twice in HBSS, intracellular DCF fluorescence, proportional to the amount of ROS/RNS, was evaluated by EnSight fluorescence 96-plate reader (EnSight™ Multimode Plate Reader, PerkinElmer) with excitation and emission wavelengths of 492 and 527 nm, respectively.

2.5 Subcellular Fractionation for Nrf2 Nuclear Translocation

Nuclear protein extracts were prepared by washing HEK-293 cells twice with ice-cold PBS. Cells were subsequently homogenized 15 times using a glass-glass dounce homogenizer in 0.32M sucrose buffered with 20mM Tris hydrochloride (Tris-HCl)(pH 7.4) containing 2mM ethylenediaminetetraacetic acid (EDTA), 0.5mM ethylene glycol-bis(2-aminoethylether)-N,N,N',N' - tetraacetic acid (EGTA), 50mM β-mercaptoethanol, and 20 µg/mL leupeptin, aprotinin, and pepstatin. The homogenate was centrifuged at 300g for 5 minutes to obtain the nuclear fraction. An aliquot of the nuclear fraction was used for protein assay by the Bradford method, whereas the remaining was boiled for 5 min after dilution with sample buffer and subjected to polyacrylamide gel electrophoresis and immunoblotting as described below.

2.6 Western Blot Analysis

Total protein extracts were prepared by harvesting cells in 80 µL of lysis buffer containing 50mM Tris-HCl (pH 7.6), 150mM sodium chloride (NaCl), 5mM EDTA, 1mM phenyl methyl sulphonyl fluoride, 0.5 mg/mL leupeptin, 5 mg/mL aprotinin, and 1 mg/mL pepstatin. Samples were sonicated and centrifuged at 15,000g for 30 minutes at 4°C. The resulting supernatants were isolated, and protein content was determined by a conventional method (BCA protein assay Kit, Pierce, Rockford, IL) before processing for Western blot analysis. Protein samples (30 µg) of both total and nuclear extracts were

electrophoresed in 10% or 12% acrylamide gel and electroblotted onto nitrocellulose membranes (Sigma-Aldrich, Merck KGaA, Darmstadt, Germany). Membranes were blocked for 1 h in 5% w/v bovine serum albumin in TBS-T (0.1M Tris-HCl pH7.4, 0.15M NaCl, and 0.1% Tween 20) and incubated overnight at 4°C with primary antibodies. Primary antibodies were anti-Mn-superoxide dismutase (anti-SOD2, 1:200, Sigma-Aldrich, Merck KGaA, Darmstadt, Germany), anti-Cu-Zn superoxide dismutase (anti-SOD1, 1:300, Santa Cruz Biotechnology Inc., Heidelberg, Germany), anti-Nrf2 (1:2000, Novus, Bio-technie, Minneapolis, USA), anti-NQO1 (1:100, Novus, Bio-technie, Minneapolis, USA), anti HO-1 (1:2000, Novus, Bio-technie, Minneapolis, USA), anti- β -actin (1:1000, BD Biosciences, Franklin Lakes, NJ, USA), anti-lamin A/C (1:1000, BD Biosciences, Franklin Lakes, NJ, USA), and anti- α tubulin (1:1000, Sigma-Aldrich, Merck KGaA, Darmstadt, Germany). IRDye near-infrared dyeconjugated secondary antibodies (LI-COR, Lincoln, Nebraska, USA) were used. The immunodetection was performed using a dual-mode western imaging system Odyssey FC (LI-COR, Lincoln, Nebraska, USA). Quantification was performed using Image Studio Software (LI-COR, Lincoln, Nebraska, USA), and the results were normalized over the α -tubulin, β -actin, or lamin A/C signal.

2.7 Antioxidant Enzyme Activities

SOD activity was measured following the inhibition of epinephrine oxidation according to McCord's method [30]. Total protein extracts and epinephrine 0.1M (Sigma-Aldrich, Merck KGaA, Darmstadt, Germany) were added to G buffer (0.05M glycine and 0.1M NaCl at pH10.34), and the reaction was monitored measuring the decrease of absorbance at 480nm. The activity of purified SOD enzyme (3000 U/mg, Sigma-Aldrich, Merck KGaA, Darmstadt, Germany) was also measured in each experiment as a positive control. Data were normalized for protein amount, and the results were expressed as U/mg using the molar extinction coefficient of 402 at 480 nm. CAT activity was measured monitoring the decomposition of H₂O₂ according to Shangari and O'Brien [31]. In particular, total protein extracts were incubated in a substrate (65 μ M H₂O₂ in 6.0mM PBS buffer pH7.4) at 37°C for 60 s. The enzymatic reaction was stopped by the addition of 32.4mM ammonium molybdate

(Sigma-Aldrich, Merck KGaA, Darmstadt, Germany) and measured at 405 nm. The results were extrapolated by a standard curve (ranging from 12U/mL to 0.25 U/mL) performed with purified CAT enzyme (20,100 U, Sigma-Aldrich, Merck KGaA, Darmstadt, Germany). GPx activity was performed in accordance with Awasthi *et al.* [32], measuring NADPH oxidation at 340nm in the reaction that involved oxidation of reduced glutathione (GSH) to glutathione (GSSG) followed by its reduction by glutathione reductase (GR). Total protein extracts were mixed with a reaction mix, containing 50mM PBS with 0.4mM EDTA at pH7.0, 1.0mM sodium azide solution, 1.0mg β -NADPH, 100 U/mL GR, 200mM GSH, and 10 μ L of 0.042% H₂O₂. The activity of purified GPx enzyme (116U/mg) was also measured in each experiment as positive control. All the reagents were purchased from Sigma-Aldrich, Merck KGaA, Darmstadt, Germany. GPx activity was measured as nmol NADPH oxidized to NADP⁺/mg protein by using the molar extinction coefficient of 0.00622 at 340 nm, and the data were expressed as U/mg.

2.8 Quantitative Real-Time PCR

Total RNA was extracted from 5×10^6 cells following TRIzol[®] reagent protocol (Invitrogen Corporation, Carlsbad, CA, USA). 2 μ g of total RNA was retrotranscribed with MMLV reverse transcriptase (Promega, Madison, Wisconsin, USA), using random hexamers in a final volume of 40 μ L. Parallel reactions containing no reverse transcriptase were used as negative controls to confirm the removal of all genomic DNA. Nrf2, Keap1, NQO1, HO-1, and GAPDH primers were provided by Qiagen (Qiagen, Hilden, Germany). GAPDH was used as endogenous reference. Quantitative RT-PCR was performed with the ViiA7 Real-Time PCR System (Applied Biosystems, Foster City, CA, USA) using the iQ[™]SYBR Green Supermix method (Bio-Rad Laboratories, Richmond, CA, USA) according to manufacturer's instructions.

2.9 Statistical Analysis

The results are reported as mean \pm standard error mean (SEM) or standard deviation (SD) of at least three independent experiments. Statistical differences were determined by the analysis of variance (one-way ANOVA)

followed, when significant, by an appropriate *post hoc* test as indicated in figure legends. p value of ≤ 0.05 was considered statistically significant.

3. Results

3.1 Oryzanol Prevents H_2O_2 -Induced ROS/RNS Generation and Cell Death

The antioxidant properties of ORY were evaluated in HEK-293 cells in baseline redox steady-state condition and after an acute oxidative insult. Cells were pretreated for 24 h with ORY (ORY_{24h}) at different concentrations ranging from 1 to 20 $\mu\text{g}/\text{mL}$ followed by an acute oxidative insult elicited by 100 μM H_2O_2 . After 24 h, cell viability was evaluated with MTT assay. As shown in **Figure 1 (a)**, ORY_{24h} did not affect cell viability at any examined concentration. H_2O_2 alone reduced cell viability about 35% ($p \leq 0.001$), but this mortality was rescued by ORY_{24h} at 5 $\mu\text{g}/\text{mL}$ ($p \leq 0.05$) (**Figure 1 (a)**). The minimum efficient concentration (5 $\mu\text{g}/\text{mL}$) was used for the following experiments.

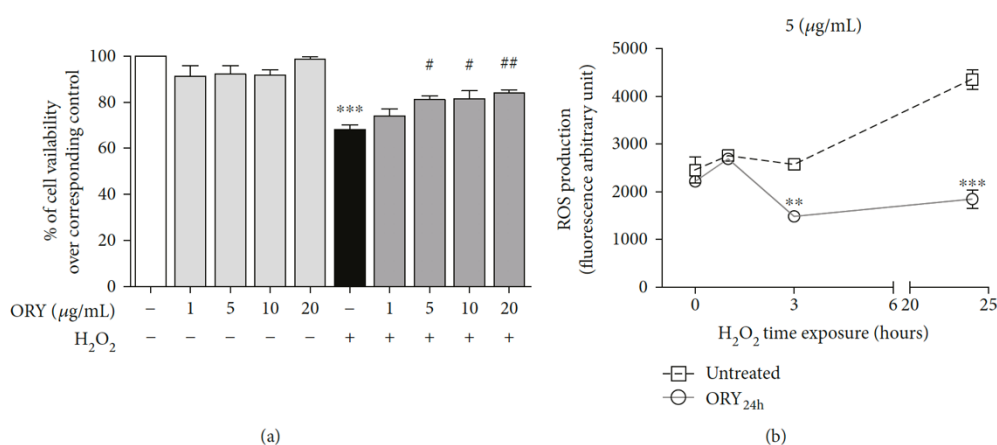


Figure 1. Oryzanol protects from cell death and decreases H_2O_2 -induced ROS/RNS generation. (a) HEK-293 cells were pretreated for 24 h with ORY (ORY_{24h}) at different concentrations and then stressed by the addition of 100 μM H_2O_2 for 24 h. Cell viability was

evaluated with MTT assay. Data are shown as percentage of cell viability compared with untreated cells; *** $p \leq 0.001$ versus untreated cells and ## $p \leq 0.01$ and # $p \leq 0.05$ versus H₂O₂ group. **(b)** Effects of 5 µg/mL ORY_{24h} on H₂O₂-induced ROS/RNS production were determined by H₂DCF-DA oxidation using a fluorescence microplate reader. Fluorescence intensity of ORY_{24h} (open square symbol) after oxidative insult significantly decreased over time with ** $p \leq 0.01$ at 3 h and *** $p \leq 0.001$ at 24 h versus the corresponding untreated control group (open circle symbol). Bonferroni's multiple comparison test was used.

The effect of 5 µg/mL ORY_{24h} on H₂O₂-induced ROS/RNS production was studied by monitoring the oxidation of the 2'-7'-dichlorofluorescein (DCF) probe from nonfluorescent-reduced state to be fluorescent in the presence of free radicals. 100 µM H₂O₂ exposure initially induced a moderate production of ROS/RNS which significantly increased over time as assessed by accumulation of oxidized DCF (**Figure 1 (b)**, open square symbol). ORY_{24h} reverted H₂O₂-induced ROS/RNS generation at 3 h, and this effect was sustained at least until 24 h (**Figure 1 (b)**, open circle symbol).

3.2 Oryzanol Modulates the Antioxidant Enzyme Activities

Different studies suggested that ORY could exert its antioxidant effects by modulating the endogenous antioxidant enzyme activities. In particular, SOD has been found to be positively regulated by ORY [26, 33, 34]. Here, we evaluated the protein expression and activity of SOD enzymes in the presence of ORY_{24h} alone or followed by oxidative insult. H₂O₂ insult did not affect the protein expression of the mitochondrial MnSOD (SOD2, **Figure 2 (a)**) but significantly increased the cytosolic Cu-Zn SOD protein levels (SOD1, **Figure 2 (b)**) that also reflected an increase of SOD activity induced by the oxidative insult (**Figure 2 (c)**). ORY_{24h} alone significantly enhanced the protein expression of both SOD2 (mean ± SEM: untreated cells 0.078 ± 0.014 versus ORY_{24h} 0.143 ± 0.006; $p \leq 0.001$) and SOD1 (mean ± SEM: untreated cells 0.059 ± 0.005 versus ORY_{24h} 0.150 ± 0.011; $p \leq 0.01$) (**Figures 2 (a)** and **2 (b)**) as well as the total SOD activity (mean ± SEM: untreated cells 0.098 ± 0.066 versus ORY_{24h} 0.566 ± 0.072; $p < 0.001$ **Figure 2 (c)**). In SOD1 protein expression, the combination of ORY_{24h} followed by H₂O₂ significantly maintained higher compared to untreated cells (mean ± SEM: 0.097 ± 0.007; $p \leq 0.05$), but no difference was highlighted compared to H₂O₂ alone (mean ± SEM: 0.107 ± 0.019). Interestingly, in the presence of an acute oxidative

insult (3 h of H₂O₂), ORY_{24h} maintained higher total SOD activity compared to H₂O₂ alone (mean \pm SEM: ORY_{24h} + H₂O₂ 0.4448 ± 0.085 versus H₂O₂ 0.214 ± 0.048 **Figure 2 (c)**). We also evaluated the activity of CAT and GPx, two enzymes that work downstream of SOD. No differences in terms of CAT activity were found compared to the different treatments (data not shown). Differently, GPx activity was found to be modulated by ORY. ORY_{24h} alone increased GPx activity (mean \pm SEM: 0.43 ± 0.016) compared to untreated one (mean \pm SEM: 0.27 ± 0.011 ; $p \leq 0.001$ **Figure 2 (d)**). H₂O₂ acute insults at 3 h also induced an increase in GPx activity that was confirmed by the ORY pretreatment without further affecting the activity levels. A long-lasting oxidative insult of H₂O₂ at 24 h which showed ORY_{24h} pretreatment still maintained higher GPx activity suggesting an active alarm system to detoxify from radicals. Altogether, these data confirmed the antioxidant effects of ORY through the modulation of endogenous antioxidant enzyme activities.

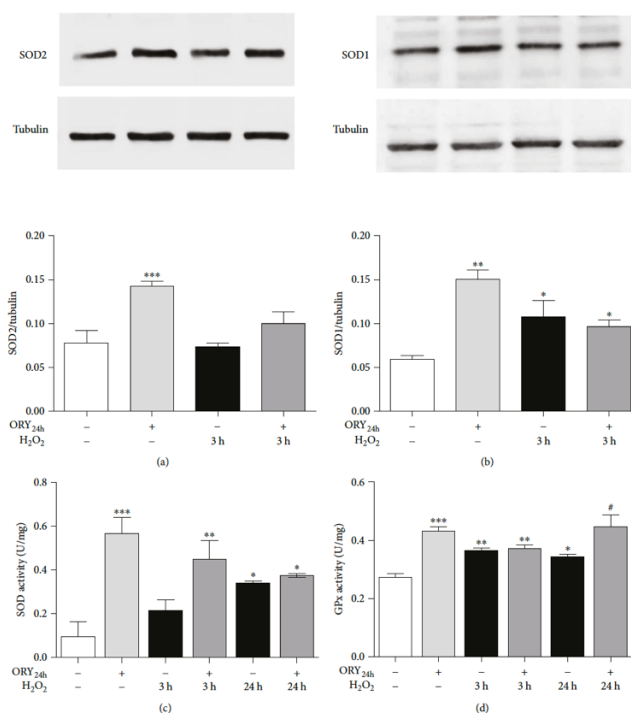


Figure 2. Oryzanol effect on antioxidant enzyme activities and MnSOD and Cu-ZnSOD expression. HEK-293 cells were pretreated with 5 μ g/mL ORY for 24 h followed by 100

$\mu\text{M H}_2\text{O}_2$ for 3 h or 24 h. **(a, b)** Effect of $\text{ORY}_{24\text{h}}$ on the expression of MnSOD (SOD2) and Cu-ZnSOD (SOD1) in H_2O_2 -induced oxidative stress. The protein expression was assessed by Western blotting. Tubulin expression was used as loading control. Data are presented as mean \pm SEM; *** $p \leq 0.001$ and ** $p \leq 0.01$ versus untreated cells. The activity of total SOD **(c)** and GPx **(d)** enzymes was assessed, as reported in the Material and Methods, before and after 3 h and 24 h of H_2O_2 oxidative insult. The results are represented as mean \pm SEM; *** $p \leq 0.001$, ** $p \leq 0.01$, and * $p \leq 0.05$ versus untreated cells and # $p < 0.05$ versus the corresponding H_2O_2 control group. Bonferroni's multiple comparison test was used.

3.3 Oryzanol Activates Nrf2 Pathway

Activation of the Keap1/Nrf2 pathway and the consequent induction of its antioxidant genes trigger an elaborate network of protective mechanisms against oxidative damage [35]. When exposed to an oxidative insult, Keap1 undergoes conformational changes thereby disrupting its binding to Nrf2, which in turn promotes the Nrf2 translocation into the nucleus and activates the transcription-mediated protective responses. [36].

Thus, ORY was investigated to verify whether it might affect the Nrf2 pathway. We focused on the activation of Nrf2 signaling by analyzing its translocation into the nucleus and its ability to induce NQO1 and HO-1, the two prototypical cytoprotective Nrf2-target genes related to cellular stress response.

In basal condition, 3 h exposure of ORY significantly increased Nrf2 nuclear expression which was further enhanced at 6 h and decreased at 24 h in comparison with untreated cells (mean \pm SEM: $\text{ORY}_{3\text{h}}$ 1.28 ± 0.11 ; $\text{ORY}_{6\text{h}}$ 1.76 ± 0.25 ; $\text{ORY}_{24\text{h}}$ 1.03 ± 0.02 versus untreated 0.64 ± 0.07 ; $p \leq 0.01$, $p \leq 0.001$, and $p \leq 0.05$, respectively, **Figure 3 (a)**). As a positive control, 100 $\mu\text{M H}_2\text{O}_2$ at 3 h treatment increased higher Nrf2 nuclear levels than those found in untreated cells (mean 1.01 ± 0.07 ; $p \leq 0.05$) and $\text{ORY}_{24\text{h}}$ (**Figure 3 (a)**). The pretreatment of $\text{ORY}_{24\text{h}}$ followed by 3 h H_2O_2 did not significantly differ in the extent of activation from the $\text{ORY}_{24\text{h}}$ or H_2O_2 alone. To further sustain these results, we also investigated the Nrf2 expression in the cytosolic fraction. At 3, 6, and 24 h, ORY did not modify the Nrf2 cytoplasmatic expression, which

expressed as ratio Nrf2/tubulin (**Figure 3 (b)**). Likewise, a similar trend was observed in the presence of H₂O₂ alone or with ORY (**Figure 3 (b)**).

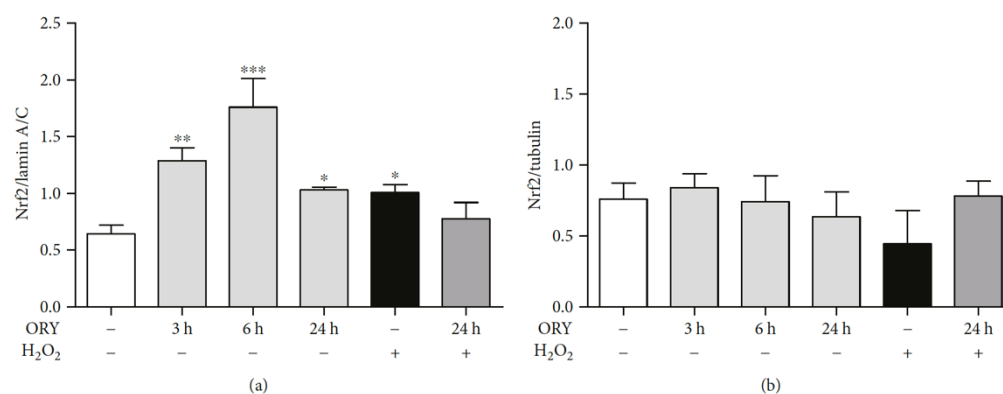


Figure 3. Nrf2 nuclear translocation induced by oryzanol. HEK-293 cells were pretreated with ORY for 3, 6, and 24 h and then stressed with 100 μ M H₂O₂ for 3 h. Nuclear and cytoplasmic fractions were isolated as described in the Material and Methods. **(a)** Nuclear expression of Nrf2 was assessed by Western blotting and lamin A/C expression was used as loading control. Data are represented as mean \pm SD; *** $p \leq 0.001$, ** $p \leq 0.01$, and * $p \leq 0.05$ versus untreated cells, Dunnett's multiple comparison test. **(b)** Cytoplasmic expression of Nrf2 was assessed by Western blotting, and tubulin expression was used as loading control. Data are represented as mean \pm SD.

The mRNA expression of Nrf2 was also evaluated in cells pretreated with ORY_{24h} alone or followed by H₂O₂ exposure in a time course (**Figure 4 (a)**). H₂O₂ alone transiently increased mRNA levels of Nrf2. ORY_{24h} alone did not affect Nrf2 expression. However, when the oxidative insult was present, ORY_{24h} significantly increased its mRNA levels at 1 and 3 h without changing the transient pattern. The increase of mRNA presented also an increase of Nrf2 protein levels at 24 h after H₂O₂ in presence or absence of ORY_{24h} (**Figure 5 (a)**).

Since Keap1 is the other key factor involved in the regulation of Nrf2 pathway activation, its mRNA expression was also investigated (**Figure 4 (b)**). ORY_{24h} did not change Keap1 mRNA levels with respect to untreated cells. H₂O₂ alone significantly increased Keap1 mRNA level only at 3 h. The combined treatment of ORY_{24h} and H₂O₂ although appeared to further enhance Keap1 mRNA, only the results at 3 h were significant.

To verify the complete activation of the Nrf2 pathway, we further analyzed the induction of the cytoprotective Nrf2 target genes. **Figures 4** and **5** showed the mRNA expression and protein levels of HO-1 and NQO1 in cells exposed to ORY_{24h} alone or followed by H₂O₂.

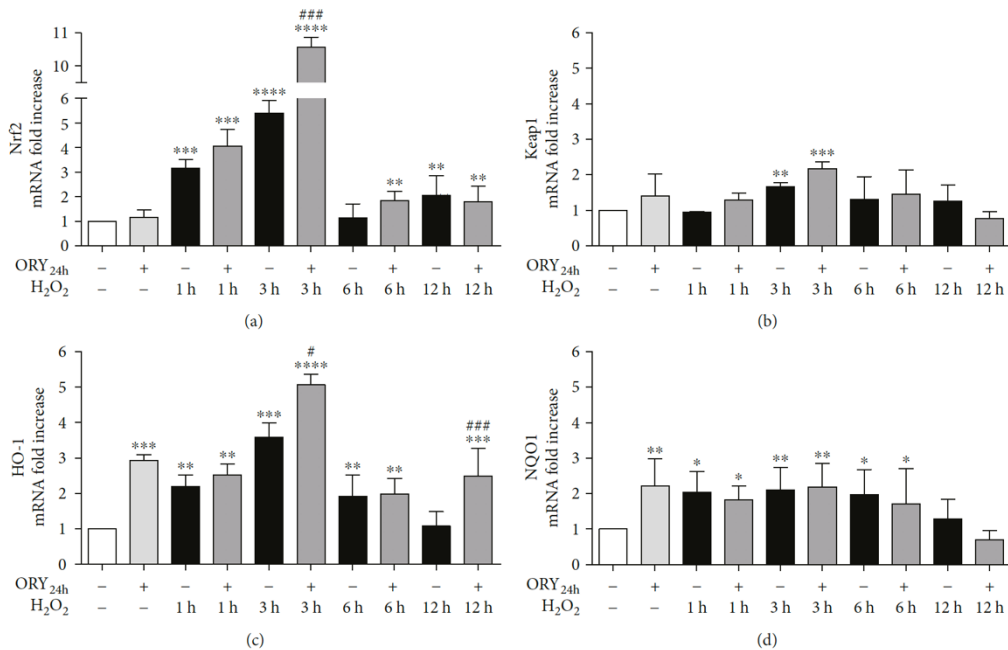


Figure 4. Oryzanol activates the transcription of Nrf2 target genes. HEK-293 cells were pretreated with 5 $\mu\text{g}/\text{mL}$ ORY for 24 h followed by a time course of 100 μM H₂O₂ (1, 3, 6, and 12 h). Cells were then processed for measuring Nrf2 **(a)**, Keap1 **(b)**, HO-1 **(c)**, and NQO1 **(d)** mRNA levels by real-time PCR. GAPDH was used to normalize the results. Data are shown as mean \pm SEM. Statistically significant differences were represented as follows: **** $p \leq 0.0001$, *** $p \leq 0.001$, ** $p \leq 0.01$, and * $p \leq 0.05$ versus untreated cells and ### $p \leq 0.001$ and # $p \leq 0.05$ versus the corresponding H₂O₂ control group, Bonferroni's multiple comparison test.

ORY_{24h} treatment increased the mRNA levels of HO-1 and NQO1 by nearly twofold and onefold, respectively (**Figures 4 (c)** and **4 (d)**). HO-1 mRNA expression was also transiently induced by H₂O₂ with the highest expression at 3 h, which returned to the basal level at 12 h. Interestingly, after treatment with ORY_{24h} followed by the H₂O₂, HO-1 mRNA remained high at 12 h (**Figure 4 (c)**). HO-1 protein expression reflected the mRNA results showing a

significant increase after ORY_{24h} or H₂O₂ alone and remaining high after the combined treatment of ORY_{24h} plus H₂O₂ (**Figure 5 (b)**).

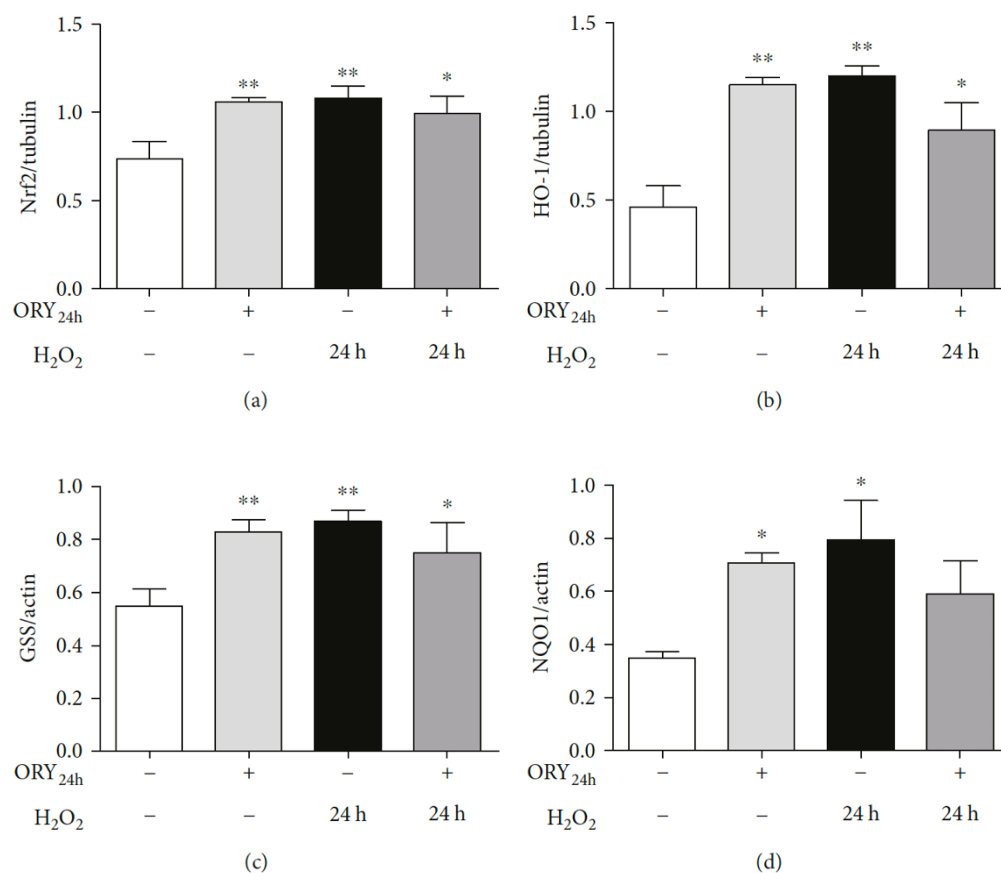


Figure 5. Oryzanol induces an increase in Nrf2 target gene protein levels. HEK-293 cells were pretreated with 5 μ g/mL ORY for 24 h followed by 24 h of 100 μ M H₂O₂. Cells were then processed for measuring Nrf2 (**a**), HO-1 (**b**), GSS (**c**), and NQO1 (**d**) protein levels by Western blotting. Tubulin and actin were used as loading control according with the molecular weight of the above investigated proteins. Data are shown as mean \pm SD; ** p \leq 0.01 and * p \leq 0.05 versus untreated cells, Dunnett's multiple comparison test.

Similarly, NQO1 mRNA was transiently increased by H₂O₂ alone or in combination with ORY_{24h}, while the magnitude of fold increase was lower than that observed for HO-1 at any time points (**Figure 4 (d)**). NQO1 protein expression reflected the mRNA results showing a significant increase after

ORY_{24h} or H₂O₂ alone and then decreasing after the combined treatment ORY_{24h} plus H₂O₂ (**Figure 5 (d)**). Since the increase in GPx activity due to ORY pretreatment, we also decided to investigate protein levels of GSS, another Nrf2 target gene. GSS protein expression was in accordance with the results obtained from HO-1 since it significantly increased after ORY_{24h} or H₂O₂ alone and decreased after the combined pretreatment with ORY and H₂O₂. These data confirmed an early activation of Nrf2 pathway due to ORY pretreatment highlighting its ability to modulate efficiently the relative expression of Nrf2 target genes at both mRNA and protein levels.

4. Discussion

Before the westernization of Eastern countries, the introduction, and the diffusion of Western foods, the Eastern populations were known for their longevity and low incidence of certain illness such as cardiovascular disease [37]. Rice has been at the base of diet of such populations. Moreover, it has been related to the prevention of aging and age-related diseases, but its importance and consumption are not really well claimed. Rice exerts beneficial effects on health as a source of fiber, minerals, vitamins, and phenols with antioxidant activities [19, 20, 38, 39]. Rice-derived ORY has been well studied for its ability to prevent oxidative stress by inducing antioxidant enzyme expression and activity [16, 22].

Our results have showed the antioxidant effects exerted by ORY in an *in vitro* model via inhibition of H₂O₂-induced ROS/RNS generation. In particular, we showed that in basal condition, ORY regulated the protein expression and the activity of SOD enzymes. Furthermore, GPx enzyme activity was also enhanced by ORY in H₂O₂-induced ROS/RNS and baseline condition. In addition, following the H₂O₂ treatment, ORY was able to sustain the antioxidant cellular response and maintain a higher enzymatic activity, thus efficiently turning off ROS/RNS generation. Through this mechanism, ORY might represent a valid first line of defense against oxidative stress. Moreover, beyond its antioxidant properties, ORY was found to possess further potential

functions such as antihyperlipidemic, antidiabetic, and antiinflammatory effects, suggesting a potential role against the development of the related diseases [16, 22, 39-41]. All these disorders are related to redox imbalance, thus suggesting that other mechanisms associated with the regulation of redox homeostasis and the protection against long-lasting oxidative insults could be involved. Here, we showed that ORY exhibited a remarkable free radical scavenging property, and we further deepened the antioxidant profile of ORY by suggesting its ability to trigger the Nrf2 pathway in terms of upregulation of Nrf2 expression, translocation into the nucleus, and induction of the Nrf2-dependent defensive genes such as HO-1, NQO1, and GSS. These results are very interesting because they might promote ORY or ORY-inspired compounds as an integrative intervention to impact the aging process and longevity together with the decrease of oxidative stress [42, 43].

Induction by oxidative stress is the best-understood mechanism of Nrf2 activation. In our experimental model, H₂O₂ was able to induce Nrf2 translocation and activation of its target genes involved in cellular responses against xenobiotics. NQO1, HO-1 mRNA, and protein levels were found enhanced in HEK-293 cells treated with H₂O₂. SOD1 is another target gene of Nrf2. H₂O₂ induced an increase in the expression of SOD1 suggesting that it could be under the regulation of Nrf2. The mechanism by which free radicals activated Nrf2 pathway is via the modification of cysteine residues on Keap1, thus resulting in Nrf2 accumulation in the cytoplasm and translocation into the nucleus. The oxidative insult also induced the increase of mRNA and protein expression of Nrf2 (**Figure 4 (a)**). Two ARE-like motifs in the 5' flanking regions of the Nrf2 promoter are responsible for the induction of Nrf2 upon activation [44] ensuring a feed-forward process with Nrf2 activation promoting its own expression, thus facilitating a profound cellular response to stress. Therefore, all these data highlighted that the cells were unable to detoxify themselves from the oxidative stress induced by ROS/RNS production. In addition, Nrf2 can also be activated by different phytochemicals [45-47] as well as various pharmaceuticals (reviewed in [48]) via overlapping and distinct mechanisms. Here, we demonstrated that ORY alone was able to transiently induce Nrf2 translocation that was still present when oxidative insult was added. Our hypothesis is that the mechanism by

which ORY is able to modulate Nrf2 pathway might be due to its intrinsic chemical structure (**Figure 6**) [49]. The presence of ROS/RNS induces the hydroxyl group on the phenolic ring of ORY [16, 22] resulting in the formation of a phenoxy radical, which might be involved in the modification of cysteine thiols of Keap1 leading to the inhibition of Keap1-Nrf2 binding. As a consequence of Nrf2 nuclear translocation, its target genes are transactivated. Here, we found that ORY_{24h} induced the transient transcription of HO-1, NQO1, and GSS genes by the increase of their protein expression. It is noteworthy that HO-1 mRNA was still higher after 12 h of pretreatment with ORY followed by H₂O₂ exposure suggesting the presence of alternative mechanisms to sustain in parallel its expression. Finally, after ORY_{24h} pretreatment, the increase of SOD1 protein expression could be also influenced by the Nrf2 pathway.

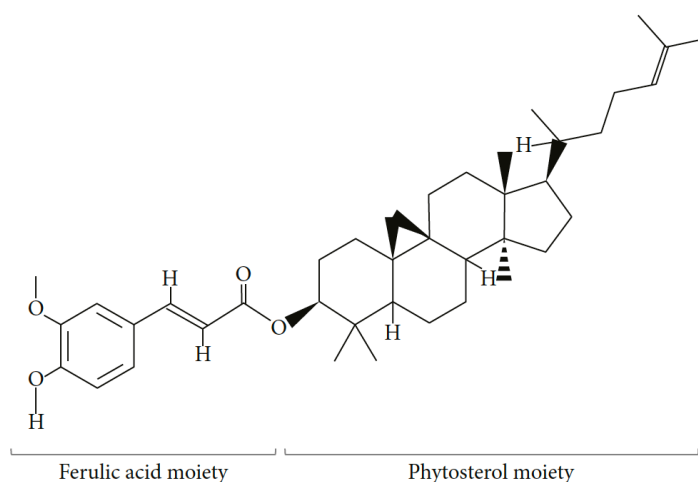


Figure 6. Molecular structure of oryzanol. The structure of ORY consists of two moieties: ferulic acid and phytosterols (National Center for Biotechnology Information; PubChem Compound Database, CID = 6450219.)

In conclusion, this study suggested that the antioxidant effects of ORY could also be sustained by the Nrf2 pathway. Nrf2 is involved in regulating longevity and age-related diseases and has also been proposed as a master regulator

of the aging process. Further *in vitro* and *in vivo* studies of ORY as a potential longevity-promoting inducer could be studied in the future.

References

- [1] D. Harman, "Aging: a theory based on free radical and radiation chemistry," *Journal of Gerontology*, vol. 11, no. 3, pp. 298-300, 1956.
- [2] R. Olinski, A. Siomek, R. Rozalski *et al.*, "Oxidative damage to DNA and antioxidant status in aging and age-related diseases," *Acta Biochimica Polonica*, vol. 1, pp. 11-26, 2007.
- [3] B. Uttara, A. Singh, P. Zamboni, and R. Mahajan, "Oxidative stress and neurodegenerative diseases: a review of upstream and downstream antioxidant therapeutic options," *Current Neuropharmacology*, vol. 7, no. 1, pp. 65-74, 2009.
- [4] G. Cenini, C. Cecchi, A. Pensalfini *et al.*, "Generation of reactive oxygen species by beta amyloid fibrils and oligomers involves different intra/extracellular pathways," *Amino Acids*, vol. 38, no. 4, pp. 1101-1106, 2010.
- [5] J. M. McCord, "The evolution of free radicals and oxidative stress," *The American Journal of Medicine*, vol. 108, no. 8, pp. 652-659, 2000.
- [6] Y. Z. Fang, S. Yang, and G. Wu, "Free radicals, antioxidants, and nutrition," *Nutrition*, vol. 18, no. 10, pp. 872-879, 2002.
- [7] N. Ghosh, R. Ghosh, and S. C. Mandal, "Antioxidant protection: a promising therapeutic intervention in neurodegenerative disease," *Free Radical Research*, vol. 45, no. 8, pp. 888-905, 2011.
- [8] J. I. Castillo-Quan, K. J. Kinghorn, and I. Bjedov, "Genetics and pharmacology of longevity," *Advances in Genetics*, vol. 90, pp. 1-101, 2015.
- [9] D. R. Bruns, J. C. Drake, L. M. Biela, F. F. Peelor, B. F. Miller, and K. L. Hamilton, "Nrf2 signaling and the slowed aging phenotype: evidence from long-lived models," *Oxidative Medicine and Cellular Longevity*, vol. 2015, Article ID 732596, 15 pages, 2015.
- [10] G. P. Sykiotis, I. G. Habeos, A. V. Samuelson, and D. Bohmann, "The role of the antioxidant and longevity-promoting Nrf2 pathway in metabolic regulation," *Current Opinion in Clinical Nutrition and Metabolic Care*, vol. 14, no. 1, pp. 41-48, 2011.
- [11] A. J. Wilson, J. K. Kerns, J. F. Callahan, and C. J. Moody, "Keap calm, and carry on covalently," *Journal of Medicinal Chemistry*, vol. 56, no. 19, pp. 7463-7476, 2013.
- [12] K. Itoh, T. Chiba, S. Takahashi *et al.*, "An Nrf2/small Maf heterodimer mediates the induction of phase II detoxifying enzyme genes through antioxidant response elements," *Biochemical and Biophysical Research Communications*, vol. 236, no. 2, pp. 313-322, 1997.
- [13] M. C. Lu, J. A. Ji, Z. Y. Jiang, and Q. D. You, "The Keap1-Nrf2-ARE pathway as a potential preventive and therapeutic target: an update," *Medicinal Research Reviews*, vol. 36, no. 5, pp. 924-963, 2016.

- [14] N. Ismail, M. Ismail, M. U. Imam *et al.*, "Mechanistic basis for protection of differentiated SH-SY5Y cells by oryzanol-rich fraction against hydrogen peroxide-induced neurotoxicity," *BMC Complementary and Alternative Medicine*, vol. 14, no. 1, 2014.
- [15] N. Ismail, M. Ismail, S. Farhana Fathy *et al.*, "Neuroprotective effects of germinated brown rice against hydrogen peroxide induced cell death in human SH-SY5Y cells," *International Journal of Molecular Sciences*, vol. 13, no. 12, pp. 9692-9708, 2012.
- [16] M. Shafiqul Islam, R. Nagasaka, K. Ohara *et al.*, "Biological abilities of rice bran-derived antioxidant phytochemicals for medical therapy," *Current Topics in Medicinal Chemistry*, vol. 11, no. 14, pp. 1847-1853, 2011.
- [17] K. Masisi, T. Beta, and M. H. Moghadasian, "Antioxidant properties of diverse cereal grains: a review on *in vitro* and *in vivo* studies," *Food Chemistry*, vol. 196, pp. 90-97, 2016.
- [18] M. A. Soobrattee, V. S. Neergheen, A. Luximon-Ramma, O. I. Aruoma, and T. Bahorun, "Phenolics as potential antioxidant therapeutic agents: mechanism and actions," *Mutation Research*, vol. 579, no. 1-2, pp. 200-213, 2005.
- [19] S. Butsat and S. Siriamornpun, "Antioxidant capacities and phenolic compounds of the husk, bran and endosperm of Thai rice," *Food Chemistry*, vol. 119, no. 2, pp. 606-613, 2010.
- [20] M. J. Lerma-García, J. M. Herrero-Martínez, E. F. Simó-Alfonso, C. R. B. Mendonça, and G. Ramis-Ramos, "Composition, industrial processing and applications of rice bran γ -oryzanol," *Food Chemistry*, vol. 115, no. 2, pp. 389-404, 2009.
- [21] R. Kaneko and T. Tsuchiya, "New compound in rice bran and germ oils," *The Journal of the Society of Chemical Industry, Japan*, vol. 57, no. 7, p. 526, 1954.
- [22] I. Minatel, F. Francisqueti, C. Corrêa, and G. Lima, "Antioxidant activity of γ -oryzanol: a complex network of interactions," *International Journal of Molecular Sciences*, vol. 17, no. 12, 2016.
- [23] I. O. Minatel, S. I. Han, G. Aldini *et al.*, "Fat-soluble bioactive components in colored rice varieties," *Journal of Medicinal Food*, vol. 17, no. 10, pp. 1134-1141, 2014.
- [24] Z. Xu, N. Hua, and J. S. Godber, "Antioxidant activity of tocopherols, tocotrienols, and γ -oryzanol components from rice bran against cholesterol oxidation accelerated by 2,2'-azobis(2-methylpropionamide) dihydrochloride," *Journal of Agricultural and Food Chemistry*, vol. 49, no. 4, pp. 2077-2081, 2001.
- [25] M. Jin Son, C. W. Rico, S. Hyun Nam, and M. Young Kang, "Influence of oryzanol and ferulic acid on the lipid metabolism and antioxidative status in high fat-fed mice," *Journal of Clinical Biochemistry and Nutrition*, vol. 46, no. 2, pp. 150-156, 2010.
- [26] S. M. Araujo, M. T. de Paula, M. R. Poetini *et al.*, "Effectiveness of γ -oryzanol in reducing neuromotor deficits, dopamine depletion and oxidative stress in a *Drosophila melanogaster* model of Parkinson's disease induced by rotenone," *Neurotoxicology*, vol. 51, pp. 96-105, 2015.
- [27] M. I. Waly, M. S. Al Moundhri, and B. H. Ali, "Effect of curcumin on cisplatin- and oxaliplatin-induced oxidative stress in human embryonic kidney (HEK) 293 cells," *Renal Failure*, vol. 33, no. 5, pp. 518-523, 2011.

-
- [28] D. Dinu, G. O. Bodea, C. D. Ceapa *et al.*, "Adapted response of the antioxidant defense system to oxidative stress induced by deoxynivalenol in Hek-293 cells," *Toxicol*, vol. 57, no. 7-8, pp. 1023-1032, 2011.
- [29] A. R. N. Reddy, Y. N. Reddy, D. R. Krishna, and V. Himabindu, "Multi wall carbon nanotubes induce oxidative stress and cytotoxicity in human embryonic kidney (HEK293) cells," *Toxicology*, vol. 272, no. 1-3, pp. 11-16, 2010.
- [30] J. M. McCord and I. Fridovich, "Superoxide dismutase. An enzymic function for erythrocyte hemocuprein," *The Journal of Biological Chemistry*, vol. 22, pp. 6049-6055, 1969.
- [31] N. Shangari and P. J. O'Brien, "Catalase activity assays," *Curr Protoc Toxicol*, 2006, chapter 7, unit 7.7.1-15.
- [32] Y. C. Awasthi, D. D. Dao, A. K. Lal, and S. K. Srivastava, "Purification and properties of glutathione peroxidase from human placenta," *The Biochemical Journal*, vol. 177, no. 2, pp. 471-476, 1979.
- [33] S. S. Panchal, R. K. Patidar, A. B. Jha, A. A. Allam, J. Ajarem, and S. B. Butani, "Anti-inflammatory and antioxidative stress effects of oryzanol in glaucomatous rabbits," *Journal of Ophthalmology*, vol. 2017, Article ID 1468716, 9 pages, 2017.
- [34] S. B. Ghatak and S. S. Panchal, "Anti-diabetic activity of oryzanol and its relationship with the anti-oxidant property," *International Journal of Diabetes in Developing Countries*, vol. 32, no. 4, pp. 185-192, 2012.
- [35] L. Baird and A. T. Dinkova-Kostova, "The cytoprotective role of the Keap1-Nrf2 pathway," *Archives of Toxicology*, vol. 85, no. 4, pp. 241-272, 2011.
- [36] T. Suzuki and M. Yamamoto, "Molecular basis of the Keap1-Nrf2 system," *Free Radical Biology & Medicine*, vol. 88, pp. 93-100, 2015.
- [37] A. O. Odegaard, W. P. Koh, J. M. Yuan, M. D. Gross, and M. A. Pereira, "Western-style fast food intake and cardiometabolic risk in an eastern country," *Circulation*, vol. 126, no. 2, pp. 182-188, 2012.
- [38] T. Laokuldilok, C. F. Shoemaker, S. Jongkaewwattana, and V. Tulyathan, "Antioxidants and antioxidant activity of several pigmented rice brans," *Journal of Agricultural and Food Chemistry*, vol. 59, no. 1, pp. 193-199, 2011.
- [39] C. Saenjum, "Antioxidant and anti-inflammatory activities of gamma-oryzanol rich extracts from Thai purple rice bran," *Journal of Medicinal Plants Research*, vol. 6, no. 6, 2012.
- [40] J. Parrado, E. Miramontes, M. Jover *et al.*, "Prevention of brain protein and lipid oxidation elicited by a water-soluble oryzanol enzymatic extract derived from rice bran," *European Journal of Nutrition*, vol. 42, no. 6, pp. 307-314, 2003.
- [41] S. Sakai, T. Murata, Y. Tsubosaka, H. Ushio, M. Hori, and H. Ozaki, "γ-Oryzanol reduces adhesion molecule expression in vascular endothelial cells via suppression of nuclear factor-κB activation," *Journal of Agricultural and Food Chemistry*, vol. 60, no. 13, pp. 3367-3372, 2012.

- [42] A. Safdar, J. deBeer, and M. A. Tarnopolsky, "Dysfunctional Nrf2-Keap1 redox signaling in skeletal muscle of the sedentary old," *Free Radical Biology & Medicine*, vol. 49, no. 10, pp. 1487-1493, 2010.
- [43] J. H. Suh, S. V. Shenvi, B. M. Dixon *et al.*, "Decline in transcriptional activity of Nrf2 causes age-related loss of glutathione synthesis, which is reversible with lipoic acid," *Proceedings of the National Academy of Sciences of the United States of America*, vol. 101, no. 10, pp. 3381-3386, 2004.
- [44] M. K. Kwak, K. Itoh, M. Yamamoto, and T. W. Kensler, "Enhanced expression of the transcription factor Nrf2 by cancer chemopreventive agents: role of antioxidant response element-like sequences in the nrf2 promoter," *Molecular and Cellular Biology*, vol. 22, no. 9, pp. 2883-2892, 2002.
- [45] Y.-J. Surh, J. Kundu, and H.-K. Na, "Nrf2 as a master redox switch in turning on the cellular signaling involved in the induction of cytoprotective genes by some chemopreventive phytochemicals," *Planta Medica*, vol. 74, no. 13, pp. 1526-1539, 2008.
- [46] E. L. Donovan, J. M. McCord, D. J. Reuland, B. F. Miller, and K. L. Hamilton, "Phytochemical activation of Nrf2 protects human coronary artery endothelial cells against an oxidative challenge," *Oxidative Medicine and Cellular Longevity*, vol. 2012, Article ID 132931, 9 pages, 2012.
- [47] D. J. Reuland, S. Khademi, C. J. Castle *et al.*, "Upregulation of phase II enzymes through phytochemical activation of Nrf2 protects cardiomyocytes against oxidant stress," *Free Radical Biology & Medicine*, vol. 56, pp. 102-111, 2013.
- [48] B. M. Hybertson, B. Gao, S. K. Bose, and J. M. McCord, "Oxidative stress in health and disease: the therapeutic potential of Nrf2 activation," *Molecular Aspects of Medicine*, vol. 32, no. 4-6, pp. 234-246, 2011.
- [49] "National Center for Biotechnology Information," *PubChem Compound Database*, CID=6450219, December 2017, <https://pubchem.ncbi.nlm.nih.gov/compound/6450219>.

PART II

The following manuscript was published in *ACS Chemical Neuroscience* in 2019 as:

Prenylated Curcumin Analogues as Multipotent Tools To Tackle Alzheimer's Disease

Federica Bisceglia, Francesca Seghetti, Massimo Serra, Morena Zusso, Silvia Gervasoni, Laura Verga, Giulio Vistoli, Cristina Lanni, **Michele Catanzaro**, Ersilia De Lorenzi and Federica Belluti

Abstract

Alzheimer's disease is likely to be caused by copathogenic factors including aggregation of A β peptides into oligomers and fibrils, neuroinflammation, and oxidative stress. To date, no effective treatments are available, and because of the multifactorial nature of the disease, it emerges the need to act on different and simultaneous fronts. Despite the multiple biological activities ascribed to curcumin as neuroprotector, its poor bioavailability and toxicity limit the success in clinical outcomes. To tackle Alzheimer's disease on these aspects, the curcumin template was suitably modified, and a small set of analogues was attained. In particular, derivative 1 turned out to be less toxic than curcumin. As evidenced by capillary electrophoresis and transmission electron microscopy studies, 1 proved to inhibit the formation of large toxic A β oligomers, by shifting the equilibrium toward smaller nontoxic assemblies and to limit the formation of insoluble fibrils. These findings were supported by molecular docking and steered molecular dynamics simulations which confirmed the superior capacity of 1 to bind A β structures of different complexity. Remarkably, 1 also showed *in vitro* anti-inflammatory and antioxidant properties. In summary, the curcumin-based analogue 1 emerged as multipotent compound worthy to be further investigated and exploited in the Alzheimer's disease multitarget context.

Keywords: Alzheimer's disease; amyloid beta oligomers and fibrils; capillary electrophoresis; curcumin analogues; oxidative stress.

Prenylated Curcumin Analogues as Multipotent Tools To Tackle Alzheimer's Disease

Federica Bisceglia,[†] Francesca Seghetti,[‡] Massimo Serra,[†] Morena Zusso,[§] Silvia Gervasoni,^{||} Laura Verga,[⊥] Giulio Vistoli,^{||} Cristina Lanni,[†] Michele Catanzaro,[†] Ersilia De Lorenzi,^{*,†} and Federica Belluti[‡]

[†]Department of Drug Sciences, University of Pavia, Viale Taramelli 12, 27100 Pavia, Italy

[‡]Department of Pharmacy and Biotechnology, Alma Mater Studiorum-University of Bologna, Via Belmeloro 6, 40126 Bologna, Italy

[§]Department of Pharmaceutical and Pharmacological Sciences, University of Padua, Largo Meneghetti 2, 35131 Padua, Italy

^{||}Department of Pharmaceutical Sciences, University of Milan, Via Mangiagalli 25, 20133 Milan, Italy

[⊥]Department of Molecular Medicine, Unit of Pathology, University of Pavia IRCCS Policlinico S. Matteo Foundation, Via Forlanini 14, 27100 Pavia, Italy

INTRODUCTION

Alzheimer's disease (AD) is the most common form of dementia,¹ and despite impressive efforts, so far the setup of a successful anti-AD drug discovery strategy has been extremely difficult, mainly because of the multifactorial nature of the disease.^{1,2} In the last years, numerous AD-modifying therapeutics failed clinical trials and, to date, only five drugs mainly targeting cholinesterases have been approved by United States Food and Drug Administration. Compelling evidence considers extracellular amyloid-beta ($A\beta$) deposits in the brain as one of the main AD hallmarks:^{1,3,4} they trigger microglia and astrocytes activation, which in turn results in chronic inflammation and cellular oxidative stress.^{3,5,6} All these mechanisms, together with mitochondria and neurovascular dysfunctions, are mutually involved in a feed-forward loop, ultimately leading to progressive neurodegeneration.^{1,6}

$A\beta$ protein includes natively disordered peptides, ranging from 36–43 amino acids, that are produced from the sequential metabolism of amyloid precursor protein by β - and γ -secretases;⁴ in particular, the predominant species found in plaques is the most toxic and amyloidogenic $A\beta_{1-42}$ ($A\beta_{42}$). Monomeric $A\beta_{42}$ peptide is prone to self-assembly into oligomeric species, which aggregate to form protofibrils and then mature amyloid fibrils.^{2,4} Some

well-defined A β peptide regions are involved in the aggregation process.⁷ The glycosaminoglycan (GAGs) binding site (HHQK) assists, via a α -helix intermediate, the conformational transition of monomers from normal random coil to β -sheet structure which is characterized by an increased tendency to aggregate into dimers and oligomers.⁸ The stabilization of the soluble A β monomers conformation, or the prevention of the α -to- β conformational transition, represents suitable strategies to avoid oligomers formation. The self-recognition hydrophobic core (¹⁶KLVFFA²¹), located in the central region of the A β peptide, constitutes a nucleation site that initiates the A β -A β interaction.⁹ In particular, π - π stacking involving the two Phe residues may play a significant role in the self-assembly process. The emerging π - π -hypothesis suggests that drugs able to block these interactions may effectively control the amyloid diseases.¹⁰ After this primary lag step, spherical oligomers transform into larger aggregates (nucleation phase) and an equilibrium between hydrophobic and hydrophilic interactions, involving Glu²²-Gly²⁹ residues, is thought to affect this stage.

Notably, in the last 25 years, attention has been shifted from amyloid fibrils to soluble prefibrillar A β oligomers which, unlike other amyloidoses, are found to be more toxic than mature fibrils.¹¹ A β ₄₂ oligomers bind to hippocampal neurons and hamper synaptic plasticity, manifested as inhibition of the long-term potentiation, which is involved in learning and memory.^{4,12} To date, it is not clear which particular oligomeric state is mainly involved in eliciting neurotoxic effects and by which specific mechanism. Indeed, the transient and non-covalent nature makes it difficult their identification and characterization.^{2,13,14} On the other hand, also insoluble fibril deposits are found to be neurotoxic since, being in equilibrium with oligomers, they may serve as a reservoir and catalyze oligomer formation through secondary nucleation pathways. Consequently, both oligomers and fibrils represent important targets. In this scenario, a multitarget approach based on the simultaneous inhibition of some relevant AD targets offers promises to achieve a successful therapeutic outcome.¹⁵

Curcumin (**Figure 1**), the primary bioactive compound found in the rhizome of *Curcuma longa*, has been reported to interfere with A β aggregation and to

attenuate oxidative stress and neuroinflammation.^{16–18} The 4-hydroxy,3-methoxy-phe-nyl (vanillin) rings of curcumin were shown to adopt a correct

position to establish π – π interactions with Phe¹⁹ and Phe²⁰ residues of A β ,^{19–21} as a result of the appropriate length and flexibility of the heptatrienone central linker.^{22,23} In addition, the curcumin coplanar rearrangement allows the intercalation between the A β fibrils, thus hampering the β -sheets assembly and in turn the fibrillation pathways.²⁰ Nevertheless, curcumin does not have success in clinical trials, due to its poor bioavailability and possible toxic effects, mainly ascribed to the 4-hydroxy,3-methoxy substitution pattern of the two aryl rings.^{22,24} Together with a large number of multipotent compounds such as quinones, catechols, and isothiazolones, curcumin has been included among pan-assay interfering compounds (PAINS), since they can display apparent bioactivity and/or interfere with assay readouts.^{24,25} It is not definite whether compounds containing a PAINS-related substructure behave as reactive chemicals rather than selective drugs; indeed the reactivity of a compound or other effects might be also context-dependent.²⁶ However, a number of curcumin-based compounds, when properly decorated, have been shown to exert significant biological activities,^{21,27} thus confirming the great potential of the curcumin scaffold for drug discovery. In this context, the key chemical features for an A β ligand have been identified to comprise two sterically bulky aromatic moieties, connected by a flexible linker of suitable length, to ensure their optimal spatial arrangement.²³ The resulting elongated and flat molecule demonstrated to hamper the characteristic π – π stacking interactions between the aromatic residues of A β monomers, oligomers, or filaments.^{19,20}

In order to identify multipotent AD disease-modifying drug candidates^{15,28} with an improved biological profile as compared to the reference compound curcumin, a small series of newly synthesized analogues was here tested for anti-oligomeric and antifibrillogenic activity, while toxicity was evaluated on both neuroblastoma and microglia cells. Molecular docking and steered molecular dynamics (SMD) simulations were performed in order to assess the molecular recognition of the derivatives with either monomeric or aggregated A β ₄₂ and to assess the stability of the corresponding complexes

which are responsible for the inhibitory activity. The identification of probes able to modulate A β aggregation, inflammation and oxidative stress could allow to shed light into this crosstalk and represents a crucial issue in the AD drug discovery scenario. Therefore, the most promising compounds in terms of anti-oligomeric and antifibrillogenic activity were also evaluated for their anti-inflammatory and antioxidant properties.

RESULTS AND DISCUSSION

Design and Synthesis of Curcumin Analogues

The aromatic 4-hydroxy,3-methoxy substitution patterns of curcumin (cur, **Figure 1**) were sequentially replaced with the para-3,3-dimethylallyloxy (4-prenyloxy), to obtain 1 as asymmetrical compound, bearing both vanillin and 4-prenyloxyphenyl functions, and 2 (**Figure 1**), as symmetrical counterpart in which both side rings were decorated with the 4-prenyloxy group. This moiety, found in a large number of natural products, proved to be often associated to neuroprotective effects, such as anti-inflammatory and antioxidant, among others ^{27,28}. This flexible mono-unsaturated function could also impart to the molecule an increased capability to establish hydrophobic contacts with A β monomers. Furthermore, the importance of the hepta-1,4,6-trien-3-one central linker was studied by its proper simplification into a penta-1,4-dien-3-one, obtaining the corresponding compounds 3 and 4 (**Figure 1**). Since this structural modification has been successfully introduced in the design of curcumin derivatives with increased anti-proliferative and anti-inflammatory activities ²⁹, we wondered if the same increased activity would have been observed in AD multi-target context. Indeed, the maintenance of the carbonyl α,β -unsaturated electrophile reactive centre, together with the length of the linker (6–19 Å) and its rigidity are some of the key chemical features required to effectively inhibit amyloid aggregation ²².

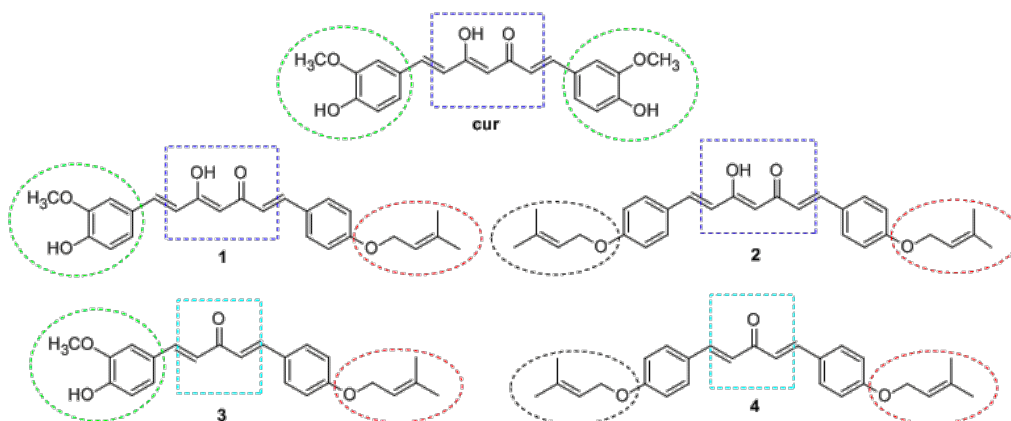
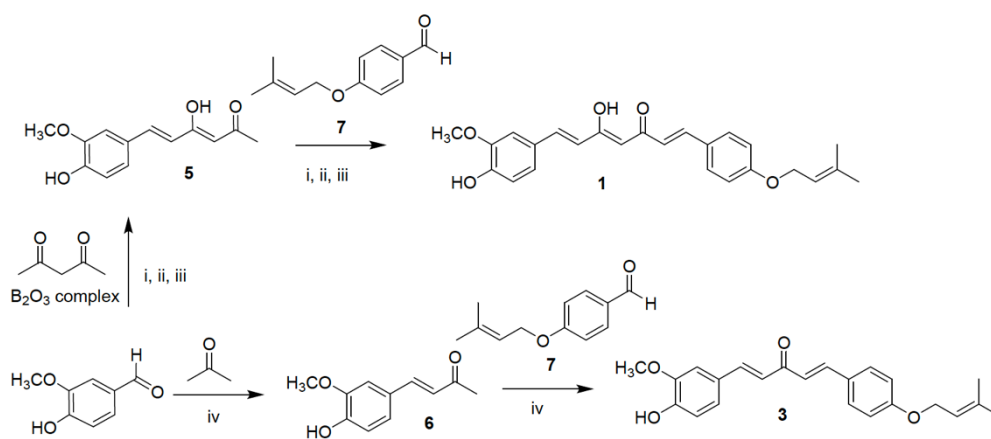


Figure 1. Design strategy toward the curcumin-based analogues 1-4. Structures of curcumin (cur), the newly synthesized curcuminoids (1, 2) and their monocarbonyl analogues (3, 4).

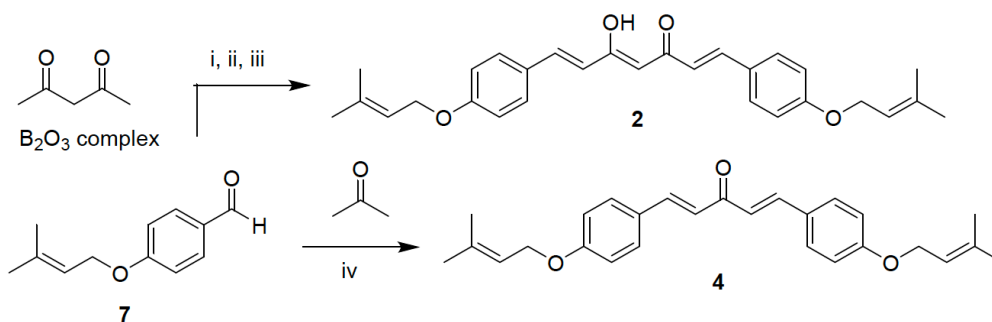
Chemistry

The synthetic route for the attainment of the target curcumin-based compounds (1-4) is outlined in **Schemes 1** and **2**. Compounds 1 and 2 were prepared by two-consecutive steps, applying the Pabon reaction^{26,30}. Analogues 3 and 4 were synthesized through base-catalyzed Claisen-Schmidt procedure. In the classical Pabon procedure pentane-2,4-dione was complexed with B_2O_3 in EtOAc to avoid the methylene-centred reactivity toward the Knoevenagel reaction and to favor the nucleophilic attack at the side methyl groups. The boric complex was then condensed with the suitable aldehyde and then a step-wise addition of n-tributylborate and n-butylamine was carried out. Acidic treatment caused the dissociation of the complex, providing the desired curcumin-based analogue. This reaction has been reported to give the curcuminoid as β -keto-enol tautomer. In the classical Claisen-Schmidt aldol condensation, acetone was reacted with the appropriate aldehyde in EtOH and in the presence of a 50% KOH/H₂O solution. In details, by condensing pentane-2,4-dione or acetone with two different selected aldehydes, namely 4-hydroxy-3-

methoxybenzaldehyde (vanillin) and 4-(3,3-dimethylallyloxy)benzaldehyde, a mixture of the desired compounds could be obtained, among which the asymmetrical and the two symmetrical curcuminoids, including the semi-reaction products. Consequently, obtaining the desired compounds in a good purity grade would require several chromatographic purifications. To avoid this drawback, the synthesis of asymmetric curcumin analogues **1** and **3** (**Scheme 1**) was performed through two sequential steps, in which the semi-synthetic intermediates were first prepared reacting pentane-2,4-dione and acetone with vanillin under the appropriate reaction condition to give **5** and **6**, respectively. Subsequently, a second reaction with 4-(3,3-dimethylallyloxy) benzaldehyde, allowed the attainment of the desired asymmetrical compounds. In order to prepare the symmetrical analogues **2** and **4** (**Scheme 2**) a one-pot procedure, by using a 1:2 stoichiometric ratio for the ketone and the benzaldehyde, was performed. The 4-(3,3-dimethylallyloxy) benzaldehyde (**7**) was obtained by exploiting a Williamson ether synthesis between 4-hydroxybenzaldehyde and 3,3-dimethylallylbromide in the presence of K_2CO_3 as base.



Scheme 1. Reagents and conditions: i) $B(n-BuO)_3$; ii) $n-BuNH_2$, 80 °C; iii) HCl , 80 °C; iv) KOH 50%. EtOH, rt.



Scheme 2. Reagents and conditions: i) $B(n-BuO)_3$; ii) $n-BuNH_2$, 80 °C; iii) HCl , 80 °C; iv) KOH 50%. EtOH, rt.

Cell toxicity of curcumin and analogues

In view of evaluating if the $A\beta_{42}$ oligomers-induced toxicity is ameliorated in presence of the newly synthesized analogues (1-4), the intrinsic toxicity was assessed on neuroblastoma (SH-SY5Y) and microglia cells by using cur as reference compound. Cells were exposed to compound concentrations ranging from 1 to 50 μM for 24 hours or from 1 to 40 μM for 16 hours, respectively. As shown in **Figure S1 a**), high concentrations (20-50 μM) of all tested compounds induced a significant loss of neuroblastoma cell viability in comparison to cells exposed to culture medium only. The di-prenoxylated derivatives 2 and 4 showed a significant and comparable profile, as toxic effects were observed at 5 μM concentration. At high concentrations (20-50 μM), 3 considerably reduced cell viability, conversely, at concentrations ranging from 1-10 μM it was found to be not toxic, alike cur and 1.

Compound 2 exerted a similar effect on microglia cell viability, showing a cytotoxic activity from 1 μM concentration. Interestingly, treatment of microglia with 1, even at 20 and 40 μM concentrations, did not significantly affect cell viability in comparison with vehicle-treated control cells, whereas the same concentrations of cur were cytotoxic (**Figure S1 b**)), confirming previously published results³¹.

Inhibition of A β ₄₂ aggregation

On the basis of the amyloid hypothesis, a variety of anti-amyloid agents have been developed over the years, with the aim of interfering either with A β peptides oligomerization or fibrillogenesis or with both events^{2,14}. Despite the efforts made, results are not yet encouraging. The assays employed in *in vitro* aggregation studies show limitations in providing simultaneous and comparable information on both fibrils and oligomers, as well as among oligomers of different size. As a consequence, it is clear that more than one technique has to be used, since a potential inhibitor of the oligomerization may not be identified by using a specific assay for fibrils¹⁴.

The evidence of fibril formation or inhibition is commonly given by well established techniques, such as transmission electron microscopy (TEM) and thioflavin T (ThT) fluorescence. Conversely, the identification and characterization of soluble A β oligomers involved in the pathological cascade are extremely challenging; indeed, to date, a specific oligomeric state to target is missing^{2,14}. In particular, the difficulties in obtaining well characterized A β oligomers in solution, as well as the dynamic equilibrium among oligomers which keep on aggregating during the *in vitro* experiments, represent important issues in the search for modulators of fibrillogenesis³².

In this context, it has been demonstrated that capillary electrophoresis (CE) can play an alternative role in the *in vitro* aggregation studies of A β peptides. Since it works in free solution and in the absence of secondary equilibria, CE allows a real snapshot of A β while assembling into soluble oligomers inside the capillary, until sample precipitation³³. The use of CE to identify agents able to interfere with A β ₄₂ oligomerization has been pioneered by us and also reported by others³⁴⁻³⁶. Furthermore, the combination of CE analysis of A β ₄₂ solutions in the presence of an anti-aggregating candidate with the TEM images of the final precipitate, provides integrated information on the anti-oligomerization and anti-fibrillogenesis activity³²⁻³⁵.

Anti-oligomeric activity. In this work, we exploited one of the analytical

platforms recently reported by us that were optimized and standardized to correlate aggregation state, structure and toxicity of A β ₄₂ oligomers separated by CE, in view of coincubation experiments³².

Before carrying out any analysis of an A β ₄₂ sample in the presence of an inhibitor of aggregation, the setup of a reproducible protocol for A β ₄₂ sample preparation and in turn of a reproducible CE separation of the prepared oligomers are mandatory prerequisites. A β ₄₂ peptide aggregates and precipitates very rapidly, therefore, to appreciate differences in oligomer formation kinetics or to detect reduction/abrogation of oligomer building-up by a coincubated compound, it is necessary to keep the assemblies in solution for a suitable time window. Moreover, the toxicity of the oligomeric populations detected and separated by CE has to be known, for identifying the target species of the small molecules evaluated.

In particular, for observing the effect of coincubated molecules, the least aggregating sample preparation protocol was selected³⁷, as it allows a wider time window if compared with other methods³⁴⁻³⁶. Since cur and compounds 1-4 are soluble in pure ethanol, an adjustment of the original A β ₄₂ sample preparation protocol was necessary (see Experimental Section), to account for the percentage of ethanol in buffer when coincubating the peptide and the compounds. The comparison of the CE profile and mobility values reported in³² with those of A β ₄₂ control (i.e. in the absence of compounds) shown in **Figure 2 a)** and **Table S1** (Supplementary material), demonstrate that the kinetics of formation of oligomers and all electrophoretic parameters are not affected by a concentration of ethanol in buffer as high as 3.26%. Therefore, precise peak identification, molecular weight range and toxicity of the separated oligomers can be considered the same. Briefly, **Figure 2 a)** shows the analysis of A β ₄₂ peptide injected in the CE system after different elapsed times from sample solubilization (t₀): monomers and dimers (peaks 1 and 2) progressively convert over time into neurotoxic aggregates larger than dodecamers (peak 3)³². At late times from solubilization, large aggregates are the most abundant species, until insoluble fibrils are formed, and no more soluble species are detected. As small oligomers are not toxic³², a compound is considered

active if it interferes with the formation of the assemblies migrating under peak 3. All coincubation studies were carried out in triplicate and electrophoretic traces were recorded for cur and all analogues, at different concentrations and at different elapsed times from sample redissolution.

Figure 2 b) shows the effect on the normalized area percentage of peak 3 in the presence of a given compound at the highest concentration tested (50 μM), at a time point where, for the control sample, the formation of toxic species is maximized (first bar). All compounds show some activity, although it is clear that the asymmetrical hepta-1,4,6-trien-3-one-based analogue 1 turns out to be the most effective of the series in suppressing the building up of toxic oligomers, followed by cur and then 2, while the 1,4-dien-3-one analogues 3 and 4 are remarkably less active. Complete information on many time points from solubilization up to precipitation is reported in **Figure S2**, to appreciate how 1, even at later times, is evidently more potent than cur.

Based on these results, experiments have been performed at 10 μM compound concentration, focusing the attention on cur, 1 and 2, both endowed with the curcuminoid scaffold. **Figure S3** (as compared to **Figure 2 b)**) shows how the activity is kept, in the same order, albeit with decreasing potency. Electropherograms in **Figures 2 c) d) and e)** easily visualize how derivative 1 (red trace) is best in suppressing the formation of large toxic oligomers (peak 3). The lower anti-aggregation activity of compound 2 (blue trace) could be partially ascribed at the lack of aromatic substituents capable of taking part in hydrogen bonding, which, conversely, are highly conserved in most amyloid ligands of natural origin²².

Complete evaluation at decreasing concentrations down to 1 μM is reported in **Figure 3**. Here the observations on the reduction of the toxic large oligomers (peak 3) can be summarized as follows: i) independently on the concentration tested, the symmetrical analogue 2 only slows down the formation of toxic oligomers, that are eventually formed as abundant as they are in the control sample; ii) both cur and 1 show concentration-dependent activity down to 1 μM (see also Figure S3); iii) at the lowest concentration and in comparison with cur, not only does 1 show a more consistent reduction

(nearly double) of the toxic oligomers at the end point of the analyses, but it also keeps their abundance constantly low over time.

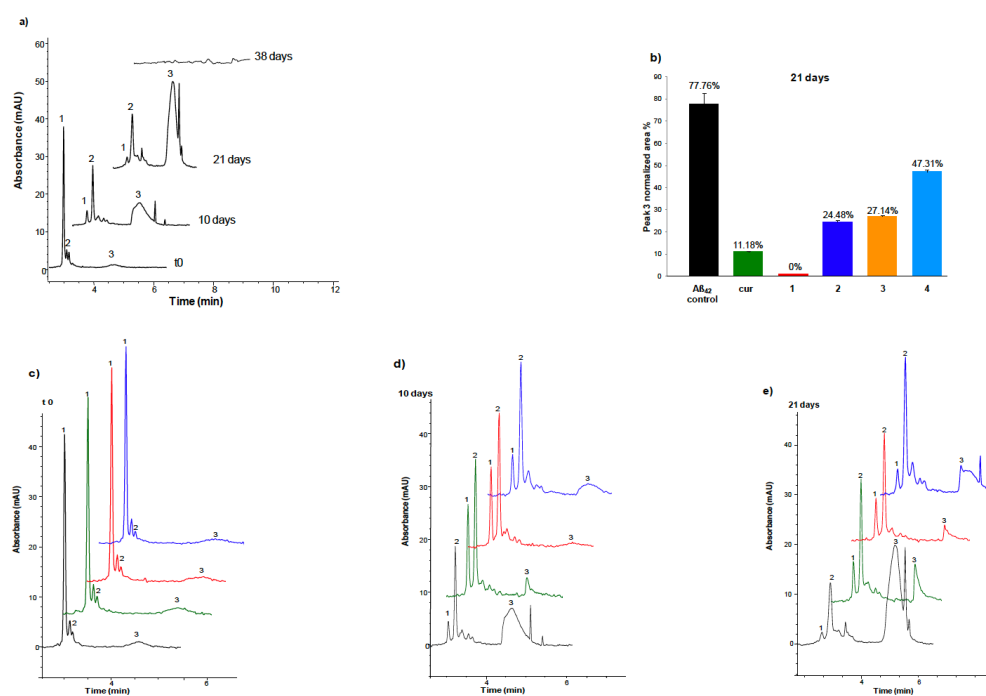


Figure 2. Oligomerization of 100 μ M A β ₄₂ in the absence or in the presence of cur and of compounds 1-4. **a)** Electrophoretic profiles of A β ₄₂ control (solubilized in 3.26% EtOH in 20 mM phosphate buffer pH 7.4, see Experimental section) at selected elapsed times from t₀ until precipitation: monitoring over time by CE. **b)** Anti-aggregation activity of 50 μ M cur and compounds 1-4: normalized area % of peak 3 at 21 days from sample redissolution as observed in control peptide and in the presence of compounds. Data are expressed as mean \pm standard deviation, for n=3. **c-e)** Comparison between electrophoretic profiles of 100 μ M A β ₄₂ control (black trace) and in the presence of 10 μ M cur (green traces), 1 (red traces) and 2 (blue traces) at different elapsed times from redissolution. Electropherograms are representative of n=3.

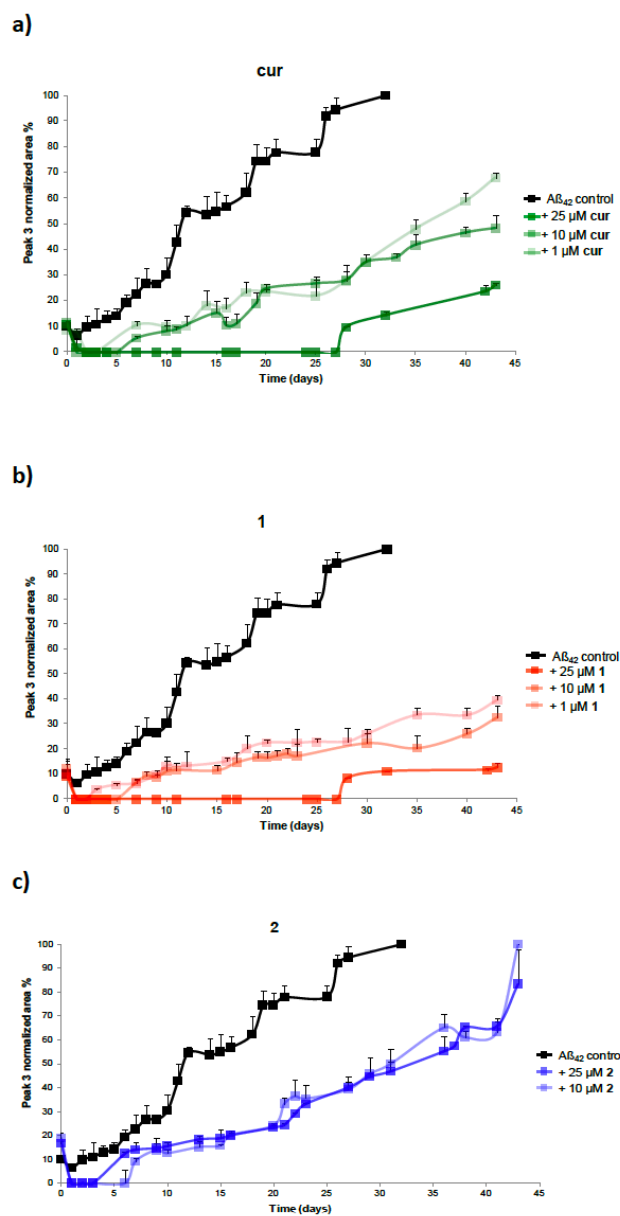


Figure 3. Anti-oligomeric effect of compounds on toxic large oligomers (peak 3) over time. Normalized area percentage plot of peak 3 of 100 μM Aβ₄₂ control and in the presence of decreasing concentrations of: **a)** cur, **b)** 1, **c)** 2. Data are expressed as mean ± standard deviation, for n=3.

Figure 2 e) also provides information on the effect that coincubation of compounds exerts on the persistence in solution of non toxic monomers and dimers (earlier migrating peaks 1 and 2). In particular, it is clear that dimers (peak 2) are always kept in solution for very long times, in comparison with A β ₄₂ control sample. This effect is consistent with the stabilization of A β dimers induced by curcumin²⁰. Notably, from **Figure S4**, where the trend of the normalized area of dimers over time is reported, it can be derived that this effect is markedly induced by cur and by its mono 4-prenyloxy-aryl substituted 1, in a concentration dependent manner.

It can be summarized that CE data are consistent with the activity expected by virtue of the progressive structural modifications performed on 1. In particular, the further substitution of the 4-hydroxy,3-methoxy group with the 4-prenyloxy (as for 2) and the simplification of the β -keto enol function (as for 3) result in a gradual decrease of the anti-oligomeric activity, that is lowest for 4, in which both modifications are combined. The order of potency observed is 1 > cur > 2 > 3 > 4.

Anti-fibrillogenic activity. Because of the intrinsic fluorescence of curcumin, ThT fluorescence assay is precluded³⁸, therefore TEM has been here employed to appreciate the effect of cur and 1-4 on fibril formation, fibril morphology and fibril density. Conclusions are drawn on data obtained for three independent samples each one measured in duplicate.

As shown in **Figure 4**, A β ₄₂ peptide alone contains fibrils already at early stages from solubilization (24 hours), although, as explained in³², these are not injected in the capillary of the CE system. Conversely to the control peptide and already after 24 hours, A β ₄₂ samples coincubated with cur or 1 contain amorphous aggregates only. The absence of amyloid fibrils is kept at later stages of oligomerization (after 21 days). This evidence can be correlated with the anti-oligomeric activity induced by both compounds relative to large oligomers (**Figure S2**, 21 days) and consistently with the persistence in solution of dimers (**Figure 2 e**).

The sample containing cur eventually precipitates into dense amyloid fibrils. This is not overly surprising, as also recent reports suggested that curcumin only inhibits oligomerization while promoting fibrillization^{39,40}; despite a growing evidence on the anti-amyloid effect of curcumin, the exact mechanism of action is still debated.

Contrary to samples coincubated with cur, only sporadic fibrils are detected in precipitated samples of A β ₄₂ in the presence of derivative 1. Surprisingly, compound 2 abrogates the formation of the fibrils observed after 24 hours, as only amorphous granular assemblies are detected at sample precipitation. In accordance with the poor anti-oligomeric activity, both monocarbonyl derivatives (3 and 4) lead to amyloid fibrils already after 24 hours and as end products of the aggregation (**Figure 4**).

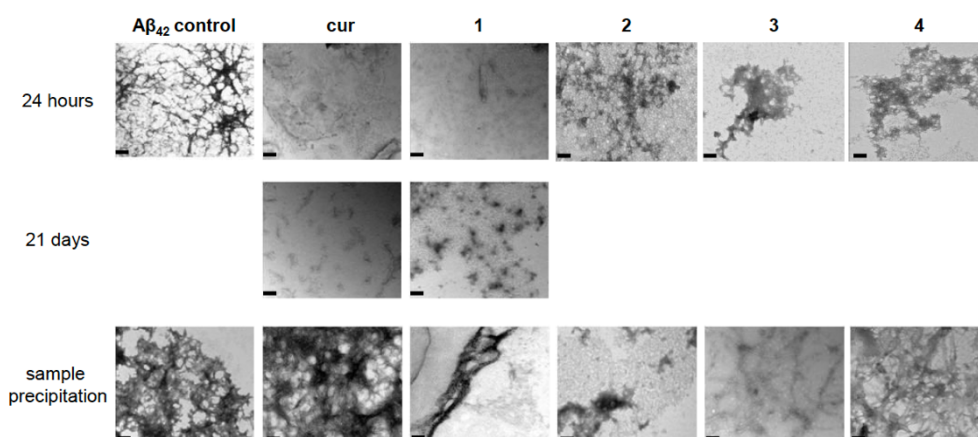


Figure 4. TEM images of A β ₄₂ control peptide (100 μ M) and 100 μ M A β ₄₂ coincubated with 50 μ M cur and 1-4 analyzed at different times from redissolution. Scale bar=100nm. 60000x. n=3.

Modeling Studies

Docking simulations were carried out to corroborate the effects of the curcumin-based analogues on A β ₄₂ aggregation process and to elucidate

by which specific interactions with A β residues the tested compounds are able to modify it. Even though the A β_{42} peptide shows a marked flexibility and can assume almost all secondary motifs, docking simulations were focused on the peptide in its alpha-helix form because this is the only available resolved structure.

Figures 5 a) b) and c) show the best complexes obtained for cur, 1 and 2 with the monomeric A β_{42} peptide. As expected, the ligands approach the amyloid region corresponding to the above mentioned ¹⁶KLVFFA²¹ sequence which is well-known to be involved in ligand recognition. In the computed complexes, the curcumin analogues assume slightly bent conformations which are in line with the curcumin geometries found in the resolved structures. For instance, the curcumin molecule included in the resolved complex with human transthyretin (PDB Id: 4PMF) shows an angle, as defined by the central carbonyl and the two aromatic rings, of 107.87 while, in the here generated complex, the same angle of cur is equal to 106.99 (see **Figure 5 a)**). Moreover, and in all considered complexes, the β -keto-enol central core elicits H-bonds with Glu²² and Ser²⁶, while a ligand phenyl ring stabilizes a clear π - π stacking contact with Phe¹⁹. The other interactions stabilized by the phenyl moieties depend on the polarity of the substituents. Thus, cur, through a side vanillin group, elicits H-bonds with Gln¹⁵ and Asn²⁷, while asymmetrical analogue 1 retains the same polar contacts and, through its prenyloxy function, adds clear hydrophobic interactions with Ile³¹. The diprenoxylated 2 loses the H-bond with Gln¹⁵ and adds apolar contacts with Val¹⁸. Both monocarbonyl analogues (3 and 4) lose the key polar interactions with Glu²² (complexes not shown). As depicted in **Figure S5**, the complexes as computed by considering more extended amyloid structures show comparable ligand poses even though the involvement of more amyloid segments increases the number of interacting residues especially concerning the hydrophobic residues.

While contacting the same well-known amyloid region, **Figure 5 d) e) and f)** show that the simulated ligands assume different poses when interacting with the fibril structures. In particular, the ligands assume rather extended geometries by which they contact six different amyloid segments. As seen

for 1, the ligands contact the same residues of all involved segments: in detail, they elicit i) extended hydrophobic contacts with six Leu¹⁸ residues which contact both phenyl ring and alkyl chains and ii) extended H-bonds with six Lys¹⁶ residues, which approach both the β -keto-enol central core and the substituents on phenyl rings. Not to mention that these protonated residues can also stabilize charge-transfer interactions with the phenyl rings. Taken together, one may observe that, while the ligands assume comparable poses in all simulated amyloid structures, the relevance of hydrophobic contacts increases when increasing the complexity of the simulated amyloid structure and finds its maximum expression with the fibril structure where the ligands are supported by a basis completely composed of apolar residues. These observations suggest that the interaction with simple amyloid structures are enhanced by a fine balance between polar and apolar contacts as seen for 1 in the monomeric protein, while the interaction with complex amyloid structures appears to be strongly governed by hydrophobic contacts.

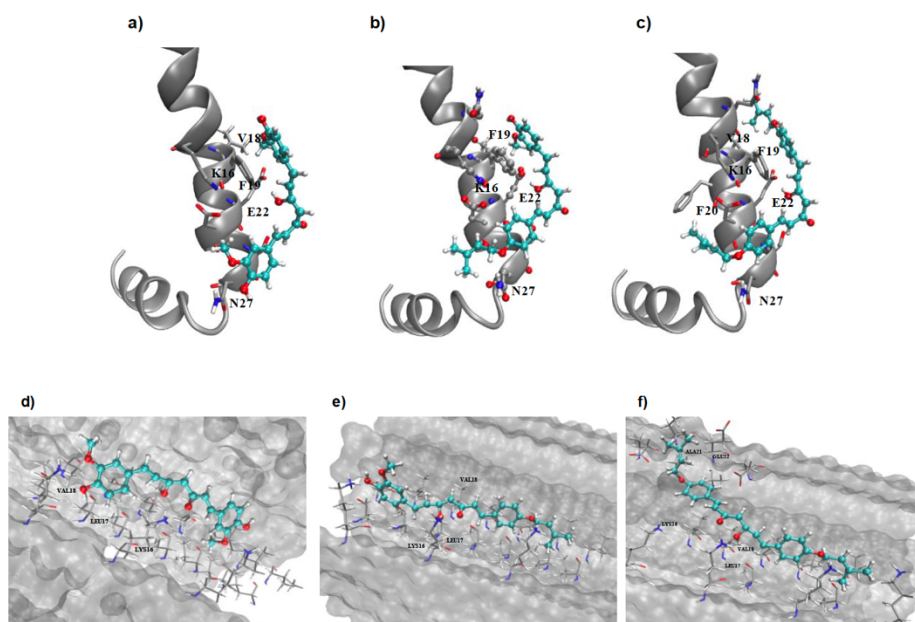


Figure 5. Main interactions stabilizing the putative complexes with monomeric A β_{42} for **a)** cur, **b)** 1 and **c)** 2, and with the amyloid fibril structure for **d)** cur, **e)** 1 and **f)** 2.

The described molecular docking results find encouraging validations by SMD simulations involving A β ₄₂ tetramers and fibrils and comparing 1 and 2 with cur. In these simulations the ligand is forced to unbind from the A β ₄₂ structures and the required pulling force is monitored during the time. As compiled in **Table S2**, each simulated ligand is thus characterized by the time required to unbind the ligand (i.e. until the monitored force is 0 pN) as well as by the force mean required for unbinding. A third relevant parameter is the AUC value of the plot limited to the residence time which accounts for both the total force and required time. With regards to A β ₄₂ tetramers, Table S2 shows that the most polar cur compound requires an initial marked force to break its key polar interactions (as reflected in the highest force mean) but then is unable to prolong its binding and indeed it shows a residence time and AUC values clearly lower than 1 and 2. These results confirm that only a proper balance between polar and hydrophobic interactions is able to increase the stability of the complex with A β ₄₂ oligomers over the time. In contrast and when simulating the fibrils, the ligands reveal rather similar values in all reported parameters. This observation may indicate that the ligands are here similarly governed by the sole hydrophobic contacts and indeed the most apolar compound (2) shows the best force mean and AUC value. All proposed compounds were submitted to SwissADME online web-server (<http://www.swissadme.ch>) and resulted completely devoid of PAINS alerts with a predicted pharmacokinetic profile roughly comparable with that of the parent compound (results not shown).

Evaluation of anti-inflammatory properties

The prenylation of aromatic natural products results in derivatives with an improved pharmacological profile when compared with not-prenylated compounds and prenylated natural compounds proved to be useful for the treatment of cancer and inflammation²⁷. As this latter represents an important pathological condition in AD^{3,4}, the functionalization of cur by the introduction of a prenyl function could enhance the anti-inflammatory potential. Thus, the most promising compound 1 in terms of anti-oligomeric

and anti-fibrillogenic activity, was selected to be tested for its anti-inflammatory properties, in comparison to cur. Lipopolysaccharide (LPS) is the major component of the outer membrane of gram-negative bacteria and a potent immune activator of a variety of mammalian cell types, including microglia. Inhibition of LPS-induced release of the proinflammatory cytokines IL-1 β and TNF- α by microglia was examined to assess the anti-inflammatory effects of analogue 1 and cur. Microglia cells were exposed to non-cytotoxic concentrations of test compounds for 1 hour and then stimulated with LPS for 16 hours to induce an inflammatory response. In unstimulated cells low or undetectable amounts of IL-1 β and TNF- α were released and these basal levels remained unchanged after treatment with the tested compounds (white bars, **Figure 6**). As expected, LPS stimulation induced an increased release of IL-1 β and TNF- α (taken as 100%). Not only was this effect significantly suppressed by cur, as we previously showed^{31,41}, but also by its prenylated analogue 1, starting from the concentration of 5 μ M.

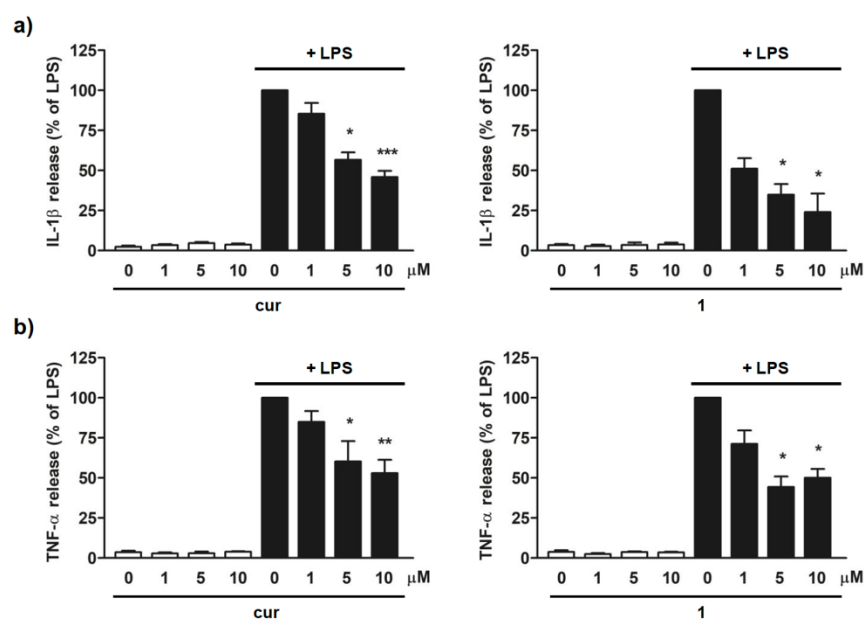


Figure 6. Effects of cur and analogue 1 on cytokine release from LPS-stimulated cortical microglia cells. **a)** IL-1 β and **b)** TNF- α release. Data are mean \pm SEM (n=3). * $p < 0.05$, ** $p < 0.01$ and *** $p < 0.001$ vs LPS stimulated cultures, Kruskal-Wallis followed by *post-hoc* Dunn's test.

Evaluation of antioxidant properties

In addition to the anti-inflammatory activity, we then investigated the potential of compounds 1 and 2 as antioxidants. We evaluated in SH-SY5Y neuroblastoma cells their scavenger ability when co-incubated with H_2O_2 , using cur as reference. In comparison to untreated cells, (grey line, **Figure 7 a**)), the intracellular DCFH-fluorescence intensity in H_2O_2 -treated cells significantly increased (black line, **Figure 7 a**)). Treatment with cur and compounds 1 and 2 reduced H_2O_2 -induced intracellular ROS production, albeit to a different extent. At any time tested, cur showed the strongest scavenger activity when compared to analogues 1 and 2. In particular, the presence of both vanillin moieties (as for cur) appears to be important for this antioxidant activity. Compound 2, lacking 4-hydroxy,3-methoxy group on both aromatic rings, was less effective than compound 1, where one of the two vanillin functions of curcumin are preserved.

Further studies were carried out on the mechanism of action of 1 and 2 on the Nrf2 cellular pathway, for investigating their ability to modulate the expression of the Nrf2 transcription factor⁴². Recent evidence further showed that Nrf2 activation suppresses inflammation through redox control⁴³. Therefore, we investigated the activation of Nrf2 pathway by analyzing its translocation into nucleus. A concentration of 5 μ M of cur and 1 induced Nrf2 nuclear translocation, whereas 2 did not show to be a Nrf2-inducer. The asymmetrical analogue 1, at the concentration of 10 μ M, did not produce statistically significant results in our experimental setting, although we could assume an increasing trend as compared to control (**Figure 7 b**)).

These data suggest that 1 may modulate antioxidant response by acting through different pathways, besides Nrf2 activation. Evidence from literature supports the ability of different natural products, including polyphenols in general, to interact with selected miRNAs, thus targeting multiple genes and showing pleiotropic activity⁴⁴. Hence, the differential Nrf2 activation by 10 μ M 1 may be putatively related to the modulation of the levels of certain miRNAs associated with the Nrf2 signaling pathway. On the basis of these observations, the investigation of miRNA modulation could potentially be

important and will be next further evaluated to better understand the underlying antioxidant mechanism of natural products and their derivatives.

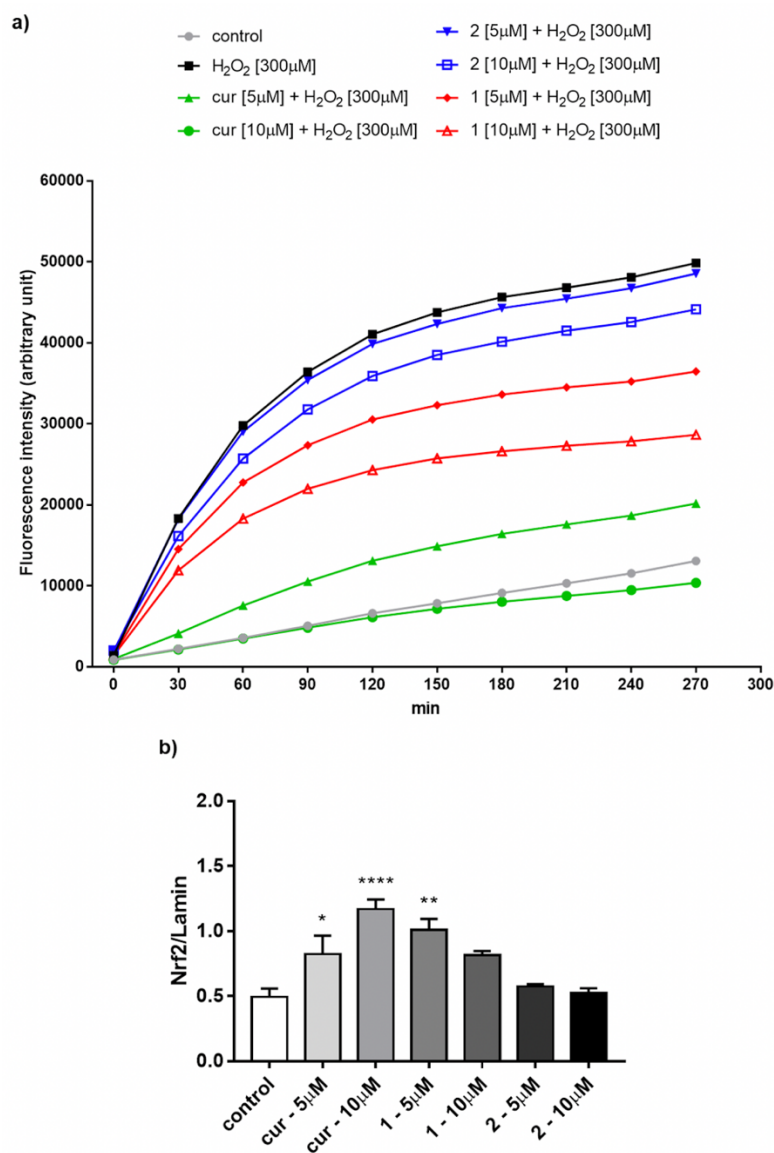


Figure 7. Antioxidant activity of cur and analogues 1 and 2. a) Reduction of H₂O₂-induced intracellular ROS production: fluorescence intensity for all compounds is significant at any time from 30 to 270 min with $p < 0.001$ vs H₂O₂, with exception of compound 2 at the concentration

of 5 μM . For compound 2 the significance is as follows: $p < 0.05$ at 90 min; $p < 0.01$ at 120 min and 270 min; $p < 0.001$ at 150, 180, 210 and 240 min. Dunnett's multiple comparison test; **b)** Activation of Nrf2 pathway: SH-SY5H cells were treated for 3 hours with compounds. Results are shown as ratio Nrf2/lamin \pm SEM; * $p < 0.05$, ** $p < 0.01$, **** $p < 0.0001$ versus control; Dunnett's multiple comparison test.

CONCLUSIONS

The curcumin scaffold was rationally modified, and a small set of structurally related compounds was obtained and tested against $\text{A}\beta_{42}$ oligomer and fibril formation, inflammation and oxidative stress, i.e. copathogenic factors related to AD. To this aim, derivatives were obtained in which i) a prenyloxy function was introduced as substituent in one or both the cur side aryl functions, and ii) the cur keto-enol central linker was simplified. Two couples of analogues 1-2, and 3-4, respectively were obtained.

The new compounds were firstly evaluated for their anti-amyloid effects, leading to identify cur and analogue 1, both endowed with the hepta-trien-3-one linker, as the most effective agents in slowing down the formation of toxic $\text{A}\beta$ oligomers. Interestingly, CE and TEM analyses showed how 1 potently inhibits oligomers building up and, contrary to cur, it does not lead to the formation of a dense network of fibrils. Due to its remarkably lower toxicity on microglia cells if compared to 2 and even to cur, analogue 1 was then selected to investigate its anti-inflammatory effect on microglia activation. In particular, at 5 μM concentration, a suppression of pro-inflammatory cytokines release was detected. This analogue also showed an antioxidant potential, with particular reference to the capability to induce, at 5 μM , Nrf2 nuclear translocation. By contrast, the symmetrical curcuminoid 2, in comparison to 1, showed a remarkably weaker antioxidant activity and a lower efficacy in contrasting oligomer formation. Notably, fibrils were not observed in presence of compound 2 and this suggests that the two prenyloxy substituents may serve as β -sheet breakers by intercalating in the amyloid fibrillar core. The anti-amyloid effects of 1 and 2, compared to those of cur, were evidently corroborated by molecular docking and SMD

simulations which revealed the growing role of the hydrophobic interactions when simulating A β structures of increasing complexity. The simplified counterparts 3 and 4 failed to block both the formation of large A β assemblies and the deposition of fibrils.

Taken together, these data underlined the pivotal role of the curcumin scaffold in eliciting anti-amyloidogenic effects, in particular when both the 4-hydroxy,3-methoxy and prenyloxy aryl substitution patterns are present. Indeed, among the newly synthesized compounds, 1 turned out to be a very promising anti-AD tool, endowed with a better biological profile with respect to cur. Due to its multipotent behaviour it could be a lead compound, worthy further optimization to obtain effective AD-modifying drug candidates.

METHODS

Chemicals and Materials

Synthetic A β_{42} was purchased from Bachem (Bubendorf, Switzerland) as lyophilized powder and stored at -20°C. 1,1,1,3,3,3-Hexafluoropropan-2-ol (HFIP), acetonitrile (ACN), dimethylsulfoxide (DMSO) and sodium carbonate (Na₂CO₃) were from Sigma-Aldrich (St. Louis, MO, USA). Ethanol 96° was supplied by Carlo Erba (Cornaredo, Italy). Sodium hydroxide (NaOH) and sodium dodecyl sulphate (SDS) were provided by Merck (Darmstadt, Germany). Na₂HPO₄ and NaH₂PO₄, supplied by Sigma-Aldrich, were used for the preparation of the background electrolyte (BGE) in the CE analyses. BGE solutions were prepared daily using Millipore Direct-Q™ deionized water (Bedford, MA, USA) and filtered on 0.45 μ m Sartorius membrane filters (Göttingen, Germany). Uncoated fused-silica capillary was from Polymicro Technologies (Phoenix, AZ, USA). All cell culture reagents, culture medium and chemicals were purchased from Sigma-Aldrich. Curcumin was purchased from Sigma Aldrich (analytical standard, purity \geq 98%). All samples containing curcumin and curcumin-derivatives were kept protected from light throughout all experiments.

Chemistry

General Procedures. Starting materials, unless otherwise specified in the Experimental Section, were used as high-grade commercial products. Solvents were of analytical grade. Melting points were determined in open glass capillaries, using a Büchi apparatus and are uncorrected. $^1\text{H-NMR}$ and $^{13}\text{C-NMR}$ spectra were recorded on Varian INOVA spectrometer operating at 400 MHz. Chemical shifts are reported as parts per million (ppm δ value). Standard abbreviations indicating spin multiplicities are given as follows: s (singlet), d (doublet), dd (doublet of doublet), t (triplet), br (broad), q (quartet) or m (multiplet). High-resolution mass spectra (HRMS) were acquired with an LTQ Orbitrap XL instrument (Thermo Fisher Scientific, Rodano, Milano). Resolution was set at 30000 (FWHM at 400 m/z) and scan range was 250-1000 m/z with a target of 5×10^5 ions per scan. Instrument control and data analysis/elaboration were provided by the software Xcalibur (version 2.07, ThermoFisher Scientific, Rodano, MI, Italy). Chromatographic separations were performed on silica gel columns using the flash method (Kieselgel 40, 0.040-0.063 mm, Merck). Reactions were followed by thin layer chromatography (TLC) on precoated silica gel plates (Merck Silica Gel 60 F254) and then visualized with a UV lamp. Purities of all tested compounds used in the biological assays were determined by HPLC using the area percentage method on the UV trace recorded at 254 nm. The analyses were performed under reversed-phase conditions on a Phenomenex Luna 5 μm C 18 column (150 \times 4.60 mm), by using a ternary mixture of 0.1% $\text{H}_3\text{PO}_4/\text{MeCN}/\text{MeOH}$ (40:40:20, v/v) as mobile phase, flow rate: 0.7 mL / min. A liquid chromatograph PU-1587 UV model equipped with a 20 μL loop valve (Jasco Europe, Italy) was employed. All compounds were found to have >95% purity, as confirmed by NMR spectra (see Supplementary material). Compounds were named using Chem-BioDraw Ultra 14.0 IUPAC name algorithm developed by CambridgeSoft Corporation.

4-(3,3-dimethylallyloxy) benzaldehyde (7). 4-hydroxybenzaldehyde (1.00 g, 8.19 mmol) and 3,3-dimethylallyl bromide (1.14 mL, 9.83 mmol) were allowed to react according to the general procedure of the Williamson reaction for 8 h to give the crude product that was purified by crystallization from PE; yellow

oil, 83 % yield. $^1\text{H-NMR}$ (400 MHz, CDCl_3): δ 1.76 (s, 3H, CH_3), 1.81 (s, 3H, CH_3), 4.60 (d, 2H, $J = 6.8$ Hz, OCH_2), 5.45 (t, 1H, $J = 6.8$ Hz, $\text{CH}=\text{}$), 7.00 (d, 2H, $J = 8.8$ Hz, H-3' and H-5'), 7.83 (d, 2H, $J = 8.8$ Hz, H-2' and H-6'), 9.88 (s, 1H, CHO).

Pabon reaction: general procedure for the synthesis of compounds 1, 2, and 5. To a stirred solution of pentane-2,4-dione (1.00 mmol) in EtOAc (1.0 mL), B_2O_3 (1.0 molar equiv) was added, and the suspension was stirred for 30 min at 80 °C before addition of a solution of the appropriate aldehyde/s, (0.9 molar equiv for monoaryl or 1.8 molar equiv for bi-aryl curcumin derivatives), tri-*n*-butyl borate (2.0 molar equiv for monoaryl or 4.0 molar equiv for bi-aryl curcumin derivatives), in EtOAc (0.5 mL). The reaction mixture was stirred at 80 °C for 30 min, then a solution of *n*-butylamine (0.4 molar equiv in 1.0 mL of EtOAc) was added over a period of 15 min. The mixture was heated to 80 °C for 8 h and then, after cooling to r.t., it was acidified with 0.5 N HCl (30 mL) and then stirred at 80 °C for 30 min. The organic phase was separated, and the aqueous layer was extracted with EtOAc (3 x 10 mL). The combined organic layers were sequentially washed with saturated aqueous NaHCO_3 and brine, dried over Na_2SO_4 , filtered, and concentrated under reduced pressure. The crude residue was purified by flash column chromatography using a mixture of petroleum ether/ethyl acetate (PE/EtOAc) as eluent, followed by crystallization from suitable solvent.

3Z,5E-4-hydroxy-6-(4-hydroxy-3-methoxyphenyl)hexa-3,5-dien-2-one (5) ²⁶. Reaction of pentane-2,4-dione (0.50 g, 5.00 mmol), B_2O_3 (0.45 g, 5.00 mmol), and vanillin (0.69 g, 4.5 mmol), in EtOAc (7.5 mL), gave a crude product that was purified by flash chromatography (PE / EtOAc, 9.75:0.25), yellow powder, 55% yield, mp 144-146 °C (EtOH). $^1\text{H NMR}$ (400 MHz, CDCl_3): δ 2.16 (s, 3H, CH_3), 3.94 (s, 3H, OCH_3), 5.40 (br, 1H, OH), 5.63 (s, 1H, keto-enol-CH), 6.33 (d, $J = 16.0$ Hz, 1H, $\text{CH}=\text{CH}$), 6.92 (d, $J = 8.0$ Hz, 1H, H-5), 7.02 (d, $J = 1.8$ Hz, 1H, H-2), 7.09 (dd, $J = 1.8, 8.0$ Hz, 1H, H-6), 7.53 (d, $J = 16.0$ Hz, 1H, $\text{CH}=\text{CH}$).

(1E,4Z,6E)-5-hydroxy-7-(4-hydroxy-3-methoxyphenyl)-1-(4-((3-methylbut-2-en-1-yl)oxy)phenyl)hepta-1,4,6-trien-3-one (1). Reaction of intermediate 5 (0.23 g, 1.00 mmol) and 7 (0.17 g, 0.9 mmol) gave a crude product that was purified by flash chromatography (PE/EtOAc, 8.5:1.5) and further

crystallization from EtOH affording 1 as orange solid, 41 % yield, mp 144-146 °C. ¹H-NMR (CDCl₃): δ 1.77 (s, 3H, CH₃), 1.82 (s, 3H, CH₃), 3.96 (s, 3H, OCH₃), 4.56 (d, J = 6.8 Hz, 2H, OCH₂), 5.50 (t, J = 6.8 Hz, 1H, CH=C), 5.80 (s, 1H, keto-enol-CH), 5.85 (br s, 1H, OH), 6.49 (d, J = 15.6 Hz, 1H, CH=CH), 6.50 (d, J = 15.6 Hz, 1H, CH=CH), 6.94 (d, J = 8.0 Hz, 2H, H-3' and H-5'), 6.95 (d, J = 8.0 Hz, 1H, H-5), 7.07 (s, 1H, H-2), 7.13 (d, J = 8.0 Hz, 1H, H-6), 7.51 (d, J = 8.8 Hz, 2H, H-2' and H-6'), 7.60 (d, J = 15.6 Hz, 1H, CH=CH), 7.63 (d, J = 15.6 Hz, 1H, CH=CH). ¹³C-NMR (CDCl₃): δ 18.4, 26.0, 56.1, 65.1, 101.4, 109.7, 115.0, 115.2 (2C), 119.4, 122.0, 121.9, 123.1, 127.8, 127.9, 129.9 (2C), 138.9, 140.4, 140.6, 146.9, 148.0, 160.8, 183.4, 183.5. HRMS (ESI) calcd. for C₂₅H₂₇O₅ ¹⁴⁺ 407.18530; found 407.18533 (Δ = 0.1 ppm).

(1*E*,4*Z*,6*E*)-5-hydroxy-1,7-bis(4-((3-methylbut-2-en-1-yl)oxy)phenyl)hepta-1,4,6-trien-3-one (2). Reaction of pentane-2,4-dione (0.15 mL, 1.46 mmol) and 7 (0.5 g, 2.63 mmol) gave the crude product that was purified by flash chromatography (PE/EtOAc, 9.75:0.25) and further crystallization from EtOH, affording 2 as yellow solid, 45 % yield, mp 165-167 °C. ¹H-NMR (400 MHz, CDCl₃): δ 1.76 (s, 6H, CH₃), 1.81 (s, 6H, CH₃), 4.56 (d, J = 6.8 Hz, 4H, OCH₂), 5.50 (t, J = 6.8 Hz, 2H, CH=C), 5.78 (s, 1H, keto-enol-CH), 6.51 (d, J = 15.6 Hz, 2H, CH=CH), 6.93 (d, J = 8.4 Hz, 4H, H-3' and H-5'), 7.51 (d, J = 8.4 Hz, 4H, H-2' and H-6'), 7.63 (d, J = 15.6 Hz, 2H, CH=CH). ¹³C-NMR (100 MHz, CDCl₃): δ 18.4 (2C), 26.0 (2C), 65.1 (2C), 101.5, 115.2 (4C), 119.4 (2C), 121.9 (2C), 127.9 (2C), 129.9 (4C), 138.8 (2C), 140.3 (2), 160.8 (2C), 183.5 (2C). HRMS (ESI) calcd. for C₂₉H₃₃O₄ ¹⁴⁺ 445.23734; found 445.23553 (Δ = -1.6 ppm).

Claisen-Schmidt Reaction: general procedure for the synthesis of compounds 3, 4, and 6. To a solution of ketone (1.0 mmol) and the selected aldehyde (1.1 mmol or 2.2 mmol) in EtOH (10 mL), a KOH aqueous solution (50% p/v, 1 mL) was added dropwise. The reaction mixture was stirred overnight at room temperature, then diluted with H₂O and acidified with aqueous 6N HCl. The separated solid was collected by vacuum filtration and purified by flash chromatography or by crystallization.

(*E*)-4-(4-hydroxy-3-methoxyphenyl)but-3-en-2-one (6). Reaction of propan-2-one (0.25 g, 5.00 mmol), vanillin (0.98 g, 5.5 mmol), in EtOH (5.0 mL), gave a

crude product that was purified by crystallization from EtOH to give **6** as white solid, 75% yield, mp 95-98 °C. ¹H NMR (400 MHz, CDCl₃): δ 2.37 (s, 3H, CH₃), 3.94 (s, 3H, OCH₃), 5.99 (br, 1H, OH), 6.59 (d, J = 16.0 Hz, 1H, CH=CH), 6.94 (d, J = 8.4 Hz, 1H, H-6), 7.06 (d, J = 2.0 Hz, 1H, H-2), 7.09 (dd, J = 2.0, 8.4 Hz, 1H, H-5), 7.46 (d, J = 16.0 Hz, 1H, CH=CH).

(1*E*,4*E*)-1-(4-hydroxy-3-methoxyphenyl)-5-(4-((3-methylbut-2-en-1-yl)oxy)phenyl)penta-1,4-dien-3-one (**3**). Reaction of intermediate **6** (0.19 g, 1.00 mmol) and **7** (0.21 g, 1.1 mmol), gave the crude product that was purified by flash chromatography (PE/EtOAc, 7:3) and further crystallization from EtOH, affording **3** as pale orange solid 85% yield, mp 101-113 °C. ¹H NMR (400 MHz, CDCl₃): δ 1.77 (s, 3H, CH₃), 1.82 (s, 3H, CH₃), 3.96 (s, 3H, OCH₃), 4.56 (d, J = 6.8 Hz, 2H, OCH₂), 5.50 (t, J = 6.8 Hz, 1H, CH=C), 5.97 (br, 1H, OH), 6.91-7.00 (m, 5H, CH=CH, H-5, H-3', H-5'), 7.12 (d, J = 1.6 Hz, 1H, H-2), 7.18 (dd, J = 2.0, 8.4 Hz, 1H, H-6), 7.57 (d, J = 8.8 Hz, 2H, H-2' and H-6'), 7.67 (d, J = 15.2 Hz, 1H, CH=CH), 7.71 (d, J = 15.2 Hz, 1H, CH=CH). ¹³C NMR (100 MHz, CDCl₃): δ 18.4, 26.0, 56.1, 65.1, 109.9, 115.0, 115.2 (2C), 119.3, 123.2, 123.5, 123.8, 127.6, 130.2 (2C), 138.9, 142.9, 143.2, 147.0, 148.3, 161.1, 189.0. HRMS (ESI) calcd. for C₂₃H₂₅O₄¹⁴⁺ 365.17474; found 365.17471 (Δ = -0.1 ppm).

(1*E*,4*E*)-1,5-bis(4-((3-methylbut-2-en-1-yl)oxy)phenyl)penta-1,4-dien-3-one (**4**)⁴⁵. Reaction of propan-2-one (0.25 g, 5.00 mmol), vanillin (1.95 g, 11.0 mmol), in EtOH (5.0 mL), gave a crude product that was purified by crystallization from EtOH to give **4** as yellow solid, 87% yield, mp 74-76 °C. ¹H NMR (400 MHz, CDCl₃): δ 1.77 (s, 6H, CH₃), 1.82 (s, 6H, CH₃), 4.56 (d, J = 6.8 Hz, 4H, OCH₂), 5.50 (t, J = 6.8 Hz, 2H, CH=C), 6.94-6.98 (m, 6H, CH=CH, H-3, H-5), 7.56 (d, J = 8.8 Hz, 4H, H-2 and H-6), 7.70 (d, J = 16.0 Hz, 2H, CH=). ¹³C NMR (CDCl₃): δ 18.3 (2C), 25.9 (2C), 65.0 (2C), 115.2 (4C), 119.3 (2C), 123.5 (2C), 127.6 (2C), 130.1 (4C), 138.8 (2C), 142.8 (2C), 161.0 (2C), 189.0. HRMS (ESI) calcd. for C₂₇H₃₁O₃¹⁴⁺ 403.22677; found 403.22675 (Δ = 0.0 ppm).

Capillary electrophoresis

Aβ₄₂ peptide was solubilized by following the procedure described in ³⁷. Briefly, lyophilized Aβ₄₂ was dissolved in HFIP and then the solvent was left to

evaporate after an appropriate incubation time. The A β ₄₂ aliquots were redissolved in a basic mixture (ACN/300 μ M Na₂CO₃/250 mM NaOH, 48.3:48.3:3.4, v/v/v) to obtain 500 μ M A β ₄₂. This solution was then diluted to the operative concentration (100 μ M A β ₄₂ control peptide) with 20 mM phosphate buffer pH=7.4, with or without small molecules. Stock solutions of cur and of curcumin-based analogues (1.53 mM) were prepared in pure ethanol. For co-incubation studies, 500 μ M A β ₄₂ peptide (in the basic mixture) was resuspended in an appropriately diluted compound solution, so as to keep the peptide concentration at 100 μ M and obtain different peptide/compound ratios: 1:100, 1:10, 1:4, 1:2 for cur and 1; 1:10, 1:4, 1:2 for 2 and 1:2 for 3 and 4. The final percentage of ethanol was equal or lower than 3.26%. The aggregation process of A β ₄₂ in the presence or not of cur and of curcumin-based analogues was monitored by an Agilent Technologies 3D CE system with built-in diode-array detector (Waldbronn, Germany), following the analytical method reported in ³². For the separation, a fused silica capillary (Polymicro Technologies, Phoenix, AZ, USA) of 33 cm (24.5 cm, effective length) was employed. The background electrolyte (BGE, 80 mM Na₂HPO₄/NaH₂PO₄ (pH 7.4)) was prepared daily and filtered on 0.45 μ m membrane filters. The injection of the samples was carried out by applying a pressure of 30 mbar for 3 s. The capillary was thermostatted with circulating air at 25°C and separations were carried out at 12 kV (operative current: 75–78 μ A) with the anode at the sample injection end. The acquisition wavelength was 200 nm. Oligomeric species were identified on the basis of effective mobilities (μ_{eff}), which are calculated by subtracting the contribute of the electrosmotic flow (μ_{EOF}) from the apparent mobility (μ_{app}). Electrosmotic flow is measured as a perturbation of the baseline due to the sample solvent mixture. Semiquantitative analyses were performed based on the normalized area % ³².

Transmission Electron Microscopy

Amyloid fibril identification was carried out by using a JEOL JEM 1400-Plus electron microscope (Peabody, MA, USA) operating at 80 kV. When no more peaks are detected by CE, precipitated samples were prepared as follows: A β ₄₂ sample suspensions with or without cur and analogues 1-4 were diluted

at 10 μ M with 20 mM $\text{Na}_2\text{HPO}_4/\text{NaH}_2\text{PO}_4$ and then 10 μ L of diluted suspensions were left to sediment on carbon-coated Formvar nickel grids (200 mesh) (Electron Microscopy Sciences, Washington, PA, USA). After 15 minutes the excess of sample was drained off by means of a filter paper. The negative staining was performed with 10 μ L of 2%w/v uranyl acetate solution (Electron Microscopy Sciences).

Docking studies

In order to rationalize the different activity of curcumin and the here proposed derivatives, molecular docking simulations were performed involving the resolved $\text{A}\beta_{42}$ peptide (PDB Id:1IYT), which was simulated in its monomeric, dimeric and tetrameric forms. Calculations also included the resolved amyloid fibril (PDB Id: 2MXU). The ligands were simulated in their keto-enolic form and their conformational space was explored by combining MonteCarlo simulations and PM7-based semi-empirical minimizations as previously described⁴⁶. In detail, the amyloid monomer was minimized by keeping fixed the backbone atoms to preserve the resolved folding and utilized to build the corresponding dimer by following the computational procedure as described by Rao and co-workers⁴⁷. Briefly, two optimized monomers were initially aligned at an average distance between the backbone atoms of the two monomers of about 10 Å and then the monomers were progressively approached and optimized to reach a final average distance of about 5 Å. The resolved fibril structure underwent the same refinement protocol as described for monomer before docking simulations. Thus, SMD simulations involved $\text{A}\beta_{42}$ in its monomeric, dimeric and fibril forms and were performed by using PLANTS and by including the entire amyloid structure in its searches⁴⁸. For each simulated ligand, 20 poses were generated and ranked by ChemPLP score with a speed equal to 1. All obtained poses were then minimized. The best dimeric complexes were finally utilized to generate the corresponding tetramers by docking on them a second dimer structure. Such a dimer-dimer docking was performed using PatchDock by adopting its default parameters and the so generated 20 docking results were finally refined by FireDock⁴⁹. The so produced best tetrameric complexes were finally minimized by keeping fixed the backbone atoms. The computed

tetrameric and fibril complexes for 1, 2 and cur were then neutralized and inserted into an 80 Å side box of water. After a preliminary minimization, the systems underwent 3 ns SMD simulations with the same characteristics as described in ⁵⁰.

Inhibition of cytokines release

All animal-related procedures complied with the ARRIVE guidelines and were performed in accordance with EU guidelines for the care and use of laboratory animals and those of the Italian Ministry of Health (D.Lg. 26/2014) and were approved by the Institutional Review Board for Animal Research (Organismo Preposto al Benessere Animale, OPBA) of the University of Padua and by the Italian Ministry of Health (Protocol number 958/2016-PR). One-day old Sprague-Dawley rat pups (CD strain) were rapidly decapitated, minimizing suffering, discomfort or stress. Primary microglia cells were isolated from mixed glial cell cultures prepared from cerebral cortex, as previously described ⁵¹. Briefly, upon reaching confluence (7-10 days after isolation) microglia adhering to the astroglial monolayer were dislodged by shaking (200 r.p.m. for 1 h at 37°C), resuspended in high-glucose Dulbecco's Modified Eagle's Medium (DMEM) supplemented with 2 mM L-glutamine, 10% heat-inactivated fetal bovine serum (FBS), 100 U/mL penicillin, 100 µg/mL streptomycin and 50 µg/mL gentamicin and plated on uncoated plastic wells at a density of 1.25×10^5 cells/cm². Cells were allowed to adhere for 45 min and then washed to remove non-adhering cells. After a 24 h incubation period, the medium was replaced with serum-free medium containing the agents under study. Purity of the cultures was confirmed by immunocytochemistry using a primary polyclonal antibody against ionized calcium binding adaptor molecule 1 (Iba1, 1:800, Wako Chemicals USA Inc., Richmond, VA, USA). Ninety-seven per cent of the cells were Iba1 immunopositive. Cells were maintained at 37°C in a humidified atmosphere containing 5% CO₂/95% air.

Microglia were pre-treated for 1 hour with non-cytotoxic concentrations of cur and 1 and then stimulated with 100 ng/mL Ultra-Pure LPS-EB for an additional 16 hours. At the end of incubation, culture medium was collected and the

levels of IL-1 β and TNF- α released by microglia were assayed using a commercially available ELISA kits (Antigenix America, Huntington Station, NY, USA), according to the manufacturer's instructions. Cytokine concentrations (pg/mL) in the medium were determined by reference to standard curves obtained with known amounts of IL-1 β and TNF- α and the results expressed as percentage relative to LPS-stimulated cultures. Data were analyzed using GraphPad software, version 3.03 (GraphPad Software, Inc., La Jolla, CA, USA) and expressed as mean \pm SEM of at least 3 independent experiments. As raw values varied between experiments and the variability could obscure the treatment effect, data were expressed as percentage LPS treatment, taken as baseline of each independent experiment. Data were analyzed by means of Kruskal-Wallis one-way analysis of variance followed by *post-hoc* Dunn's test for multiple comparisons vs LPS treatment. Significance level was set at $p < 0.05$. Additional details are provided in the figure legends, where appropriate.

Measurement of intracellular ROS

The fluorescent probe 2,7-dichlorodihydrofluorescein diacetate (DCFH-DA) (Merck KGaA, Darmstadt, Germany) was used as a specific marker for quantitative intracellular ROS formation. Cells (2×10^4 cells per well) were loaded with 25 μ M DCFH-DA for 45 min. After centrifugation DCFH-DA was removed and cells were exposed to 5 and 10 μ M of cur, compounds 1 and 2 and 300 μ M H₂O₂. ROS levels were determined from 0 to 270 min using Synergy HT multidetection microplate reader (BioTek) with excitation and emission wavelengths of 485 and 530 nm, respectively.

Immunodetection of Nrf2

The expression of Nrf2 in nuclear cell lysates was assessed using Western blot analysis. Cell monolayers were washed twice with ice-cold PBS, harvested and subsequently homogenized 15 times using a glass-glass dounce homogenizer in ice-cold fractionation buffer (20 mM Tris/HCl pH 7.4, 2 mM EDTA, 0.5 mM EGTA, 0.32 M sucrose, 50 mM β -mercaptoethanol). The homogenate was centrifuged at $300 \times g$ for 5 min to obtain the nuclear

fraction. An aliquot of the nuclear extract was used for protein quantification, whereas the remaining extract was prepared for Western blot by mixing the nuclear cell lysate with 2X sample buffer (125 mM Tris-HCl pH 6.8, 4% SDS, 20% glycerol, 6% β -mercaptoethanol, 0.1% bromophenol blue) and then denaturing at 95°C for 5 min. Equivalent amounts of nuclear extracted proteins were loaded into a SDS-PAGE gel, electrophoresed under reducing conditions, transferred to a PVDF membrane (Merck KGaA, Darmstadt Germany) and then blocked for 1 hour with 5% w/v BSA in Trisbuffered saline containing 0.1% Tween 20 (TBS-T). Membranes were immunoblotted with rabbit antihuman Nrf2 (1:2000) diluted in 5% w/v BSA in TBS-T. Detection was carried out by incubation with horseradish peroxidase conjugated goat anti-rabbit IgG (1:5000 dilution in 5% w/v BSA in TBS-T) for 1 hour at room temperature. Membranes were then washed three times with TBS-T and proteins of interest were visualized using an enhanced chemiluminescent reagent (Pierce, Rockford, IL, USA). Lamin A/C was performed as a control for gel loading.

SUPPLEMENTARY MATERIAL

The Supporting Information is available free of charge on the ACS Publications website at DOI: 10.1021/acschemneuro.8b00463.

REFERENCES

- (1) Winblad, B., Amouyel, P., Andrieu, S., Ballard, C., Brayne, C., Brodaty, H., Cedazo-Minguez, A., Dubois, B., Edvardsson, D., Feldman, H., Fratiglioni, L., Frisoni, G. B., Gauthier, S., Georges, J., Graff, C., Iqbal, K., Jessen, F., Johansson, G., Jonsson, L., Kivipelto, M., Knapp, M., Mangialasche, F., Melis, R., Nordberg, A., Rikkert, M. O., Qiu, C., Sakmar, T. P., Scheltens, P., Schneider, L. S., Sperling, R., Tjernberg, L. O., Waldemar, G., Wimo, A., and Zetterberg, H. (2016) Defeating Alzheimer's disease and other dementias: a priority for European science and society. *Lancet Neurol* 15, 455-532.
- (2) Chiti, F., and Dobson, C. M. (2017) Protein Misfolding, Amyloid Formation, and Human Disease: A Summary of Progress Over the Last Decade, *Annu Rev Biochem* 86, 35.1-35.42.

-
- (3) Calsolaro, V., and Edison, P. (2016) Neuroinflammation in Alzheimer's disease: Current evidence and future directions. *Alzheimers Dement* 12, 719-732.
 - (4) Querfurth, H. W., and LaFerla, F. M. (2010) Alzheimer's disease, *N Engl J Med* 362, 329-344.
 - (5) Younkin, S. G. (1995) Evidence that A beta 42 is the real culprit in Alzheimer's disease, *Ann Neurol* 37, 287-288.
 - (6) Da Mesquita, S., Ferreira, A. C., Sousa, J. C., Correia-Neves, M., Sousa, N., and Marques, F. (2016) Insights on the pathophysiology of Alzheimer's disease: The crosstalk between amyloid pathology, neuroinflammation and the peripheral immune system, *Neurosci Biobehav Rev* 68, 547-562.
 - (7) Maji, S. K., Ogorzalek Loo, R. R., Inayathullah, M., Spring, S. M., Vollers, S. S., Condrón, M. M., Bitan, G., Loo, J. A., and Teplow, D. B. (2009) Amino acid position-specific contributions to amyloid beta-protein oligomerization, *J Biol Chem* 284, 23580-23591.
 - (8) Liao, M. Q., Tzeng, Y. J., Chang, L. Y., Huang, H. B., Lin, T. H., Chyan, C. L., and Chen, Y. C. (2007) The correlation between neurotoxicity, aggregative ability and secondary structure studied by sequence truncated Aβ peptides. *FEBS Lett* 581, 1161-1165.
 - (9) Tjernberg, L. O., Lilliehook, C., Callaway, D. J., Naslund, J., Hahne, S., Thyberg, J., Terenius, L., and Nordstedt, C. (1997) Controlling amyloid beta-peptide fibril formation with protease-stable ligands, *J Biol Chem* 272, 12601-12605.
 - (10) Belluti, F., Rampa, A., Gobbi, S., and Bisi, A. (2013) Small-molecule inhibitors/modulators of amyloid-beta peptide aggregation and toxicity for the treatment of Alzheimer's disease: a patent review (2010 - 2012), *Expert Opin Ther Pat* 23, 581-596.
 - (11) Cleary, J. P., Walsh, D. M., Hofmeister, J. J., Shankar, G. M., Kuskowski, M. A., Selkoe, D. J., and Ashe, K. H. (2005) Natural oligomers of the amyloid-beta protein specifically disrupt cognitive function. *Nat Neurosci* 8, 79-84.
 - (12) Walsh, D. M., Klyubin, I., Fadeeva, J. V., Cullen, W. K., Anwyl, R., Wolfe, M. S., Rowan, M. J., and Selkoe, D. J. (2002) Naturally secreted oligomers of amyloid beta protein potently inhibit hippocampal long-term potentiation *in vivo*, *Nature* 416, 535-539.
 - (13) Benilova, I., Karran, E., and De Strooper, B. (2012) The toxic Aβ oligomer and Alzheimer's disease: an emperor in need of clothes, *Nat Neurosci* 15, 349-357.
 - (14) Lee, S. J., Nam, E., Lee, H. J., Savellieff, M. G., and Lim, M. H. (2017) Towards an understanding of amyloid-beta oligomers: characterization, toxicity mechanisms, and inhibitors, *Chem Soc Rev* 46, 310-323.
 - (15) Leon, R., Garcia, A. G., and Marco-Contelles, J. (2013) Recent advances in the multitarget-directed ligands approach for the treatment of Alzheimer's disease, *Med Res Rev* 33, 139-189.
 - (16) Di Martino, R. M. C., Bisi, A., Rampa, A., Gobbi, S., and Belluti, F. (2017) Recent progress on curcumin-based therapeutics: a patent review (2012-2016). Part II: curcumin derivatives in cancer and neurodegeneration, *Expert Opin Ther Pat* 27, 953-965.
 - (17) Esatbeyoglu, T., Huebbe, P., Ernst, I. M., Chin, D., Wagner, A. E., and Rimbach, G. (2012) Curcumin - from molecule to biological function, *Angew Chem Int Ed Engl* 51, 5308-5332.

- (18) Prasad, S., Gupta, S. C., Tyagi, A. K., and Aggarwal, B. B. (2014) Curcumin, a component of golden spice: from bedside to bench and back. *Biotechnol Adv* 32, 1053-1064.
- (19) Masuda, Y., Fukuchi, M., Yatagawa, T., Tada, M., Takeda, K., Irie, K., Akagi, K., Monobe, Y., Imazawa, T., and Takegoshi, K. (2011) Solid-state NMR analysis of interaction sites of curcumin and 42-residue amyloid beta-protein fibrils, *Bioorg Med Chem* 19, 5967-5974.
- (20) Zhao, L. N., Chiu, S. W., Benoit, J., Chew, L. Y., and Mu, Y. (2012) The effect of curcumin on the stability of Abeta dimers, *J Phys Chem B* 116, 7428-7435.
- (21) Orlando, R. A., Gonzales, A. M., Royer, R. E., Deck, L. M., and Vander Jagt, D. L. (2012) A chemical analog of curcumin as an improved inhibitor of amyloid Abeta oligomerization, *PLoS One* 7, e31869.
- (22) Reinke, A. A., and Gestwicki, J. E. (2007) Structure-activity relationships of amyloid beta-aggregation inhibitors based on curcumin: influence of linker length and flexibility. *Chem Biol Drug Des* 70, 206-215.
- (23) Nelson, K. M., Dahlin, J. L., Bisson, J., Graham, J., Pauli, G. F., and Walters, M. A. (2017) The Essential Medicinal Chemistry of Curcumin, *J Med Chem* 60, 1620-1637.
- (24) Baell, J., and Walters, M. A. (2014) Chemistry: Chemical con artists foil drug discovery. *Nature* 513, 481-483.
- (25) Jasial, S., Hu, Y., and Bajorath, J. (2017) How Frequently Are Pan-Assay Interference Compounds Active? Large-Scale Analysis of Screening Data Reveals Diverse Activity Profiles, Low Global Hit Frequency, and Many Consistently Inactive Compounds, *J Med Chem* 60, 3879-3886.
- (26) Di Martino, R. M., De Simone, A., Andrisano, V., Bisignano, P., Bisi, A., Gobbi, S., Rampa, A., Fato, R., Bergamini, C., Perez, D. I., Martinez, A., Bottegoni, G., Cavalli, A., and Belluti, F. (2016) Versatility of the Curcumin Scaffold: Discovery of Potent and Balanced Dual BACE-1 and GSK-3beta Inhibitors, *J Med Chem* 59, 531-544.
- (27) Kuzuyama, T., Noel, J. P., and Richard, S. B. (2005) Structural basis for the promiscuous biosynthetic prenylation of aromatic natural products, *Nature* 435, 983-987.
- (28) Brezani, V., Smejkal, K., Hosek, J., and Tomasova, V. (2018) Anti-inflammatory Natural Prenylated Phenolic Compounds - Potential Lead Substances. *Curr Med Chem* 25, 1094-1159.
- (29) Marchiani, A., Rozzo, C., Fadda, A., Delogu, G., and Ruzza, P. (2014) Curcumin and curcumin-like molecules: from spice to drugs. *Curr Med Chem* 21, 204-222.
- (30) Pabon, H. J. J. (1964) A synthesis of curcumin and related compounds. *Recl Trav Chim Pay B* 83, 379-386.
- (31) Mercanti, G., Ragazzi, E., Toffano, G., Giusti, P., and Zusso, M. (2014) Phosphatidylserine and curcumin act synergistically to down-regulate release of interleukin-1beta from lipopolysaccharide-stimulated cortical primary microglial cells, *CNS Neurol Disord Drug Targets* 13, 792-800.
- (32) Bisceglia, F., Natalello, A., Serafini, M. M., Colombo, R., Verga, L., Lanni, C., and De Lorenzi, E. (2018) An integrated strategy to correlate aggregation state, structure and toxicity of Ass 1-42 oligomers. *Talanta* 188, 17-26.

-
- (33) Sabella, S., Quaglia, M., Lanni, C., Racchi, M., Govoni, S., Caccialanza, G., Calligaro, A., Bellotti, V., and De Lorenzi, E. (2004) Capillary electrophoresis studies on the aggregation process of beta-amyloid 1-42 and 1-40 peptides, *Electrophoresis* 25, 3186-3194.
- (34) Colombo, R., Carotti, A., Catto, M., Racchi, M., Lanni, C., Verga, L., Caccialanza, G., and De Lorenzi, E. (2009) CE can identify small molecules that selectively target soluble oligomers of amyloid beta protein and display antifibrillogenic activity, *Electrophoresis* 30, 1418-1429.
- (35) Butini, S., Brindisi, M., Brogi, S., Maramai, S., Guarino, E., Panico, A., Saxena, A., Chauhan, V., Colombo, R., Verga, L., De Lorenzi, E., Bartolini, M., Andrisano, V., Novellino, E., Campiani, G., and Gemma, S. (2013) Multifunctional cholinesterase and amyloid Beta fibrillization modulators. Synthesis and biological investigation, *ACS Med Chem Lett* 4, 1178-1182.
- (36) Brinet, D., Gaie-Levrel, F., Delatour, V., Kaffy, J., Onger, S., and Taverna, M. (2017) *In vitro* monitoring of amyloid beta-peptide oligomerization by Electrospray differential mobility analysis: An alternative tool to evaluate Alzheimer's disease drug candidates. *Talanta* 35, 84-91.
- (37) Bartolini, M., Bertucci, C., Bolognesi, M. L., Cavalli, A., Melchiorre, C., and Andrisano, V. (2007) Insight into the kinetic of amyloid beta (1-42) peptide self-aggregation: elucidation of inhibitors' mechanism of action, *Chembiochem* 8, 2152-2161.
- (38) Hudson, S. A., Ecroyd, H., Kee, T. W., and Carver, J. A. (2009) The thioflavin T fluorescence assay for amyloid fibril detection can be biased by the presence of exogenous compounds. *FEBS J* 279, 5960-5972.
- (39) Thapa, A., Jett, S. D., and Chi, E. Y. (2016) Curcumin Attenuates Amyloid-beta Aggregate Toxicity and Modulates Amyloid-beta Aggregation Pathway, *ACS Chem Neurosci* 7, 56-68.
- (40) Necula, M., Kaye, R., Milton, S., and Glabe, C. G. (2007) Small molecule inhibitors of aggregation indicate that amyloid beta oligomerization and fibrillization pathways are independent and distinct, *J Biol Chem* 282, 10311-10324.
- (41) Zusso, M., Mercanti, G., Belluti, F., Di Martino, R. M. C., Pagetta, A., Marinelli, C., Brun, P., Ragazzi, E., Lo, R., Stifani, S., Giusti, P., and Moro, S. (2017) Phenolic 1,3-diketones attenuate lipopolysaccharide induced inflammatory response by an alternative magnesium-mediated mechanism, *Br J Pharmacol* 174, 1090-1103.
- (42) Baird, L., and Dinkova-Kostova, A. T. (2011) The cytoprotective role of the Keap1-Nrf2 pathway, *Arch Toxicol* 85, 241-272.
- (43) Ahmed, S. M., Luo, L., Namani, A., Wang, X. J., and Tang, X. (2017) Nrf2 signaling pathway: Pivotal roles in inflammation. *Biochim Biophys Acta* 1863, 585-597.
- (44) Pandima Devi, K., Rajavel, T., Daglia, M., Nabavi, S. F., Bishayee, A., and Nabavi, S. M. (2017) Targeting miRNAs by polyphenols: Novel therapeutic strategy for cancer. *Semin Cancer Biol* 46, 146-157.
- (45) Liu, Z., Tang, L., Zou, P., Zhang, Y., Wang, Z., Fang, Q., Jiang, L., Chen, G., Xu, Z., Zhang, H., and Liang, G. (2014) Synthesis and biological evaluation of allylated and prenylated

mono-carbonyl analogs of curcumin as anti-inflammatory agents, *Eur J Med Chem* 74, 671-682.

- (46) Vistoli, G., Colzani, M., Mazzolari, A., Maddis, D. D., Grazioso, G., Pedretti, A., Carini, M., and Aldini, G. (2016) Computational approaches in the rational design of improved carbonyl quenchers: focus on histidine containing dipeptides, *Future Med Chem* 8, 1721-1737.
- (47) Rao, P. P., Mohamed, T., Teckwani, K., and Tin, G. (2015) Curcumin Binding to Beta Amyloid: A Computational Study, *Chem Biol Drug Des* 86, 813-820.
- (48) Korb, O., Stutzle, T., and Exner, T. E. (2009) Empirical scoring functions for advanced protein-ligand docking with PLANTS. *J Chem Inf Model* 49, 84-96.
- (49) Mashiach, E., Schneidman-Duhovny, D., Andrusier, N., Nussinov, R., and Wolfson, H. J. (2008) FireDock: a web server for fast interaction refinement in molecular docking, *Nucleic Acids Res* 36, W229-232.
- (50) Vistoli, G., Treumann, A., Zglinicki, T., and Miwa, S. (2016) Data from molecular dynamics simulations in support of the role of human CES1 in the hydrolysis of Amplex Red, *Data Brief* 6, 865-870.
- (51) Skaper, S. D., Argentini, C., and Barbierato, M. (2012) Culture of neonatal rodent microglia, astrocytes, and oligodendrocytes from cortex and spinal cord, *Methods Mol Biol* 846, 67-77.

PART III

The following manuscript was published in *European Journal of Medicinal Chemistry* in 2019 as:

Merging memantine and ferulic acid to probe connections between NMDA receptors, oxidative stress and amyloid- β peptide in Alzheimer's disease

Michela Rosini, Elena Simoni, Roberta Caporaso, Filippo Basagni, **Michele Catanzaro**, Izuddin F. Abu, Francesca Fagiani, Federica Fusco, Sara Masuzzo, Diego Albani, Cristina Lanni, Ian R. Mellor and Anna Minarini

Abstract

N-methyl-D-aspartate receptors (NMDAR) are critically involved in the pathogenesis of Alzheimer's disease (AD). Acting as an open-channel blocker, the anti-AD drug memantine preferentially targets NMDAR overactivation, which has been proposed to trigger neurotoxic events mediated by amyloid- β peptide (A β) and oxidative stress. In this study, we applied a multifunctional approach by conjugating memantine to ferulic acid, which is known to protect the brain from A β neurotoxicity and neuronal death caused by ROS. The most interesting compound (**7**) behaved, like memantine, as a voltage-dependent antagonist of NMDAR (IC₅₀ = 6.9 μ M). In addition, at 10 μ M concentration, **7** exerted antioxidant properties both directly and indirectly through the activation of the Nrf2 pathway in SH-SY5Y cells. At the same concentration, differently from the parent compounds memantine and ferulic acid alone, it was able to modulate A β production, as revealed by the observed increase of the non-amyloidogenic sAPP α in H4-sw cells. These findings suggest that compound **7** may represent a promising tool for investigating NMDAR-mediated neurotoxic events involving A β burden and oxidative damage.

Keywords: memantine; ferulic acid; NMDA receptors; oxidative stress; amyloid- β peptide.



Contents lists available at ScienceDirect

European Journal of Medicinal Chemistry

journal homepage: <http://www.elsevier.com/locate/ejmech>

Research paper

Merging memantine and ferulic acid to probe connections between NMDA receptors, oxidative stress and amyloid- β peptide in Alzheimer's disease



Michela Rosini ^{a,*}, Elena Simoni ^a, Roberta Caporaso ^a, Filippo Basagni ^a,
Michele Catanzaro ^b, Izuddin F. Abu ^{c,d}, Francesca Fagiani ^{b,e}, Federica Fusco ^f,
Sara Masuzzo ^f, Diego Albani ^f, Cristina Lanni ^b, Ian R. Mellor ^c, Anna Minarini ^{a,**}

^a Department of Pharmacy and Biotechnology, Alma Mater Studiorum – University of Bologna, Via Belmeloro 6, 40126, Bologna, Italy

^b Department of Drug Sciences (Pharmacology Section), University of Pavia, V.le Taramelli 14, 27100, Pavia, Italy

^c School of Life Sciences, University of Nottingham, University Park, Nottingham, NG7 2RD, UK

^d Universiti Kuala Lumpur, Institute of Medical Science Technology, A1-1, Jalan TKS1, Taman Kajang Sentral, 43000, Kajang, Selangor, Malaysia

^e Scuola Universitaria Superiore IUSS Pavia, P.zza Vittoria, 15, 27100, Pavia, Italy

^f Department of Neuroscience, Istituto di Ricerche Farmacologiche Mario Negri IRCCS, Via Mario Negri 2, 20156, Milan, Italy

1. Introduction

Synaptic loss is a major feature in Alzheimer's disease (AD). This chronic neurodegenerative condition, which is currently afflicting about 47 million people worldwide, slowly destroys neurons leading to progressive cognitive disabilities [1]. How synapses are affected in the disease process remains unclear. The mechanistic understanding of synaptic damage represents a challenging goal and may offer new possibilities for the prevention and cure of the disease. N-methyl-D-aspartate receptors (NMDAR) are ionotropic glutamate receptors known to play an important role for synaptic plasticity in the healthy brain [2]. They are primarily involved in neuronal excitatory synaptic transmission that underlies learning and memory but also in excitotoxic damage occurring during acute brain injuries and chronic neurodegenerative conditions. Targeting NMDAR therapeutically is therefore complicated by the dichotomous nature of their downstream signaling. It is the common view that these opposite effects depend on receptor localization: activation of synaptic NMDAR (sNMDAR) may contribute to cell survival and plasticity, while activation of extrasynaptic NMDAR (eNMDAR) may preferentially signal to neuronal death [3,4]. In particular, overactivation

of eNMDAR has been associated with glutamate-mediated oxidative damage potentially leading to aberrant, misfolded proteins [5]. The amyloid- β peptide ($A\beta$) is a pathogenic feature of AD development. Produced by the sequential cleavage of the amyloid precursor protein (APP) by β - and γ -secretases, as an alternative to the non-amyloidogenic cleavage performed by α -secretase, $A\beta$ monomers aggregate into soluble oligomeric forms, which are believed to be mainly responsible for amyloid-driven synaptotoxicity [6]. A toxic positive feedback is established between $A\beta$ production and eNMDAR overactivation, which involves cytoplasmic Ca^{2+} upregulation and aberrant redox-mediated reactions [7].

Memantine is an anti-AD drug currently in use for the treatment of moderate-to-severe forms of the disease. It is an uncompetitive/fast off-rate NMDAR antagonist. By acting as an open-channel blocker, it preferentially enters the channel's pore in conditions of excessive and prolonged glutamate exposure [8,9]. Its favorable kinetics has been proposed to selectively direct memantine's efficacy toward extrasynaptic/tonically-activated NMDAR over synaptic/phasicly-activated NMDAR [10], accounting for the clinical tolerability of the drug. Further, this peculiar profile seems to play a crucial role in determining memantine's ability to alleviate $A\beta$ -induced synaptic dysfunction and to rescue both neuronal oxidative stress and the transient memory impairment caused by $A\beta$ oligomers [11]. Unfortunately, however, like other available anti-AD drugs, memantine offers only a symptomatic relief to patients and is not able to halt the disease progression.

Based on these premises, we sought to combine in a single molecule memantine, which specifically modulates NMDAR-mediated excitotoxicity, responsible for ROS- and $A\beta$ -mediated neurotoxic events, with the antioxidant ferulic acid (FA), whose well-established biological properties include the ability to protect the brain from $A\beta$ neurotoxicity and neuronal death caused by ROS [12]. Following this rationale, we designed and synthesized memantine-FA conjugates following the two routes shown in **Figure 1**.

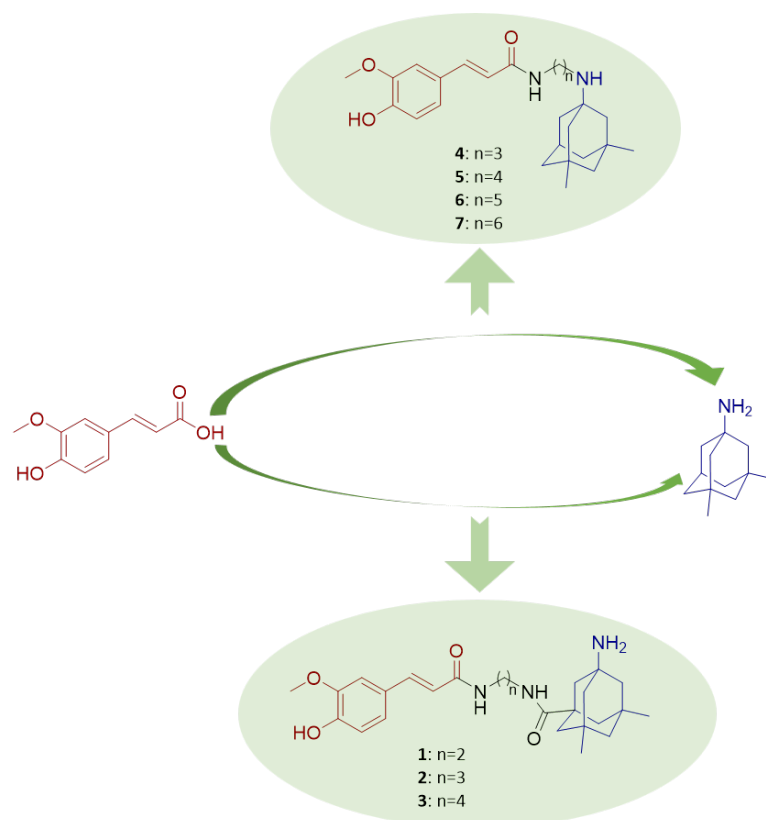


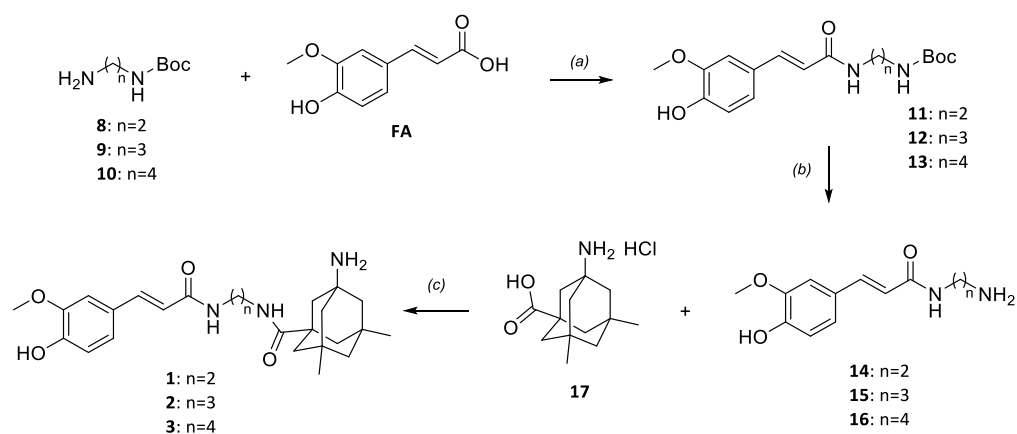
Figure 1. Drug design of compounds 1-7.

It is well known that memantine's primary amine plays a crucial role in receptor binding [13]. Thus, to preserve this moiety, we functionalized the adamantane nucleus of memantine with a carboxylic function, which acted as the reactive point for FA conjugation, affording compounds 1-3. Further, in compounds 4-7, we explored the possibility to introduce FA appendages on the nitrogen atom of memantine, whose conversion to a secondary amine has previously emerged as a feasible strategy to gain memantine-based NMDAR antagonists [14,15]. Synthesized compounds were first tested against NMDAR. Based on their NMDAR blocking properties, compounds were selected to study their direct and indirect antioxidant efficacy, as well as the ability to modulate the amyloidogenic pathway.

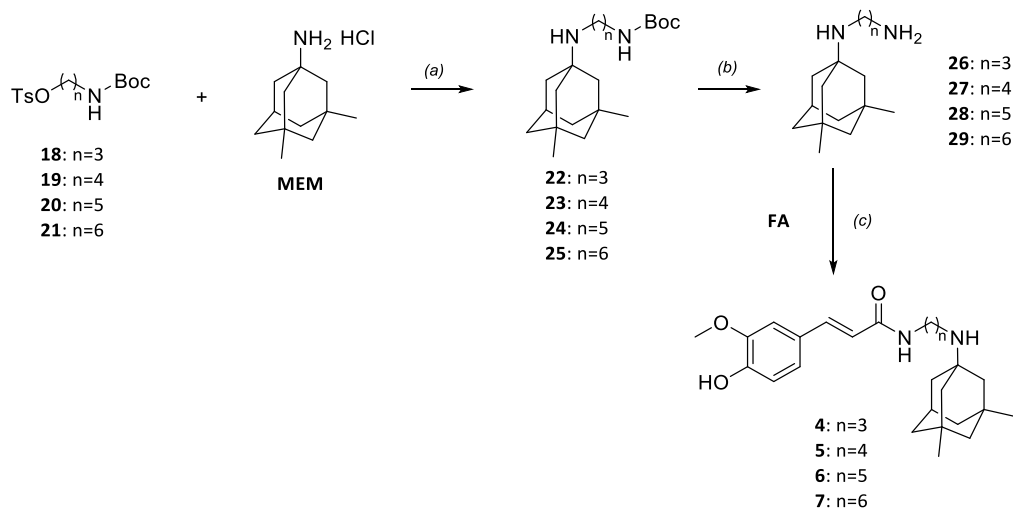
2. Results and Discussion

Chemistry

Memantine-FA hybrids 1-7 were prepared following two different synthetic routes (**Schemes 1** and **2**), depending on the way the two pharmacophores were connected. For the synthesis of compounds 1-3, the appropriate mono Boc-protected diamine (8-10) [16,17] was condensed with FA to give intermediates 11-13. Cleavage of the protecting group in acidic conditions led to compounds 14-16. Conjugation of 14-16 with 17 hydrochloride, which was obtained following a Ritter-type protocol as previously reported by Wanka *et al.* [18], afforded final compounds 1-3 (**Scheme 1**). To gain compounds 4-7, memantine hydrochloride (MEM) was alkylated with the appropriate tosyl-activated alcohol (18-21) under basic conditions to give intermediates 22-25 which, after carbamate deprotection (26-29), were coupled with FA in the presence of EDC and HOBT (**Scheme 2**).



Scheme 1. Reagents and conditions: (a) EDC, HOBT, DMF, Et₃N, N₂, 12 h, 0°C-rt; (b) HCl 4 M in dioxane, CH₂Cl₂, 90', 0°C-rt; (c) EDC, HOBT, DMF, N₂, 36 h, 0°C-rt.



Scheme 2. Reagents and conditions: (a) K_2CO_3 , KI, DMF, $140^\circ C$, 1h, MW; (b) HCl 4 M in dioxane, CH_2Cl_2 , 20', $0^\circ C$ -rt; (c) EDC, HOBT, Et_3N , DMF, N_2 , 12 h, $0^\circ C$ -rt.

NMDAR blocking activity

All the compounds were initially investigated to assess their effect at NMDAR. In particular, the antagonism of responses to NMDA and glycine were measured by voltage-clamp recordings on GluN1-1a/GluN2A NMDAR expressed in *Xenopus laevis* oocytes at -60 mV, with compounds 1-7 applied in tenfold increments in the range 0.01 to 100 μM . Memantine was used as the reference compound. Compounds 1-3, which retain the primary amine function of memantine, demonstrated very low or no potency to block NMDAR (**Figure 2A**). Conversely, employing memantine's amine for connecting FA appendages resulted in significant blocking of NMDA/glycine responses (**Figure 2A**).

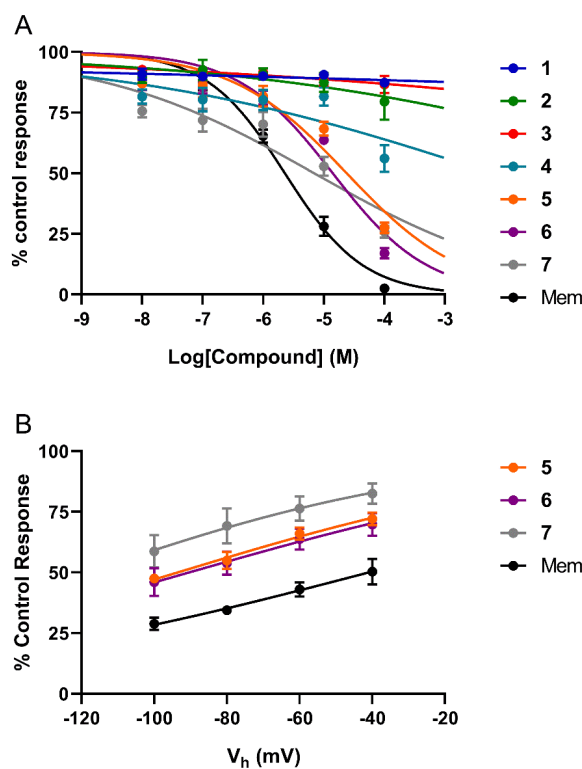


Figure 2. A) Concentration-inhibition curves for compounds 1-7 in comparison to memantine (Mem). Data are mean % of control response to 100 μ M NMDA (+10 μ M glycine) \pm SEM ($n = 5-7$ separate oocytes). The curves are fits to Equation 1 and IC_{50} values are given in Table 1. **B)** Voltage dependence of inhibition by compounds 5-7 (30 μ M, 20 μ M and 10 μ M respectively) in comparison to memantine (Mem; 3 μ M). Data are plotted as mean % control response to 100 μ M NMDA (+10 μ M glycine) \pm SEM against the holding potential (V_h) ($n = 5-6$ separate oocytes). The curves are fits of Equation 2 and δ values are given in Table 1.

Compounds 5-7 presented a micromolar profile, with IC_{50} values ranging from 6.9 to 23.9 μ M, while the shorter compound 4 had an IC_{50} greater than 100 μ M, thus suggesting its inefficacy (Table 1). Blocking properties toward NMDAR were influenced by the chain length separating the pharmacophoric functions, with compound 7, carrying a hexamethylene spacer, emerging as the most efficacious. Compounds with considerable blocking properties (5-7) were assessed for voltage dependency. The compounds were diluted to their approximate IC_{50} concentrations and block of NMDA/glycine responses

mediated by GluN1-1a/GluN2A was measured at four different holding potentials (-40, -60, -80 and -100 mV).

Compound	IC ₅₀ [95% CI] μ M (n)	$\delta \pm$ SE (n)
1	$\gg 100$ (7)	nd
2	$\gg 100$ (6)	nd
3	$\gg 100$ (6)	nd
4	>100 (5)	nd
5	23.9 [13.0–49.4] (5)	0.46 ± 0.07 (6)
6	14.1 [8.7–22.6] (5)	0.43 ± 0.12 (6)
7	6.9 [3.0–19.2] (5)	0.51 ± 0.17 (6)
memantine	2.3 [1.7–3.0] (6)	0.39 ± 0.08 (5)

nd = not determined (because inhibition was too weak).

Table 1. IC₅₀ and δ values for compounds 1-7 and memantine

Compounds presented a voltage-dependent behavior, acting, like memantine, as open channel blockers of the receptor. Data were fitted with the Woodhull equation to determine their δ values, and thus estimate the position of the binding site within the membrane electric field [19,20]. The results of this study showed that three of the new molecules yielded δ values comparable to memantine. Compounds 5, 6 and 7 had δ values in the range 0.43 to 0.51, which are just slightly higher to that of memantine, 0.39. Based on their δ values, we can suggest these compounds may have a binding site midway through the pore, maybe a little deeper but overlapping with that of memantine. This is consistent with binding adjacent to the Q/R/N-site that determines ion selectivity in ionotropic glutamate receptors.

Cell Toxicity Assay

Compounds 5-7, presenting appreciable NMDAR blocking properties, were selected for deepening their antioxidant profile in SH-SY5Y human neuroblastoma cells. To this aim, we assessed the cytotoxicity of compounds 5-7 to define the concentration range to be used in cellular experimental settings. The antioxidant FA was used for comparison. Cells were exposed to

the compounds at concentrations ranging from 1 to 50 μM for 24 h and cell viability was determined by MTT assay. As shown in **Figure 3**, all the compounds were devoid of any toxicity at a concentration up to 20 μM , while only the shorter derivative 5 retained, like FA, good tolerability up to 50 μM . Lack of toxicity was verified also for compound 4, carrying a three-methylene spacer, at all the concentrations investigated (data not shown), confirming that the spacer length significantly influenced compound tolerability in favor of shorter derivatives.

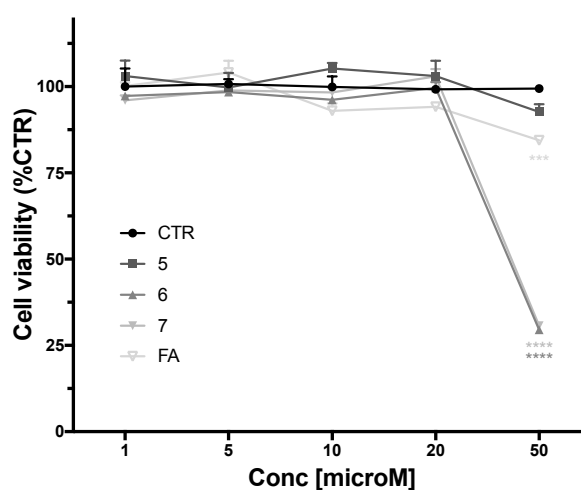


Figure 3. Cellular toxicity of hybrid compounds (5-7) and Ferulic Acid (FA) on human neuroblastoma SH-SY5Y. Cells were treated with compounds for 24 h at different concentrations ranging from 1 to 50 μM . Cell viability was assessed by MTT assay. Data are expressed as percentage of cell viability versus CTR; *** $p < 0.001$, and **** $p < 0.0001$ versus CTR; Dunnett's multiple comparison test, $n=3$.

Protective Effect toward H_2O_2 -Induced Damage

To determine the antioxidant efficacy of compounds 5-7, we first studied their ROS scavenging activity when coincubated with 300 μM H_2O_2 , using FA for comparison. The scavenger effect was evaluated in SH-SY5Y cells by using the fluorescent probe dichlorodihydrofluorescein diacetate (DCFH-DA) as a marker for quantitative intracellular ROS formation. The DCFH-fluorescence

intensity significantly increased in H₂O₂-treated cells (black line, **Figure 4A**) with respect to untreated cells (dashed grey line, **Figure 4A**). All compounds, at a concentration of 10 μ M, were able to markedly reduce H₂O₂-induced intracellular ROS formation, being, however, less effective than FA. To assess if indirect antioxidant effects could accompany radical scavenger properties, further experiments were performed pretreating SH-SY5Y cells with compounds 5-7 (10 μ M) for 24 h before adding 300 μ M H₂O₂ (**Figure 4B**). Again, compounds 5-7 produced a significant reduction in DCFH-fluorescent intensity, albeit an inversion in the trend of efficacy was observed. Indeed, with this experimental setting, compound 7 emerged as the most efficacious, reaching FA ability to counteract H₂O₂-induced ROS formation. Based on these results, we could speculate that, at least for 7, antioxidant properties might derive from both direct and indirect effects.

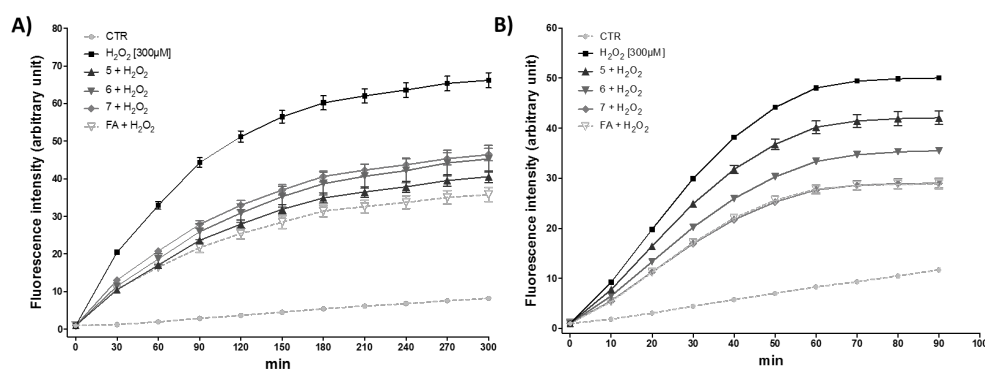


Figure 4. Hybrid compounds reverse ROS formation induced by H₂O₂. (A) After the loading with DCFH-DA, SH-SY5Y cells were exposed to 10 μ M compounds or FA in combination with 300 μ M of H₂O₂. The fluorescence intensity for all compounds tested is significant at any time starting from 60 to 300 min with $p < 0.0001$ versus H₂O₂. At 30 min the significance versus H₂O₂ is $p < 0.01$ for compound 7, $p < 0.001$ for compound 6 and $p < 0.0001$ for compound 5 and FA. Dunnett's multiple comparison test. (B) SH-SY5Y cells were pre-treated with 10 μ M of each compound for 24 hours, loaded with DCFH-DA and then exposed to 300 μ M H₂O₂. Fluorescence intensity for all compounds tested is significant at any time from 30 to 90 min with $p < 0.0001$ versus H₂O₂. At time 10 min, the fluorescence intensity did not reach statistical significance for compound 5, whereas for 6 the significance is $p < 0.01$ and for 7 and FA is $p < 0.0001$ vs H₂O₂. At 20 min, the significance is $p < 0.001$ for compound 5 and $p < 0.0001$ for compound 7 and AF vs H₂O₂. Dunnett's multiple comparison test.

Activation of Nrf2 Pathway in SH-SY5Y Cells

The nuclear factor (erythroid-derived 2)-like 2 (Nrf2) transcriptional pathway is a major player of inducible antioxidant defense [21]. Activation of the Nrf2 pathway, and the subsequent transcription of downstream cytoprotective genes, is triggered by the disruption of interaction and binding of Nrf2 with the cytosolic Nrf2 repressor Kelch-like ECH-associated protein 1 (Keap 1) [22]. A variety of electrophiles from synthetic or natural sources is emerging for their ability to hamper this interaction by targeting key cysteine residues of Keap1, which act as sensors of oxidative insults [23]. In particular, the electrophilic motif recurring in FA and its derivatives, namely the α,β -unsaturated carbonyl group, has already been shown to trigger the Nrf2-driven transcriptional process in a series of hydroxy-cinnamic derivatives for which trapping Keap1 through covalent adduct formation was proposed to be the initiating event [24,25]. Thus, we studied compounds 5-7 and FA in SH-SY5Y neuroblastoma cells to verify whether they may affect the Nrf2 pathway and indirect mechanisms could therefore contribute to their overall antioxidant profile. To this aim, we first assessed their ability to modulate the mRNA levels of Nrf2 by real-time PCR, using 10 μ M of each compound incubated for 6 h. Notably, only compound 7 determined a significant increase in Nrf2 mRNA expression (**Figure 5, panel A**), while cells treated with FA or compounds 5 and 6 behaved like untreated cells. Coherently with these results, the same trend was observed when we investigated the ability of compounds to tune the mRNA levels of heme oxygenase-1 (HO-1), a prototypical Nrf2-target gene related to oxidative stress response. Indeed, mRNA levels of the inducible cytoprotective gene raised to about 150% of control following pretreatment with 10 μ M 7, while no effect was elicited by FA or compounds 5 and 6 (**Figure 5, panel B**).

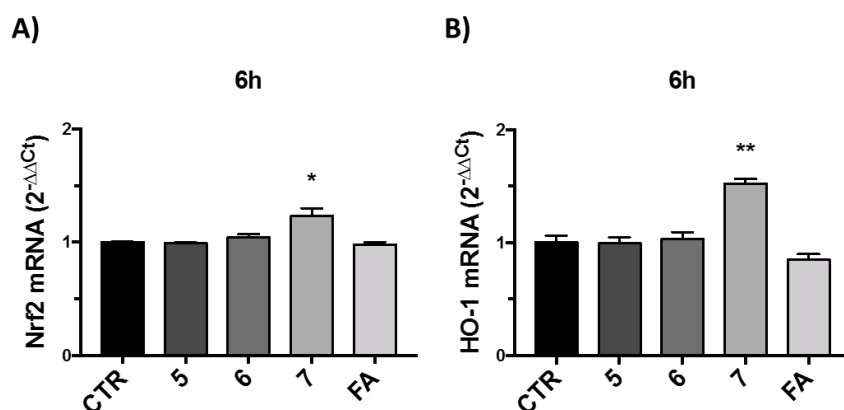


Figure 5. Hybrid compounds modulate Nrf2 and HO-1 mRNA levels. RNA was obtained from cellular extracts of SH-SY5Y cells treated for 6 h with compounds 5-7 and FA at 10 μ M and analyzed for Nrf2 (**A**) and HO-1 (**B**) mRNA expression by RT-PCR. GAPDH was used as housekeeping gene. Results are shown as mean \pm SEM; * p < 0.05, ** p < 0.01 versus CTR; Dunnett's multiple comparison test, $n=3$.

Then, we sought to verify whether the increase in HO-1 mRNA expression determined by compound 7 could effectively result in enhanced HO-1 protein levels. To this aim, HO-1 induction was analyzed by means of Western immunoblotting in the same cell line after treatment for 24 h with 7 at 10 or 20 μ M. Interestingly, compound 7 caused a dose-dependent increase of HO-1 expression, with cells treated with 20 μ M 7 almost doubling HO-1 protein levels of control (**Figure 6**). These results confirm that compound 7 is a multimodal antioxidant, which combines radical scavenging properties to the ability of potentiating the Nrf2/HO-1 axis. Further, the lack of indirect antioxidant efficacy verified for compounds 5, 6 and FA, all carrying the α,β -unsaturated carbonyl feature, reveal that an electrophilic moiety is not per se sufficient for activating redox sensor proteins, and shape complementarity may play a pivotal role in this respect. Particularly, we might speculate that compounds 5-7, varying in the linker length, and FA could differently orient their cysteine-reactive group toward nucleophilic traps of Keap1 affecting target recognition and, consequently, a compound's reactivity and specificity.

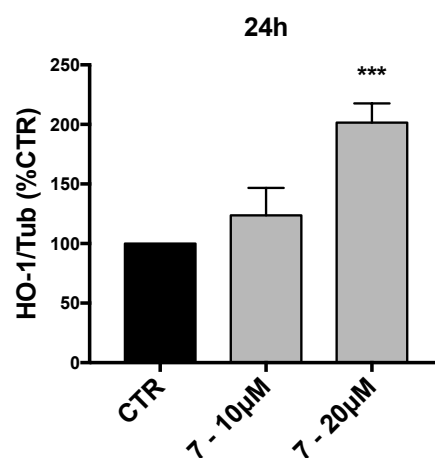


Figure 6. Effect of compound 7 on HO-1 protein levels. Cellular extracts of SH-SY5Y cells treated for 24 h with compound **7** at 10 or 20 µM were analyzed for HO-1 protein levels by Western Blot. Anti-tubulin was used as protein loading control. Results are shown as ratio (% of CTR) ± SEM; *** $p < 0.001$ versus CTR; Dunnett's multiple comparison test, $n=3$.

APP processing in H4-SW cells

In AD, a direct link exists between eNMDAR overactivation and increased neuronal A β production [26]. NMDAR have been proposed to modulate α -secretase activity, shifting APP metabolism towards a non-amyloidogenic pathway. Memantine has been shown to lower A β synthesis in a number of studies [27,28]. Mechanisms potentially involved in memantine-driven A β modulation are not completely clear, and both NMDAR-mediated and NMDAR-independent mechanisms have been proposed [29]. In this context, we sought to investigate whether the most promising compounds 5-7 could affect the APP processing favoring the production of the non-amyloidogenic soluble amyloid precursor protein α (sAPP α). Current research suggests that sAPP α plays a role in synaptic growth and plasticity, featuring neuroprotective and neurotrophic properties [30]. Thus, we studied the effect of the compounds on sAPP α levels in the human H4 cell line expressing the Swedish mutant form of APP (H4-SW), after 24 h treatment. Compounds 5-7 were tested at 10 µM concentration, which had no impact on cell viability, as

confirmed by a dose-response curve where memantine, FA and compounds 5-7 had no toxic effect up to 20 μM concentration (data not shown). Memantine and FA alone were used for comparison. The Western blot analysis reported in **Figure 7** shows that compound 7, but not compounds 5 and 6, significantly increased sAPP α levels (**Figure 7, panel A**).

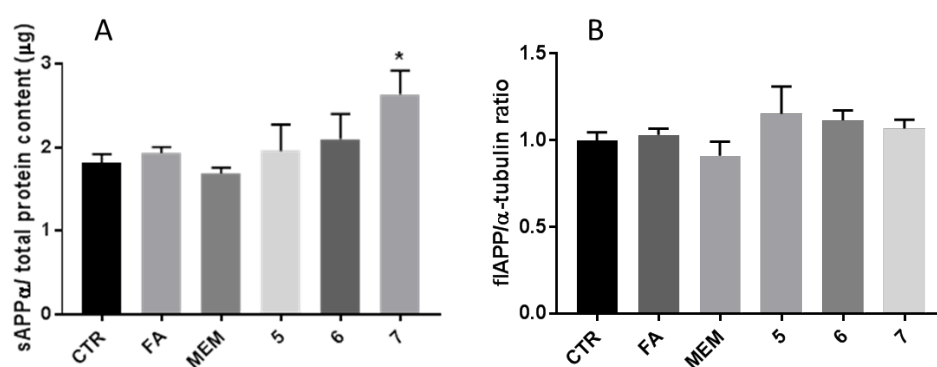


Figure 7. Assessment of the effect of compounds 5-7, MEM and FA on amyloid precursor protein (APP) proteolytic processing in H4-SW cells. (A) Determination of sAPP α levels. Cells were treated with 10 μM of each compound and after 24 h conditioned media were collected and sAPP α content assessed by Western blotting. The graph shows the densitometric quantification of the Western blotting bands, normalized to the total protein content of plated cells. * $p < 0.05$, one-way ANOVA and *post-hoc* test. **(B) Determination of full-length amyloid precursor protein (flAPP) expression.** Cells were treated with 10 μM of each compound. After 24 h, H4-SW were lysed and flAPP expression assessed by Western blotting. The graph shows the densitometric quantification of the Western blotting bands, normalized to α -tubulin as internal reference.

Notably, compounds 5-7 were not able to affect full-length APP (fl-APP) expression levels, which was determined in the same cells to evaluate the effect of the compounds on total intracellular APP (**Figure 7, panel B**). By enhancing sAPP α levels without affecting the levels of total intracellular APP, compound 7 seems to stimulate APP processing towards the α -secretase (non-amyloidogenic) pathway, which should result in decreased A β production. Noteworthy, at the same concentration, memantine and FA alone showed no effect on APP processing, strengthening the value of the design of a hybrid molecule. The lack of efficacy of memantine, whose potency as NMDAR antagonist is 3-fold higher than that of 7, suggests that the effect of

7 on APP processing we observed in this experimental setting seems to be not principally mediated by NMDAR. Interestingly, lengthening of the linker between the pharmacophoric functions up to six methylenes switched on the efficacy toward both APP processing and Nrf2 activation, pointing to 7 as the most promising molecule of the series.

3. Conclusions

NMDAR play a crucial role in the pathophysiology of AD. Excessive activation of NMDAR can compromise synapse function by triggering neurotoxic events, which involve A β peptide and oxidative stress. By preferentially blocking extrasynaptic rather than synaptic currents, the anti-AD drug memantine limits neurotoxicity mediated by excessive NMDAR activity while relatively sparing physiological neurotransmission. This peculiar NMDAR profile prompted us to conjugate memantine with the bioactive payload FA, aiming to synergistically modulate the critical partnership occurring between oxidative damage, A β burden, and hyperfunctioning NMDAR. For compounds 4-7, which exploit memantine's nitrogen for FA connection, chain lengthening positively influenced NMDAR blocking properties. The longer derivative 7, carrying a hexamethylene spacer between the pharmacophoric functions, presented a micromolar profile as NMDAR antagonist (IC₅₀=6.9 μ M), being only three times less effective than the parent compound memantine (IC₅₀= 2.3 μ M). Further, compound 7 also shares with memantine the binding site midway through the pore and a voltage-dependent behavior, suggesting that conjugation with FA produced only a modest perturbation of memantine's NMDAR binding mode. Compounds with appreciable NMDAR blocking properties were studied in SH-SY5Y cells to assess their antioxidant properties. All compounds tested showed notable free radical scavenging effects. Conversely, only 7 was able to significantly potentiate the expression of Nrf2 and its downstream protective gene HO-1 at the concentration of 10 μ M, therefore emerging as a multimodal antioxidant. Notably, the lack of indirect antioxidant efficacy observed for 5 and 6, varying in the linker length, and FA, suggests the importance of target recognition as a pre-requisite for electrophile reactivity, excluding an indiscriminate effect driven by the α,β -unsaturated carbonyl group. At the same concentration (10 μ M), compound

7, and not shorter derivatives 5 and 6, significantly enhanced sAPP α levels in H4-SW cells, suggesting that it may stimulate APP processing in favor of the α -secretase (non-amyloidogenic) pathway and consequently limit A β formation. Thus, the most potent NMDAR antagonist 7 was also able to activate inducible protective pathways which play a crucial role in contrasting the neurotoxic cascade driven by eNMDAR overactivation. The multimodal profile of compound 7 was well balanced, in the micromolar-range, and not accompanied by any cytotoxicity in both SH-SY5Y and H4-SW cells up to the concentration of 20 μ M. Based on these findings, compound 7 emerges as a promising pharmacologic tool for deepening our insight on the significance of NMDAR-mediated neurotoxic events involving ROS formation and A β damage.

4. Experimental section

Chemistry

Chemical reagents were purchased from Sigma-Aldrich, Fluka and Lancaster (Italy) and used without further purification. Chromatographic separations were performed on silica gel columns (Kieselgel 40, 0.040-0.063 mm, Merck) by chromatography. Reactions were followed by TLC on Merck (0.25 mm) glass-packed precoated silica gel plates (60 F254), then visualized with an UV lamp, bromocresol green or KMnO₄. Melting points were measured in glass capillary tubes on a Büchi SMP-20 apparatus and are uncorrected. Microwave assisted synthesis was performed by using CEM Discover[®] SP apparatus (2.45 GHz, maximum power of 300W). NMR spectra were recorded at 400 MHz for ¹H and 100 MHz for ¹³C on Varian VXR 400 spectrometer. Chemical shifts (δ) are reported in parts per millions (ppm) relative to tetramethylsilane (TMS), and spin multiplicities are given as s (singlet), br s (broad singlet), d (doublet), t (triplet), q (quartet), or m (multiplet). Direct infusion ESI-MS mass spectra were recorded on a Waters ZQ 4000 apparatus. Final compounds 1-7 were >95% pure as determined by HPLC analyses. The analyses were performed under reversed-phase conditions on a Phenomenex Jupiter C18 (150 \times 4.6

mm I.D.) column, using a binary mixture of 0.1% TFA in H₂O/acetonitrile (70/30, v/v for 5; 65/35, v/v for 3, 4, 6, 7; 80/20, v/v for 1, 2) as the mobile phase, UV detection at $\lambda = 302$ nm and a flow rate of 1 mL/min. Analyses were performed on a liquid chromatograph model PU-2089Plus UV equipped with a 20 μ L loop valve (Jasco Europe, Italy). Compounds were named relying on the naming algorithm developed by CambridgeSoft Corporation and used in Chem-BioDrawUltra 15.1.

General procedure for the intermediates 11-13. To an ice-cooled solution of ferulic acid (FA, 1 equiv) in dry DMF (3-4 mL) were added HOBt (1.3 equiv) and EDC (1.3 equiv). The reaction mixture was stirred for 10 min, followed by addition of Et₃N (1.3 equiv) and the appropriate mono-protected diamine (8-10) (1 equiv). Stirring was then continued at room temperature overnight, and the solvent evaporated under *vacuum*. The crude was purified by flash chromatography on silica gel using dichloromethane/methanol (9.5:0.5) as mobile phase.

tert-butyl (E)-(2-(3-(4-hydroxy-3-methoxyphenyl)acrylamido)ethyl)carbamate (11). Synthesized from FA (400 mg, 2.06 mmol) and 8 [17] (330 mg, 2.06 mmol) to afford 11 as waxy solid: 200 mg (30%); ¹H NMR (400 MHz, CDCl₃) δ 7.50 (d, $J = 15.6$ Hz, 1H), 6.99 (d, $J = 8$ Hz, 1H), 6.94 (s, 1H), 6.88 (d, $J = 8.4$ Hz, 1H), 6.60 (br s, 1H), 6.26 (d, $J = 15.6$ Hz, 1H), 5.33 (br s, 1H), 3.85 (s, 3H), 3.50-3.46 (m, 2H), 3.33-3.30 (m, 2H), 1.42 (s, 9H).

tert-butyl (E) - (3 - (3 - (4 - hydroxy - 3 - methoxyphenyl) acrylamido) propyl) carbamate (12). Synthesized from FA (100 mg, 0.51 mmol) and 9 [16] (174 mg, 0.51 mmol) to afford 12 as waxy solid: 100 mg (56%); ¹H NMR (400 MHz, CDCl₃) δ 7.55 (d, $J = 15.2$ Hz, 1H), 7.05 (d, $J = 8$ Hz, 1H), 7.01 (s, 1H), 6.90 (d, $J = 8$ Hz, 1H), 6.50 (br s, 1H), 6.30 (d, $J = 15.2$ Hz, 1H), 4.96 (br s, 1H), 3.92 (s, 3H), 3.44-3.40 (m, 2H), 3.23-3.19 (m, 2H), 1.67-1.61 (m, 2H), 1.45 (s, 9H).

tert-butyl (E)-(4-(3-(4-hydroxy-3-methoxyphenyl)acrylamido)butyl)carbamate (13). Synthesized from FA (400 mg, 2.06 mmol) and 10 [31] (188 mg, 2.06 mmol) to afford 13 as waxy green solid: 230 mg (33%); ¹H NMR (400 MHz, CDCl₃) δ 7.52 (d, $J = 15.2$ Hz, 1H), 7.03 (d, $J = 8.4$ Hz, 1H), 6.98 (s, 1H), 6.88

(d, $J = 8$ Hz, 1H), 6.25 (d, $J = 15.2$ Hz, 1H), 6.01 (br s, 1H), 4.64 (br s, 1H), 3.89 (s, 3H), 3.39-3.38 (m, 2H), 3.17-3.13 (m, 2H), 1.60-1.55 (m, 4H), 1.43 (s, 9H).

General procedure for the intermediates 14-16. To an ice-cooled solution of the appropriate Boc-protected intermediate (11-13, 1 equiv) in CH_2Cl_2 (2-3 mL) was added HCl 4 M in dioxane (2-3 mL) and the reaction mixture was stirred at 0 °C for 90 min. The solvent was evaporated, and the crude purified by flash chromatography on silica gel using dichloromethane/methanol/aqueous ammonia 33% (8:2:0.2) affording desired intermediates as free bases.

(E) - N - (2-aminoethyl) - 3 - (4-hydroxy-3-methoxyphenyl) acrylamide (14). Synthesized from 11 (200 mg, 0.60 mmol) to afford 14 as pale yellow solid: 120 mg (86%); ^1H NMR (400 MHz, $\text{DMSO}-d_6$) δ 8.34 (t, $J = 5.4$ Hz, 1H), 7.72 (d, $J = 15.6$ Hz, 1H), 7.53 (s, 1H), 7.41-7.38 (m, 1H), 7.20 (d, $J = 7.6$ Hz, 1H), 6.86 (d, $J = 15.6$ Hz, 1H), 4.21 (s, 3H), 3.59-3.55 (m, 2H), 3.04-3.00 (m, 2H), 2.92 (br s, 2H).

(E) - N - (3-aminopropyl) - 3 - (4-hydroxy-3-methoxyphenyl) acrylamide (15). Synthesized from 12 (100 mg, 0.30 mmol) to afford 15 as pale green solid: 71 mg (99%); ^1H NMR (400 MHz, CD_3OD) δ 7.40 (d, $J = 15.6$ Hz, 1H), 7.10 (s, 1H), 7.00-6.98 (m, 1H), 6.77 (d, $J = 8.4$ Hz, 1H), 6.48 (d, $J = 15.6$ Hz, 1H), 3.84 (s, 3H), 3.38 (t, $J = 6.4$ Hz, 2H), 2.96 (t, $J = 7.2$ Hz, 2H), 1.95-1.88 (m, 2H).

(E) - N - (4-aminobutyl) - 3 - (4-hydroxy-3-methoxyphenyl) acrylamide (16). Synthesized from 13 (230 mg, 0.63 mmol) to afford 16 as pale green solid: 160 mg (96%); ^1H NMR (400 MHz, CD_3OD) δ 7.39 (d, $J = 15.6$ Hz, 1H), 7.05 (s, 1H), 6.96 (d, $J = 7.6$ Hz, 1H), 6.73 (d, $J = 8.4$ Hz, 1H), 6.40 (d, $J = 15.6$ Hz, 1H), 3.82 (s, 3H), 3.31-3.23 (m, 2H), 2.80-2.78 (m, 2H), 1.59-1.58 (m, 4H).

General procedure for compounds 1-3. To an ice-cooled solution of the hydrochloride salt 17 [18] (1 equiv) in dry DMF (3 mL) were added HOBT (1.3 equiv) and EDC (1.3 equiv) under N_2 atmosphere. The reaction mixture was stirred for 10 min, followed by addition of the appropriate intermediates (14-16) (2 equiv). Stirring was continued at room temperature for 36-48 h, and

then the solvent evaporated under *vacuum*. The crude was purified by column chromatography on silica gel using dichloromethane /methanol/aqueous ammonia 33% (8.5:1.5:0.15) as mobile phase.

(1r,3s,5R,7S)-3-amino-*N*-(2-((*E*)-3-(4-hydroxy-3-methoxyphenyl) acrylamido) ethyl)-5,7-dimethyladamantane-1-carboxamide (1). Synthesized from 17 (64 mg, 0.24 mmol) and 14 (115 mg, 0.48 mmol) to afford 1 as green solid: 80 mg (74%); mp 122-124 °C; ¹H NMR (400 MHz, DMSO-*d*₆) δ 7.99 (br s, 1H), 7.46 (br s, 1H), 7.32 (d, *J* = 15.6 Hz, 1H), 7.11 (s, 1H), 6.99-6.97 (m, 1H), 6.80 (d, *J* = 8.4 Hz, 1H), 6.40 (d, *J* = 15.6 Hz, 1H), 3.80 (s, 3H), 3.20-3.17 (m, 2H), 3.15-3.12 (m, 2H), 1.40 (s, 2H), 1.29-1.23 (m, 4H), 1.16-1.12 (m, 4H), 1.01 (s, 2H), 0.82 (s, 6H). ¹³C NMR (100 MHz, DMSO-*d*₆) δ 176.77, 166.17, 148.84, 148.27, 139.54, 126.70, 121.97, 119.25, 116.10, 111.23, 55.96, 51.30, 49.90, 49.79, 49.03, 46.18, 44.55, 44.10, 38.90, 32.95, 30.19. MS [ESI+] *m/z* 442 [M+1]⁺.

(1r,3s,5R,7S)-3-amino-*N*-(3-((*E*)-3-(4-hydroxy-3-methoxyphenyl) acrylamido) propyl)-5,7-dimethyladamantane-1-carboxamide (2). Synthesized from 17 (37 mg, 0.14 mmol) and 15 (71 mg, 0.28 mmol) to afford 2 as green solid: 31 mg (52%); mp 118-119 °C; ¹H NMR (400 MHz, CD₃OD) δ 7.43 (d, *J* = 16 Hz, 1H), 7.11 (s, 1H), 7.03-7.00 (m, 1H), 6.78 (d, *J* = 8 Hz, 1H), 6.41 (d, *J* = 16 Hz, 1H), 3.87 (s, 3H), 3.29 (t, *J* = 8 Hz, 2H), 3.22 (t, *J* = 8 Hz, 2H), 1.73-1.66 (m, 2H), 1.63 (s, 2H), 1.44 (s, 4H), 1.32-1.26 (m, 4H), 1.14 (s, 2H), 0.92 (s, 6H). ¹³C NMR (100 MHz, CD₃OD) δ 177.79, 168.00, 148.87, 148.00, 140.82, 126.55, 121.91, 117.08, 115.16, 110.09, 54.95, 50.48, 48.96, 48.41, 48.28, 44.09, 43.78, 43.43, 36.40, 36.37, 32.47, 28.98, 28.60. MS [ESI+] *m/z* 455 [M+1]⁺.

(1r,3s,5R,7S)-3-amino-*N*-(4-((*E*)-3-(4-hydroxy-3-methoxyphenyl) acrylamido) butyl)-5,7-dimethyladamantane-1-carboxamide (3). Synthesized from 17 (89 mg, 0.30 mmol) and 16 (160 mg, 0.61 mmol) to afford 3 as green solid: 68 mg (48%); mp 116-117 °C; ¹H NMR (400 MHz, CD₃OD) δ 7.40 (d, *J* = 15.6 Hz, 1H), 7.05 (s, 1H), 6.98-6.95 (m, 1H), 6.73 (d, *J* = 8 Hz, 1H), 6.37 (d, *J* = 15.6 Hz, 1H), 3.82 (s, 3H), 3.27-3.24 (m, 2H), 3.18-3.15 (m, 2H), 1.54-1.49 (m, 6H), 1.38-1.36 (m, 4H), 1.24 (s, 4H), 1.07 (s, 2H), 0.86 (s, 6H). ¹³C NMR (100 MHz, CD₃OD) δ 177.94, 167.83, 149.83, 148.29, 140.76, 126.04, 122.02, 116.86, 115.46,

110.03, 54.92, 49.76, 49.12, 49.09, 48.47, 44.22, 44.09, 43.91, 38.77, 38.63, 32.46, 28.76, 26.53, 26.44. MS [ESI+] m/z 470 [M+1]⁺.

General procedure for the intermediates 22-25. A mixture of memantine hydrochloride (MEM, 1 equiv), K₂CO₃ (2 equiv), KI (1 equiv) and the appropriate intermediate (18-21, 1 equiv) in dry DMF (2-5 ml) was placed in a microwave (140°C, 250 Psi, 100 W) and left stirring for 1 h. The solvent was removed under reduced pressure and the crude purified by chromatography on silica gel using dichloromethane/methanol/aqueous ammonia 33% (9:1:0.2) as mobile phase.

*tert-butyl (3-(((1*r*,3*R*,5*S*,7*r*)-3,5-dimethyladamantan-1-yl) amino) propyl) carbamate (22).* Synthesized from 18 [14](0.4 g, 1.2 mmol) to afford 22 as a pale oil: 0.24 g (59%); ¹H NMR (400 MHz, CDCl₃) δ 5.34 (br s, 1H), 3.16-3.14 (m, 2H), 2.65 (t, $J = 6.6$ Hz, 2H), 2.09-2.07 (m, 1H), 1.67-1.64 (m, 2H), 1.49 (s, 2H), 1.38 (s, 9H), 1.32-1.23 (m, 8H), 1.06-1.05 (m, 2H), 0.78 (s, 6H).

*tert-butyl (4-(((1*r*,3*R*,5*S*,7*r*)-3,5-dimethyladamantan-1-yl) amino) butyl) carbamate (23).* Synthesized from 19 [32](0.4 g, 1.5 mmol) to afford 23 as a pale oil: 0.35 g (87%); ¹H NMR (400 MHz, CDCl₃) δ 5.32 (br s, 1H), 3.00-2.99 (m, 2H), 2.63 (t, $J = 7.2$ Hz, 2H), 2.06-2.04 (m, 1H), 1.59-1.55 (m, 4H), 1.48-1.43 (m, 2H), 1.37-1.28 (m, 13H), 1.24-1.13 (m, 4H), 1.02-1.01 (m, 2H), 0.73 (s, 6H).

*tert-butyl (5-(((1*r*,3*R*,5*S*,7*r*)-3,5-dimethyladamantan-1-yl) amino) pentyl) carbamate (24).* Synthesized from 20 [33](0.4 g, 1 mmol) to afford 24 as a pale oil: 0.22 g (55%); ¹H NMR (400 MHz, CDCl₃) δ 5.31 (br s, 1H), 3.11-3.09 (m, 2H), 2.59 (t, $J = 7.4$ Hz, 2H), 2.15-2.13 (m, 1H), 1.54-1.42 (m, 15H), 1.40-1.25 (m, 10H), 1.16-1.11 (m, 2H), 0.85 (s, 6H).

*tert-butyl (6-(((1*r*,3*R*,5*S*,7*r*)-3,5-dimethyladamantan-1-yl) amino) hexyl) carbamate (25).* Synthesized from 21 [34](0.6 g, 1.6 mmol) to afford 25 as a pale oil: 0.4 g (79%); ¹H NMR (400 MHz, CDCl₃) δ 4.61 (br s, 1H), 2.99-2.97 (m, 2H), 2.48 (t, $J = 7.4$ Hz, 2H), 2.03-2.02 (m, 1H), 1.41-1.32 (m, 15H), 1.24-1.15 (m, 12H), 1.01-1.00 (m, 2H), 0.73 (s, 6H).

General procedure for the intermediates 26-29. To an ice-cooled appropriate Boc-protected intermediate (22-25, 1 equiv) was added HCl 4 M in dioxane (4 mL) and the reaction mixture was stirred at 0°C for 15-20 min under N₂ atmosphere. The solvent was evaporated, and the crude purified by flash chromatography on silica gel using dichloromethane/methanol/aqueous ammonia 33% (8:2:0.4) affording desired intermediates as free bases.

*N*¹-((1*r*,3*R*,5*S*,7*r*)-3,5-dimethyladamantan-1-yl)propane-1,3-diamine (26). Synthesized from 22 (0.24 g, 0.7 mmol) to afford 26 as a pale oil: 0.09 g (54%); ¹H NMR (400 MHz, DMSO-*d*₆) δ 3.94 (br s, 3H), 2.74-2.73 (m, 2H) 2.59 (t, *J* = 6.8 Hz, 2H), 2.06-2.04 (m, 1H), 1.57- 1.50 (m, 2H), 1.42-1.41 (m, 2H), 1.26-1.18 (m, 8H), 1.09-1.00 (m, 2H), 0.78 (s, 6H).

*N*¹-((1*r*,3*R*,5*S*,7*r*)-3,5-dimethyladamantan-1-yl)butane-1,4-diamine (27). Synthesized from 23 (0.35 g, 1 mmol) to afford 27 as a pale oil: 0.18 g (72%); ¹H NMR (400 MHz, CDCl₃) δ 2.66-2.62 (m, 5H), 2.53 (t, *J* = 6.8 Hz, 2H), 2.06-2.03 (m, 1H), 1.48-1.40 (m, 6H), 1.26-1.17 (m, 8H), 1.05-0.98 (m, 2H), 0.74 (s, 6H).

*N*¹-((1*r*,3*R*,5*S*,7*r*)-3,5-dimethyladamantan-1-yl)pentane-1,5-diamine (28). Synthesized from 24 (0.22 g, 0.6 mmol) to afford 28 as a pale oil: 0.11 g (70%); ¹H NMR (400 MHz, CDCl₃) δ 2.63 (t, *J* = 7.1 Hz, 2H), 2.52 (t, *J* = 7.1 Hz, 2H), 2.07-2.06 (m, 1H), 1.59 (br s, 3H), 1.42-1.38 (m, 6H), 1.31-1.17 (m, 10H), 1.05-1.04 (m, 2H), 0.78 (s, 6H).

*N*¹-((1*r*,3*R*,5*S*,7*r*)-3,5-dimethyladamantan-1-yl)hexane-1,6-diamine (29). Synthesized from 25 (0.4 g, 1.06 mmol) to afford 29 as a pale oil: 0.16 g (54%); ¹H NMR (400 MHz, CDCl₃) δ 2.63 (t, *J* = 7.2 Hz, 2H), 2.52 (t, *J* = 7.2 Hz, 2H), 2.38 (br s, 3H), 2.08-2.07 (m, 1H), 1.44-1.38 (m, 6H), 1.30-1.19 (m, 12H), 1.06-1.05 (m, 2H), 0.78 (s, 6H).

General procedure for compounds 4-7. To an ice-cooled solution of FA (1 equiv) in dry DMF (3-4 mL) was added HOBt (1.3 equiv) and EDC (1.3 equiv) under N₂ atmosphere. The reaction mixture was stirred for 10 min at 0°C, followed by addition of Et₃N (1.3 equiv) and the appropriate amine (26-29) (1

equiv). Stirring was then continued at room temperature overnight, then the solvent was evaporated under reduced pressure and the crude purified by chromatography on silica gel.

(*E*) - *N* - (3-(((1*r*,3*R*,5*S*,7*r*)-3,5-dimethyladamantan-1-yl) amino) propyl) - 3 - (4-hydroxy-3-methoxyphenyl) acrylamide (4). Synthesized from 26 (90 mg, 0.38 mmol), purified by chromatography on silica gel using petroleum ether/dichloromethane/methanol/aqueous ammonia 33% (2:6.5:1.5:0.16) as mobile phase to afford 4 as a yellow solid: 61.5 mg (39%); mp 213-215 °C; ¹H NMR (400 MHz, CDCl₃) δ 7.66 (br s, 1H), 7.49 (d, *J* = 15.6 Hz, 1H), 7.09 (s, 1H), 7.08-7.04 (m, 1H), 6.88 (d, *J* = 8 Hz, 1H), 6.64 (d, *J* = 15.6 Hz, 1H), 3.90 (s, 3H), 3.57-3.52 (m, 2H), 2.94-2.91 (m, 2H), 2.24 (m, 3H), 1.89-1.88 (m, 2H), 1.72-1.63 (m, 4H), 1.43-1.32 (m, 4H), 1.20 (s, 2H), 0.85 (s, 6H). ¹³C NMR (100 MHz, CDCl₃) δ 167.60, 147.53, 147.02, 140.33, 127.35, 122.15, 119.07, 114.87, 110.05, 59.04, 56.03, 49.88, 44.16, 41.92, 39.60, 38.59, 37.00, 32.57, 29.67, 26.77, 24.06. MS [ESI+] *m/z* 413 [M+1]⁺.

(*E*) - *N* - (4-(((1*r*,3*R*,5*S*,7*r*)-3,5-dimethyladamantan-1-yl) amino) butyl) - 3 - (4-hydroxy-3-methoxyphenyl) acrylamide (5). Synthesized from 27 (72.5 mg, 0.28 mmol), purified by chromatography on silica gel using petroleum ether/dichloromethane/methanol/aqueous ammonia 33% (2:6.5:1.5:0.07) as mobile phase to afford 5 as a yellow solid: 39.6 mg (32%); mp 174-175 °C; ¹H NMR (400 MHz, CDCl₃) δ 7.83 (br s, 1H), 7.41 (d, *J* = 15.6 Hz, 1H), 7.04 (s, 1H), 6.95 (d, *J* = 8.2 Hz, 1H), 6.86 (d, *J* = 8.2 Hz, 1H), 6.70 (d, *J* = 15.6 Hz, 1H), 3.81 (s, 3H), 3.33-3.32 (m, 2H), 2.82 (t, *J* = 7.4 Hz, 2H), 2.17 (s, 1H), 1.89-1.88 (m, 4H), 1.71-1.62 (m, 4H), 1.37-1.23 (m, 6H), 1.14 (s, 2H), 0.84 (s, 6H). ¹³C NMR (100 MHz, CDCl₃) δ 167.60, 147.53, 147.02, 140.33, 127.35, 122.15, 119.07, 114.87, 110.05, 59.04, 56.03, 49.88, 44.16, 41.92, 39.60, 38.59, 37.00, 32.57, 29.67, 26.77, 24.06. MS [ESI+] *m/z* 427 [M+1]⁺.

(*E*) - *N* - (5-(((1*r*,3*R*,5*S*,7*r*)-3,5-dimethyladamantan-1-yl) amino) pentyl) - 3 - (4-hydroxy-3-methoxyphenyl) acrylamide (6). Synthesized from 28 (54 mg, 0.2 mmol), purified by chromatography on silica gel using petroleum ether/dichloromethane/methanol/aqueous ammonia 33% (2:6.5:1.5:0.09) as mobile phase to afford 6 as a yellow solid: 27.7 mg (31%); mp 200-202 °C; ¹H

NMR (400 MHz, CDCl₃) δ 7.51 (d, *J* = 15.6 Hz, 1H), 7.03 (d, *J* = 7.6 Hz, 1H), 6.96 (s, 1H), 6.86 (d, *J* = 7.6 Hz, 1H), 6.31 (d, *J* = 15.6 Hz, 1H), 5.82 (br s, 1H), 3.86 (s, 3H), 3.37-3.33 (m, 2H), 2.61 (t, *J* = 7.2 Hz, 2H), 2.13-2.11 (m, 1H), 1.58-1.53 (m, 4H), 1.36-1.24 (m, 12H), 1.10-1.09 (m, 2H), 0.82 (s, 6H). ¹³C NMR (100 MHz, CDCl₃) δ 166.21, 147.43, 146.81, 140.72, 127.33, 121.93, 118.40, 114.84, 109.72, 55.86, 50.83, 48.43, 42.89, 40.83, 40.37, 39.52, 32.37, 30.24, 30.19, 29.45, 24.78. MS [ESI+] *m/z* 441 [M+1]⁺.

(*E*) - *N* - (6-(((1*r*,3*R*,5*S*,7*r*)-3,5-dimethyladamantan-1-yl) amino) hexyl) - 3 - (4-hydroxy-3-methoxyphenyl) acrylamide (7). Synthesized from 29 (0.1 g, 0.36 mmol), purified by chromatography on silica gel using petroleum ether/dichloromethane/methanol/aqueous ammonia 33% (2:6.5:1.5:0.1) as mobile phase to afford 7 as a yellow solid: 95.9 mg (59%); mp 203-204°C; ¹H NMR (400 MHz, CDCl₃) δ 7.51 (d, *J* = 15.2 Hz, 1H), 7.03 (d, *J* = 8.4 Hz, 1H), 6.97 (s, 1H), 6.86 (d, *J* = 8.4 Hz, 1H), 6.25 (d, *J* = 15.2 Hz, 1H), 5.73 (br s, 1H), 3.88 (s, 3H), 3.36-3.31 (m, 2H), 2.57 (t, *J* = 7.4 Hz, 2H), 2.12-2.09 (m, 1H), 1.54-1.45 (m, 6H), 1.33-1.23 (12H), 1.13-1.05 (m, 2H), 0.82 (s, 6H). ¹³C NMR (100 MHz, CDCl₃) δ 166.20, 147.57, 146.90, 140.74, 127.26, 121.96, 118.35, 114.90, 109.75, 55.85, 50.85, 48.42, 42.90, 40.79, 40.45, 39.54, 32.37, 30.24, 30.20, 29.50, 27.03, 26.73. MS [ESI+] *m/z* 455 [M+1]⁺.

Electrophysiological assays

Inhibition of NMDARs by compounds 1-7 and memantine was assessed by the expression of GluN1-1a and GluN2A subunits in *Xenopus* oocytes followed by voltage clamp recording. Oocytes were obtained from the European *Xenopus* Resource Centre (University of Portsmouth, UK) directly following their removal from mature female *Xenopus laevis* according to UK Home Office guidelines. Sections of the ovary were cut into smaller pieces and treated with 1 mg/mL collagenase type 1A (Sigma-Aldrich) in Ca²⁺-free modified Barth's media containing 96 mM NaCl, 2 mM KCl, 1 mM MgCl₂, 5 mM HEPES, 2.5 mM pyruvic acid, 0.5 mM theophylline, 0.05 mg/mL gentamicin, pH 7.5, with shaking at 18°C for 40-60 minutes, in order to separate them into individual defolliculated oocytes. The oocytes were then rinsed in Ca²⁺-free modified Barth's media multiple times until the solution

was clear and stored in modified Barth's media (as per Ca²⁺-free but including 1.8 mM CaCl₂). Oocytes were injected with 50 nL of cRNA encoding both the GluN1-1a and GluN2A subunits (1:1 by weight ratio; total 250 ng/μL). The cRNA was synthesized from linearized plasmid DNA (pRK7) containing the GluN-encoding genes using an mMessage mMachine kit (Invitrogen). Following injection, oocytes were kept in modified Barth's media at 18 °C for 3-4 days before electrophysiological testing. Voltage-clamp recording was conducted using an Axoclamp-2A voltage-clamp amplifier (Axon Instruments, USA). Microelectrodes were pulled from borosilicate glass capillaries (TW150F-4, World Precision Instruments) using a Sutter P-97 programmable micropipette puller to have a resistance of 0.5-2 MΩ when filled with 3 M KCl. Oocytes were placed in a perfusion chamber and constantly perfused (~5 mL/min) with solution containing 96 mM NaCl, 2 mM KCl, 1.8 mM CaCl₂, 10 mM HEPES, pH 7.5, and voltage-clamped at holding potentials (V_h) between -40 and -100 mV. NMDAR currents were initiated by application of 100 μM NMDA + 10 μM glycine. Once the current had reached a steady state (~30 s) the test compounds were introduced at concentrations ranging from 0.01 to 100 μM until a new plateau (inhibited current) was achieved. All agonists and test compounds were applied using an Automate Valvelink 8 perfusion system. Analogue output from the amplifier was digitized by a CED 1401 plus A/D converter at 100 Hz and recorded on a windows PC using WinEDR software (Dr John Dempster, University of Strathclyde, UK). NMDA/glycine-evoked current in the presence of test compound was normalized to that in its absence just before test compound addition (% control response) and plotted against concentration. Concentration-inhibition data were fit by:

$$\% \text{ control response} = \frac{100}{1 + 10^{((\log_{10} IC_{50} - X) \times HillSlope)}} \quad \text{Equation 1}$$

to obtain IC₅₀ values, where X = Log₁₀[compound]; using Graphpad Prism 7. All points were means of at least 5 separate oocytes. For voltage dependence studies the test compounds were applied at a single (~IC₅₀) concentration but at four V_hs in the range -40 to -100 mV. Data were normalized as above and fit by:

$$\% \text{ control response} = \frac{100}{(1 + [B]/K_D)e^{z\delta(FE/RT)}} \quad \text{Equation 2}$$

to obtain δ values (fraction of the membrane electric field crossed by the blocking compound), where [B] is the concentration of the blocker, K_D is the dissociation constant at 0 mV, z is the charge valence of the blocker, F is Faraday's constant, E is the membrane potential, R is the universal gas constant and T is absolute temperature; using Graphpad Prism 7. All points were means of at least 5 separate oocytes.

Reagents for cellular experiments (SH-SY5Y cells)

All hybrid compounds were solubilized in DMSO (at stock concentrations) and frozen (-20°C) in aliquots that were diluted immediately prior to use. For each experimental setting, one stock aliquot was thawed out and diluted to minimize compound damage due to repeated freeze and thaw cycles. The final concentration of DMSO in culture medium was $<0.1\%$. Ferulic Acid was purchased from Sigma Aldrich (Merck KGaA, Darmstadt, Germany). Rabbit polyclonal anti-human HO-1 (NBP1-31341) antibody was purchased from Novus (Biotechnie, Minneapolis USA). Mouse monoclonal anti- β -tubulin (T0198) was purchased from by Sigma Aldrich (Merck KGaA, Darmstadt, Germany).

Cell cultures

All culture media, supplements and Foetal Bovine Serum (FBS) were purchased from Sigma Aldrich (Merck KGaA, Darmstadt, Germany). Human neuroblastoma SH-SY5Y cells from the European Collection of Cell Cultures (ECACC No. 94030304) were cultured in a medium with equal amounts of Eagle's minimum essential medium and Nutrient Mixture Ham's F-12, supplemented with 10% heat-inactivated FBS, 2 mM glutamine, 0.1 mg/mL streptomycin, 100 IU/mL penicillin and non-essential aminoacids at 37°C in 5% CO_2 and 95% air atmosphere. H4-SW cells were cultured in D-MEM medium (Invitrogen, Carlsbad, CA) supplemented with 10% fetal bovine serum (FBS), 100 U/mL penicillin, 100 $\mu\text{g}/\text{mL}$ streptomycin and 2 mM L-

glutamine. Hygromycin B and Blastidicin S were used as selection antibiotics for SW mutation maintenance.

Cell Viability

The mitochondrial dehydrogenase activity that reduces 3-(4,5-dimethylthiazol-2-yl)-2,5-diphenyl-tetrazolium bromide (MTT, Sigma Aldrich, Merck KGaA, Darmstadt, Germany) was used to determine cellular viability, in a quantitative colorimetric assay. At day 0, SH-SY5Y cells were plated at a density of 2.5×10^4 viable cells per well in 96-well plates. After treatment, according to the experimental setting, cells were exposed to an MTT solution in complete medium (1 mg/mL). Following 4 h incubation with MTT and treatment with sodium dodecyl sulfate (SDS) for 24 h, cell viability reduction was quantified by using a Synergy HT multidetection microplate reader (Bio-Tek).

Measurement of Intracellular ROS

DCFH-DA (Sigma Aldrich, Merck KGaA, Darmstadt, Germany) was used to estimate intracellular ROS following two different experimental setting described in each figure legend. In each setting, cells were loaded with 25 μ M DCFH-DA for 45 min. After centrifugation DCFH-DA was removed, and the results were visualized using Synergy HT multidetection microplate reader (BioTek) with excitation and emission wavelengths of 485 and 530 nm, respectively.

Real-time PCR (RT-PCR)

For RNA extraction, 2×10^6 cells were used. Total RNA was extracted using a Direct-zol™ RNA MiniPrep (Zymo Research, Irvine, USA) following the manufacturer's instructions. QuantiTect reversion transcription kit and QuantiTect Sybr Green PCR kit (Qiagen, Valencia, CA, USA) were used for cDNA synthesis and gene expression analysis, following the manufacturer's specifications. Nrf2, HO-1, and GAPDH primers were provided by Qiagen. GAPDH was used as an endogenous reference.

Immunodetection of HO-1, flAPP and sAPP α

The expression of HO-1 in whole cell lysates was assessed by Western blot analysis. After treatment, cell monolayers were washed twice with ice-cold PBS, lysed on the culture dish by the addition of ice-cold homogenization buffer (50 mM Tris-HCl pH 7.4, 150 mM NaCl, 5 mM EDTA, 0.5% Triton X-100 and protease inhibitor mix) and an aliquot was used for protein quantification, whereas the remainder was prepared for western blot by mixing the cell lysate with 2X sample buffer (125 mM Tris-HCl pH 6.8, 4% SDS, 20% glycerol, 6% β -mercaptoethanol, 0.1% bromophenol blue) and then denaturing at 95°C for 5 min. Equivalent amounts of extracted proteins were loaded into a SDS-PAGE gel, electrophoresed under reducing conditions, transferred to a PVDF membrane (Sigma Aldrich, Merck KGaA, Darmstadt, Germany) and then blocked for 1 h with 5% w/v BSA in Tris-buffered saline containing 0.1% Tween 20 (TBS-T). The proteins were visualized using primary antibodies for HO-1, full length (fl) APP or soluble APP alpha (sAPP α) and α - or β -tubulin (1:1000) followed by secondary horseradish peroxidase conjugated antibody (1:5000) diluted in 5% w/v BSA in TBS-T. Tubulins were performed as a control for gel loading. Signal development was carried out using an enhanced chemiluminescent method (Pierce, Rockford, IL, USA).

Densitometry and statistics

All experiments, unless specified, were performed at least three times with representative results being shown. Data are expressed as mean \pm SEM. The relative densities of the acquired images of Western blotting bands were analyzed with ImageJ software. Statistical analyses were performed using Prism software version 7.0 (GraphPad Software, La Jolla, CA, USA). Statistical differences were determined by analysis of variance (ANOVA) followed, when significant, by an appropriate *post hoc* test as indicated in figure legends. A *p* value of <0.05 was considered statistically significant.

REFERENCES

1. Niu H, Álvarez-Álvarez I, Guillén-Grima F, Aguinaga-Ontoso I. Prevalence and incidence of Alzheimer's disease in Europe: A meta-analysis. *Neurologia*, 32(8), 523-532 (2017).

2. Traynelis SF, Wollmuth LP, McBain CJ *et al.* Glutamate receptor ion channels: structure, regulation, and function. *Pharmacol Rev*, 62(3), 405-496 (2010).
3. Müller MK, Jacobi E, Sakimura K, Malinow R, von Engelhardt J. NMDA receptors mediate synaptic depression, but not spine loss in the dentate gyrus of adult amyloid Beta (A β) overexpressing mice. *Acta Neuropathol Commun*, 6(1), 110 (2018).
4. Hardingham GE, Fukunaga Y, Bading H. Extrasynaptic NMDARs oppose synaptic NMDARs by triggering CREB shut-off and cell death pathways. *Nat Neurosci*, 5(5), 405-414 (2002).
5. Lipton SA. NMDA receptor activity regulates transcription of antioxidant pathways. *Nat Neurosci*, 11(4), 381-382 (2008).
6. Lanni C, Fagiani F, Racchi M *et al.* Beta-amyloid short- and long-term synaptic entanglement. *Pharmacol Res*, 139, 243-260 (2019).
7. Tu S, Okamoto S, Lipton SA, Xu H. Oligomeric A β -induced synaptic dysfunction in Alzheimer's disease. *Mol Neurodegener*, 9, 48 (2014).
8. Xia P, Chen HS, Zhang D, Lipton SA. Memantine preferentially blocks extrasynaptic over synaptic NMDA receptor currents in hippocampal autapses. *J Neurosci*, 30(33), 11246-11250 (2010).
9. Song X, Jensen M, Jogini V *et al.* Mechanism of NMDA receptor channel block by MK-801 and memantine. *Nature*, 556(7702), 515-519 (2018).
10. Takahashi H, Xia P, Cui J *et al.* Pharmacologically targeted NMDA receptor antagonism by NitroMemantine for cerebrovascular disease. *Sci Rep*, 5, 14781 (2015).
11. Figueiredo CP, Clarke JR, Ledo JH *et al.* Memantine rescues transient cognitive impairment caused by high-molecular-weight a β oligomers but not the persistent impairment induced by low-molecular-weight oligomers. *J Neurosci*, 33(23), 9626-9634 (2013).
12. Benchekroun M, Romero A, Egea J *et al.* The Antioxidant Additive Approach for Alzheimer's Disease Therapy: New Ferulic (Lipoic) Acid Plus Melatonin Modified Tacrines as Cholinesterases Inhibitors, Direct Antioxidants, and Nuclear Factor (Erythroid-Derived 2)-Like 2 Activators. *J Med Chem*, 59(21), 9967-9973 (2016).
13. Lipton SA. Paradigm shift in neuroprotection by NMDA receptor blockade: memantine and beyond. *Nat Rev Drug Discov*, 5(2), 160-170 (2006).
14. Simoni E, Daniele S, Bottegoni G *et al.* Combining galantamine and memantine in multitargeted, new chemical entities potentially useful in Alzheimer's disease. *J Med Chem*, 55(22), 9708-9721 (2012).
15. Reggiani AM, Simoni E, Caporaso R *et al.* *In Vivo* Characterization of ARN14140, a Memantine/Galantamine-Based Multi-Target Compound for Alzheimer's Disease. *Sci Rep*, 6, 33172 (2016).
16. Minniti E, Byl JAW, Riccardi L *et al.* Novel xanthone-polyamine conjugates as catalytic inhibitors of human topoisomerase II α . *Bioorg Med Chem Lett*, 27(20), 4687-4693 (2017).

17. Riva E, Comi D, Borrelli S *et al.* Synthesis and biological evaluation of new camptothecin derivatives obtained by modification of position 20. *Bioorg Med Chem*, 18(24), 8660-8668 (2010).
18. Wanka L, Cabrele C, Vanejews M, Schreiner P. gamma-aminoadamantanecarboxylic acids through direct C-H bond amidations. *European Journal of Organic Chemistry*, (9), 1474-1490 (2007).
19. Sobolevsky A, Koshelev S, Khodorov B. Probing of NMDA channels with fast blockers. *Journal of Neuroscience*, 19(24), 10611-10626 (1999).
20. Woodhull AM. Ionic blockage of sodium channels in nerve. *J Gen Physiol*, 61(6), 687-708 (1973).
21. Cuadrado A, Rojo AI, Wells G *et al.* Therapeutic targeting of the NRF2 and KEAP1 partnership in chronic diseases. *Nat Rev Drug Discov*, 18(4), 295-317 (2019).
22. Dinkova-Kostova AT, Kostov RV, Canning P. Keap1, the cysteine-based mammalian intracellular sensor for electrophiles and oxidants. *Arch Biochem Biophys*, 617, 84-93 (2017).
23. Basagni F, Lanni C, Minarini A, Rosini M. Lights and shadows of electrophile signaling: focus on the Nrf2-Keap1 pathway. *Future Med Chem*, 11(7), 707-721 (2019).
24. Simoni E, Serafini MM, Caporaso R *et al.* Targeting the Nrf2/Amyloid-Beta Liaison in Alzheimer's Disease: A Rational Approach. *ACS Chem Neurosci*, 8(7), 1618-1627 (2017).
25. Simoni E, Bergamini C, Fato R *et al.* Polyamine conjugation of curcumin analogues toward the discovery of mitochondria-directed neuroprotective agents. *J Med Chem*, 53(19), 7264-7268 (2010).
26. Bordji K, Becerril-Ortega J, Nicole O, Buisson A. Activation of extrasynaptic, but not synaptic, NMDA receptors modifies amyloid precursor protein expression pattern and increases amyloid- β production. *J Neurosci*, 30(47), 15927-15942 (2010).
27. Folch J, Busquets O, Ettcheto M *et al.* Memantine for the Treatment of Dementia: A Review on its Current and Future Applications. *J Alzheimers Dis*, 62(3), 1223-1240 (2018).
28. Alley GM, Bailey JA, Chen D *et al.* Memantine lowers amyloid-beta peptide levels in neuronal cultures and in APP/PS1 transgenic mice. *J Neurosci Res*, 88(1), 143-154 (2010).
29. Bordji K, Becerril-Ortega J, Buisson A. Synapses, NMDA receptor activity and neuronal A β production in Alzheimer's disease. *Rev Neurosci*, 22(3), 285-294 (2011).
30. Habib A, Sawmiller D, Tan J. Restoring Soluble Amyloid Precursor Protein α Functions as a Potential Treatment for Alzheimer's Disease. *J Neurosci Res*, 95(4), 973-991 (2017).
31. Palermo G, Minniti E, Greco M *et al.* An optimized polyamine moiety boosts the potency of human type II topoisomerase poisons as quantified by comparative analysis centered on the clinical candidate F14512. *Chemical Communications*, 51(76), 14310-14313 (2015).
32. Nguyen C, Ruda GF, Schipani A *et al.* Acyclic nucleoside analogues as inhibitors of *Plasmodium falciparum* dUTPase. *J Med Chem*, 49(14), 4183-4195 (2006).

33. Lamanna G, Smulski C, Chekkat N et al. Multimerization of an Apoptogenic TRAIL-Mimicking Peptide by Using Adamantane-Based Dendrons. *Chemistry-a European Journal*, 19(5), 1762-1768 (2013).
34. Zanichelli V, Bazzoni M, Arduini A et al. Redox-Switchable Calix[6]arene-Based Isomeric Rotaxanes. *Chemistry*, 24(47), 12370-12382 (2018).

CHAPTER 3

Immune response in COVID-19:
a critical dissertation of potential pharmacological treatments

PART I

The following manuscript was published in *Signal Transduction and Targeted Therapy* in 2020 as:

Immune response in COVID-19: addressing a pharmacological challenge by targeting pathways triggered by SARS-CoV-2

Michele Catanzaro, Francesca Fagiani, Marco Racchi, Emanuela Corsini, Stefano Govoni and Cristina Lanni

Abstract

To date, no vaccines or effective drugs have been approved to prevent or treat COVID-19 and the current standard care relies on supportive treatments. Therefore, based on the fast and global spread of the virus, urgent investigations are warranted in order to develop preventive and therapeutic drugs. In this regard, treatments addressing the immunopathology of SARS-CoV-2 infection have become a major focus. Notably, while a rapid and well-coordinated immune response represents the first line of defense against viral infection, excessive inflammatory innate response and impaired adaptive host immune defense may lead to tissue damage both at the site of virus entry and at systemic level. Several studies highlight relevant changes occurring both in innate and adaptive immune system in COVID-19 patients. In particular, the massive cytokine and chemokine release, the so-called "cytokine storm", clearly reflects a widespread uncontrolled dysregulation of the host immune defense. Although the prospective of counteracting cytokine storm is compelling, a major limitation relies on the limited understanding of the immune signaling pathways triggered by SARS-CoV-2 infection. The identification of signaling pathways altered during viral infections may help to unravel the most relevant molecular cascades implicated in biological processes mediating viral infections and to unveil key molecular players that may be targeted. Thus, given the key role of the immune system in COVID-19, a deeper understanding of the mechanism behind the immune dysregulation might give us clues for the clinical management of the severe cases and for preventing the transition from mild to severe stages.

Keywords: SARS-CoV-2; inflammation; immune signaling; NF- κ B; JAK/STAT; sphingosine-1-phosphate.



REVIEW ARTICLE OPEN

Immune response in COVID-19: addressing a pharmacological challenge by targeting pathways triggered by SARS-CoV-2

Michele Catanzaro¹, Francesca Fagiani^{1,2}, Marco Racchi¹, Emanuela Corsini³, Stefano Govoni¹ and Cristina Lanni¹

¹Department of Drug Sciences (Pharmacology Section), University of Pavia, V.le Taramelli 14, 27100 Pavia, Italy; ²Scuola Universitaria Superiore IUSS Pavia, P.zza Vittoria, 15, 27100 Pavia, Italy and ³Laboratory of Toxicology, Department of Environmental and Political Sciences, Università Degli Studi di Milano, Via Balzaretti 9, 20133 Milano, Italy
Correspondence: Cristina Lanni (cristina.lanni@unipv.it)
These authors contributed equally: Michele Catanzaro, Francesca Fagiani

INTRODUCTION

The outbreak of the novel coronavirus disease 2019 (COVID-19), induced by severe acute respiratory syndrome coronavirus 2 (SARS-CoV-2), originated in Wuhan, in the Hubei province of China, in December 2019, has rapidly spread worldwide, becoming a global public health emergency. On 11th March 2020, the World Health Organization (WHO) declared COVID-19 a pandemic. As of April 28, 2020, WHO reports more than 2,8 million confirmed cases and 198 842 deaths worldwide (WHO, 2020, <https://covid19.who.int>). After the isolation of SARS-CoV-2, the viral genome was sequenced, thus facilitating diagnostic testing, epidemiologic tracking, as well as investigations on potential preventive and therapeutic strategies in the management of COVID-19. To date, despite the intense scientific effort demonstrated by more than 600 clinical trials currently underway (typing SARS-CoV-2 on clinicaltrials.gov), no vaccines or effective drugs have been approved to prevent or treat COVID-19 and the current standard care is supportive treatment. Therefore, based on the fast and global spread of the virus, urgent investigations are warranted in order to develop effective therapies. Within this context, treatments addressing the immunopathology of the infection have become a major focus.

VIROLOGY AND HOST-PATHOGEN INTERACTION

The new human-infecting severe acute respiratory syndrome coronavirus 2 (SARS-CoV-2) is a positive-sense single-stranded RNA-enveloped virus belonging to CoV family.¹ Among the six CoVs pathogenic to humans, four of them have been associated with mild respiratory symptoms,² while two SARS-CoV and the Middle East respiratory syndrome (MERS) CoV (MERS-CoV), whose epidemic outbreaks took place in 2002 and 2012 respectively, caused severe respiratory diseases in affected individuals.² SARS-CoV-2 is the seventh identified CoV and, after SARS-CoV and MERS-CoV, the third zoonotic virus of CoVs that has been transmitted from animals to humans via an intermediate mammalian host.^{3,4} In particular, based on genetic analysis, Chinese horseshoe bats have been proposed to serve as natural reservoir hosts for SARS-CoV-2, similar to SARS-CoV and MERS-CoV.⁴⁻⁶ Moreover, genomic analysis indicates that SARS-CoV-2 is in the same beta-CoV clade as SARS-CoV and MERS-CoV.¹ In particular, SARS-CoV-2 has been observed to share almost 80% of the genome with SARS-CoV^{1,6,7} and almost all encoded proteins of SARS-CoV-2 are homologous to SARS-CoV proteins.¹ In contrast, SARS-CoV-2 has been found to be more distant from MERS-CoV, with only 50% identity.¹ Moreover, the entry of SARS-CoV-2 into human host cells has been found to rely on the same receptor as SARS-CoV: the surface angiotensin-converting enzyme 2 (ACE2), which is expressed in the type II surfactant-secreting alveolar cells of the lungs.^{8,9} Consistently, despite amino acid variations at specific key residues, homology modelling revealed a structural similarity between the receptor-binding domains of SARS-CoV and SARS-CoV-2.¹ However, further studies are necessary to compare SARS-CoV and SARS-CoV-2 affinities to ACE2 receptor that might explain the increased transmissibility and greater virulence of SARS-CoV-2 compared to SARS-CoV.⁸

Two independent groups provided key insights into the first step of SARS-CoV2 infection, by demonstrating that ACE2 host receptor is required for host cell entry of SARS-CoV-2.^{8,10} Noteworthy, the expression of ACE2 receptors is not only restricted to the lung, and extrapulmonary spread of SARS-CoV in ACE-expressing tissues has been demonstrated.¹¹⁻¹³ Hence the same pattern

may be expected for SARS-CoV-2, with most of human tissues, such as oral mucosa and gastrointestinal tract, kidney, heart, blood vessels expressing ACE2 receptors, particularly prone to SARS-CoV-2 infection.^{14,15} The viral entry of SARS-CoV-2 has been further found to be prevented by a clinically proven inhibitor of the cellular host type 2 transmembrane serine protease TMPRSS2 (camostat mesylate).⁸ Priming of the envelope-located trimeric spike (S) protein by host proteases, which cleave at the S1/S2 and the S2' sites, has been described as a fundamental step for viral entry, and the host protease TMPRSS2 emerged as a key cellular factor necessary for the priming of S protein and for the consequent membrane fusion and viral internalization by endocytosis in the pulmonary epithelium.⁸ Hence, TMPRSS2 has been proposed as a potential target for clinical intervention^{6,8} and its inhibitor camostat mesylate, approved for human use in Japan to treat pancreatic inflammation, has attracted the attention of the scientific community. Currently, a randomized, placebo-controlled, phase IIa trial is investigating the use of camostat mesylate (NCT04321096) and is expected to run until December 2020, whereas another independent trial will start in June 2020 to evaluate the efficacy of camostat mesilate in combination with hydroxychloroquine in hospitalized patients with moderate coronavirus disease 2019 (COVID-19) infection (NCT04338906).

A detailed analysis of additional mechanisms of cellular viral infection for SARS-CoV-2 is still missing and would be fundamental to identify further potential biological substrates to target.

IMMUNOPATHOLOGY OF COVID-19

The majority of COVID-19 cases (about 80%) is asymptomatic or exhibits mild to moderate symptoms, but approximately the 15% progresses to severe pneumonia and about 5% eventually develops acute respiratory distress syndrome (ARDS), septic shock and/or multiple organ failure.^{16,17} As for SARS and MERS, the most common symptoms of COVID-19 are fever, fatigue, and

respiratory symptoms, including cough, sore throat and shortness of breath.^{16,18}

Notably, SARS-CoV-2 infection activates innate and adaptive immune response, thus sustaining the resolution of COVID-19. While a rapid and well-coordinated immune response represents the first line of defense against viral infection, excessive inflammatory innate response and dysregulated adaptive host immune defense may cause harmful tissue damage at both at the site of virus entry and at systemic level. The excessive pro-inflammatory host response has been hypothesized to induce an immune pathology resulting in the rapid course of acute lung injury (ALI) and ARDS occurring in SARS-CoV-2 infected patients.¹⁶⁻¹⁸ For example, the massive cytokine and chemokine release, the so-called "cytokine storm", clearly reflects a widespread uncontrolled dysregulation of host immune defense. Thus, given the key role of the immune system in COVID-19, a deeper understanding of the mechanism behind the immune dysregulation, as well as of SARS-CoV-2 immune-escape mechanisms might give us clues for the clinical management of the severe cases and for preventing the transition from mild to severe stages. Moreover, although no within the goal of the present review, future investigations concerning the systemic effects of uncontrolled immune system on other physiological systems, such as the gastrointestinal tract, neuroendocrine, renal and cardiovascular are urgent.

Immune response to SARS-CoV-2

Several studies highlight relevant changes occurring both in innate and adaptive immune system in COVID-19 patients. In particular, lymphocytopenia and a modulation in total neutrophils are common hallmarks and seem to be directly correlated with disease severity and death.^{6,18} In patients with severe COVID-19, a marked decrease in the levels of absolute number of circulating CD4⁺ cells, CD8⁺ cells, B cells and natural killers (NK) cells,^{16,17,19} as well as a decrease in monocytes, eosinophils and basophils has been reported.¹⁹⁻²¹ In addition, most of patients with severe COVID-19 displayed significantly increased serum levels of pro-inflammatory cytokines (e.g. IL-6, IL-1 β , IL-2, IL-8, IL-17, G-CSF, GM-CSF, IP-10, MCP-1,

CCL3, and TNF α).^{20,22} Although no direct evidence for pro-inflammatory cytokines and chemokines involvement in lung pathology in COVID-19 has been reported, an increase in serum cytokine and chemokine levels, as well as in neutrophil-lymphocyte-ratio (NLR) in SARS-CoV-2 infected patients has been correlated with the severity of the disease and adverse outcomes, suggesting a possible role for hyper-inflammatory responses in COVID-19 pathogenesis.²⁰ Moreover, a recent multicenter retrospective cohort study analyzing data from the Early Risk Stratification of Novel Coronavirus Pneumonia (ERS-COVID-19) study (ChiCTR2000030494) showed that patients with COVID-19 had elevated high-sensitivity C-reactive protein (Hs-CRP) and procalcitonin serum levels, two major inflammation markers associated with high risks of mortality and organ injury.²³

Noteworthy, MERS-CoV has been demonstrated to infect THP-1 cells, human peripheral blood monocyte-derived macrophages and dendritic cells, and SARS-CoV to directly infect macrophages and T cells,²⁴ thereby inducing delayed but elevated levels of pro-inflammatory cytokines and chemokines.^{25,26} However, ACE2 receptor is only minimally expressed in monocytes, macrophages, and T cells in the lung, hence, the mechanism by which SARS-CoV directly infects immune cells is still unknown.²⁷ Taking into account the similarities between SARS-CoV and SARS-CoV-2, it is likely that also this latter may infect monocytes and macrophages by a mechanism that has to be still unveiled. In this regard, it is possible that the virus may be capable to bind other specific receptors and/or other mechanisms of viral entry mode can be exploited by the virus.

As far as concerns the adaptive immunity, the novel SARS-CoV-2 has been demonstrated to mainly affect lymphocyte counting and balance. In particular, Li *et al.* reported that, compared to survivors, dead COVID-19 patients showed lower percentage and count in CD3⁺, CD4⁺, and CD8⁺ lymphocytes populations, strong predictive values for in-hospital mortality, organ injury, and severe pneumonia.²³

In a retrospective, single-center study enrolling a cohort of 452 patients with COVID-19 in Wuhan, patients with severe COVID-19 displayed a significantly

lower number of total T cells, both helper T cells and suppressor T cells.²⁰ In particular, among helper T cells, a decrease in regulatory T cells, with a more pronounced reduction according to the severity of the cases, and in memory T cells has been observed, whereas the percentage of naïve T cells was found increased.²⁰ Notably, naïve and memory T cells are essential immune components, whose balance is crucial for maintaining a highly efficient defensive response. Naïve T cells enable the defenses against new and previously unrecognized infection by a massive and tightly coordinated release of cytokines, whereas memory T cells mediate antigen-specific immune response. A dysregulation in their balance, favoring naïve T cells activity compared to regulatory T cells, could highly contribute to hyperinflammation. A reduction in memory T cells on the other hand could be implicated in COVID-19 relapse, since a number of recurrences has been reported in recovered cases of COVID-19.^{6,28} These data are consistent with results reported by Tan *et al.*²⁹ Overall, the lymphopenia observed in COVID-19 patients may depend on the fact that SARS-CoV-2 may directly infect lymphocytes minimally expressing ACE2, leading to lymphocyte death or, alternatively, may directly damage lymphatic organs since they express ACE2 receptors.²⁹ However, to date no data are available on lymph nodes and spleen shrinking and lymphocytes functionalities, hence such speculations need to be further investigated to confirm these hypotheses.

As far as concerns B cells, by using single-cell RNA sequencing to characterize the transcriptome landscape of blood immune cell subsets during the recovery stage of COVID-19, Wen *et al.* found significant changes in B cells.³⁰ In particular, while the naïve B cells have been reported to be decreased, the plasma cells have been found remarkably increased in peripheral blood mononuclear cells.³⁰ Moreover, several new B cell-receptor changes have been identified (e.g. IGHV3-23 and IGHV3-7).³⁰ In addition, isotypes, including IGHV3-15, IGHV3-30, and IGKV3-11, previously used for virus vaccine development have been confirmed.³⁰ The strongest pairing frequencies, IGHV3-23-IGHJ4, has been suggested to indicate a monoclonal state associated with SARS-CoV-2 specificity.³⁰ Moreover, given the pivotal role of B cells in the control of infections, tracking the antibody seroconversion response is an important process for the clinical evaluation of

infections. In COVID-19 patients, while serum samples from patients with COVID-19 showed no cross-binding to the S1 subunit of the SARS-CoV spike antigen, some cross-reactivity of serum samples has been observed from patients with COVID-19 to nucleocapsid antigens of SARS-CoV.³¹ Interestingly, this study reports that 96.8% of tested patients achieved seroconversion of IgG or IgM within 20 days after symptom onset with a titer plateaued within 6 days after seroconversion.³¹ Moreover, 100% of patients had positive virus-specific IgG approximately 17-19 days after symptom onset.³¹ Instead, 94.1% patients showed positive virus-specific IgM approximately 20-22 days after symptom onset.³¹

In addition to these observations about immunity, a critical aspect has to be raised concerning the ability to escape from anti-viral host defenses. Viral evasion of host immune response is in fact believed to play a major role in disease severity.³² As an example, SARS-CoV and MERS-CoV escape and suppress the signaling pathways mediated by type I Interferon (IFN), a key cytokine secreted by virus-infected cells to enroll nearby cells to heighten their anti-viral immune defenses.³³ Based on genomic sequence comparison and on partial identity of SARS-CoV-2 with SARS-CoV, it is speculative that SARS-CoV-2 can adopt similar strategies to modulate the host innate immune response, thus evading immune detection and dampening human defenses.

Inflammatory cytokine storm and lung damage

Mounting clinical evidence from severe COVID-19 patients suggests that extensive changes in the serum levels of several cytokines play a pivotal role in the pathogenesis of COVID-19.^{22,34,35} Such hypercytokinemia, the so-called "cytokine storm", has been proposed as one of the key leading factors that trigger the pathological processes leading to plasma leakage, vascular permeability, and disseminated vascular coagulation, observed in COVID-19 patients, and accounting for life-threatening respiratory symptoms.¹⁷ Huang *et al.* found that plasma concentrations of IL-1 β , IL-1ra, IL-7, IL-8, IL-9, IL-10, basic FGF, G-CSF, G-MCSF, IFN γ , IP-10, MCP1, MIP-1 α , MIP-1 β , PDGF, TNF α , and VEGF were higher in both ICU (intensive care unit) patients and non-ICU patients than in healthy adults.¹⁶ Moreover, when comparing ICU and non-

ICU patients, plasma concentrations of IL-2, IL-7, IL-10, G-CSF, IP-10, MCP-1, MIP-1 α , and TNF α were higher in ICU patients than non-ICU patients, thus indicating that the cytokine storm might be correlated with disease severity.¹⁶ Another study on a small set of patients with severe COVID-19 pneumonia, found 15 cytokines (IFN- α 2, IFN- γ , IL-1ra, IL-2, 4, 7, 10, 12 and 17, chemokine IP-10, as well as G-CSF and M-CSF) associated with lung injury based on Murray score.³⁵ Evidence from literature indicates that the cytokine storm observed in COVID-19 resembles that occurring in Cytokines Release Syndrome (CRS), a form of systemic inflammatory response syndrome, and in secondary haemophagocytic lymphohistiocytosis (sHLH), an hyperinflammatory syndrome characterized by fulminant and fatal hypercytokinemia with multiorgan failure, mainly induced by viral infections.^{22,36} Therefore, as detailed below, existing pharmaceutical modulators of cytokines might be repurposed as therapeutic strategy to attenuate the hypercytokinemia in COVID-19 patients.

Interestingly, Gou *et al.* recently reported that the disruption of gut microbiome features by host and environmental factors may predispose healthy individuals to abnormal inflammatory response observed in COVID-19.³⁷ In particular, the authors constructed a blood proteomic risk score for the prediction of COVID-19 progression to clinically severe phase and observed that core gut microbiota features were significantly correlated with proinflammatory cytokines in a set of 366 individuals, using a machine learning model.³⁷ Specifically, *Bacteroides* genus, *Streptococcus* genus and *Clostridiales* order have been negatively correlated with most of the tested inflammatory cytokines, whereas *Ruminococcus* genus, *Blautia* genus and *Lactobacillus* genus have been positively associated.³⁷ Moreover, fecal metabolomics analysis indicated some potential amino acid-related pathways (e.g. aminoacyl-tRNA biosynthesis pathway, arginine biosynthesis pathway, and valine, leucine and isoleucine biosynthesis pathway) that correlate core microbial features with host inflammation among 987 participants.³⁷ Thus, the core intestinal microbiological characteristics, along with its related metabolites, should be further investigated as potential predictors for the individual susceptibility to COVID-19 progression and severity and might represent potential targets for the prevention of

susceptible populations, as well as for the development of therapeutic approaches to manage COVID-19.

PUTATIVE SIGNALING PATHWAYS TRIGGERED BY SARS-COV-2

It is well-established that, upon binding of the viral spike protein to the host cells by the entry receptor ACE2, the viral RNAs, as pathogen-associated molecular patterns (PAMPs), are detected by the pattern recognition receptors, which include the family of Toll-like receptors (TLRs). In particular, for RNA virus such as CoVs, viral genomic RNA or the intermediates during viral replication, including dsRNA, are recognized by either the endosomal RNA receptors, TLR3 and TLR7/8, and the cytosolic RNA sensor, retinoic acid-inducible gene (RIG-I)/MDA5.³⁸ Consistently, such TLRs have been found to activate different signaling pathways in human CD14⁺ monocytes, correlating with differential type I IFN and cytokine secretion involved in CD4⁺ T cells polarization.³⁸ As a result of virus recognition, downstream transduction pathways, crucial for proper antiviral response, such as IRF3 (IFN regulatory factor-3), nuclear factor κ B (NF- κ B), JAK (Janus kinase)/STAT (signal transducer and activator of transcription) signaling pathways, are activated.³⁹ The identification of the most relevant intracellular signaling pathways involved in the modulation of host immune systems may give important hints on how to overcome the infectious disease driven by SARS-CoV-2. In particular, taking into account the structural similarities of SARS-CoV-2 as well as the analogies in the infection mechanisms with pathogenic SARS-CoV, it is tempting to speculate that the viral infection may induce the activation of shared intracellular pathways, in particular of those mainly involved in the innate immune response. However, to date, it has to be demonstrated whether such sequence similarities between SARS-CoV and SARS-CoV-2 can be directly translated into similar biological outcomes. Taking into account such limitation, the identification of signaling pathways altered during viral infections may help to unravel the most relevant molecular cascades implicated in biological processes mediating viral infections and to unveil key molecular players that may be targeted. The advantage of targeting

intracellular molecules rather than viral proteins is that their effect is not likely to be negated by mutations in the virus genome. In fact, antiviral drugs inhibiting virus replication may select for mutational escape, thus rendering the therapy ineffective. Thus, the modulation of the host immune response shows the potential advantage of exerting less-selective pressure on viral populations.⁴⁰ Repurposing of existing drugs targeting specific signal transducers will be discussed as potential treatment options for the management of COVID-19, as schematized in **Figure 1**.

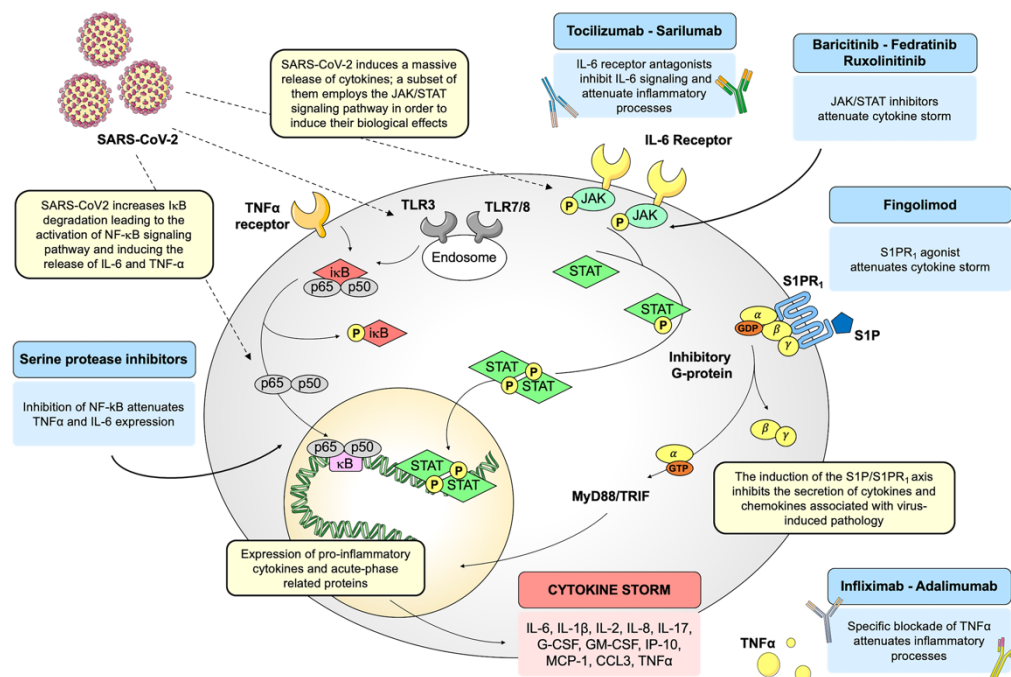


Figure 1. Schematic representation of SARS-CoV-2-driven signaling pathways and potential drug targets. Schematic representation of host intracellular signaling pathways induced by SARS-CoV-2 infection. Selected drugs, acting on these pathways, are repurposed to manage the cytokine storm induced by the viral infection. SARS-CoV-2, severe acute respiratory syndrome coronavirus 2; I κ B, inhibitor of nuclear factor κ B; NF- κ B, p65-p50, nuclear factor κ B; IL-6, interleukin 6; IL-1 β , interleukin 1 β ; IL-2, interleukin 2; IL-8, interleukin 8; IL-17, interleukin 17; G-CSF, granulocyte-colony stimulating factor; GM-CSF, granulocyte macrophage-colony stimulating factor; IP-10, IFN- γ -induced protein 10; MCP-1, monocyte chemoattractant protein 1; CCL3, chemokine (C-C motif) ligand 3; TNF α , Tumor necrosis factor

α ; JAK, Janus kinase; STAT, signal transducer and activator of transcription; S1P, sphingosine-1-phosphate; S1PR1, sphingosine-1-phosphate receptor 1; MyD88, myeloid differentiation primary response gene 88; TRIF, TIR-domain-containing adapter-inducing IFN- β .

The NF- κ B/TNF α signaling pathway

The transcription factor NF- κ B is a critical regulator of both innate and adaptive immunity.⁴¹ Under basal conditions, NF- κ B is retained in the cytoplasm by the inhibitory proteins (I κ Bs). A variety of cellular stimuli, including pathogens, induce I κ B phosphorylation, ubiquitination and degradation by the proteasome, thereby promoting NF- κ B nuclear translocation.⁴¹ In the nucleus, NF- κ B induces the transcription of a wide spectrum of genes encoding pro-inflammatory cytokines and chemokines, stress-response proteins, and anti-apoptotic proteins. NF- κ B activity is essential for survival and activation, and for initiating and propagating optimal immune responses.⁴² By contrast, the constitutive activation of the NF- κ B pathway is often associated with inflammatory diseases, such as rheumatoid arthritis and asthma. Notably, the exacerbation of NF- κ B activation has been reported to be implicated in lung inflammatory immunopathology induced by respiratory viruses, including SARS-CoV.^{43,44} Moreover, Wang and collaborators demonstrated that, in murine macrophages cell line (RAW264.7), the exposure to recombinant SARS-CoV spike protein induced a massive protein release of IL-6 and TNF α in a time- and concentration-dependent manner in the supernatants and that such increase in IL-6 and TNF α secretion relies on the activation of NF- κ B signaling pathway.⁴⁵ In fact, SARS-CoV spike protein has been associated with an increase in I κ B α degradation, an essential step required for the activation of NF- κ B signaling pathway.⁴⁵ Accordingly, transfection with dominant-negative NIK, which inhibits NF- κ B activation, produced a strong reduction in spike protein IL-6 and TNF α release in RAW264.7 cells, thus demonstrating that NF- κ B is required for the induction of IL-6 and TNF α by SARS-CoV spike protein.⁴⁵ Such *in vitro* data were consistent with results obtained *in vivo*, where treatments with drugs inhibiting NF- κ B activation (such as caffeic acid phenethyl ester (CAPE), Bay11-7082, and parthenolide) reduced inflammation by suppressing the mRNA expression of TNF α , CXCL2, and MCP-1 in the lung of SARS-CoV-infected mice. Moreover, pharmacological

inhibition of NF- κ B protected against pulmonary pathology and enhanced mice survival after SARS-CoV infection.⁴³

In line with these findings, Smits *et al.* demonstrated that SARS-CoV-infected aged macaques show in the lungs an increase in NF- κ B nuclear translocation, as a result of NF- κ B activation, and developed a stronger host response to virus infection compared to young adult macaques, with a significant increase in the expression of pro-inflammatory genes mainly regulated by NF- κ B.⁴⁴

Taken together these data suggest that NF- κ B inhibition might be an effective strategy to counteract pathogenic SARS-CoV. However, targeting NF- κ B is an approach strongly limited by intrinsic pathways complexity. Molecules blocking NF- κ B lack for specificity and interfere with NF- κ B physiological roles in cellular homeostasis, resulting in increased risk of undesired side effects, such as a broad suppression of innate immunity.⁴⁶ Moreover, within the context of viral infection, a major limitation of targeting NF- κ B signaling depends on the ability of viruses to efficiently escape, by encoding proteins specifically blocking this pathway.⁴⁶ Thus, a promising strategy may rely on directly targeting the downstream effectors of the pathway, such as TNF α , whose expression is mainly controlled by NF- κ B transcriptional activity. While TNF α is known to play a key role in the coordination and development of the inflammatory response, especially in the acute phase, long-lasting and excessive production of TNF α may become less effective by possibly altering TNF/TNF receptor signaling threshold which, after an initial wave of NF- κ B activation, favors sustained basal NF- κ B activity.⁴⁷ In addition, despite many other pro-inflammatory cytokines and mediators are involved in the cytokine storm, specific blockade of TNF α has been reported to be clinically effective in several pathological conditions. Accordingly, TNF α blockers, such as infliximab and adalimumab, have been successfully used for the treatment of several immune-mediated disorders, such as psoriasis, rheumatoid arthritis, inflammatory bowel diseases and ankylosing spondylitis.^{48,49} Hence, anti-TNF α monoclonal antibodies are likely to attenuate inflammatory processes occurring in COVID-19, reducing the release of other inflammatory-exacerbating mediators. Indeed, when an anti-TNF α is administered in patients with active rheumatoid arthritis, it has been demonstrated to induce

a rapid decrease of a broad spectrum of cytokines (e.g. IL-6 and IL-1), as well as of others acute-phase related proteins and vascular permeability factor.⁵⁰⁻⁵²

Furthermore, the envelope viral spike protein of SARS-CoV has been found to promote the activity of TNF α -converting enzyme (TACE)-dependent shedding of ACE2 receptor, which is a fundamental step for virus entry into the cell.⁵³ Thus, TNF α blockers represent effective therapeutic tools to counteract SARS-CoV infection by exerting a dual mechanism of action: attenuation of inflammation and inhibition of viral infection.⁴⁵ However, warnings about the potential increased risk of bacterial and fungal superinfections due to anti-TNF α therapy have to be taken into account.⁵⁴ Taking into account the sequence similarities between SARS-CoV and SARS-CoV-2 and the strong limitation in directly inhibiting NF- κ B, to date, a clinical trial investigating adalimumab for the management of COVID-19 has been registered in the Chinese Clinical Trial Registry (ChiCTR2000030089) and is expected to run until August 2020. However, further investigations concerning the use and safety of TNF α -blockers in COVID-19 patients are urgently needed.

In addition, concerning a potential intervention on NF- κ B signaling pathway, serine protease inhibitors of trypsin-like serine proteases (e.g. camostat mesylate, nafamostat mesylate, gabexate mesylate, ulinastatin), used for the treatment of pancreatitis, disseminated intravascular coagulation, and anticoagulant for hemodialysis,^{55,56} have been found to inhibit viral replication^{57,58} and to attenuate inflammatory processes in different pathological contexts, such as asthma, chronic allergic pulmonary inflammation, and inflammatory myocardial injury.⁵⁹⁻⁶² For instance, nafamostat mesylate and gabexate mesylate have been demonstrated to attenuate allergen-induced airway inflammation and eosinophilia in mouse model of allergic asthma,⁶¹ thus reducing mast cell activation, eosinophils infiltrations in the lung, and *Dermatophagoides pteronyssinus*-driven IL-4 and TNF α production in bronchoalveolar lavage fluid.⁶¹ Furthermore, treatment with nafamostat mesylate downregulated the expression of IL-1 β , TNF α , IL-6, eotaxin, inducible NO synthase (iNOS), CD86, and NF- κ B activation, but

enhanced the expression of IL-12 and IL-10 in *Dermatophagoides pteronyssinus*-driven IL-4 and TNF α production in bronchoalveolar lavage fluid.⁶¹ Moreover, gabexate mesylate has been found to inhibit LPS-induced TNF α production in human monocytes by blocking both NF- κ B and mitogen-activated protein kinase activation.⁶³ Thus, the pharmacological profile of serine protease inhibitors, as inhibitors of complement pathways and broad-spectrum anti-inflammatory agents, provide a strong rationale for their use in the management of COVID-19. However, the specific mechanism of action through which serine protease inhibitors induce their anti-inflammatory effects is still unknown.

The IL-6/JAK/STAT signaling pathway

First discovered as the primary mediator of intracellular signaling induced by IFN in hematopoietic and immune cells, the JAK/STAT signaling is a key pathway transducing extracellular signals transmitted by a large number of cytokines, lymphokines and growth factors. In particular, a subset of cytokines employs the JAK/STAT signaling pathway in order to induce their biological effects. Notably, one of the major activators of JAK/STAT signaling is the cytokine IL-6, which has been reported to be dramatically increased in COVID-19 patients,^{20,22} with a strong implication in acute inflammation and cytokine storm. In particular, IL-6 has been reported to activate numerous cell types expressing the glycoprotein (gp130) receptor and the membrane-bound IL-6 receptor, as well as a soluble form of IL-6 receptor interacting with gp130, thereby promoting the downstream activation of JAK/STAT signaling.⁶⁴ In turn, the activation of JAK/STAT pathway has been reported to stimulate the production of IL-6.⁶⁵ Such signaling pathway has been reported to be aberrantly activated in patients with chronic inflammation conditions, such as arthritis rheumatoid, and it is likely that its excessive overactivation may also occur in COVID-19 patients, thereby exacerbating the host inflammatory response. Noteworthy, chronic elevation of circulating IL-6 has been widely recognized as a predictor for increased risk of cardiovascular events.^{66,67} Consistently, IL-6 is produced from several tissues, including activated macrophages and endothelial and smooth muscle cells, where it promotes the secretion of other cytokines and, among others, it stimulates

MCP1 secretion from macrophages to promote atherogenesis,⁶⁸ increases the expression of cell adhesion molecules,^{69,70} and stimulates the proliferation and migration of vascular smooth muscle cells.⁷¹ Thus, the abnormal increase in IL-6 levels may be implicated, at least in part, in the occurrence cardiovascular diseases (e.g. coronary atherosclerosis, inflammation in the vascular system resulting in diffuse microangiopathy with thrombosis) observed in COVID-19 patients.⁷² Accordingly, the synthesis and secretion of IL-6 has been demonstrated to be induced by angiotensin II, which is locally produced by the inflamed vessels in a JAK/STAT-dependent manner.⁷³ In particular, angiotensin II binding to Angiotensin II receptor type 1 (AT₁ receptor) has been found to activate JAK/STAT pathway and to promote the downstream production of IL-6.^{73,74} Increased angiotensin II enhances IL-6 production in AT₁/JAK/STAT dependent manner, thus establishing a positive inflammatory feedback loop. Interestingly, the spike protein of SARS-CoV has been demonstrated to downregulate ACE2 expression, thus resulting in over-production of angiotensin II by the related enzyme ACE.^{75,76} In a similar way, it could be hypothesized that SARS-CoV-2 may downregulate ACE2 receptors, thus leading to an over-production of angiotensin II, in turn enhancing IL-6 production in AT₁/JAK/STAT dependent manner, and ultimately driving to vascular inflammation and lung injury, clinical signatures of COVID-19 (**Figure 2**). Moreover, the angiotensin II/AT₁ receptor axis has been reported to also activate both NF-κB and ADAM17.⁷⁷ Notably, an important substrate for ADAM17 is ACE2, whose cleavage by ADAM17 has been reported to inactivate it, enhancing angiotensin II retention, thus leading to hypertension, cardiovascular remodeling, and other types of pathophysiology associated with enhancement of the renin-angiotensin system.⁷⁷ Beside its implication in the shedding of ACE2 receptor, fundamental for virus entry,⁵³ ADAM17 induction has been found to process the membrane form of IL-6Rα to the soluble form (sIL-6Rα), followed by the gp130-mediated activation of STAT3 via the sIL-6Rα-IL-6 complex in a variety of IL-6Rα-negative non-immune cells.⁷⁸ The activation of STAT3 has been reported to be required for the complete induction of NF-κB pathway.⁷⁸ Thus, SARS-CoV-2 infection may activate both NF-κB and STAT3 signaling, which in turn can promote the IL-6 amplifier mechanism, required for the hyper-activation of NF-κB by STAT3, thereby inducing multiple inflammatory and

autoimmune diseases.⁷⁸ The IL-6 amplifier promotes the production and secretion of several pro-inflammatory cytokines and chemokines, such as IL-6, and the recruitment of lymphoid and myeloid cells, sustaining the IL-6 amplifier-driven positive feedback loop (as proposed by Hirano and Murakami)⁷⁹ (**figure 2**). Furthermore, the metalloprotease ADAM17 has been found to mediate angiotensin II-induced EGFR (epidermal growth factor receptor) transactivation by generating the mature form of heparin-binding EGF-like growth factor in vascular smooth muscle cells, thus leading to vascular remodeling.⁷⁷ Notably, EGFR transactivation is critical for angiotensin II-mediated cardiovascular complications.⁷⁷ In this regard, the EGFR kinase inhibitor Erlotinib has been recently repurposed for the treatment of COVID-19, based on its capability to reduce the infectivity of a wide range of viruses.⁸⁰⁻⁸² Beside its antiviral activity, the implication of EGFR transactivation in cardiovascular complications represent another theoretical foundation for the use of erlotinib in the management of COVID-19 patients.

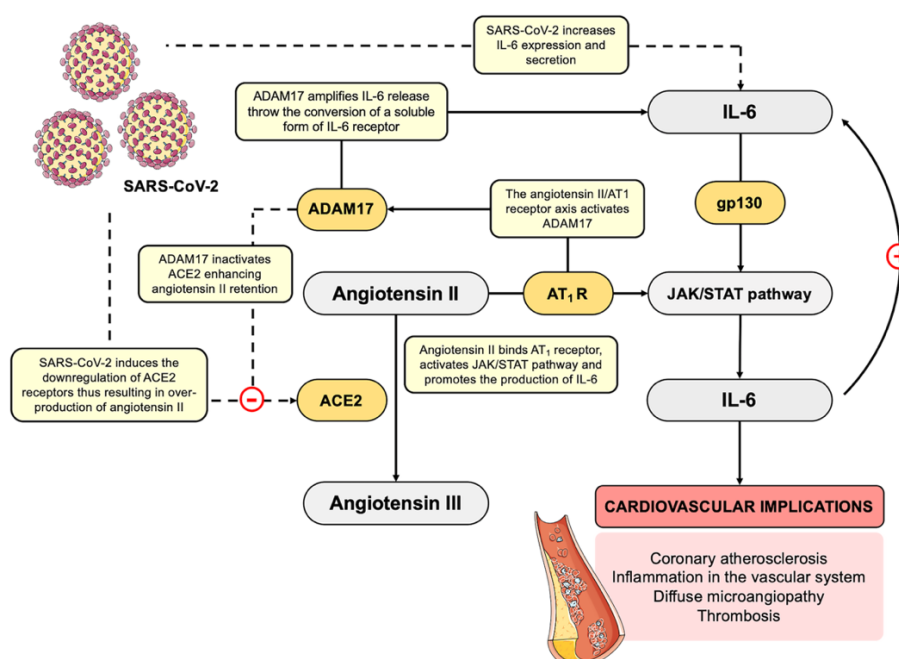


Figure 2. Hypothetical mechanism by SARS-CoV-2 in establishing an inflammatory feedback loop between IL-6 and angiotensin II. Cytokine IL-6 has been found increased in

COVID-19 patients, thus suggesting a direct role of SARS-CoV-2 in a massive cytokine release. IL-6 is able to activate a soluble form of IL-6 receptor interacting with gp130, thereby promoting the downstream activation of JAK/STAT signaling, and the production of IL-6. Moreover, SARS-CoV-2 has been directly related with the occurrence of cardiovascular implications, such as coronary atherosclerosis, inflammation in the vascular system and diffuse microangiopathy with thrombosis. Synthesis and secretion of IL-6 are directly implicated in cardiovascular damages. Indeed, IL-6 production is also induced by angiotensin II in AT₁/JAK/STAT-dependent manner. As observed in SARS-CoV, also SARS-CoV-2 may be hypothesized to downregulate ACE2 expression, thus resulting in over-production of angiotensin II by the related enzyme ACE. In turn, increased angiotensin II enhances IL-6 production via JAK/STAT pathway, thus establishing a positive inflammatory feedback loop, ultimately resulting in the exacerbation of vascular and lung injuries. Moreover, the angiotensin II/AT₁ receptor axis activates ADAM17 that cleaves and inactivates ACE2, enhancing angiotensin II retention. In addition, ADAM17 induction has been found to process the membrane form of IL-6R α to the soluble form (sIL-6R α), followed by the gp130-mediated activation of STAT3 via the sIL-6R α -IL-6 complex in a variety of IL-6R α -negative non-immune cells. The IL-6 amplifier promotes the production and secretion of several pro-inflammatory cytokines and chemokines, such as IL-6, sustaining the IL-6 amplifier-driven positive feedback. SARS-CoV-2, severe acute respiratory syndrome coronavirus 2; IL-6, interleukin 6; ACE2, angiotensin-converting enzyme 2; AT₁, angiotensin II receptor type 1; JAK, Janus Kinase; STAT, Signal Transducer and Activator of Transcription; ADAM17, A Disintegrin And Metalloproteinase domain-containing protein 17.

Moreover, given the importance of angiotensin II/AT₁ receptor axis, the attempt to use angiotensin II-receptor blockers as a therapeutic benefit in COVID-19 by targeting the host response to the virus has been made.⁸³ However, their use needs to be deepened, since ACE inhibitors and angiotensin II-receptor blockers have been suggested to further increase the risk of COVID-19 infection by up-regulating ACE2.⁸⁴ Whether patients affected by COVID-19 and hypertension, taking an ACE inhibitors or angiotensin II-receptor blockers, should switch to another antihypertensive drug is still a matter of debate, and further evidence is required.

Since IL-6 appears a key driver of cytokine storm and of its consequent detrimental effects, monoclonal antibodies against IL-6, such as tocilizumab and sarilumab, have been also proposed to dampen this process. Tocilizumab, a monoclonal antibody IL-6 receptor antagonist, approved for the treatment of rheumatoid arthritis and CRS, has been used in clinical practice in order to manage severe cases of COVID-19 and it has been included in the current Chinese national treatment guidelines (<https://www.chinalawtranslate.com/wp-content/uploads/2020/03/Who->

translation.pdf). To date, 40 clinical trials (typing COVID-19 and tocilizumab on clinicaltrials.gov and, clinicaltrialsregister.eu) are underway to test tocilizumab, alone or in combination, in patients with COVID-19. Moreover, 18 clinical trials (typing COVID-19 and tocilizumab on clinicaltrials.gov and, clinicaltrialsregister.eu) will study the efficacy and safety of another IL-6 receptor antagonist, sarilumab, approved for the treatment of rheumatoid arthritis in patients with COVID-19.

Beside monoclonal antibodies specifically targeting IL-6, approved drugs inhibiting IL-6/JAK/STAT signaling may represent a valuable tool. In particular, JAK signaling inhibitors, such as baricitinib, fedratinib, and ruxolitinib – approved for indications such as rheumatoid arthritis and myelofibrosis – have been reported to attenuate the host inflammatory response associated with massive pro-inflammatory cytokine and chemokine release.⁸⁵ Based on this anti-inflammatory effect, they are likely to be effective against the consequences of the elevated levels of cytokines typically observed in patients with COVID-19.⁸⁰ Among them, baricitinib, a selective inhibitor of JAK 1 and 2, has been predicted by crystallographic studies to inhibit two members of the numb-associated kinase family, such as AP2-associated protein kinase 1 (AAK1) and cyclin G-associated kinase (GAK), thus hindering viral endocytosis into lung cells, at the concentration approved for the treatment of arthritis rheumatoid.⁸⁶ However, despite such undeniable advantages, the repurposing of baricitinib and, in general, of JAK inhibitors for the management of COVID-19 is debated. In particular, concerns arise mainly from evidence reporting that the activation of JAK/STAT pathway, mediated by IFNs, is required for the induction of many IFN-regulated genes, playing a pivotal role as innate early defense system against viral infections. The defensive role of JAK/STAT pathway is corroborated by evidence demonstrating that the majority of virus have developed escaping strategies, such as the production of viral-encoded factors blocking this pathway, which are recognized as crucial determinants of virulence.⁸⁷ Therefore, inhibition of JAK/STAT signaling is likely to produce an impairment of IFN-related antiviral response, exacerbating SARS-CoV-2 infection. However, since several benefits, such as the blockage of virus entry and the attenuation of host excessive inflammatory response, as well as vascular and lung damage,

provide a strong rationale for the use of baricitinib in the management of COVID-19 patients, the balance between positive and negative aspects of JAK/STAT signaling inhibition has to be still drawn up.

To date, several clinical trials are testing the efficacy and safety JAK inhibitors in COVID-19 patients (typing COVID-19 and JAK inhibitors on clinicaltrials.gov and clinicaltrialsregister.eu).

The sphingosine-1-phosphate receptor 1 pathway

The sphingosine-1-phosphate (S1P) 1 has emerged as a crucial signaling lipid regulator of inflammation and immune response, including lymphocyte trafficking, vascular integrity, and cytokine and chemokine production.⁸⁸ Beside S1P role of second messenger during inflammation, most of S1P effects on innate and adaptive immunity are mediated by its binding to five G-protein-coupled receptors (S1PR₁₋₅), which are differentially expressed in tissues.⁸⁸ Among them, S1P₁ receptor is ubiquitously expressed and coupled with a G inhibitory protein.⁸⁹ The activation of S1P₁ receptor is associated with Ras/ERK, PI3K/Akt/eNOS, and PLC/Ca²⁺ downstream pathways.⁸⁹ Notably, under physiological and pathological conditions, the S1P/S1PR₁ axis has been demonstrated to regulate the trafficking and migration of numerous types of immune cells, including T and B lymphocytes, NK cells, dendritic cells.⁸⁸ Moreover, the S1P₁ receptor signaling pathways have been reported to inhibit the pathological damage induced by the host innate and adaptive immune responses, thus attenuating the cytokine storm observed in influenza virus infection.⁴⁰ In particular, Teijaro *et al.* demonstrated that, in mice infected with A/Wisconsin/WSLH34939/09 influenza virus, S1P₁ receptor subtype regulates a crucial signaling loop fundamental for the initiation of cytokine storm in respiratory endothelial cells.⁴⁰ The administration of S1P₁ agonist blunted cytokine storm, by significantly inhibiting secretion of cytokines and chemokines associated with influenza virus-induced pathology, such as IFN- α , CCL2, IL-6, TNF α , and IFN- γ .⁴⁰ Notably, in endothelial cells, suppression of early innate immune responses through S1P₁ signaling has been found to decrease mortality during influenza virus infection in mice.⁴⁰ Interestingly, in a later work by the same group, activation of S1P₁ signaling

has been demonstrated to block cytokine and chemokine production, as well as immune cell activation and recruitment in the lungs of mice infected with the H1N1 WSN strain of influenza virus.⁹⁰ Moreover, S1P₁ agonism has been found to reduce cytokine storm independently of TLR3 and TLR7 signaling, as well as of multiple endosome and cytosolic innate pathogen-sensing pathways.⁹⁰ In contrast, S1P₁R agonism has been found to suppress cytokine and chemokine production by targeting MyD88 (myeloid differentiation primary response gene 88)/TRIF (TIR-domain-containing adapter-inducing IFN- β) signaling, two common actors with NF- κ B pathway.⁹⁰ However, S1P₁R agonism is likely to modulate other signaling pathways that have not yet identified.

Thus, based on the effects of S1P receptor signaling on multiple immunological processes indicating such pathway a promising for the modulation of harmful inflammatory responses, the application of therapies targeting S1P and S1P signaling may be repurposed for immune-mediated disorders and inflammatory conditions, such as COVID-19. For instance, SP1 agonists, approved for multiple sclerosis, such as fingolimod, might be used as therapeutic tools to dampen cytokine and chemokine responses in those patients displaying excessive immune responses. To date, only one non-randomized phase II clinical trial is underway to establish the efficacy of fingolimod in the treatment of COVID-19 (NCT04280588) (typing COVID-19 and fingolimod on clinicaltrials.gov).

CONCLUDING REMARKS: A GLIMPSE INTO THE FUTURE

The COVID-19 pandemic, induced by the novel SARS-CoV-2, represents one of the greatest global public health emergencies since the pandemic influenza outbreak of 1918 and provides an unprecedented challenge for the identification of both preventive and therapeutic drugs. In particular, vaccines and effective therapeutics to tackle this novel virus are urgently needed. Fortunately, in the last decade vaccine technology has significantly evolved, with the development of several RNA and DNA vaccine candidates, licensed

vectored vaccines, recombinant proteins and cell-culture based vaccines for many indications.⁹¹ Moreover, given the similarities of SARS-CoV-2 with SARS-CoV, the ideal target for the vaccine, the spike S protein on the surface of the virus required for viral entry, has been quickly identified, providing a target antigen to incorporate into advanced vaccine platforms. Thus, antibodies specifically targeting the S protein can block the binding of SARS-CoV-2 to the host ACE2 receptor, thus neutralizing the virus. However, given the lesson learned from SARS and MERS, the development of the vaccine against SARS-CoV-2 is likely to be an uphill road with several obstacles. In fact, several vaccines for SARS-CoV, including recombinant S protein-based vaccines, have been already developed and tested in animal models, but many did not produce sterilizing immunity in animal models and/or induced severe side effects, such as lung and liver damage.^{92,93} To date, no human CoV vaccines have been approved so far. Moreover, to complicate this scenario, it has to be still unveiled whether infection with CoVs induces long-lived antibody response protecting against the risk of relapsing infections. Thus, scientific community has to overcome several issues for the development of an effective and safe SARS-CoV-2 vaccine. In this regard, Ling *et al.* recently detected SARS-CoV-2-specific humoral and cellular immunity in 8 COVID-19 patients, recently become virus-free and consequently discharged.⁹⁴ In addition, the neutralizing antibody titers have been significantly correlated with the numbers of nucleocapsid protein-specific T cells.⁹⁴ Such evidence indicates that both B and T cells cooperate to protect the host from viral infection. Notably, despite the small sample size, this study laid a theoretical foundation for the diagnosis of infectious diseases, the tracing of past infections, as well as the development of therapeutic antibody drugs and the design of an effective vaccine. Consistently, Long *et al.* reported acute antibody responses to SARS-CoV-2 in a cohort of 285 patients with COVID-19.³¹ In particular, 19 days after symptom onset, 100% of patients have been tested positive for antiviral IgG and seroconversion for IgG and IgM have been reported to occur simultaneously or sequentially.³¹ Thus, serological testing might be useful to identify suspected patients with negative RT-PCR results as well as asymptomatic infections.³¹

However, the speed at which SARS-CoV-2 is spreading has emphasized the urgent need to identify alternative therapeutic strategies in order to contain viral infection and to attenuate the excessive host immune response during the lag of vaccine availability, especially in a scenario where the virus may become endemic and recurrent seasonal epidemics may occur. In this regard, several antiviral drugs, such as remdesivir, lopinavir and ritonavir, are currently tested in several clinical trials, either alone or in combination, and compassionate use of these drugs has already been reported for SARS-CoV-2.^{95,96} However, antiviral drugs might select for mutational escape, thus rendering this therapeutic approach ineffective. Moreover, still unconfirmed reports indicate sufficient pre-clinical rationale and evidence regarding the use of chloroquine and hydroxychloroquine as prophylactic agent,⁹⁷ with evidence of safety from long-time use in clinical practice for the treatment of malaria and autoimmune diseases.⁹⁸ However, their use needs further evidence and clinical evaluation. Chloroquine and hydroxychloroquine are known to potentially cause heart rhythm problems, that may be exacerbated whether combined with other drugs with similar effects on the heart, and induce adverse liver, kidney and cerebral effects.⁹⁹ Thus, as discussed in this review, treatments addressing the immunopathology of the infection, such as immunomodulatory drugs approved for different clinical indications, have become a major focus. Such approaches show the advantage to override viral mutational escape and to exert less-selective pressure on viral population. Although the prospective of counteracting cytokine storm is compelling, a major limitation relies on the limited understanding of the immune signaling pathways triggering such process. Hence, future dissection of immune signaling pathways triggered by SARS-CoV-2 will provide novel insight on the effects of the virus on human immune system and may reveal relevant biological players that can be targeted to blunt cytokine storm. Notably, since it is well established that innate immune responses trigger the activation of multiple and redundant signaling pathways, an effective therapy may require to acting, at the same time, on multiple signaling pathways. In this regard, cocktails of immunomodulatory drugs, such as monoclonal antibody targeting a specific cytokine (e.g. TNF- inhibitors, IL-1-inhibitors, IL-6 inhibitors), corticosteroids (e.g., prednisone, methylprednisolone and dexamethasone), and S1PR₁ agonists (e.g. fingolimod), rather than a single

drug, might be more effective in the management of COVID-19, by exerting either synergic or additive effects. In this regard, it would be of key importance to assess whether patients with immune-mediated disorders treated with immunomodulatory drugs, such as cytokine blockers, are more resistant to the excessive immune response observed in COVID-19 patients and more protected against SARS-CoV-2-driven pneumonia. However, to date, no evidence reporting either decreased or increased risk of SARS-CoV-driven pneumonia has been documented in this patients and further investigations are required to verify this hypothesis.

Furthermore, another aspect to better investigate concerns the possibility that the uncontrolled immune response to viral infection may cause detrimental systemic effects on several physiological systems, such as the nervous, endocrine, renal and cardiovascular systems. Accordingly, it is likely that the massive cytokine and chemokine release may critically impact on these physiological systems, thereby inducing both short- and long-term detrimental effects. As an example, the neuro-invasive potential of SARS-CoV and MERS-CoV has been previously reported.¹⁰⁰ Thus, given the high similarity between SARS-CoV and SARS-CoV-2, it is likely that this latter displays a similar potential.¹⁰¹⁻¹⁰³ As a matter of fact, a study carried out in 214 COVID-19 patients reported that about 88% of severe COVID-19 cases showed neurologic manifestations, such as acute cerebrovascular diseases and impaired consciousness.¹⁰⁴

Finally, beside the putative long-term effects directly induced by SARS-CoV-2 infection, another key issue to address concerns the long-term effects of empirical and experimental treatments in COVID-19 patients. In this regard, a study carried out in 25 recovered SARS patients, recruited 12 years after the viral infection, reported significant differences in the serum metabolomes in recovered SARS patients compared to controls.¹⁰⁵ In particular, a significant metabolic alteration - increased levels of phosphatidylinositol and lysophosphatidylinositol - has been found to coincide with the effect of methylprednisolone administration,¹⁰⁵ thus suggesting that high-dose pulses of steroid treatment may induce long-term systemic damage associated with serum metabolic alterations.¹⁰⁵

Therefore, all the challenges discussed above highlight some of the major gaps in our knowledge of COVID-19 clinical spectrum, underlying immune signaling pathways, systemic effects, and long-term pathological signatures, which need to be urgently fulfilled by future investigations.

REFERENCES

1. Lu, R. *et al.* Genomic characterisation and epidemiology of 2019 novel coronavirus: implications for virus origins and receptor binding. *Lancet Lond. Engl.* **395**, 565-574 (2020).
2. Corman, V. M., Lienau, J. & Witznath, M. [Coronaviruses as the cause of respiratory infections]. *Internist* **60**, 1136-1145 (2019).
3. Chan, J. F. W. *et al.* Middle East respiratory syndrome coronavirus: another zoonotic betacoronavirus causing SARS-like disease. *Clin. Microbiol. Rev.* **28**, 465-522 (2015).
4. Mackenzie, J. S. & Smith, D. W. COVID-19: a novel zoonotic disease caused by a coronavirus from China: what we know and what we don't. *Microbiol. Aust.* MA20013 (2020) doi:10.1071/MA20013.
5. Lau, S. K. P. *et al.* Severe acute respiratory syndrome coronavirus-like virus in Chinese horseshoe bats. *Proc. Natl. Acad. Sci. U. S. A.* **102**, 14040-14045 (2005).
6. Zhou, L., Liu, K. & Liu, H. G. [Cause analysis and treatment strategies of 'recurrence' with novel coronavirus pneumonia (covid-19) patients after discharge from hospital]. *Zhonghua Jie He He Hu Xi Za Zhi Zhonghua Jiehe He Huxi Zazhi Chin. J. Tuberc. Respir. Dis.* **43**, E028 (2020).
7. Chan, J. F.-W. *et al.* Genomic characterization of the 2019 novel human-pathogenic coronavirus isolated from a patient with atypical pneumonia after visiting Wuhan. *Emerg. Microbes Infect.* **9**, 221-236 (2020).
8. Hoffmann, M. *et al.* SARS-CoV-2 Cell Entry Depends on ACE2 and TMPRSS2 and Is Blocked by a Clinically Proven Protease Inhibitor. *Cell* **181**, 271-280.e8 (2020).
9. Wan, Y., Shang, J., Graham, R., Baric, R. S. & Li, F. Receptor Recognition by the Novel Coronavirus from Wuhan: an Analysis Based on Decade-Long Structural Studies of SARS Coronavirus. *J. Virol.* **94**, (2020).
10. Ou, X. *et al.* Characterization of spike glycoprotein of SARS-CoV-2 on virus entry and its immune cross-reactivity with SARS-CoV. *Nat. Commun.* **11**, 1620 (2020).
11. Ding, Y. *et al.* Organ distribution of severe acute respiratory syndrome (SARS) associated coronavirus (SARS-CoV) in SARS patients: implications for pathogenesis and virus transmission pathways. *J. Pathol.* **203**, 622-630 (2004).
12. Gu, J. *et al.* Multiple organ infection and the pathogenesis of SARS. *J. Exp. Med.* **202**, 415-424 (2005).

13. Hamming, I. *et al.* Tissue distribution of ACE2 protein, the functional receptor for SARS coronavirus. A first step in understanding SARS pathogenesis. *J. Pathol.* **203**, 631–637 (2004).
14. Xu, H. *et al.* High expression of ACE2 receptor of 2019-nCoV on the epithelial cells of oral mucosa. *Int. J. Oral Sci.* **12**, 8 (2020).
15. Zhao, Y. *et al.* Single-cell RNA expression profiling of ACE2, the putative receptor of Wuhan 2019-nCoV. *Biorxiv* 2020(1):26.919985, (2020).
16. Huang, C. *et al.* Clinical features of patients infected with 2019 novel coronavirus in Wuhan, China. *Lancet Lond. Engl.* **395**, 497–506 (2020).
17. Xu, Z. *et al.* Pathological findings of COVID-19 associated with acute respiratory distress syndrome. *Lancet Respir. Med.* **8**, 420–422 (2020).
18. Wu, F. *et al.* A new coronavirus associated with human respiratory disease in China. *Nature* **579**, 265–269 (2020).
19. Shi, Y. *et al.* Immunopathological characteristics of coronavirus disease 2019 cases in Guangzhou, China. *medRxiv* 2020.03.12.20034736 (2020) doi:10.1101/2020.03.12.20034736.
20. Qin, C. *et al.* Dysregulation of immune response in patients with COVID-19 in Wuhan, China. *Clin. Infect. Dis. Off. Publ. Infect. Dis. Soc. Am.* (2020) doi:10.1093/cid/ciaa248.
21. Zhang, B. *et al.* Immune phenotyping based on neutrophil-to-lymphocyte ratio and IgG predicts disease severity and outcome for patients with COVID-19. *medRxiv* 2020.03.12.20035048 (2020) doi:10.1101/2020.03.12.20035048.
22. Mehta, P. *et al.* COVID-19: consider cytokine storm syndromes and immunosuppression. *Lancet Lond. Engl.* **395**, 1033–1034 (2020).
23. Li, D. *et al.* Immune dysfunction leads to mortality and organ injury in patients with COVID-19 in China: insights from ERS-COVID-19 study. *Signal Transduct. Target. Ther.* **5**, 62 (2020).
24. Perlman, S. & Dandekar, A. A. Immunopathogenesis of coronavirus infections: implications for SARS. *Nat. Rev. Immunol.* **5**, 917–927 (2005).
25. Tynell, J. *et al.* Middle East respiratory syndrome coronavirus shows poor replication but significant induction of antiviral responses in human monocyte-derived macrophages and dendritic cells. *J. Gen. Virol.* **97**, 344–355 (2016).
26. Zhou, J. *et al.* Active replication of Middle East respiratory syndrome coronavirus and aberrant induction of inflammatory cytokines and chemokines in human macrophages: implications for pathogenesis. *J. Infect. Dis.* **209**, 1331–1342 (2014).
27. Zhu, N. *et al.* A Novel Coronavirus from Patients with Pneumonia in China, 2019. *N. Engl. J. Med.* **382**, 727–733 (2020).
28. Chen, D. *et al.* Recurrence of positive SARS-CoV-2 RNA in COVID-19: A case report. *Int. J. Infect. Dis. IJID Off. Publ. Int. Soc. Infect. Dis.* **93**, 297–299 (2020).
29. Tan, L. *et al.* Lymphopenia predicts disease severity of COVID-19: a descriptive and predictive study. *Signal Transduct. Target. Ther.* **5**, 33 (2020).

30. Wen, W. *et al.* Immune Cell Profiling of COVID-19 Patients in the Recovery Stage by Single-Cell Sequencing. *medRxiv* 2020.03.23.20039362 (2020) doi:10.1101/2020.03.23.20039362.
31. Long, Q.-X. *et al.* Antibody responses to SARS-CoV-2 in patients with COVID-19. *Nat. Med.* (2020) doi:10.1038/s41591-020-0897-1.
32. Alcami, A. & Koszinowski, U. H. Viral mechanisms of immune evasion. *Immunol. Today* **21**, 447-455 (2000).
33. de Wit, E., van Doremalen, N., Falzarano, D. & Munster, V. J. SARS and MERS: recent insights into emerging coronaviruses. *Nat. Rev. Microbiol.* **14**, 523-534 (2016).
34. Wan, S. *et al.* Characteristics of lymphocyte subsets and cytokines in peripheral blood of 123 hospitalized patients with 2019 novel coronavirus pneumonia (NCP). *medRxiv* 2020.02.10.20021832 (2020) doi:10.1101/2020.02.10.20021832.
35. Liu, Y. *et al.* Elevated plasma level of selective cytokines in COVID-19 patients reflect viral load and lung injury. *Natl. Sci. Rev.* (2020) doi:10.1093/nsr/nwaa037.
36. Favalli, E. G. *et al.* COVID-19 infection and rheumatoid arthritis: Faraway, so close! *Autoimmun. Rev.* **19**, 102523 (2020).
37. Gou, W. *et al.* Gut microbiota may underlie the predisposition of healthy individuals to COVID-19. *medRxiv* 2020.04.22.20076091 (2020) doi:10.1101/2020.04.22.20076091.
38. de Marcken, M., Dhaliwal, K., Danielsen, A. C., Gautron, A. S. & Dominguez-Villar, M. TLR7 and TLR8 activate distinct pathways in monocytes during RNA virus infection. *Sci. Signal.* **12**, (2019).
39. Olejnik, J., Hume, A. J. & Mühlberger, E. Toll-like receptor 4 in acute viral infection: Too much of a good thing. *PLoS Pathog.* **14**, e1007390 (2018).
40. Teijaro, J. R. *et al.* Endothelial cells are central orchestrators of cytokine amplification during influenza virus infection. *Cell* **146**, 980-991 (2011).
41. Li, Q. & Verma, I. M. NF-kappaB regulation in the immune system. *Nat. Rev. Immunol.* **2**, 725-734 (2002).
42. Hayden, M. S., West, A. P. & Ghosh, S. NF- κ B and the immune response. *Oncogene* **25**, 6758-6780 (2006).
43. DeDiego, M. L. *et al.* Inhibition of NF- κ B-Mediated Inflammation in Severe Acute Respiratory Syndrome Coronavirus-Infected Mice Increases Survival. *J. Virol.* **88**, 913 (2014).
44. Smits, S. L. *et al.* Exacerbated innate host response to SARS-CoV in aged non-human primates. *PLoS Pathog.* **6**, e1000756 (2010).
45. Wang, W. *et al.* Up-regulation of IL-6 and TNF-alpha induced by SARS-coronavirus spike protein in murine macrophages via NF-kappaB pathway. *Virus Res.* **128**, 1-8 (2007).
46. Hiscott, J., Nguyen, T.-L. A., Arguello, M., Nakhaei, P. & Paz, S. Manipulation of the nuclear factor-kappaB pathway and the innate immune response by viruses. *Oncogene* **25**, 6844-6867 (2006).

47. Clark, J., Vagenas, P., Panesar, M. & Cope, A. P. What does tumour necrosis factor excess do to the immune system long term? *Ann. Rheum. Dis.* **64** Suppl 4, iv70-76 (2005).
48. Silva, L. C. R., Ortigosa, L. C. M. & Benard, G. Anti-TNF- α agents in the treatment of immune-mediated inflammatory diseases: mechanisms of action and pitfalls. *Immunotherapy* **2**, 817-833 (2010).
49. Lapadula, G. *et al.* Adalimumab in the treatment of immune-mediated diseases. *Int. J. Immunopathol. Pharmacol.* **27**, 33-48 (2014).
50. Charles, P. *et al.* Regulation of cytokines, cytokine inhibitors, and acute-phase proteins following anti-TNF-alpha therapy in rheumatoid arthritis. *J. Immunol. Baltim. Md 1950* **163**, 1521-1528 (1999).
51. Feldmann, M. & Maini, R. N. Anti-TNF alpha therapy of rheumatoid arthritis: what have we learned? *Annu. Rev. Immunol.* **19**, 163-196 (2001).
52. Dvorak, H. F., Brown, L. F., Detmar, M. & Dvorak, A. M. Vascular permeability factor/vascular endothelial growth factor, microvascular hyperpermeability, and angiogenesis. *Am. J. Pathol.* **146**, 1029-1039 (1995).
53. Haga, S. *et al.* Modulation of TNF-alpha-converting enzyme by the spike protein of SARS-CoV and ACE2 induces TNF-alpha production and facilitates viral entry. *Proc. Natl. Acad. Sci. U. S. A.* **105**, 7809-7814 (2008).
54. Galloway, J. B. *et al.* Anti-TNF therapy is associated with an increased risk of serious infections in patients with rheumatoid arthritis especially in the first 6 months of treatment: updated results from the British Society for Rheumatology Biologics Register with special emphasis on risks in the elderly. *Rheumatol. Oxf. Engl.* **50**, 124-131 (2011).
55. Hirano, T. Pancreatic injuries in rats with fecal peritonitis: protective effect of a new synthetic protease inhibitor, sepinostat mesilate (FUT-187). *J. Surg. Res.* **61**, 301-306 (1996).
56. Takahashi, H. *et al.* Combined treatment with nafamostat mesilate and aspirin prevents heparin-induced thrombocytopenia in a hemodialysis patient. *Clin. Nephrol.* **59**, 458-462 (2003).
57. Zhirnov, O. P., Klenk, H. D. & Wright, P. F. Aprotinin and similar protease inhibitors as drugs against influenza. *Antiviral Res.* **92**, 27-36 (2011).
58. Yamaya, M. *et al.* The serine protease inhibitor camostat inhibits influenza virus replication and cytokine production in primary cultures of human tracheal epithelial cells. *Pulm. Pharmacol. Ther.* **33**, 66-74 (2015).
59. Ishizaki, M. *et al.* Nafamostat mesilate, a potent serine protease inhibitor, inhibits airway eosinophilic inflammation and airway epithelial remodeling in a murine model of allergic asthma. *J. Pharmacol. Sci.* **108**, 355-363 (2008).
60. Florencio, A. C. *et al.* Effects of the serine protease inhibitor rBmTI-A in an experimental mouse model of chronic allergic pulmonary inflammation. *Sci. Rep.* **9**, 12624 (2019).
61. Chen, C.-L. *et al.* Serine protease inhibitors nafamostat mesilate and gabexate mesilate attenuate allergen-induced airway inflammation and eosinophilia in a murine model of asthma. *J. Allergy Clin. Immunol.* **118**, 105-112 (2006).

62. Lin, C.-C. *et al.* The Effect of Serine Protease Inhibitors on Airway Inflammation in a Chronic Allergen-Induced Asthma Mouse Model. *Mediators Inflamm.* **2014**, 879326 (2014).
63. Yuksel, M., Okajima, K., Uchiba, M. & Okabe, H. Gabexate mesilate, a synthetic protease inhibitor, inhibits lipopolysaccharide-induced tumor necrosis factor-alpha production by inhibiting activation of both nuclear factor-kappaB and activator protein-1 in human monocytes. *J. Pharmacol. Exp. Ther.* **305**, 298-305 (2003).
64. Zhang, C., Wu, Z., Li, J.-W., Zhao, H. & Wang, G.-Q. The cytokine release syndrome (CRS) of severe COVID-19 and Interleukin-6 receptor (IL-6R) antagonist Tocilizumab may be the key to reduce the mortality. *Int. J. Antimicrob. Agents* 105954 (2020) doi:10.1016/j.ijantimicag.2020.105954.
65. Lee, C. *et al.* Janus kinase-signal transducer and activator of transcription mediates phosphatidic acid-induced interleukin (IL)-1beta and IL-6 production. *Mol. Pharmacol.* **69**, 1041-1047 (2006).
66. Wainstein, M. V. *et al.* Elevated serum interleukin-6 is predictive of coronary artery disease in intermediate risk overweight patients referred for coronary angiography. *Diabetol. Metab. Syndr.* **9**, 67 (2017).
67. Zhang, B., Li, X.-L., Zhao, C.-R., Pan, C.-L. & Zhang, Z. Interleukin-6 as a Predictor of the Risk of Cardiovascular Disease: A Meta-Analysis of Prospective Epidemiological Studies. *Immunol. Invest.* **47**, 689-699 (2018).
68. Biswas, P. *et al.* Interleukin-6 induces monocyte chemotactic protein-1 in peripheral blood mononuclear cells and in the U937 cell line. *Blood* **91**, 258-265 (1998).
69. McLoughlin, R. M. *et al.* Differential Regulation of Neutrophil-Activating Chemokines by IL-6 and Its Soluble Receptor Isoforms. *J. Immunol.* **172**, 5676 (2004).
70. van der Meer Irene M. *et al.* Inflammatory Mediators and Cell Adhesion Molecules as Indicators of Severity of Atherosclerosis. *Arterioscler. Thromb. Vasc. Biol.* **22**, 838-842 (2002).
71. Xiang, S. *et al.* Inhibitory effects of suppressor of cytokine signaling 3 on inflammatory cytokine expression and migration and proliferation of IL-6/IFN- γ -induced vascular smooth muscle cells. *J. Huazhong Univ. Sci. Technol. Med. Sci. Hua Zhong Ke Ji Xue Xue Bao Yi Xue Ying Wen Ban Huazhong Keji Daxue Xuebao Yixue Yingdewen Ban* **33**, 615-622 (2013).
72. Qu, D., Liu, J., Lau, C. W. & Huang, Y. IL-6 in diabetes and cardiovascular complications. *Br. J. Pharmacol.* **171**, 3595-3603 (2014).
73. Schieffer, B. *et al.* Role of NAD(P)H oxidase in angiotensin II-induced JAK/STAT signaling and cytokine induction. *Circ. Res.* **87**, 1195-1201 (2000).
74. Marrero, M. B. *et al.* Direct stimulation of Jak/STAT pathway by the angiotensin II AT1 receptor. *Nature* **375**, 247-250 (1995).
75. Kuba, K. *et al.* A crucial role of angiotensin converting enzyme 2 (ACE2) in SARS coronavirus-induced lung injury. *Nat. Med.* **11**, 875-879 (2005).

76. Glowacka, I. *et al.* Differential downregulation of ACE2 by the spike proteins of severe acute respiratory syndrome coronavirus and human coronavirus NL63. *J. Virol.* **84**, 1198-1205 (2010).
77. Eguchi, S., Kawai, T., Scalia, R. & Rizzo, V. Understanding Angiotensin II Type 1 Receptor Signaling in Vascular Pathophysiology. *Hypertens. Dallas Tex 1979* **71**, 804-810 (2018).
78. Murakami, M., Kamimura, D. & Hirano, T. Pleiotropy and Specificity: Insights from the Interleukin 6 Family of Cytokines. *Immunity* **50**, 812-831 (2019).
79. Hirano, T. & Murakami, M. COVID-19: A New Virus, but a Familiar Receptor and Cytokine Release Syndrome. *Immunity* (2020) doi:10.1016/j.immuni.2020.04.003.
80. Stebbing, J. *et al.* COVID-19: combining antiviral and anti-inflammatory treatments. *Lancet Infect. Dis.* **20**, 400-402 (2020).
81. Bekerman, E. *et al.* Anticancer kinase inhibitors impair intracellular viral trafficking and exert broad-spectrum antiviral effects. *J. Clin. Invest.* **127**, 1338-1352 (2017).
82. Pu, S.-Y. *et al.* Feasibility and biological rationale of repurposing sunitinib and erlotinib for dengue treatment. *Antiviral Res.* **155**, 67-75 (2018).
83. Gurwitz, D. Angiotensin receptor blockers as tentative SARS-CoV-2 therapeutics. *Drug Dev. Res.* (2020) doi:10.1002/ddr.21656.
84. Zheng, Y.-Y., Ma, Y.-T., Zhang, J.-Y. & Xie, X. COVID-19 and the cardiovascular system. *Nat. Rev. Cardiol.* **17**, 259-260 (2020).
85. Sanchez, G. A. M. *et al.* JAK1/2 inhibition with baricitinib in the treatment of autoinflammatory interferonopathies. *J. Clin. Invest.* **128**, 3041-3052 (2018).
86. Sorrell, F. J., Szklarz, M., Abdul Azeez, K. R., Elkins, J. M. & Knapp, S. Family-wide Structural Analysis of Human Numb-Associated Protein Kinases. *Struct. Lond. Engl.* 1993 **24**, 401-411 (2016).
87. Fleming, S. B. Viral Inhibition of the IFN-Induced JAK/STAT Signalling Pathway: Development of Live Attenuated Vaccines by Mutation of Viral-Encoded IFN-Antagonists. *Vaccines* **4**, (2016).
88. Spiegel, S. & Milstien, S. The outs and the ins of sphingosine-1-phosphate in immunity. *Nat. Rev. Immunol.* **11**, 403-415 (2011).
89. Bryan, A. M. & Del Poeta, M. Sphingosine-1-phosphate receptors and innate immunity. *Cell. Microbiol.* **20**, e12836 (2018).
90. Teijaro, J. R., Walsh, K. B., Rice, S., Rosen, H. & Oldstone, M. B. A. Mapping the innate signaling cascade essential for cytokine storm during influenza virus infection. *Proc. Natl. Acad. Sci. U. S. A.* **111**, 3799-3804 (2014).
91. Amanat, F. & Krammer, F. SARS-CoV-2 Vaccines: Status Report. *Immunity* **52**, 583-589 (2020).
92. Bolles, M. *et al.* A double-inactivated severe acute respiratory syndrome coronavirus vaccine provides incomplete protection in mice and induces increased eosinophilic proinflammatory pulmonary response upon challenge. *J. Virol.* **85**, 12201-12215 (2011).

-
93. Tseng, C.-T. *et al.* Immunization with SARS coronavirus vaccines leads to pulmonary immunopathology on challenge with the SARS virus. *PLoS One* **7**, e35421 (2012).
 94. Ni, L. *et al.* Detection of SARS-CoV-2-specific humoral and cellular immunity in COVID-19 convalescent individuals. *Immunity* (2020) doi:10.1016/j.immuni.2020.04.023.
 95. Holshue, M. L. *et al.* First Case of 2019 Novel Coronavirus in the United States. *N. Engl. J. Med.* **382**, 929-936 (2020).
 96. Lim, J. *et al.* Case of the Index Patient Who Caused Tertiary Transmission of COVID-19 Infection in Korea: the Application of Lopinavir/Ritonavir for the Treatment of COVID-19 Infected Pneumonia Monitored by Quantitative RT-PCR. *J. Korean Med. Sci.* **35**, e79 (2020).
 97. Cortegiani, A., Ingoglia, G., Ippolito, M., Giarratano, A. & Einav, S. A systematic review on the efficacy and safety of chloroquine for the treatment of COVID-19. *J. Crit. Care* (2020) doi:10.1016/j.jcrc.2020.03.005.
 98. Lee, S.-J., Silverman, E. & Bargman, J. M. The role of antimalarial agents in the treatment of SLE and lupus nephritis. *Nat. Rev. Nephrol.* **7**, 718-729 (2011).
 99. Touret, F. & de Lamballerie, X. Of chloroquine and COVID-19. *Antiviral Res.* **177**, 104762 (2020).
 100. Xu, J. *et al.* Detection of severe acute respiratory syndrome coronavirus in the brain: potential role of the chemokine mig in pathogenesis. *Clin. Infect. Dis. Off. Publ. Infect. Dis. Soc. Am.* **41**, 1089-1096 (2005).
 101. Netland, J., Meyerholz, D. K., Moore, S., Cassell, M. & Perlman, S. Severe acute respiratory syndrome coronavirus infection causes neuronal death in the absence of encephalitis in mice transgenic for human ACE2. *J. Virol.* **82**, 7264-7275 (2008).
 102. Li, K. *et al.* Middle East Respiratory Syndrome Coronavirus Causes Multiple Organ Damage and Lethal Disease in Mice Transgenic for Human Dipeptidyl Peptidase 4. *J. Infect. Dis.* **213**, 712-722 (2016).
 103. Li, Y.-C., Bai, W.-Z. & Hashikawa, T. The neuroinvasive potential of SARS-CoV2 may play a role in the respiratory failure of COVID-19 patients. *J. Med. Virol.* (2020) doi:10.1002/jmv.25728.
 104. Mao, L. *et al.* Neurological Manifestations of Hospitalized Patients with COVID-19 in Wuhan, China: a retrospective case series study. *medRxiv* 2020.02.22.20026500 (2020) doi:10.1101/2020.02.22.20026500.
 105. Wu, Q. *et al.* Altered Lipid Metabolism in Recovered SARS Patients Twelve Years after Infection. *Sci. Rep.* **7**, 9110 (2017).

PART II

The following manuscript was published in *Signal Transduction and Targeted Therapy* in 2020 as:

Molecular features of IGHV3-53-encoded antibodies elicited by SARS-CoV-2


Francesca Fagiani, **Michele Catanzaro (co-first author)** and Cristina Lanni

Abstract

An elegant paper by Yuan *et al.*, recently published in *Science*, provides novel insights into the molecular features of neutralizing antibody responses to the severe acute respiratory syndrome coronavirus 2 (SARS-CoV-2).

**RESEARCH HIGHLIGHT** **OPEN**

Molecular features of IGHV3-53-encoded antibodies elicited by SARS-CoV-2

Francesca Fagiani^{1,2}, Michele Catanzaro¹ and Cristina Lanni *Signal Transduction and Targeted Therapy* (2020)5:170; <https://doi.org/10.1038/s41392-020-00287-4>

¹Department of Drug Sciences (Pharmacology Section), University of Pavia, V.le Taramelli 14, 27100 Pavia, Italy and ²Scuola Universitaria Superiore IUSS Pavia, P.zza Vittoria, 15, 27100 Pavia, Italy

Correspondence: Cristina Lanni (cristina.lanni@unipv.it)

These authors contributed equally: Francesca Fagiani, Michele Catanzaro

An elegant paper by Yuan *et al.*, recently published in *Science*, provides novel insights into the molecular features of neutralizing antibody responses to the severe acute respiratory syndrome coronavirus 2 (SARS-CoV-2).¹

According to the principles of the “reverse vaccinology 2.0” postulated by Burton *et al.*,² the authors explore the interactions between potent neutralizing antibodies from naturally infected donors and their target epitopes, providing key information about structural motifs and binding mode that may facilitate the design of vaccine antigens capable to elicit the immune response against SARS-CoV-2. The vast majority of anti-CoV neutralizing antibodies have been found to specifically target the receptor-binding domain (RBD) of the viral spike (S) protein, thus hindering SARSCoV-2 binding to the host angiotensin converting enzyme 2 (ACE2) receptor and viral entry.³

Yuan and collaborators analyzed 294 anti-SARS-CoV-2 antibodies from COVID-19 patients and demonstrated that among these antibodies the immunoglobulin heavy variable 3-53 (IGHV3-53) represents the most frequently used IGHV gene, with 10% encoded by IGHV3-53. In the cohort investigated by Yuan *et al.*, IGHV3-53 antibodies have been reported to be more potent compared to other germ lines, as well as to display lower somatic mutation rates. The authors determined the crystal structures of two antibodies, CC12.1 and CC12.3, encoded by a common IGHV353 gene, but

belonging to different clonotypes, in order to define the structural features, and to add favorable properties for RBD recognition to IGHV3-53. Notably, among the antibodies tested against live replicating SARS-CoV-2 and pseudovirus, CC12.1 and CC12.3 ($IC_{50} \sim 20$ ng/mL), isolated from COVID-19 patients, are among the top four highly potent neutralizing antibodies, with a binding affinity (K_d) of Fabs CC12.1 and CC12.3 to SARS-CoV-2 RBD of 17 and 14 nM, respectively.^{1,4} By performing competitions experiments, Yuan *et al.* demonstrated that both CC12.1 and CC12.3 bind to the ACE2 binding site on SARS-CoV-2 RBD with an identical angle of approach. Among 17 ACE2 binding residues on RBD, 15 and 11 are within the epitopes of CC12.1 and CC12.3, respectively. Remarkably, several epitope residues are not conserved between SARS-CoV-2 and SARS-CoV, thus explaining, at least in part, the absence of antibody cross-reactivity between these two CoVs.⁵ Such evidence is consistent with data, reported by Ju *et al.*, showing the lack of antibody cross-reactivity with RBDs not only from SARS-CoV, but also from middle east respiratory syndrome coronavirus (MERS-CoV), thus suggesting that SARSCoV, SARS-CoV-2, and MERS-CoV are immunologically distinct.⁵ As an example, despite SARS-CoV-2 and SARS-CoV display both sequential and structural similarities, diverse viral species-specific responses have been observed in patients.⁵ Such evidence justifies the failures of the attempts to neutralize SARS-CoV-2 by using previously isolated SARS-CoV antibodies.⁵

Moreover, the authors provided evidence that CC12.1 presents immunoglobulin kappa variable1-9 (IGKV1-9) and CC12.3 IGKV320, thereby suggesting that IGHV3-53 can pair with different light chains. Such finding indicates that the identity of the heavy chain, instead of that of the light-chain, might be critical for targeting ACE2 binding site in SARS-CoV-2 RBD.

Furthermore, the complementarity-determining regions (CDRs) of IGHV3-53 were structurally analyzed. Based on structural analysis, the presence of two structural motifs, the NY motif in the CDR H1 and an SGG motif in the CDR H2, as well as the short length of CDR H3, appear fundamental for the binding to the RBD. CDR H1 and H2 of CC12.1 and CC12.3 antibodies have been found to stabilize the CDR conformation with the surrounding framework and to establish hydrogen bonds with the carbonyl backbone of key amino acids

in the RBD. While high similarity in the interaction modes between SARS-CoV-2 RBD and CDR H1 and H2 loops has been found, significant differences in the CDR H3 sequence and conformations have been observed when comparing two antibodies. As an example, while CDR H3 of CC12.2 has been found to establish a hydrogen bond with RBD Y453, CDR H3 of CC12.3 has been observed not to form it. Notably, an interesting feature of CDR H3 region of IGHV3-53-encoded antibodies is its short length. Accordingly, CC12.1 and CC12.3 have a CDR H3 consisting of nine amino acids in lengths. This structural feature may rely on the fact that the epitopes of IGHV3-53 antibodies are relatively flat and present a small pocket to insert the CDR H3 loop. Hence, longer CDR H3 regions might not be accommodated in IGHV3-53-encoded antibodies.

In sum, based on this structural characterization, Yuan and collaborators shed lights on some key molecular features (illustrated in **Figure 1**) contributing to an effective antibody response against SARS-CoV-2 infection, demonstrating that IGHV3-53 provides a versatile framework to target the ACE2 binding site in SARS-CoV-2 RBD.

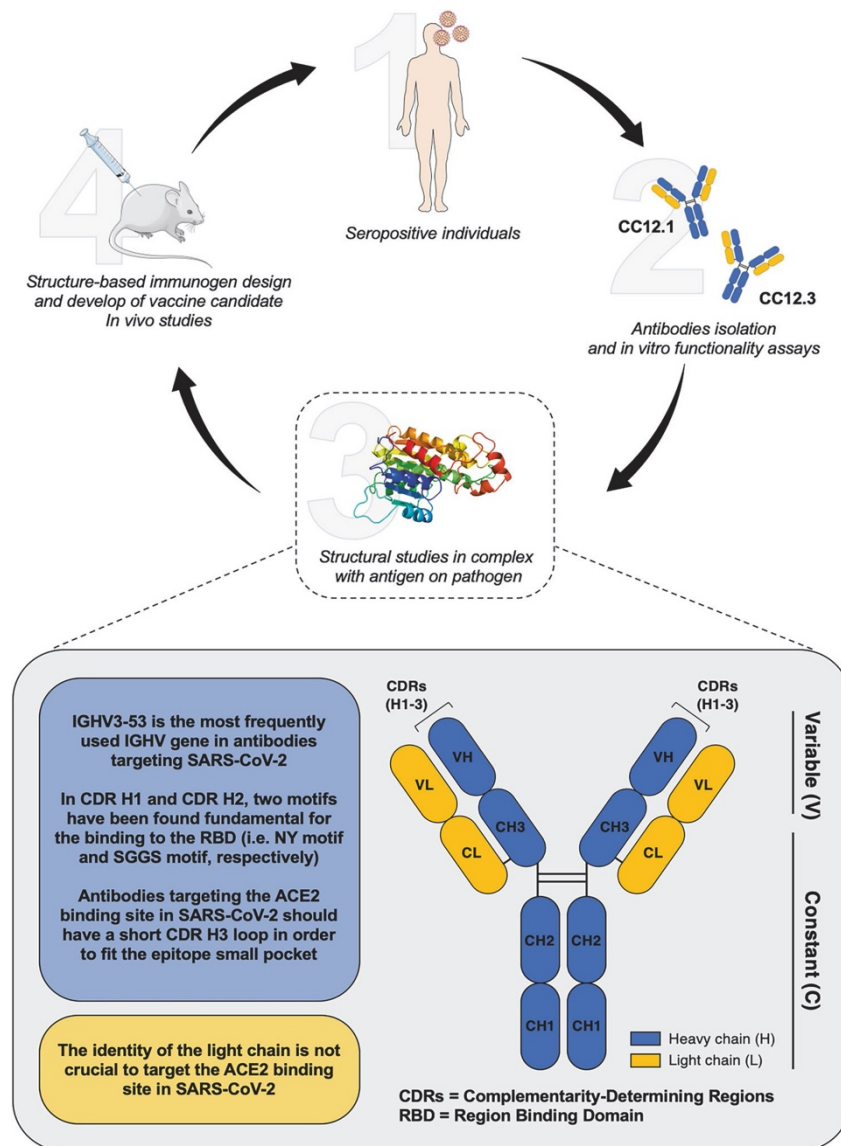


Figure 1. Representation of “reverse vaccinology 2.0” theory: focus on the molecular features of IGHV3-53-encoded antibodies. Monoclonal antibodies are obtained from seropositive subjects, isolated and structurally characterized. Based on the molecular features, a structure-based immunogen is designed and then tested in appropriate animal models.

In conclusion, understanding of IGHV3-53-encoded antibodies and, in general, of anti-SARS-CoV-2 neutralizing antibodies, produced by infected donors, is required to generate immunogens that optimally present neutralizing epitopes to the immune system. Such approach may further open new horizons toward the identification of multiple functional antibodies, derived from several donors and directed toward single epitopes regions in order to combine sites of different shapes recognizing the critical regions, thereby capturing the biological diversity of antibody response.² The characterization by Yuan *et al.* may also allow to create anti-SARS-CoV-2 antibody templates for immunogens design, thus greatly improving the sophistication in the design of immunogens and in immunization strategies.

REFERENCES

1. Yuan, M. *et al.* Structural basis of a shared antibody response to SARS-CoV-2. *Science* <https://doi.org/10.1126/science.abd2321> (2020).
2. Burton, D. R. What are the most powerful immunogen design vaccine strategies? Reverse vaccinology 2.0 shows great promise. *Cold Spring Harb. Perspect. Biol.* **9**, a030262 (2017).
3. Hoffmann, M. *et al.* SARS-CoV-2 cell entry depends on ACE2 and TMPRSS2 and is blocked by a clinically proven protease inhibitor. *Cell* **181**, 271–280.e8 (2020).
4. Rogers, T. F. *et al.* Isolation of potent SARS-CoV-2 neutralizing antibodies and protection from disease in a small animal model. *Science* <https://doi.org/10.1126/science.abc7520> (2020).
5. Ju, B. *et al.* Human neutralizing antibodies elicited by SARS-CoV-2 infection. *Nature* <https://doi.org/10.1038/s41586-020-2380-z> (2020).

CHAPTER 4

Other research activities

PART I

The following manuscript was published in *International Journal of Pharmaceutiutics* in 2019 as:

The role of chitosan as coating material for nanostructured lipid carriers for skin delivery of fucoxanthin

Leticia Malgarim Cordenonsi, Angela Faccendini, **Michele Catanzaro (co-first author)**, Maria Cristina Bonferoni, Silvia Rossi, Lorenzo Malavasi, Renata Platcheck Raffin, Elfrides Eva Scherman Schapoval, Cristina Lanni, Giuseppina Sandri and Franca Ferrari

Abstract

Fucoxanthin (FUCO) is a marine carotenoid characterized by antiproliferative properties against hyperproliferative cells. The aim of this work was to design and develop nanostructured lipidic carriers (NLCs) based on bacuri butter and tucumã oil and loaded with FUCO, intended for skin application to prevent skin hyperproliferative diseases and in particular psoriasis. The presence of FUCO should control the hyperproliferation of skin diseased cells and the lipids forming the NLC core, rich in antioxidants and characterized by wound healing properties, should favor the restoring of skin integrity. NLCs were coated with chitosan (CS) to improve their biopharmaceutical properties (bio/mucoadhesion and wound healing) and to combine the advantages of lipidic nanoparticles with the biological properties of CS. Chitosan coated and non-coated NLC were prepared by means of high shear homogenization and characterized for chemico-physical and biopharmaceutical properties (in vitro biocompatibility and cell uptake towards normal dermal human fibroblasts). Moreover, the pharmacological activity of FUCO loaded in NLCs was assessed in psoriatic-like cellular model. NLCs were characterized by dimensions ranging from about 250 to 400 nm. Moreover, the CS coating and FUCO loading determined an increase of size. Moreover, TEM and zeta potential analysis confirmed the presence of CS

coating on nanoparticle surface, thus conferring to nanoparticle good bioadhesion properties. NLCs uptake in fibroblasts was observed and NLC-FUCO-CS caused a reduction of cell viability with a less marked effect in fibroblasts rather than in psoriatic cells, highlighting the capability of this system to control skin hyperproliferation and inflammation. The loading of NLC-FUCO-CS in pullulan film should render NLCs application easy, without impair prompt interaction of the drug with the skin. Considering the overall results skin application of CS coated NLCs loaded with FUCO seems a promising approach to control skin hyperproliferation and to preserve skin integrity in psoriatic skin.

Keywords: Fucoxanthin; Natural lipids; Nanostructured lipid carriers; Chitosan; Skin hyperproliferative diseases; Psoriasis *in vitro* model.

PART II

The following manuscript was published in *CNS Drugs* in 2020 as:

Targeting Infectious Agents as a Therapeutic Strategy in Alzheimer's Disease

Tamàs Fülöp, Usma Munawara, Anis Larbi, Mathieu Desroches, Serafim Rodrigues, **Michele Catanzaro**, Andrea Guidolin, Abdelouahed Khalil, François Bernier, Annelise E. Barron, Katsuiku Hirokawa, Pascale B. Beauregard, David Dumoulin, Jean-Philippe Bellenger,

Jacek M. Witkowski and Eric Frost

Abstract

Alzheimer's disease (AD) is the most prevalent dementia in the world. Its cause(s) are presently largely unknown. The most common explanation for AD, now, is the amyloid cascade hypothesis, which states that the cause of AD is senile plaque formation by the amyloid β peptide, and the formation of neurofibrillary tangles by hyperphosphorylated tau. A second, burgeoning theory by which to explain AD is based on the infection hypothesis. Much experimental and epidemiological data support the involvement of infections in the development of dementia. According to this mechanism, the infection either directly or via microbial virulence factors precedes the formation of amyloid β plaques. The amyloid β peptide, possessing antimicrobial properties, may be beneficial at an early stage of AD, but becomes detrimental with the progression of the disease, concomitantly with alterations to the innate immune system at both the peripheral and central levels. Infection results in neuroinflammation, leading to, and sustained by, systemic inflammation, causing eventual neurodegeneration, and the senescence of the immune cells. The sources of AD-involved microbes are various body microbiome communities from the gut, mouth, nose, and skin. The infection hypothesis of AD opens a vista to new therapeutic approaches, either by treating the infection itself or modulating the immune system, its senescence, or the body's metabolism, either separately, in parallel, or in a multi-step way.

Keywords: Alzheimer's disease; infections; microbes; HSV-1; *Porphyromonas gingivalis*.

LIST OF PUBLICATIONS

(from 2017 to 2020)

1. M.M. Serafini, **M. Catanzaro**, M. Racchi, M. Rosini, C. Lanni; *Curcumin in Alzheimer's disease: can we think to new strategies and perspectives for this molecule?*; *Pharmacological Research*, 2017 Oct; 124: 146-155. doi: 10.1016/j.phrs.2017.08.004.
2. W. Rungratanawanich, G. Abate, M.M. Serafini, M. Guarienti, **M. Catanzaro**, M. Marziano, M. Memo, C. Lanni, D. Uberti; *Characterization of the antioxidant effects of gamma-Oryzanol: involvement of the Nrf2 pathway*; *Oxidative Medicine and Cellular Longevity*, 2018 Mar 14; 2018: 2987249. doi: 10.1155/2018/2987249.
3. **M. Catanzaro**, E. Corsini, M. Rosini, M. Racchi, C. Lanni; *Immunomodulators inspired by nature: a review on Curcumin and Echinacea*; *Molecules*, 2018, 23 (11), 2778. doi: 10.3390/molecules23112778.
4. F. Bisceglia, F. Seghetti, M. Serra, M. Zusso, S. Gervasoni, L. Verga, G. Vistoli, C. Lanni, **M. Catanzaro**, E. De Lorenzi, F. Belluti; *Prenylated Curcumin analogues as multipotent tools to tackle Alzheimer's disease*; *ACS Chemical Neuroscience*, 2019 Mar 20; 10 (3): 1420-1433. doi: 10.1021/acscemneuro.8b00463.
5. L. Malgarim Cordenonsi, A. Faccendini, **M. Catanzaro (co-first author)**, M.C. Bonferoni, S. Rossi, L. Malavasi, R. Platcheck Raffin, E.E. Scherman Schapoval, C. Lanni, G. Sandri, F. Ferrari; *The role of chitosan as coating of Nanostructured Lipid Carrier in skin delivery of fucoxanthin*; *International Journal of Pharmaceutics*, 2019 Aug 15; 567: 118487. doi: 10.1016/j.ijpharm.2019.118487.
6. M. Rosini, E. Simoni, R. Caporaso, F. Basagni, **M. Catanzaro**, I.F. Abu, F. Fagiani, F. Fusco, S. Masuzzo, D. Albani, C. Lanni, I.R. Mellor, A. Minarini; *Merging memantine and ferulic acid to probe connections between NMDA receptors, oxidative stress and amyloid- β peptide in Alzheimer's*

- disease; *European Journal Medicinal Chemistry*, 2019 Oct 15; 180: 111-120. doi: 10.1016/j.ejmech.2019.07.011.
7. M.M. Serafini, **M. Catanzaro (co-first author)**, F. Fagiani, E. Simoni, R. Caporaso, M. Dacrema, S. Govoni, M. Racchi, M. Rosini, M. Daglia, C. Lanni; *Modulation of oxidative stress response through activation of Keap1/Nrf2/ARE pathway by curcuma- and garlic-derived hybrids*; *Frontiers in Pharmacology*, 2019; 10: 1597. doi: 10.3389/fphar.2019.01597.
 8. T. Fülöp, U. Munawara, A. Larbi, M. Desroches, S. Rodrigues, **M. Catanzaro**, A. Khalil, F. Bernier, A. Barron, P.B. Beauregard, D. Dumoulin, J.P. Bellenger, J.M. Witkowski, E.H. Frost; *Targeting Infectious Agents as a Therapeutic Strategy in Alzheimer's Disease: Rationale and Current Status*; *CNS Drugs*, 2020 May 26; doi: 10.1007/s40263-020-00737-1.
 9. **M. Catanzaro**, F. Fagiani, M. Racchi, E. Corsini, S. Govoni, C. Lanni; *Immune response in COVID-19: addressing a pharmacological challenge by targeting pathways triggered by SARS-CoV-2*; *Signal Transduction and Targeted Therapy*, 2020 May 29; 5 (1): 84. doi: 10.1038/s41392-020-0191-1.
 10. **M. Catanzaro**, C. Lanni, F. Basagni, M. Rosini, S. Govoni, M. Amadio; *Eye-Light on Age-Related Macular Degeneration: Targeting Nrf2-Pathway as a Novel Therapeutic Strategy for Retinal Pigment Epithelium*; *Frontiers in Pharmacology*, 2020; 11: 844. doi: 10.3389/fphar.2020.00844.
 11. F. Fagiani, **M. Catanzaro (co-first author)**, E. Buoso, F. Basagni, D. Di Marino, S. Raniolo, M. Amadio, E.H. Frost, E. Corsini, M. Racchi, T. Fülöp, S. Govoni, M. Rosini, C. Lanni; *Targeting cytokine release through the differential modulation of Nrf2 and NF- κ B pathways by electrophilic/non-electrophilic compounds*; *Frontiers in Pharmacology*, 2020; 11: 1256. doi: 10.3389/fphar.2020.01256.
 12. F. Fagiani, **M. Catanzaro (co-first author)**, C. Lanni; *Molecular features of IGHV3-53-encoded antibodies elicited by SARS-CoV-2*; *Signal Transduction and Targeted Therapy*, Aug 25; 5 (1): 170. doi: 10.1038/s41392-020-00287-4.

